INVESTIGATIONS OF A POSSIBLE NOVEL DECONTAMINATION ROLE FOR A HAEMOSTATIC PRODUCT: STUDIES WITH S-[2-(DIISOPROPYLAMINO)ETHYL]-*O*-ETHYL METHYLPHOSPHONOTHIOATE (VX)

By

HELEN LOUISE LYDON

A thesis submitted to the University of Birmingham for the degree of

DOCTOR OF PHILOSOPHY

School of Biosciences

University of Birmingham

May 2012

ABSTRACT

Haemorrhage remains a leading cause of death in civilian and military environments. Recent research into emergency treatments for severe haemorrhaging injuries has resulted in production of a number of advanced haemostatic products. In certain scenarios, concomitant release of toxic materials may exacerbate trauma and ultimately reduce survival from such injuries. In particular, systemic absorption of the nerve agent VX (S-[2-(diisopropylamino)ethyl]-*O*-ethyl methylphosphonothioate) via wounds may rapidly cause muscle paralysis and death. This research explored the hypothesis that a haemostatic product could perform an additional function as a wound decontaminant.

The objectives of this project were to: (i) demonstrate that haemostatic products retain efficacy in the presence of VX using *in vitro* thrombelastography (TEG); (ii) identify candidate products which have demonstrable ability to sequester VX from damaged and undamaged skin using an established *in vitro* percutaneous penetration model and; (iii) assess the most effective candidate product *in vivo* (anaesthetised swine) when applied to a non-haemorrhaging skin wound contaminated with a 5xLD_{50} dose of ^{14}C-VX. Finally, to further investigate the mechanism of toxicity of VX and identify potential therapeutic targets, a preliminary genomic analysis of exposed animal blood samples was conducted.

Firstly, four products (WoundStat™ (WS), ProQR™ (PQR), FastAct™ and Vitagel™), from an initial list of seven, improved coagulation kinetics of swine whole blood samples compared to control samples *in vitro* and retained this property in the presence of VX. Secondly, four products (QuikClot™ (QC), Celox™, WS and PQR) and a novel decontaminant liquid (TOP) reduced penetration of ^{14}C-VX across isolated pig skin *in vitro* over a 24 hour period.

Furthermore, WS, QC and PQR also significantly reduced penetration of ^{14}C-VX across superficially damaged pig skin, to a similar extent as the current "benchmark" military decontaminant Fuller's Earth. Thirdly, when assessed *in vivo* WS was capable of significantly preventing death from intoxication, prolonging survival time and reducing the severity of signs of intoxication in the absence of additional medical intervention. However, decontamination did not significantly improve whole blood acetylcholinesterase (AChE) activity, supporting the view that AChE activity is not a useful prognostic indicator and that mechanisms of toxicity other than AChE inhibition may exist for VX. Finally, preliminary genomic analysis identified significant changes in regulation of genes involved in inflammatory processes, liver damage and oxidative stress.

In summary, this project has successfully demonstrated that haemostatic products, based on an adsorptive mechanism of action, offer a highly effective means of countering the rapidly fatal effects of the chemical warfare agent VX present in wounded skin tissue. Further development of the concept of a haemostatic decontaminant has life-saving implications.

ACKNOWLEDGEMENTS

The work presented in this Thesis could not have been completed without incredible help and support from a number of people.

I sincerely thank my supervisors, Dr Rob Chilcott and Professor Kevin Chipman, for their invaluable and unwavering advice, support and encouragement. It has been a privilege to be your student.

I am incredibly grateful to my colleagues, Charlotte, Haz and Rhys. You all helped so much. I thank you for giving me so much of your time, helping me out of tight spots, being great company, keeping me calm (most of the time) and letting me complain about the same things even when you had your own problems.

I wish to thank the staff of the Biomedical Sciences Department at the Defence Science and Technology Laboratory, Porton Down, UK, particularly Chris Dalton, for their assistance with the practical work. I would also like to thank the staff at the US Army Medical Research Institute of Chemical Defense, particularly Dr John Graham and Dr Ed Clarkson, and Professor Bob Maynard at the Health Protection Agency, for their assistance and encouragement throughout the work.

My colleagues at the Health Protection Agency and University of Birmingham were incredibly helpful throughout the project, and I particularly wish to express my gratitude to Dr Tim Williams and the Functional Genomics Facility at the University of Birmingham, and certain colleagues (Dr Awesome and friends) at the Health Protection Agency, for their help in designing and interpreting the gene expression analysis experiment. I am truly grateful to

my friends at the Health Protection Agency for scientific discussions over tea and cake. You helped more than you can know. I would also like to express my thanks to former colleagues at the University of Manchester, who were always ready with words of support and encouragement during the difficult times.

I also wish to gratefully acknowledge funding from the US Defence Threat Reduction Agency, without which this work could not have been completed.

Finally, to say “Thank you” to Jon, Charlotte and my family doesn’t come anywhere near how much I appreciate their support. I literally could not have done this without any of you and can’t believe how much time and attention you’ve given me over the last four years (and, in the case of Jon and Charlotte, still actually like me)! For that I am, and always will be, amazed and truly grateful.

TABLE OF CONTENTS

LIST OF FIGURES

LIST OF TABLES

LIST OF ABBREVIATIONS

AChE	Acetylcholinesterase
AVTUR	Aviation turpentine, see JP8
COTS	commercial "off-the-shelf"
CX	Celox™ haemostatic granules
DD	The group of animals which were exposed to a 5xLD_{50} dose of ^{14}C-VX and subsequently decontaminated with WoundStat™
DXD	The group of animals which were exposed to a 5xLD_{50} dose of ^{14}C-VX
FA	FastAct™ liquid haemostatic preparation
FE	Fuller's Earth
GC-MS	Gas chromatography mass spectrometry
HC	HemCon™ haemostatic bandage
JP8	Aviation turpentine (aviation fuel)
LD_{50}	The "median lethal dose" which results in 50% fatality rate within a population
LSC	Liquid scintillation cocktail
M291	M291 (product name), currently "in use" or "benchmark" military decontaminant
OP	Organophosphate
PQR	ProQR™ haemostatic powder
RSDL	Reactive Skin Decontamination Lotion®
QC (ACS+)	QuikClot® (Advanced Clotting Sponge Plus)™

TDLO	The lowest published toxic dose; the lowest dose that has been published for a substance which produces a toxic effect in a given species
TEG	Thrombelastography
TOP	Tetraglyme polyethyleneimine
VG	Vitagel^{TM} liquid haemostatic preparation
VX	S-[2-(diisopropylamino)ethyl]-O-ethyl methylphosphonothioate
^{14}C-VX	The radiolabelled analogue of VX
WS	WoundStat^{TM}

CHAPTER 1. Introduction

CHAPTER 1. Introduction

Haemorrhage remains a leading cause of death following trauma in both civilian and military environments[1,2]. In addition to the damage caused by the injury, further complications may manifest as a result of blood loss sustained in the interval between injury and treatment (either by first responders or at a medical centre) which can often exacerbate severe trauma[3,4]. Rapid response to haemorrhage is therefore an important factor influencing survival and recovery. In the last decade, this requirement was particularly recognised by the international military community[5]. As a result, a number of products have been developed in response to the identification of the requirement for rapid pre-hospital treatment of haemorrhage.

In certain scenarios the presence of environmental contaminants due to accidental or deliberate release, in addition to trauma and haemorrhage, may be a further complication to consider. Contaminants may: 1) aggravate the initial injury; 2) cause secondary injuries; 3) cause toxicity following systemic absorption, or; 4) affect coagulation and haemostasis. These issues could seriously affect acute and chronic outcomes.

The priority for treatment of severe haemorrhage following trauma is to achieve haemostasis and the benefit of locally applied haemostatic products is clear. However, in a situation as described above, a haemostatic product which could also provide some decontamination action would be necessary.

The purpose of the work presented in this thesis was to identify a commercially available haemostatic product intended for local application at the site of a haemorrhaging wound,

with the potential to prevent fatal blood loss and fatal poisoning with the organophosphate compound S-[2-(diisopropylamino)ethyl]-*O*-ethyl methylphosphonothioate (VX).

In support of this objective, identification of such a product should follow a structured, step-wise research programme. *In vitro* assays may be used to screen a selection of candidate products, prior to evaluation in *in vivo* models. These screens should assess suitability as a haemostat and as a decontaminant. Haemostat performance can be assessed by an *in vitro* coagulation assay. Decontaminant performance can be assessed using *in vitro* models of contaminant penetration through excised skin samples. These *in vitro* assays can use either animal or human tissue: human is the gold standard tissue source, however this is subject to variable availability. *In vitro* assays may also allow manipulation of variables, such as dose, exposure time or decontamination time, without compromising sample sizes. Contaminant penetration through damaged skin can also be evaluated *in vitro*, which is of particular importance for the ultimate target described above. These *in vitro* screens allow elimination of unsuitable products so that only promising candidates are taken forward for evaluation in *in vivo* models, thus reducing the numbers of animal experiments required. The *in vivo* models can assess whether the effects *in vitro* can be reproduced *in vivo*, first with regards to decontaminating a contaminated skin surface wound, then by preventing death from toxicity and blood loss in a haemorrhaging wound.

Part 1: Haemostatic products

1.1 Strategies for testing efficacy of advanced, local haemostatic products

The developments made in the field of "advanced haemostat" research include bandages; granular or powder absorptive packing materials or dressings; liquid sealants and "glues". Systemically administered and active treatments such as clotting factors have also been examined. Mechanisms of action vary between wound sealing, compression, passive absorption and concentration of clotting factors, and fibrin or thrombin activation[5].

Clearly, it is important that haemostatic products have demonstrable efficacy prior to clinical use. A range of experimental techniques have been developed for this purpose, based on reproducible moderate to severe haemorrhaging injuries *in vivo*. However, there is an increasing emphasis on the need to replace animal studies with suitable *in vitro* alternatives.

Until recently, reports of test haemostatic products were usually anecdotal and reported variable effect[5]. Reporting and evaluation of local haemostatic product performance in human trauma is limited to case reports from civilian and combat settings[6,7]. These reports span product use and/or outcomes in certain disease states and coagulopathies etc.; on a desperate-use basis for surgery or trauma patients where standard-of-care has been unsuccessful; and in a military setting. However, frequency of reporting, and in turn the reliability of case reports, may be particularly problematic in far-forward medical care settings. Surveys of local haemostat use on the battlefield or in far-forward medical attendance have been attempted, but without much success[6]. Efficacy and mechanism of

action of local haemostats can therefore be evaluated in more detail by *in vivo* studies using appropriate animal models of haemorrhage or trauma, or *in vitro* using blood samples.

1.1.1 In vivo models: model selection and study design

Primary targets for battlefield-intended haemostat development are injuries that may be treated without (or with minimal) medical background or training and the wounded area should be easily accessible to first responders[7]. A number of models have been developed over the last 15 years to represent clinically relevant injuries for both civilian and military trauma. In general, the pig has been more commonly used due to its larger blood volume and similarity with human anatomy and physiology. The successful demonstration of the haemostatic ability of a product using one model only demonstrates the effectiveness for that type of injury, at that level of severity and within the experimental boundaries put in place by the researchers[5]. Thus it is not possible to assess products by a single standardised haemorrhage model: models should be designed to mimic and reflect the likely conditions for the products intended deployment.

Recent development has resulted in a generally accepted battery of models including aortotomy, venous, lethal extremity, complex and lethal groin injuries and liver injuries in swine. The liver is the most commonly injured solid organ, and 50-90% mortality rates have been recorded for Grade V liver injury in humans[7–12]. The current standard of care is abdominal packing which requires re-operation for removal and is associated with serious complications. On the battlefield, certain areas of the body at the edges of personal body

armour were identified as frequent sites of injury, such as the neck, peritoneum and groin[13]. These are awkward sites to treat by tourniquets and compression dressings. The complex groin injury model was developed in response to the growing concern for haemorrhage control of injuries like these[13,14]. The merits of the model are that the injury involves damage to multiple tissues and vasculature, including complete transection of the femoral artery and vein. Ultimately this is an accepted, well defined, clinically relevant model of severe haemorrhage from accessible major, yet awkward to treat areas of a large animal.

Wound induction by arteriotomy does produce a near transection injury and (otherwise lethal) high pressure arterial haemorrhage that many modern local haemostats are theoretically designed for. The severity of the femoral arteriotomy model was demonstrated by the 100% lethality rate resulting from treatment with the gauze Army Field Bandage alone[15,16]. Modifications and individualised study designs can produce models with additional aggravation of skin, muscle and bone damage.

Battlefield injuries to the extremities present major compressible bleeding sites, and severe haemorrhage that is prospectively salvageable with effective control. In humans the aorta itself would not be a compressible injury site, but the swine aorta is suggested to be similar to the size of a human femoral artery[17,18]. Additionally, the performance of haemostats applied through a pool of blood, against high pressure, high volume (and high rate) spurting blood can be assessed.

Penetrating or impact injury to the abdomen is likely to cause trauma in multiple organs[5]. The presence of major blood vessels and multiple organs with diverse roles in close proximity to each other exacerbates the risk of major consequences from this type of

trauma. The high volume of blood received by the liver and kidneys especially is a major point of concern for haemorrhage from these sites.

The model designs can be manipulated to include complications of coagulopathy, hypothermia or metabolic acidosis which may accompany and exacerbate severe trauma; or prolonged observation periods to mimic delays between the injury and clinical treatment[19]. Physiological and post-mortem monitoring can also provide useful limits for inclusion of appropriate data and demonstration of uniformity of injury induction[10,11].

The primary endpoints which are monitored in the majority of these models include blood loss, haemorrhage control and survival, amongst others. However, few studies analyse survival over a period of days to weeks. Other endpoints such as pathology or resuscitation requirement are included less frequently.

In vivo models have also demonstrated the practical variations of dressing application which may influence performance. Granular haemostats are generally poured onto or into the wound, or sometimes poured onto gauze for application, whereas the rigidity of HemCon has been noted to restrict the ability of the dressing to conform to complex wounds. Evaluation of HemCon has sometimes required the dressing to be cut in half or pre-moulded to improve flexibility and enhance contact with the defect[15,16]. Exothermic reactions following application of QuikClot to wounds has been documented to the extent that during some experiments, a roll of gauze has been placed over QuikClot to protect against potential thermal injuries to the surgeons[3,8,15,16].

1.1.2 *In vitro* methods for *in vivo* monitoring and as alternatives to *in vivo* studies

For intra-operative monitoring of *in vivo* studies, assays invariably include prothrombin time (PT), activated partial prothromboplastin time (aPTT), fibrinogen concentrations ([fib]), and usually platelet counts and complete blood cell counts (CBC). However, local haemostat development may continue to progress away from *in vivo* studies by using *in vitro* tools. Relevant *in vitro* assays can identify and demonstrate haemostatic properties of substances, characterise mechanisms of action and screen candidate compounds, aside from *in vivo* studies. The main advantage of these studies is that human blood or plasma can be used as a model. However the appropriate choice of an *in vitro* method is essential. Investigating specific portions of the coagulation process involves manipulation of blood samples[20]. Methods which can evaluate treatment-effects in whole blood samples may be much more helpful for gross evaluation of haemostatic efficacy. The increasing inclusion of thrombelastographic measures for evaluation of haemostats is a step towards addressing this issue.

Thrombelastography

Thrombelastography is a technique which monitors and quantifies the coagulation characteristics and kinetics of whole blood. Thrombelastography (TEG) measures clotting time, clot formation time and maximum clot firmness. Empirically, the equipment consists of a pin attached to a torsion wire and a receiver: the pin is inserted into a cup containing a blood sample and either the cup or the sensor is rotated through 45° in each direction.

When the blood coagulates, the movement of the pin becomes “coupled” to the movement of the blood in the cup, thus the mechanical strength of the clot is transferred to the pin. The detected movement of the pin is reflective of coagulation progress, and ultimately the coagulation strength of the blood in the cup.

The components of the TEG trace can be divided into:

- reaction time: similar to whole blood clotting time, expressed in minutes or a trace distance for calculation (according to tracing speed);
- coagulation time (or rate of coagulation);
- rate of clot formation;
- maximum clot elastic shear modulus (i.e. maximum clot strength);
- fibrinolysis.

Thrombelastography has been primarily used so far for patients as a point-of-care diagnostic tool, for example to diagnose coagulopathy, assess coagulation status or detect abnormalities in surgical or trauma patients[21]. Recently, the technique has become increasingly utilised to assess components of products or compounds with hypothesised pro-coagulatory characteristics[22–25].

A further advantage of thrombelastography for advanced local haemostat development is the provision of data on the strength and sustainability of clots. Clot strength data could be reflective of patient survival and in turn recovery, and also may be representative of haemostat performance in cases of delayed medical attention, such as prolonged evacuation from a battlefield.

Clearly the selection of the correct model, method and observations is a delicate balance between acquiring as much data as possible and keeping the investigation relevant to the intended setting. In vivo models have to be carefully selected and procedures amended to reflect the intended deployment of the product, and the haemostat can only be verified to be as successful within the limits of the experimental design[5]. *In vitro* assays, whether alone or alongside an animal model, have numerous advantages. Blood or plasma samples can be obtained for, or modified to mimic, certain disease states, coagulopathies or situations, whilst minimising or even eliminating the use of animal subjects. *In vitro* analyses enable evaluation of haemostatic action on - or interaction with – blood, platelets, plasma and coagulation pathways, and a method of screening compounds for potential haemostatic action. Most importantly of all, *in vitro* analyses provide a means to evaluate the haemostat in its intended target: human blood. Standardisation of study designs, the definitions and methods of quantifying primary endpoints should be a priority to promote reliable comparison of haemostatic performance between studies.

Part 2: Decontamination of VX

1.2.1 Toxicity of the organophosphate compound S-[2-(diisopropylamino)ethyl]-*O*-ethyl methylphosphonothioate (VX)

Organophosphate compounds have been used in some parts of the world as pesticides for many years. The primary mechanism of action of these chemicals is to inhibit acetylcholinesterase. However, some organophosphates, such as S-[2-(diisopropylamino)ethyl]-*O*-ethyl methylphosphonothioate (VX; Figure 1.1) have sufficient known toxicity to designate them as chemical warfare agents, namely nerve agents[26,27]. These particular compounds irreversibly inhibit acetylcholinesterase to an extent to which the ensuing accumulation of the neurotransmitter acetylcholine at synapses results in symptoms known as "cholinergic crisis". These symptoms include miosis, increased secretions (including salivation, bronchorrhoea, lacrimation), fasciculations, tremors, convulsions and eventually muscle paralysis and apnoea. Following exposure to a sufficient dose, death can occur within minutes or hours[28,29].

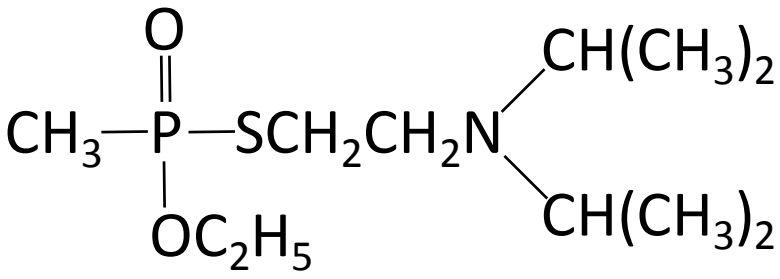

Figure 1.1: Structure of the organophosphate nerve agent, S-[2-(diisopropylamino)ethyl]-*O*-ethyl methylphosphonothioate (VX).

Mechanism of organophosphate toxicity

Organophosphates (OPs) may exert inhibitory mechanisms on various esterases, although acetylcholinesterase inhibition is considered to be the primary target resulting in toxicity. Acetylcholinesterase hydrolyses acetylcholine in the synaptic cleft, parasympathetic effector organ, or neuromuscular junction. The ester moiety of acetylcholine binds to the serine residue in the active site of acetylcholinesterase[30]. Cleavage of the enzyme-substrate complex yields choline and acetylated enzyme; hydrolysis of the acetylated intermediate completes recovery of the enzyme with intact hydroxylated serine site. Organophosphates phosphorylate or phosphonylate the serine hydroxyl group in the active site of the enzyme; the phosphonylation mechanism is more common for nerve agents. Cleavage of the OP compound yields a phosphorylated or phosphonylated serine residue rather than an acetylated serine residue. The rate of hydrolysis of the phosphorylated enzyme-complex is much slower than that of the acetylated enzyme-complex: thus the active site is obstructed and regeneration of enzyme (and hence subsequent catabolism of acetylcholine) is effectively inhibited. The resultant accumulation of acetylcholine results in depolarisation blockade and excessive stimulation of cholinergic receptors thus abnormally prolonging cholinergic effects[31]. The resultant signs of intoxication may be termed “cholinergic crisis”.

The specificity for the acetylcholinesterase enzyme, the affinity of the compound for the active site and the rate at which acetylcholinesterase may be phosphorylated varies between organophosphorous compounds, which partly accounts for variations in toxicity (particularly acute toxicity) between them[32,33]. The structure of the compound contributes to this variation[32–34]. For example, the rate of inhibition is influenced by the whole molecular structure, whereas the rate of dephosphorylation (and thus reactivation) is

determined by the structure of the group which remains complexed to the enzyme. Deacetylation is relatively quick (μs) compared to dephosphorylation (hours-days) and spontaneous reactivation by dephosphorylation is generally faster the smaller the alkyl groups which remain complexed to the enzyme.

Aging

"Aging" is a term given to describe the processes which further alter the phosphorylated enzyme and yield an intermediate so modified that reactivation may be completely prevented. The dialkyl phosphorylated enzyme-complex is dealkylated either by: 1) hydrolysis of the P-O bond, or; 2) hydrolysis of the O-C bond, yielding an alkylated enzyme-complex with increased stability. The stability of the aged enzyme increases the resistance to reactivation[34]. The rate at which "aging" occurs also depends on the structure of the inhibited enzyme. Differences in the aging half-life for compounds exist between species[34,35]. A rapid aging rate means that recovery, without (medical) intervention, would be dependent on synthesis of new enzyme. However, a slower aging half-life doesn't necessarily translate to reduced acute toxicity, as acute toxicity is attributed to accumulation of acetylcholine at synapses, not aging of acetylcholinesterase[33]. The rates of acetylcholinesterase inhibition, aging and (spontaneous) reactivation for different organophosphate nerve agents are reported to be the source of variation in susceptibility to re-activation of acetylcholinesterase by oximes[33,34,36].

Clinical signs of organophosphate intoxication

Following inhalation of nerve agents, signs of intoxication can become apparent within minutes of exposure. In comparison, the rate of absorption is slower following dermal exposure, which may delay onset and prolong effects of exposure[37]. Suspected exposure to organophosphates may be confirmed or diagnosed by measurement of acetylcholinesterase activity of blood. Clinical signs of intoxication may largely be attributed to the effect of accumulation of acetylcholine at muscarinic and nicotinic receptors at the central nervous system, nicotinic receptors at autonomic ganglia and the neuromuscular junction, and muscarinic receptors at parasympathetic effector organs[28]. Muscarinic signs arise from increased activity of acetylcholine of the parasympathetic system and include hypersecretory effects such as salivation, lacrimation, bronchorrhoea, rhinorrhea or perspiration and miosis[28,32]. Muscarinic effects on the GI tract and bladder include nausea and vomiting, cramps, and faecal and urinary incontinence[28,32]. Other muscarinic effects on the respiratory and cardiovascular systems include bronchospasms, bronchoconstriction, dyspnoea, bradycardia and reduced blood pressure[28,32,37], whilst nicotinic effects on the parasympathetic and sympathetic nerves of the cardiovascular system can cause tachycardia and increased blood pressure: the clinical effects on the cardiovascular system depend on the predominance of either muscarinic or nicotinic effects. Excessive stimulation of nicotinic receptors at the neuromuscular junction may include muscle fasciculations and cramps, muscle weakness (a contributor to respiratory depression), increased motor activity such as restlessness, tremors or convulsions and flaccid or rigid paralysis[28,32,38]. Accumulation of acetylcholine at cholinergic receptors in the brain may result in headache, confusion or reduced concentration, lethargy, drowsiness and fatigue, and ultimately unresponsive

reflexes, coma, tremors, convulsions, dyspnoea, and ultimately apnoea. Following a sufficient dose, death may be caused by respiratory paralysis resulting from central effects (depression of respiratory centres) or accumulation of acetylcholine at the neuromuscular junction.

Cases of nerve agent exposure, particularly VX

There are case reports of a very small number of accidental or deliberate exposures to VX[27,39,40]. Reports of deliberate VX exposure in humans included two murders and one recovery in Japan[27]. A structurally and toxicologically similar organophosphorous nerve agent, sarin, was released in a residential area of Matsumoto, Japan in June 1994, resulting in 7 deaths, 58 hospital admissions[41] and intoxication of approximately 600 civilians and responders. Almost a year later, in March 1995, sarin was released on five cars of the Tokyo subway network, resulting in 11 deaths and "emergency evaluation" of more than 5000 people[26]. Detection of sarin breakdown products in soil samples from bomb craters effectively confirmed the use of sarin against civilians in Iraq in 1988[42,43]. Prior to these incidents, human exposures to nerve agents had mainly been confined to military personnel, either accidentally or experimentally, and in relatively low numbers[41,44].

Treatment of organophosphorous nerve agent poisoning

Clinical assessments of the VX-recovery patient and Matsumoto patients identified an organophosphate cause[27,45]. Organophosphate exposures commonly arise from agricultural exposures, and treatment of the patients was based on that of poisoning from liquid

agricultural organophosphate chemicals[45]. Without the knowledge that the exposure had been to gaseous organophosphate, patients were treated and transported without decontamination, and protective equipment was not utilised by responders[45].

Treatment of nerve agent poisoning is based on antagonism of excessive cholinergic stimulation with atropine, regeneration of inhibited enzyme by a class of compounds termed "oximes", and treatment of the clinical signs: including muscle relaxants and anti-convulsants including diazepam and ventilatory support[41].

However, as medical treatment of nerve agent poisoning outside a clinical setting must involve combination therapies, pharmacological research into novel therapies generally use well characterised models which are relatively high through-put, in order to assess the efficacy of various drugs alone and in combination. For example, novel therapies for inclusion in auto-injectors are frequently assessed in guinea pig models[46–49]. Recent developments have included the demonstration of the efficacy of a novel oxime therapy, mononitrosoacetone, which crosses the blood brain barrier with relative ease compared with previous oxime therapies, affording effective reactivation of AChE in the CNS and peripheral tissues[50]. Recently, increasing attention has been drawn to pre-treatments and bio-scavengers. The efficacy of pre-treatment with human butyrylcholinesterase[51], paraoxonase 1[52] in response to nerve agent exposures, in particular VX, has recently been demonstrated in guinea pigs and cynomolgus monkeys[51]. Human butyrylcholinesterase has also been shown to be an effective post-exposure treatment in guinea pigs, even with a delay of 2 hours between exposure and treatment[53]. Inclusion of telemetry devices for

continuous monitoring in some models has provided useful data pertaining to the physiological effects of VX exposure at sub- and supra-lethal dose levels[37].

In vitro methods are of course invaluable for determination of comparative pharmacological activity, and dose response effects of treatments. However, appropriate *in vivo* models are essential for validation of *in vitro* pharmacological data and potential species differences in therapeutic response and, thus, efficacy[54].

Toxicokinetics of nerve agents, particularly VX

Absorption of nerve agents usually occurs via inhalation or percutaneous routes. The distribution and responses to exposure can be affected by the route of absorption. The inhalation route is generally considered to be the primary hazard of other nerve agents such as soman, as VX is relatively non-volatile. The vapour pressure of soman has been calculated as 36.4-53.4 Pa (2092-3016 mg m^{-3})[55]; in comparison, the vapour pressure of VX has been calculated as 0.06-0.12 Pa or 7.38-12.6 mg m^{-3} between 20 and 25°C[56]. Thus for VX, assessment for systemic exposure via dermal absorption has been given the most attention.

Toxicokinetic studies have detected that following percutaneous exposure, VX is primarily detected, and is persistent in, the blood and liver[57,58]. This persistence is also in contrast to other nerve agents, which are rapidly mobilised from blood *in vivo*[57,59]. Differences in distribution between species are also apparent, for example, persistence of VX in the blood of marmosets is longer than that of guinea pigs. Both models are used for medical countermeasure research, so differences in toxicokinetics are clearly an important factor to consider for such studies[59].

Metabolism of VX is generally by hydrolysis, but VX differs from other organophosphate nerve agents in that oxidation at nitrogen or sulphur is also possible[60–62]. Spontaneous hydrolysis of nerve agents is generally slower than enzymatically catalysed hydrolysis[63,64]. Some of the metabolites of VX also possess acetylcholinesterase-inhibitory activity, such as ethyl methylphosphonic acid (EMPA)[59,62,65]. Further hydrolysis reactions generate the relatively less toxic alkyl phosphonic acid (MPA)[62,65]. Other metabolites, 2-(diisopropylamino)ethanethiol (DAET) and a methylation product, 2-(diisopropylaminoethyl) methylsulphide (DAEMS), have been detected following *in vivo* exposures[66]. Recently generation of a third hydrolysis product, S-[2(diisopropylamino)ethyl] methylphosphonothioic acid (EA-2192), and a methylation product (DAET) have been confirmed *in vivo*[67–69].

Mechanisms of nerve agent toxicity other than acetylcholinesterase inhibition

Recently, attention has been increasingly drawn to mechanisms of organophosphate toxicity other than AChE inhibition[70]. Supersensitivity to various organophosphate compounds including VX has been demonstrated in AChE-knockout mice[71,72]. Also, there has been no consistent, robust correlation between lethal dose calculations for VX and levels of AChE activity[70].

Previous studies of GD or VX exposures *in vivo* have also reported various changes in biochemistry, including the thyroid hormone T4[73], Ca^{2+}, mild hyperkalaemia and hyperphosphataemia and hyperglycaemia[74]. Observations of sub-maximal AChE inhibition

following *in vivo* exposure to VX may also suggest the VX-resistance of some blood cholinesterase[74].

The general conclusions made from these findings are that mechanisms of organophosphate toxicity apart from AChE inhibition are of less primary concern, from the perspective of clinical treatment of poisoning. However, they may be of particular interest in relation to chronic low-dose exposures, such as those which may be experienced by individuals who regularly work with organophosphorous pesticides.

Part 3: Exposure to VX via the skin and the relevance for decontamination

1.3.1 Structure and function of the skin

Skin is regularly exposed to chemicals and frequently serves as a route of entry of (or exposure to) substances, whether deliberate or accidental. The skin serves as a physical, mechanical, biological and chemical barrier to exogenous substances, with the ultimate aim of preventing damage, whether local or systemic. Clearly a disease or trauma (physical or chemical) which disrupts the organisation of the skin structure may have implications for the barrier function of the organ.

Factors affecting or influencing the penetration of substances across the skin (and any resulting toxicity, whether direct or indirect) may be exogenous or endogenous[75]. The skin consists of the epidermis externally and the dermis beneath (Figure 1.2).

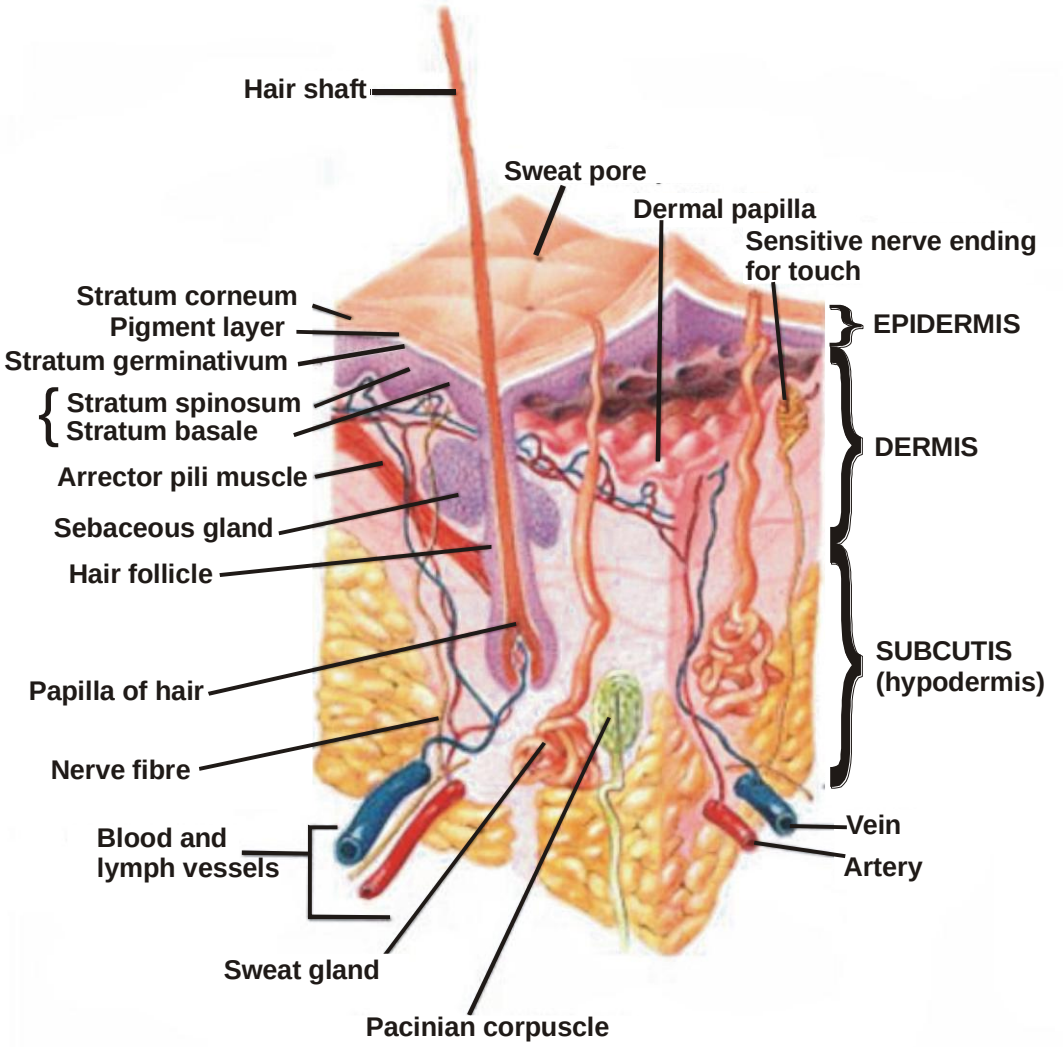

Figure 1.2: Schematic representation of the structure of human skin.

The dermis and epidermis are separated by a basement membrane. Hair follicles and sweat glands span the epidermal layers whilst blood vessels terminate in the dermis. Blood supply to the epidermis is afforded by capillaries embedded in the basement membrane. Nerve endings (e.g. the pacinican corpuscle on this diagram) are also located in the dermis. The hypodermis is populated by fibroblasts, macrophages and adipocytes and has functions related to physical padding, lipid metabolism and insulation.

Image reproduced and adapted from training pages at Surveillance Epidemiology and End Results (U.S. National Cancer Institute). Image is available from

http://training.seer.cancer.gov/melanoma/anatomy/

The basement membrane separates the two structures. Hair follicles, sebaceous glands and eccrine glands are embedded in the dermis and span the epidermis. Blood supply to the epidermis is served by capillaries embedded in the basement membrane. The dermis makes up approximately 90% of the total "skin" thickness and has an important structural supportive function. Beneath the dermis, adipocytes perform functions relating to physical padding, lipid metabolism and insulation. Collagen and elastin in the dermis provide elasticity.

The cellular structure of the epidermis mainly consists of keratinocytes, although with variable morphology[76–79]. These cells are tightly attached to each other by desmosomes, and attached to the basement membrane by hemidesmosomes.

The stratum basale is the deepest section of the epidermis: the keratinocytes here are the feeder cells for the upper layers of the epidermis as this is the only layer where keratinocytes divide. A keratinocyte's progression from the basal layer outward to the outer layers of the epidermis is accompanied by differentiation and accumulation of keratin within[76–79]. Cells of the Stratum spinosum layer begin to produce keratin, which begins to crystallise into granules within the cytoplasm in the stratum granulosum above[76–79]. Filaggrin has an important role involved in serine protease cascades contributing to maintenance of epidermal hydration and homeostasis[80]. This is a multiple layered section where the cells become compressed, increase in volume and begin to lose metabolic functions, organelles begin to degrade, and a protein layer develops beneath the cell membrane[76–79,81,82]. In certain areas of the body, a further layer of highly keratinous cells is

present: the Stratum lucidum. This is present in particularly thick skin such as the bottom of the feet or tip of the nose.

Ultimately, the differentiation processes which occur as a basal cell migrates from the stratum basale outwards builds the outermost layer of epidermal corneocytes: the stratum corneum[76–79,81]. At this level, the cells are flattened and arranged in multiple layers, the thickness of which varies with anatomical site[81]. Gradually the outermost corneocytes are shed from the outermost surface (over approximately 2 weeks), whilst being replaced as the process continues beneath (also an approximately 2 week process).

The stratum corneum is regarded as the functional barrier to contact with exogenous substances[83], but absorption of substances across the skin is affected by the physicochemical properties of the substance and the physiological state of the skin at the time of contact or exposure.

The “normal” lipid content of the intercellular space of the stratum corneum provides a hydrophobic environment which discourages transepidermal water loss. If the stratum corneum is removed, the higher water content in the intercellular spaces of the epidermis below provides an aqueous environment for hyrdrophilic compounds to diffuse into; the rete ridges provide a large surface area and sufficient vasculature for subsequent diffusion into the systemic circulation.

The extent of uptake of a substance following contact with the skin is influenced by (and may be proportional to) the substance concentration, the length of contact (time), the size of the area of skin exposed and the anatomical site of contact, the environmental conditions surrounding the point of contact, and the physicochemical properties of the substance such

as its molecular weight, lipophilicity, volatility, and the rate of diffusion through the stratum corneum[75,84–86]. Deposition and distribution of a compound in the skin relative to systemic absorption can be quantified by the octanol/water partitioning coefficient (K_{OW}), which measures the solubility of a substance. Partitioning of the substance from its vehicle into the skin will also be affected by its affinity for the vehicle: i.e. the extent to which a substance is retained in the skin relative to systemic absorption and distribution is a balance of the partitioning coefficients between the substance and its vehicle and the substance and the skin. The rate of diffusion is inversely related to the molecular weight or volume of the substance[83]. The skin is generally more permeable to hydrophobic substances of low molecular weight than hydrophilic or high molecular weight substances[83,87–90]. For substances of low molecular weight, hydrophobicity may be the limiting factor in penetration.

1.3.2 Toxicity of VX following percutaneous exposure, and treatment and decontamination thereof

The toxicity of nerve agents clearly preclude their evaluation in human volunteer studies. Data pertaining to exposures in humans are limited to early reports (circa 1950s to 1970s) of human exposure studies and case reports of poisoning[26,41,44,91–94] . Data obtained from case studies of organophosphate poisoning can provide useful supporting information. With particular regard to VX, whilst limited inhalation data are available, assessment of penetration via the percutaneous route has been given the most attention.

Much attention has been given to the use of relevant models for assessment and validation of percutaneous penetration and distribution of different compounds. Factors including type, age, sex, thickness and anatomical region of the skin; solvents or vehicles, partition co-efficient, liphophilicity, hydrophobicity, volatility, and molecular size and weight of the compound all affect the percutaneous penetration of substances[75,95,96]. Thus there is not a "one size fits all" model for assessment of percutaneous penetration of compounds: data must be obtained using the most appropriate model(s) for extrapolation and prediction of effects in humans[97].

Similarities between pig and human skin include the dermal and epidermal thickness (1-3mm), density of hair growth, and tissue elasticity[98]. Despite some differences in vasculature and the presence of apocrine glands rather than eccrine glands, pig skin has generally become an accepted model for assessment of percutaneous penetration of exogenous substances[97–99]. However, due to anatomical regional differences in skin structure and permeability, equivalent anatomical regions may not necessarily be most comparable between models[90,96,97]. A number of studies of percutaneous penetration of VX provide comparable data between pig and human skin, both *in vitro* and *in vivo*. There are comparable *in vitro* data between human and pig skin for assessment of percutaneous penetration of certain compounds. In particular, the skin of the pig ear has been repeatedly used as a suitable model for VX penetration in comparison to human forearm skin[58,74,100–102].

The percutaneous LD_{50} of VX is similar between humans and pigs (86 µg/kg and 60µg/kg respectively). The percutaneous LD_{50} of guinea pigs is also not dissimilar to that of humans or pigs (80µg/kg)[38], however, differences in the distribution of esterase enzymes in the blood

between humans, pigs and rodents, generally favour the use of pigs in studies of nerve agent toxicity and decontamination, rather than medical countermeasures[34,35,54,103,104]. Decontamination methods and barrier creams have also been assessed in the pig model, both *in vitro* and *in vivo*[100,105–110].

Part 4: Summary

1.4.1 Strategies for identification and evaluation of a haemostatic decontaminant

The primary aim of the work presented in this thesis was to identify a haemostatic product with the ability to decontaminate a wound contaminated with VX *in vivo*. Thrombelastography, an *in vitro* coagulation assay was used to test the pro-coagulatory performance of a range of commercially available haemostatic products (Chapter 3). Next, the ability of these haemostats to reduce or prevent VX penetration across intact and damaged skin was assessed using an *in vitro* diffusion cell system (Chapter 4). Following elimination of ineffective products, one candidate was selected for advanced analysis of VX-decontamination efficacy in an *in vivo* damaged skin model (Chapter 5).

1.4.2 Analysis of gene expression following exposure to VX via damaged skin

The intention of the preceding studies was to identify a haemostatic decontaminant product to facilitate haemostasis during the interval between injury and medical treatment, which could be prolonged to up to 72 hours in a battlefield environment[17]. In a case such as this, information on toxic effects other than AChE inhibition would be pertinent. In order to gather information which may be useful to identify targets or effects of VX toxicity other than AChE inhibition, gene expression during VX exposure was therefore analysed (Chapter 6).

CHAPTER 2. Materials and Methods

CHAPTER 2. Materials and Methods

Throughout the methods described in this chapter, the storage and use of CW agents was in full compliance with the Chemical Weapons Convention (1986) and animal experiments were conducted in accordance with the Home Office Animals (Scientific Procedures) Act, 1986.

2.1 In vitro coagulation assay: thrombelastography studies of coagulation in swine whole blood and the effect there-upon of haemostatic products

2.1.1 Materials

Seven local haemostatic products were included in the study: Celox™ (CX, Medtrade Products Ltd., Crewe, UK); QuikClot® Advanced Clotting Sponge Plus™ (QC ACS+, Z-Medica Corporation, Wallingford, CT, USA); HemCon™ (HC, HemCon Medical Technologies Inc, Portland, OR, USA); ProQR™ (PQR, Biolife, Sarasota, FL, USA); WoundStat™ (WS, TraumaCure, Bethesda, MD, USA); FastAct™ (FA, Wortham Laboratories Inc., Chattanooga, Tennessee, USA); Vitagel™ (Orthovita, Malvern, PA, USA). S-[2-(diisopropylamino)ethyl]-*O*-ethyl methylphosphonothioate (VX) was purchased from the Defence Science and Technology Laboratory (Dstl, Porton Down, UK) and was reported to be >98% pure by nuclear magnetic resonance (NMR) spectroscopy. Aviation turpentine fuel (AVTUR; referred to as JP8) was kindly supplied by Qinetiq (Boscombe Down, UK). Calcium chloride (0.2M) and polyethylene thrombelastography cups were purchased from Medicell, London, UK.

2.1.2 Methods

Blood sampling was carried out according to an existing Home Office license. Six female large white pigs (*Sus scrofa*) were housed individually for the period of the study (31 days). Blood samples (7.5ml) were taken daily from each animal, following sedation with

midazolam (Hypnoval®, Roche, Hertfordshire, UK) and anaesthesia (3-5% isoflurane in O_2 8 L min^{-1}). Blood was collected in trisodium citrated collection tubes (3.2% citrate; Teklab, County Durham, UK) which were placed on a roller for at least 30 minutes (and not more than 90 minutes) before thrombelastography analysis.

The thrombelastography equipment was prepared by adding 20µl 0.2M $CaCl_2$ (Medicell, London, UK) to polyethylene cups (Medicell, London, UK) and loading them on to the TEG® 5000 Thrombelastograph® Haemostasis Analyzer (TEG; Haemoscope Corporation, Niles, IL, USA). Eight TEG® channels were available and the study was designed such that four test conditions were conducted in duplicate: 1) control; 2) haemostat only; 3) contaminant only (VX or JP8); 4) haemostat and contaminant. These conditions are described below. For the contaminated conditions, 4mls of whole blood were taken from the original collection vial into a fresh plastic vial, and neat VX or neat JP8 was added to a final concentration of 0.5µl ml^{-1} (condition 3; 2µl contaminant to 4mls blood). A sample of the contaminated blood was then removed and added to a separate plastic vial containing pre-weighed test haemostat at the same ratio as the haemostat control (1 ml:4.5mg; condition 4). To mirror treatment of the contaminated samples in the non-contaminated conditions, whole blood was transferred to plastic vials (condition 1), then a sample of that blood was added to another vial containing pre-weighed test haemostats at a ratio of 1 ml:4.5 mg (condition 2). Samples were mixed and applied in 360µl aliquots to the pre-loaded TEG cups.

The time to initial fibrin formation (R; minutes); the time to reach a pre-defined clot strength (K; minutes); the trace angle (indicative of the initial rate of clot formation) and; the maximum clot strength attained (maximum amplitude of pin displacement; mm) were

analysed. Analysis continued for 30 minutes or until the sample trace reached maximum amplitude, whichever was earliest.

Statistical analysis

Statistical analyses were conducted using GraphPad Prism 5.04 (GraphPad Software, Inc.). The data were compared by Kruskal-Wallis tests with Dunn's post-test. Mann-Whitney U-tests were used to compare haemostat performance between contaminated and non-contaminated samples.

2.2 In vitro percutaneous absorption assay to assess the effect of haemostat or decontaminant application on ^{14}C-VX penetration in isolated porcine skin.

2.2.1 Materials

Seven local haemostatic products were included in the study as test decontaminants: these are listed in section 2.1.1. Additionally, a novel mixture of tetraglyme, oxime (2-PAM) and polyethyleneimine (TOP; kindly provided by Dr Richard Gordon, Walter Reid Army Institute of Research, MD, USA) and the currently used decontaminants Fuller's Earth (FE; Sigma Chemical Co., Dorset, UK), Reactive Skin Decontaminant Lotion® (RSDL; E-Z-EM Inc., Canada) and M291 (current US Army decontaminant, kindly supplied by Dr Ed Clarkson, US Army Medical Research Institute of Chemical Defense, Maryland, USA) were included as positive controls. VX (S-[2-(diisopropylamino)ethyl]-*O*-ethyl methylphosphonothioate), and the radiolabelled analogue (^{14}C-VX; Figure 2.1) were custom synthesised by TNO Defense, Security and Safety (Rijswijk, Netherlands). The radiolabelled analogue was mixed with 5g of undiluted agent to provide a stock solution with a nominal activity of ~ 1mCi g^{-1} and stored for up to two months at 4°C. Aliquots of each stock solution were diluted with unlabelled CW agent immediately prior to each experiment to provide a working solution with a nominal activity of ~0.5 µCi $µl^{-1}$. Ultima-Gold Liquid Scintillation Cocktail (LSC) was supplied by Perkin-Elmer and Sigma.

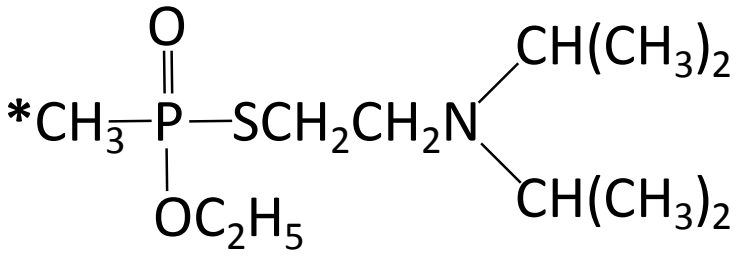

Figure 2.1: Structure of radiolabelled (^{14}C) analogue of VX (^{14}C-VX) utilised for *in vitro* and *in vivo* experiments.

The asterisk indicates the location of the ^{14}C-label.

2.2.2 Methods

1. Intact skin model

Full thickness skin was collected immediately post mortem from male and female pigs (*Sus scrofa*, large white strain, six males, six females, weight range 20 - 30 kg). Thus any cleaning methods used by external suppliers that may have damaged the skin were avoided. Skin samples were stored flat between aluminium foil sheets at -20°C until required. The skin was close clipped and dermatomed (Humeca Model D42, Eurosurgical Ltd, Guildford, UK) to a depth of 500 µm and cut into square sections (approximately 3 x 3 cm) in preparation for mounting into diffusion cells (Figure 2.2). The study was designed such that 6 replicate conditions for up to 5 decontaminants could be examined using a single skin source (Table 2.1) to eliminate inter-individual variation.

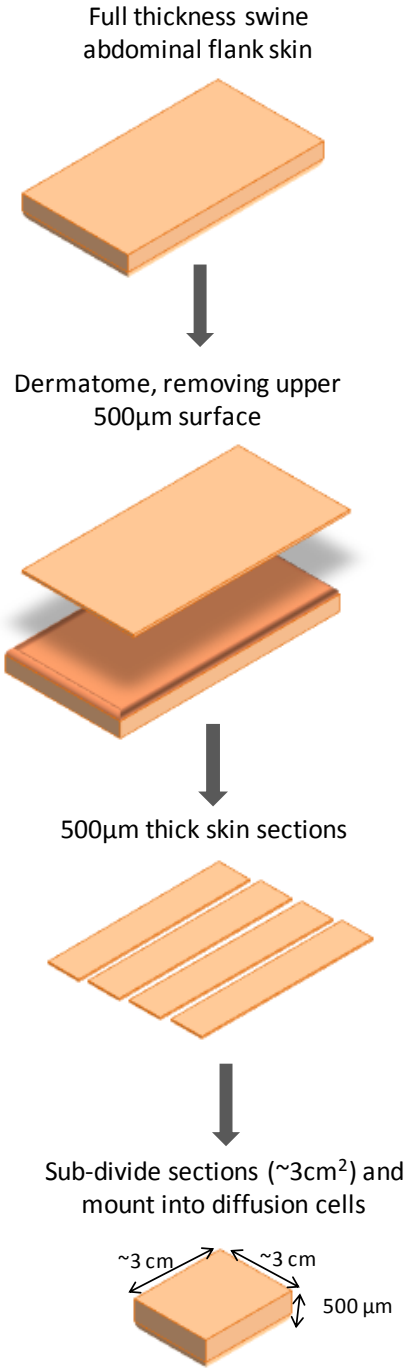

Figure 2.2: The production of intact *ex vivo* skin sections for *in vitro* percutaneous penetration studies.

Full thickness swine abdominal flank skin was obtained, in-house, immediately post-mortem, stored between aluminium foil sheets and frozen (-20°C) until used. Intact skin sections were produced by dermatoming the defrosted full thickness skin to a (nominal) depth of 500µm. The resulting strips of partial-thickness skin were then sub-divided into sections (approximately 3 x 3 cm) which were mounted into diffusion cells.

Cells	Treatment
1-6	Control: VX only
7-12	VX plus test decontaminant 1
13-18	VX plus test decontaminant 2
19-24	VX plus test decontaminant 3
25-30	VX plus test decontaminant 4
31-36	VX plus test decontaminant 5

Table 2.1: Plan of replicated conditions used for the simultaneous assessment of "test decontaminant" performance in isolated porcine skin from a single source.

The prepared skin sections were placed flat between the glass donor and receptor chambers (PermeGear, Chicago, IL., USA) and held in place with a clamp. The surface area of the skin available for exposure within the donor chamber was 1.77cm^2. The receptor chamber was filled with 50% (v/v) ethanol in deionised water solution[1] as the receptor fluid (RF), so that the meniscus in the sampling arm was level with the skin surface. Each cell was placed in a Perspex^{TM} holding apparatus, which comprised a magnetic stirrer to mix the receptor fluid in each individual cell via a Teflon^{TM}-coated iron bar placed within the receptor chamber. The receptor chambers were heated by means of surrounding water supplied by a manifold and a circulating water heater and pump (Model GD120, Grant Instruments, Cambridge, UK). This enabled the skin temperature to be maintained at ~32°C (measured with infrared thermography; FLIR Model P640 camera, Cambridge, UK). Skin integrity was assessed by measuring the resistivity across the skin surface[111], then assembled cells were left to equilibrate for ~16-24 hours.

For the experiment, 10µl ^{14}C-VX was applied to each skin section (5.7mg cm^{-2}). Test decontaminants (200mg or 200µl for liquids and gels) were added 30 seconds after dosing. Each cell condition was replicated 6 times. Samples of the receptor fluid (250µl) were withdrawn periodically and transferred straight into LSC fluid (5mls) for counting. The receptor fluid volume was replenished at each sample timepoint. Samples were collected at baseline, hourly for the first 6 hours in control cells and three hourly for all cells, for up to 24

[1] Ethanol water solution was used as the receptor fluid as opposed to isotonic saline, which is more physiologically relevant and usually used for in vitro percutaneous penetration experiments. A lipophilic receptor fluid assists removal of VX from lower skin layers, and so this deviation is intended to improve dose recovery and avoid underestimation of VX penetration rates[101].

hours. The amount of ^{14}C-VX in each sample was calculated with reference to a series of simultaneously prepared reference samples of known concentration.

2. Damaged skin model

The experimental set-up for the damaged skin model was virtually identical to the intact skin model, except for removal of the top 100µm layer from the skin by dermatome (Figure 2.3). The 400µm layer below was then removed and mounted into the diffusion cells, and the experiment conducted as described above.

Figure 2.3: The production of damaged ex vivo skin sections for *in vitro* percutaneous penetration studies.

Full thickness swine abdominal flank skin was obtained, in-house, immediately post-mortem, stored between aluminium foil sheets and frozen (-20°C) until used. Superficially damaged skin sections were produced by initially removing the upper 100 µm layer from the original full thickness skin (by dermatome), then removing the underlying layer to a (nominal) depth of 400 µm. The resulting strips of partial-thickness skin were then sub-divided into sections (approximately 3 x 3 cm) which were mounted into diffusion cells.

3. Quantification of radiolabel penetration and recovery

After 24 hours exposure, the diffusion cells were dismantled; the dosing chamber was removed and swabbed; the decontaminant (where applied) was collected and the skin section was placed into a glass scintillation vial. The skin sections were incubated in 20mls Soluene-350 until homogenised. The collected decontaminant and swabs were incubated in 100% IPA to extract any residual ^{14}C-VX: combined these extracts made up the "not penetrated" fraction. Samples of each extract (250µl) were diluted in 5mls LSC and counted in triplicate by a scintillation counter (Perkin Elmer). The mass of ^{14}C-VX in each compartment was calculated with reference to a series of simultaneously prepared reference samples (of skin, swabs and decontaminant) of known concentration.

4. Statistical analysis

Statistical analyses were conducted using GraphPad Prism 5.04 (GraphPad Software, Inc.). Experimental conditions were compared to control conditions using one-way ANOVA with Bonferroni post-test.

2.3 Decontamination of damaged ear skin of swine *in vivo*

2.3.1 Materials

Chemicals and reagents were obtained from Sigma unless otherwise stated. Test product (WoundStat™) was purchased from TraumaCure, Inc. (Bethesda, MD). The chemical warfare (CW) agent VX (S-[2-(diisopropylamino)ethyl]-*O*-ethyl methylphosphonothioate) and the corresponding ^{14}C-radiolabelled analogue (shown in Figure 2.1) were custom synthesised by TNO Defense, Security and Safety (Rijswijk, Netherlands). Both were reported to be >98% pure on synthesis. Following delivery, the radiolabelled CW agent was mixed with unlabelled agent to provide a working solution with a nominal activity of ~4 mCi g^{-1} and stored for up to three months at 4°C. Pharmaceuticals (Alfaxan® and Dolethal®) were obtained from Vétoquinol, Buckingham, UK). Ultima-Gold Liquid Scintillation Cocktail (LSC) and Soluene-350 were obtained from Sigma and Perkin Elmer (Buckinghamshire, UK).

2.3.2 Methods

The study was conducted in two cohorts. Radiometric analysis and gene expression analysis were conducted on cohort 2 animals only (Table 2.2). The animals in each cohort were divided into a positive control group and an experimental group. One group of seven animals served as a negative control group for both cohorts.

Group	Label	Number	Description
Negative control	Control	7	Undamaged skin, saline application to ear
Positive control	DXD_1	6	Damaged skin, radiolabelled VX application to ear, no decontamination, (cohort 1/2)
	DXD_2	6	
Experimental	DD_1	6	Damaged skin, radiolabelled VX application to ear, WoundStat application to ear 30s later, (cohort 1/2)
	DD_2	6	

Table 2.2: Description of the experimental groups included for analysis of decontamination of ^{14}C-VX applied to damaged ear skin of swine.

1. Animals, preparation and surgery

Female pigs (*Sus scrofa*, Yorkshire landrace cross, weight range 15-25kg) were habituated for a minimum of 7 days with food and water *ad libitum*. On the day of each experiment (and following an overnight fast) animals were placed into a weighing crate and sedated with a small dose of midazolam (4-8mls, 2mgml^{-1}: 8-16mg, dependant on animal size and activity; Hypnoval, Roche). Anaesthesia was induced in the weighing crate with 2-3% isoflurane in air with oxygen (6L min^{-1}) and nitrous oxide (2L min^{-1}) delivered via a facemask. For surgery, the animal was placed on a surgical trolley in dorsal recumbency and intubated to maintain the airway and administer inhalation anaesthesia (0.5-2% isoflurane in air with oxygen) throughout surgery. Surgery involved isolation and cannulation of the internal carotid artery and internal jugular vein (occasionally external jugular vein) to gain intravascular access, measure arterial pressure and administer intravenous anaesthesia using alfaxalone (Alfaxan®, Vétoquinol, Buckingham, UK) for the remainder of the study (rate between 12-28ml hr^{-1}, dependent on individual animal response).

Pulse rate, ECG, arterial blood pressure, breathing rate, CO_2 output, % SpO_2 were monitored throughout the experiment (Propaq Encore® monitor, Welch Allyn, Bucks, UK). Core body temperature was monitored using rectal probes, and maintained where necessary with a heated blanket or blankets. After a 30 minute stabilisation period, the animal was transferred to a trolley in ventral recumbency using a sling. The animal was moved to the fume cupboard and remained there throughout the study. All dosing and decontamination procedures took place within the fume cupboard.

Blood samples were taken just prior to commencement of Alfaxan® administration, then periodically throughout the experiment. Blood samples were collected in sodium citrated vials for radiometric and thrombelastographic analysis, and sodium EDTA vials (Teklab, County Durham, UK) for measurement of haematocrit and whole blood cholinesterase activity.

2. Wound

During the 30 minutes stabilisation period and 30 minutes pre-dosage baseline period a small area (~3cm^2 maximum) superficial wound was produced on the back surface of the ear using a dermatome to a depth of 100µm. This produced a small region of damage with localised punctate bleeding. The end of a 20ml plastic syringe barrel was secured to the ear surface around the wound with Vetbond to form a dosing chamber. The seal was checked using saline, which was also used to wipe or swab the wound to prevent any blood solidifying and creating a barrier to absorption. The ear was maintained as flat and as immobile as possible with minimal occlusion using cotton-wool covered cardboard as a flat platform scaffold underneath the ear. Autoclave tape was used to connect the dosing chamber to the cardboard, then the cardboard scaffold was clamped to the trolley arms.

3. Dosage/Exposure

Following the 30 minute pre-dosage baseline period, a 5x LD_{50} (300µg kg^{-1}) dose of neat, radiolabelled VX (^{14}C-VX; TNO, NL and Dstl, Wiltshire, UK) was applied to the wound site. In the decontamination group (DD, n=12), 2g of test haemostatic decontaminant

(WoundStat™, TraumaCure, Bethesda, USA) was poured into the dosing chamber 30 seconds after dosing, and compressed lightly using a syringe plunger. The wound and dosing site were not manipulated or occluded in any other way in the positive control group (DXD, n=12). Negative control animals (n=7) were given an equivalent volume dose of sterile isotonic saline onto undamaged skin.

Physiological parameters and signs of intoxication were monitored throughout the experiment by Propaq Encore® monitor (Welch Allyn, Buckinghamshire, UK). Death within the 6 hour study period was confirmed following 15 minutes of apnoea. At the end of the experiment (time of death or 6 hours for those animals which survived the entire study period) all animals were euthanised using an overdose of pentobarbital (Dolethal®, Vétoquinol, Buckingham, UK).

Blood was removed as thoroughly as possible using a medical suction pump and disposable liners prior to post mortem examinations. Sections of brain, heart, lung, liver, kidney, pancreas, spleen and diaphragm were removed post mortem and stored for further analysis (radiometry, cholinesterase activity, RNA expression).

4. Analysis of acetylcholinesterase activity

Cholinesterase activity was assayed in whole blood samples. Whole blood samples were stored at -20°C for at least half an hour to lyse the blood cells. Cholinesterase activity was measured using a modified Ellman assay[34,54,112,113]; (0.25mM 5,5-dithiobis-(2 nitrobenzoic) acid (DTNB); 0.45mM acetylthiocholine iodide substrate; 1.0M pH 8 phosphate buffer) and carried out at 30°C 412nm using a spectrophotometer.

5. Toxicokinetic analysis

After termination of the experiment, the area of exposed skin was excised and incubated in Soluene-350 (Perkin Elmer, Bucks, UK). A Geiger-Muller tube was used to direct excision of contaminated areas in the vicinity of the exposure site. These were collected into separate scintillation vials and treated equivalently. The decontaminant was collected and incubated in Ultima Gold liquid scintillation cocktail (LSC, Perkin Elmer and Sigma). The dose chambers were also incubated in LSC and swabs were incubated in 100% isopropanol. Samples of each extract (250µl) were diluted in 5mls LSC and counted in triplicate by a scintillation counter (Perkin Elmer). Radiolabel extracted from the dosing chamber, decontaminant and swabs made up the "not penetrated" fraction.

For analysis of radiolabel distribution in internal organs, 100mg of frozen tissue was incubated in 2mls Soluene-350 at 60°C for at least 6 hours (until dissolved, with gentle vortexing if necessary), then once cooled, the volume made up to 20mls with LSC fluid for scintillation counting. For radiometric analysis of blood samples, 0.4mls whole blood were incubated in 1ml of a 2:1 IPA:Soluene-350 solution at 60°C for 2 hours. Once cooled to room temperature, 500µl of 30% H_2O_2 was added slowly (50µl at a time) and gently mixed for approximately 5 minutes, until any foaming ceased. The mixture was incubated at room temperature for 15-30 minutes; then 60°C for 30 minutes. LSC was added to 20mls volume once the mixture was cooled. All extractions were temperature and light adapted for at least 1 hour prior to scintillation counting.

The mass of ^{14}C-VX in each compartment was calculated with reference to a series of simultaneously prepared reference samples (of each organ, blood, skin, swabs and decontaminant) of known concentration.

6. Statistical analysis

Statistical analyses were conducted using GraphPad Prism 5.04 (GraphPad Software, Inc.). Survival fractions and curve analysis were calculated using the Kaplan-Meier (log-rank) method, and Gehan-Brislow-Wilcoxon tests. One-way ANOVA with post-hoc Tukey's test was used to analyse animal weight and survival time. Toxicokinetics were usually analysed using one-tailed unpaired t-tests with Welch correction for unequal variances; except for recovery data for swabs, dosing chambers and spleen which were two-tailed unpaired t-tests with Welch correction.

2.4 Analysis of gene expression changes in blood following exposure of swine to ^{14}C-VX

This study utilised whole blood samples obtained from swine exposed to a 5xLD_{50} dose of ^{14}C-VX to damaged ear skin. A test decontaminant was also subsequently applied to experimental subjects. The methods of exposure, analysis, acquisition of blood samples and experimental protocol are described in the previous section; the results are presented in Chapter 5. An aliquot of pre-dose and final blood samples were stored in RNALater® solution (Ambion, CA, USA) at -20°C until required. Methods for analysis of gene expression in these subjects is described below.

2.4.1 Materials

Whole blood RNA extraction was performed using RNALater® and the Ambion RiboPure™ Blood RNA Isolation kit (Ambion®, CA, USA). Agilent RNA Nano 6000 chips and Porcine Gene Expression Microarray 4x44K slides, gaskets and reagents for labelling, amplification, hybridisation and washing were purchased directly from Agilent Technologies Inc. (Berkshire, UK). Labelling, amplification, hybridisation and washes were conducted according to the Agilent Low Input Quick Amp Labelling Protocol.

2.4.2 Methods

Porcine whole blood samples, obtained from a concurrent study of dermal decontamination of VX, were stored in RNALater® solution. Gene expression analysis was performed on RNA extracted from the pre-dose and final (time of death or 360 minutes exposure) blood samples from the 12 animals in cohort 2: 6 decontaminated with WoundStat and 6 with no decontamination. The final blood samples were obtained prior to administration of Dolethal®.

RNA extraction

RNA extraction from whole blood was performed using the RiboPure™ Blood kit (Ambion) according to the manufacturer's instructions except with the following adjustments. Briefly, cells (or whole blood) preserved in RNALater® were thawed and centrifuged at 16000 x g at 4°C. The pellet was re-suspended in Ambion Lysis® solution and sodium acetate by vigorous vortexing. After addition of acid phenol:chloroform the samples were inverted briefly and incubated at room temperature for 5 minutes, then centrifuged at room temperature at 16000 x g for 5 minutes. One half volume of 100% ethanol was added, then the samples were placed at -20°C for 1 hour (up to overnight). The subsequent purification steps were carried out according to the manufacturer's protocol, except for one extra wash with Wash 2/3 buffer. The RNA was eluted with 2 x 50µl of elution buffer. The concentration of RNA was measured using Nanodrop, and the quality of the extracted RNA assessed using the Agilent 2100 Bioanalyzer equipment and Agilent RNA Nano 6000 chips. The labelling, amplification, hybridisation and post-hybridisation wash steps were carried out according to

the manufacturer's instructions[114]. The labelling and amplification steps were performed using 200ng of RNA template.

Hybridised and washed microarray slides were scanned by an Agilent High-Resolution C Scanner, and data extracted using Agilent Feature Extraction software (version 11). Data analysis was conducted using Agilent GeneSpring GX software (version 12).

The pre-dose samples were used as intrinsic controls for normalisation purposes: intensity values of the final samples were normalised to the corresponding pre-dose samples. Following normalisation and filtering on flags (detected in 100% of all conditions) 10,110 probes were included in the subsequent data analysis. Initially, the basic interpretations applied were "Treatment" (decontamination, "DD", and not-decontaminated, "DXD") and "Timepoint" (pre-dose, "start", and final, "end"). Following analysis of the preceding *in vivo* data (Chapter 5), a third interpretation, "Outcome" ("survivor" or "death"), was subsequently included. Thus paired t-tests (without any false discovery rate limits set) were performed between:

- pre-dose and final blood samples in the decontaminated and not-decontaminated groups;
- pre-dose and final blood samples in the survivor or death groups;
- pre-dose and final blood samples in the survivors of the decontaminated or not-decontaminated groups;
- pre-dose and final blood samples in the deaths of the decontaminated or not decontaminated groups.

In the statistical analyses, a paired t-test between the pre-dose and final blood sample in the "survivor" group was the only comparison which returned entities (n=1730) with a Benjamini-Hochberg FDR correction. For consistency, all the statistical analyses were performed without multiple testing or false discovery rate correction. For t-tests between treatment or outcome groups, Welch's correction for unequal variances resulted in a more conservative entity list, so was employed for all comparisons. Paired t-tests were performed for comparisons between pre-dose and final blood samples.

CHAPTER 3. Thrombelastographic assessment of haemostatic products, and blood contamination with VX.

Chapter 3. Thrombelastographic assessment of haemostatic products, and blood contamination with VX.

3.1 Introduction.

Haemostatic products intended for local application to severely haemorrhaging wounds are available commercially, and a variety of strategies to test their efficacy have been described. The advantages of using *in vitro* methods to assess efficacy of haemostatic products are that: blood samples can be used, allowing experiments to be performed in the relevant species and reducing animal use; potential compounds or products may be assayed for coagulation capabilities prior to in depth *in vivo* experiments, reducing animal use further; *in vitro* assays are relatively high-throughput compared to *in vivo* methods, meaning a number of products may be evaluated simultaneously; conditions may be manipulated, for example the effect of certain conditions, such as presence of a drug, or in this case a contaminant, on blood coagulation may be assayed.

There are not many direct investigations of the effect of nerve agents on haemostasis and coagulation, although there are reports of the effects of organophosphate exposure on blood chemistry and coagulation, both experimentally and in cases of human exposure[93,115–118], however the differences in the compounds and doses examined, and the circumstances surrounding the human exposures, make comparison of the findings of these reports difficult. This study used an *in vitro* assay (Thrombelastography; TEG) to examine the effect of chemical contaminants on blood coagulation and on the efficacy of haemostatic products.

The contaminants used were the nerve agent VX; (S-[2-(diisopropylamino)ethyl]-O-ethyl methylphosphonothioate) and aviation fuel (aviation turpentine; JP8).

3.2 Materials and Methods

The materials and methods are described in detail in Chapter 2 and are briefly outlined in Figure 3.1.

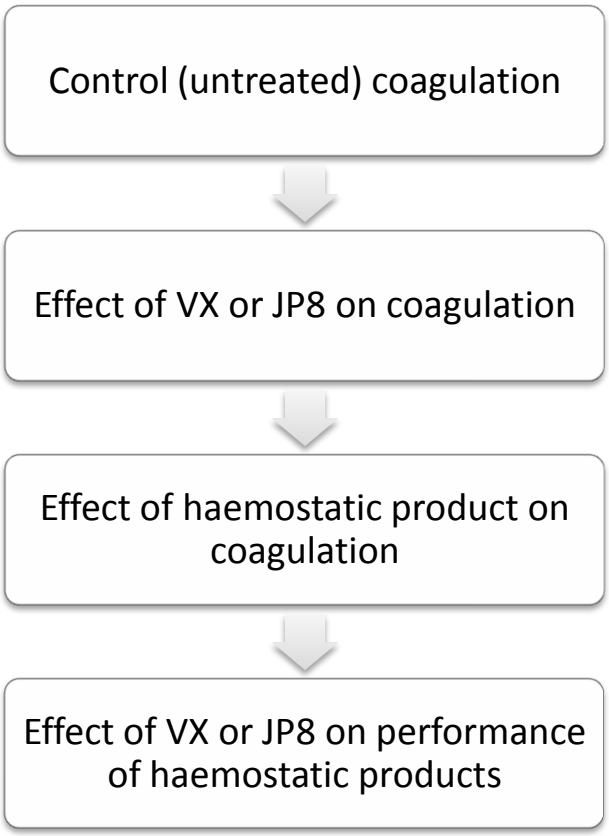

Figure 3.1: Workflow design for the *in vitro* analysis of haemostatic products within and without the presence of contaminants (VX or JP8) using thrombelastography (TEG).

3.3 Results

1. Model validation.

All control data (n=113) for each clotting parameter were pooled and subject to analysis (Shapiro-Wilk normality test) to determine the statistical distribution: R time (RT), K time (KT), angle (α) and maximum amplitude (MA) were not normally distributed ($p<0.05$). Therefore, subsequent analyses were based on non-parametric tests.

There were no significant time-dependent differences in R time, K time, trace angle or maximum amplitude between experimental days (Figures 3.2 and 3.3) as measured with the Friedman repeated measures test.

The weights of the animals were recorded every study day as an indicator of welfare, and increased steadily during the study period (Figure 3.4).

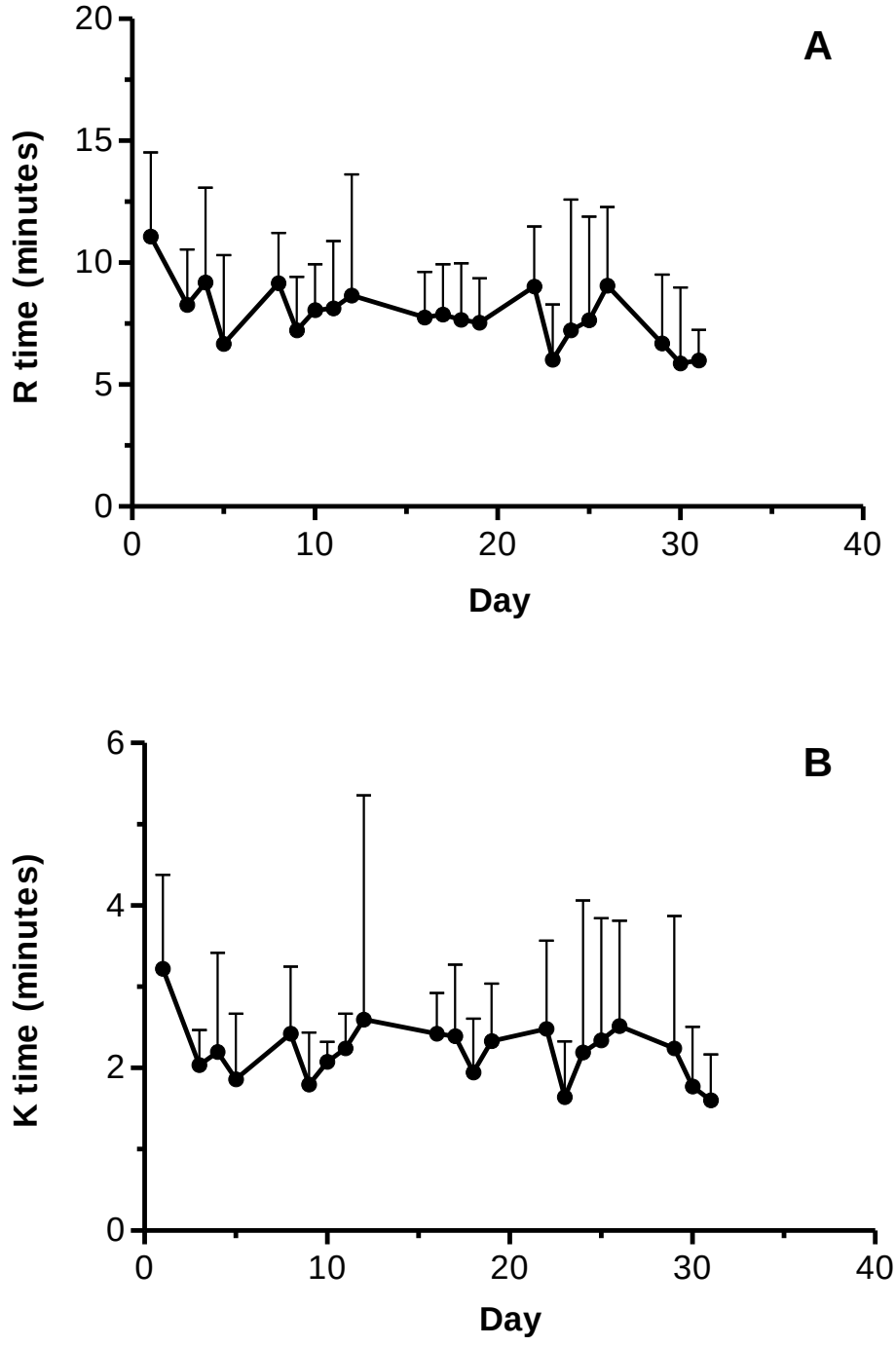

Figure 3.2: Variation in thrombelastography (TEG) clotting parameters R time (A) and K time (B) acquired from control (untreated) samples of normal whole blood acquired over the 31 day study period.

All values are average ± 95% confidence intervals (CI) of up to n=6 samples per time point. There was no significant, time-dependent change in either parameter ($p>0.05$).

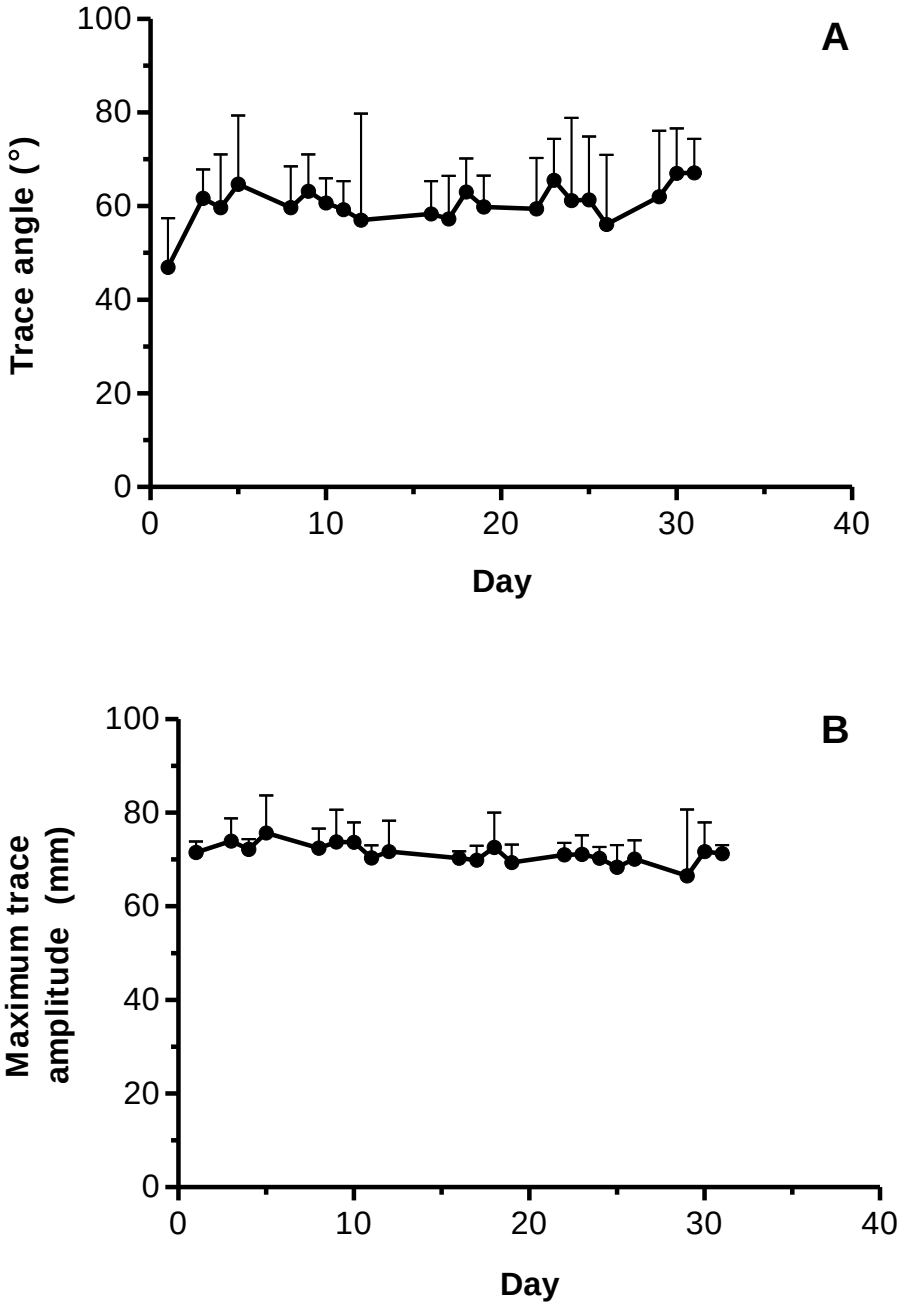

Figure 3.3: Variation in thrombelastography (TEG) clotting parameters trace angle (A) and maximum amplitude (B) acquired from control (untreated) samples of normal whole blood acquired over the 31 day study period.

All values are average ± 95% confidence intervals (CI) of up to n=6 samples per time point. There was no significant, time-dependent change in either parameter ($p>0.05$).

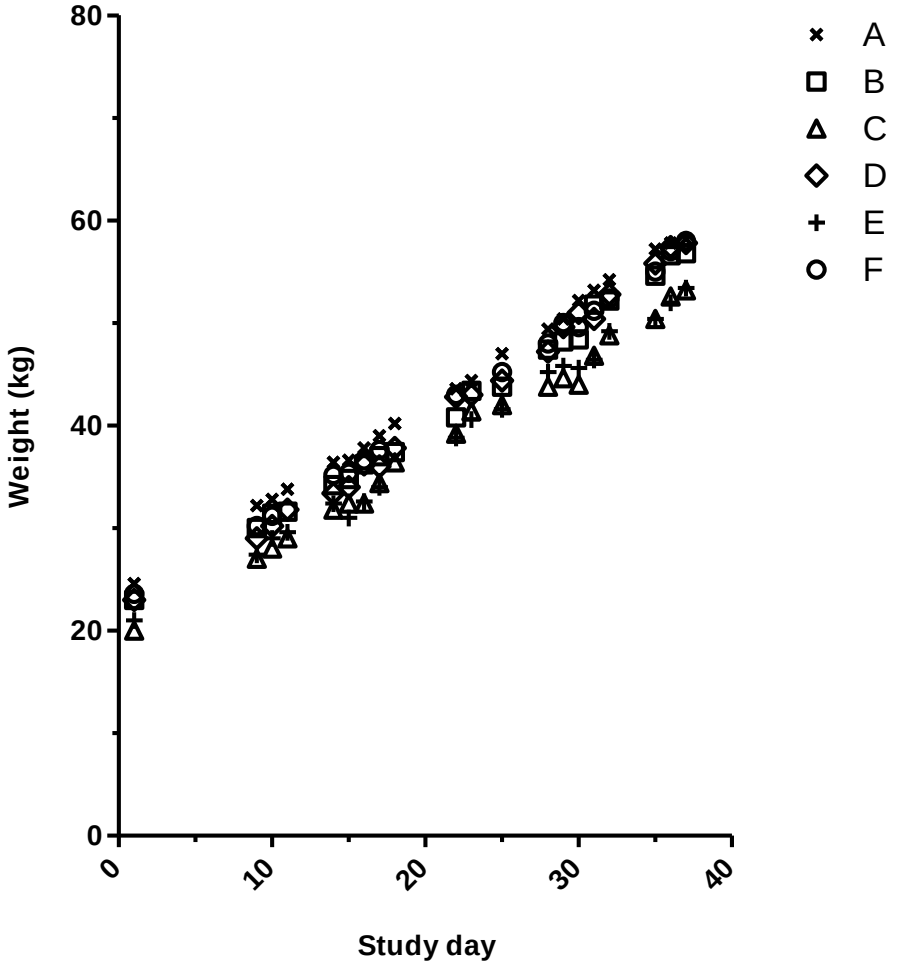

Figure 3.4: Individual plots of weight increase during the study period for all 6 animals (labelled A-F).

2. Effects of contaminants on blood clotting.

The addition of contaminants (VX or JP8) had no measurable effect on R time, K time, trace angle or maximum amplitude (Figure 3.5).

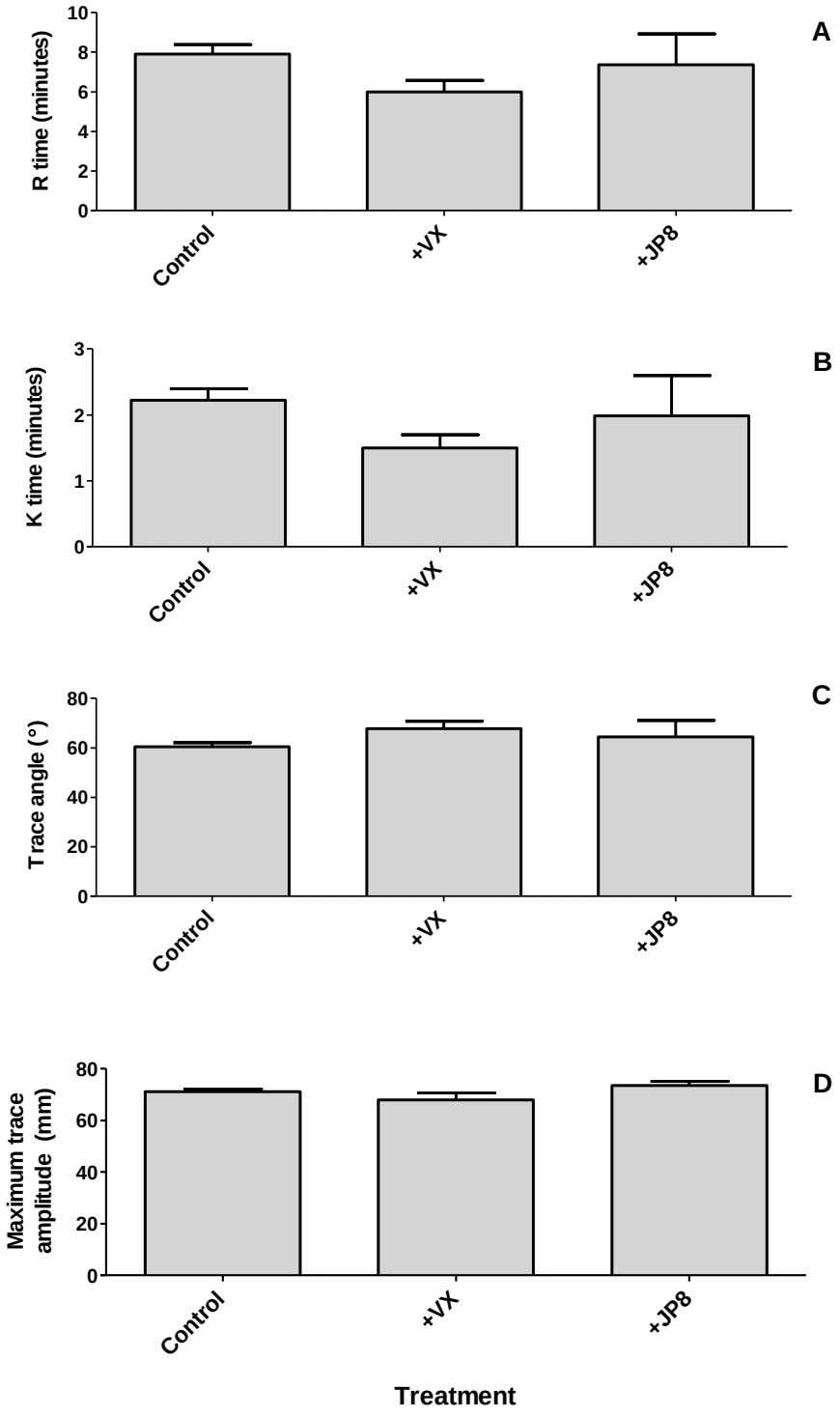

Figure 3.5: Effect of contamination with VX or JP8 on thrombelastography (TEG) clotting parameters of whole blood: clotting time (R time, A); initial clot formation time (K time, B); rate of clotting (trace angle, C); or clot strength (maximum amplitude, D).

All values are average ± 95% confidence intervals (CI) of n=113 (control), n=25 (+VX) or n=15 (+JP8) samples. There was no significant effect of contamination on blood clotting ($p>0.05$).

3. Effects of haemostatic products on blood clotting.

Treatment of whole blood with four haemostatic products (WoundStat™ (WS), FastAct™ (FA), ProQR™ (PQR) and VitaGel™ (VG)) resulted in a significant decrease ($p<0.05$) in clotting time (expressed as the R time parameter; Figure 3.6A) when compared to control (untreated) blood. In contrast, three treatments (Celox™, HemCon™ and QuikClot™) did not significantly affect R time. Correspondingly, there was a significant ($p<0.05$) reduction in K time (Figure 3.6B) and significant increase in trace angle (α; Figure 3.6C) for WS, FA, PQR and VG but no change in K time and α for CX, HC or QC ($p>0.05$). Addition of haemostatic products to whole blood resulted in no significant change in clot strength (maximum amplitude; Figure 3.6D).

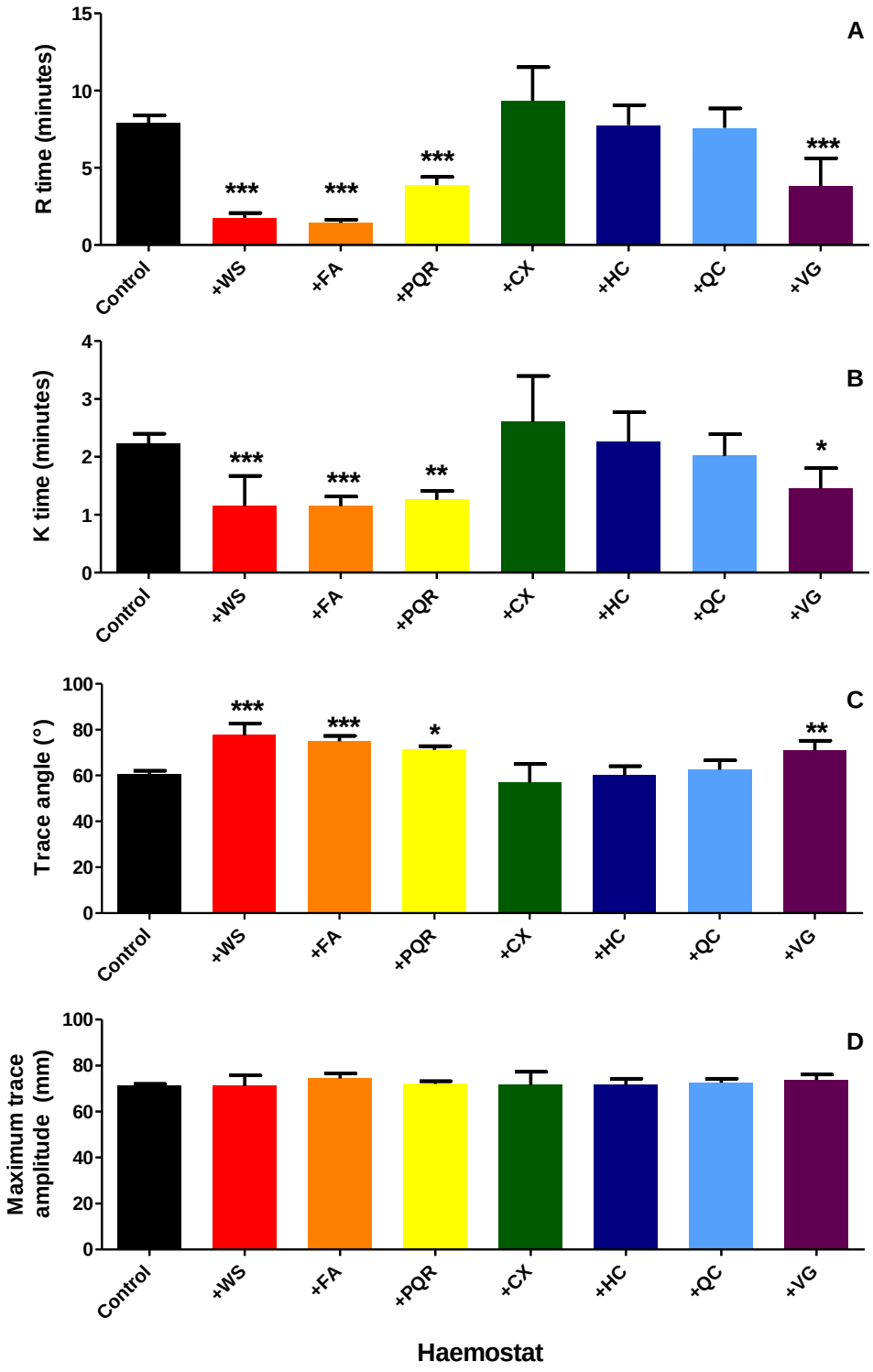

Figure 3.6: Effect of haemostatic products on R time (A); K time (B); angle (C); and maximum amplitude (D).

All values are average ± 95% confidence intervals (CI) of n=9 (CX, HC); 18 (QC, VG); 19 (PQR); 20 (FA). Asterisks indicate that value is significantly different to (untreated) control (***p<0.001; ** p<0.01; *p<0.05; Kruskal-Wallis with Dunn's post-test).

4. Efficacy of haemostatic products on blood clotting in the presence of contaminants (VX and JP8).

There were no significant differences in the measured parameters between haemostat plus contaminated blood samples and their haemostat only treated counterparts (Mann-Whitney U-tests; Figures 3.7-3.8).

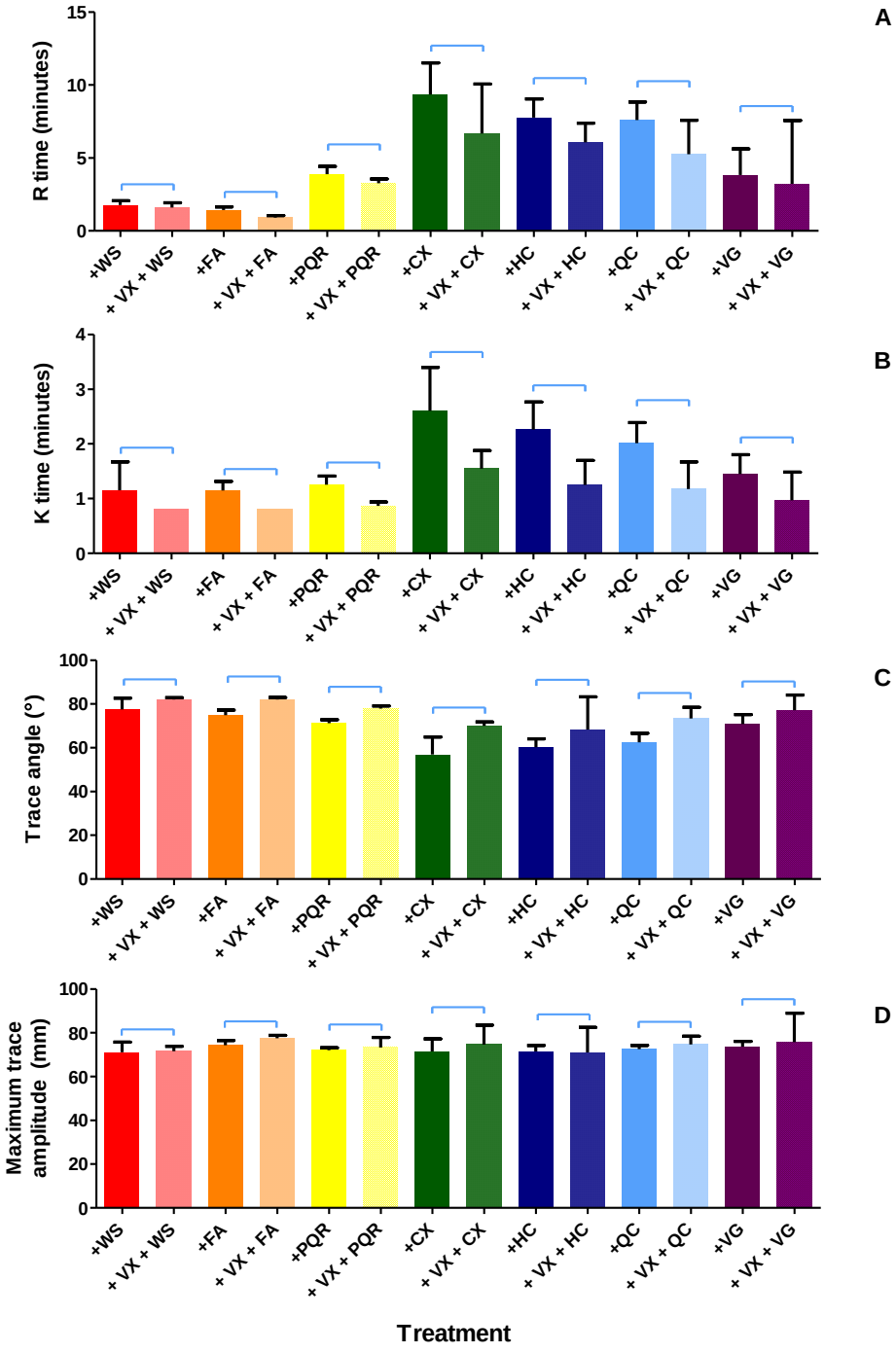

Figure 3.7: Effect of VX on the efficacy of haemostatic products, expressed as R time (A); K time (B); angle (C); and maximum amplitude (D).

All values are average ± 95% confidence intervals (CI) of up to n=6 measurements for the haemostat + contaminant condition, and up to n=20 (as Figure 3.6) for the haemostat alone condition. Efficacy of each haemostatic product was not significantly affected in the presence of VX (Mann-Whitney U-test; $p>0.05$; compared groups indicated by bars).

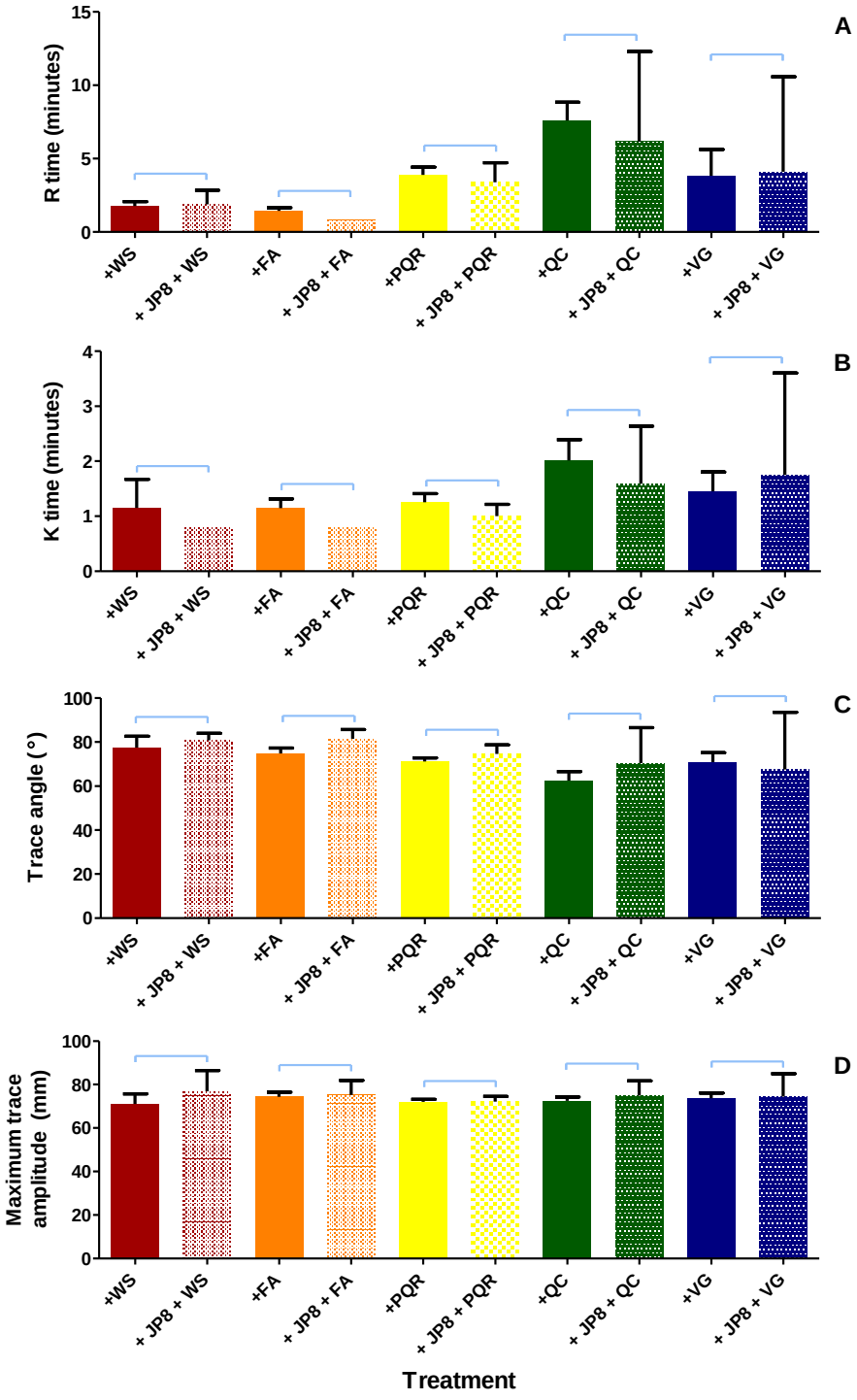

Figure 3.8: Effect of JP8 on the efficacy of haemostatic products expressed as R time (A); K time (B); angle (C); and maximum amplitude (D).

All values are average ± 95% confidence intervals (CI) of up to n=4 measurements for the haemostat + contaminant condition, and up to n=20 (as Figure 3.6) for the haemostat alone condition. Efficacy of each haemostatic product was not significantly affected in the presence of JP8 (Mann-Whitney U-test; $p>0.05$; compared groups indicated by bars).

3.4 Discussion

This *in vitro* study of coagulation has successfully demonstrated the feasibility of acquiring serial, daily blood samples from a small number of animals in order to assess seven haemostatic products by thrombelastography (TEG) and the influence of two contaminants (VX and JP8). The coagulation parameters of untreated (control) blood measured over a one month study period were shown to be reproducible and followed a non-Gaussian distribution. Four haemostatic products (WoundStat™, ProQR™, FastAct™ and Vitagel™) had a pro-coagulative effect on the parameters recorded in this study compared to control (untreated) samples, which were not affected by contamination of blood with VX or JP8. Three haemostats (Celox™, HemCon™ and QuikClot® Advanced Clotting Sponge Plus™) had no measurable effect on the coagulation parameters. Moreover, it was shown that the two contaminants did not adversely affect normal coagulation kinetics or the performance of any of the seven commercially-available haemostatic products tested. The use of TEG substantially reduced the number of animals that would be required to perform a similarly comprehensive study *in vivo* and so represents a significant contribution to the "three Rs"[119,120].

Human blood would be the "gold-standard" for the *in vitro* assessment of haemostatic products. However, human blood was unavailable for this study. Haemostatic products have been evaluated extensively in numerous pig models[5], and two previous studies have provided some limited comparative data between *in vivo* and *in vitro* measurements of haemostatic products using TEG[24,121]. Therefore, pig blood was chosen for this current *in vitro* study. There are no previous studies reporting differences in coagulation between

human and pig blood. However, data collated from untreated (control) blood in this study compare favourably with published human reference range values (Figure 3.9)[122]. Clearly, gathering evidence to further define reference ranges of coagulation parameters for relevant animal models would assist future comparisons between animal and human data.

There are several potential disadvantages of using TEG to evaluate the performance of haemostatic products. Specifically, the *in vitro* (TEG) model may not account for haemostasis caused by the "tamponade" effect or blood vessel sealing [24,121]. Indeed, three products (QC, HC and CX) did not demonstrate any pro-coagulatory effect when evaluated by TEG (Figure 3.6) despite being reportedly efficacious *in vivo*[3,4,8,9,14,17]. Thus, it could be reasonably deduced that the disparity in performance of haemostatic products between the two experimental models is due to the absence of physical factors (e.g. tamponade or wound sealing) in the *in vitro* (TEG) model. Therefore, the use of TEG may actually be advantageous for identifying inherent pro-coagulatory properties of haemostatic products such as passive absorption of plasma or stimulation of the coagulation pathway.

In this *in vitro* study, the addition of QC to whole blood did not enhance clotting kinetics. This was surprising, since the proposed mechanism of QC was via passive absorption of plasma with concomitant concentration of clotting factors[123–125]. In contrast, WS and PQR which are reported to partly act via the same mechanism of passive absorption were very effective[121]. This difference suggests that the *in vivo* clotting mechanism for QC may be more due to the tamponade effect than absorption of blood plasma.

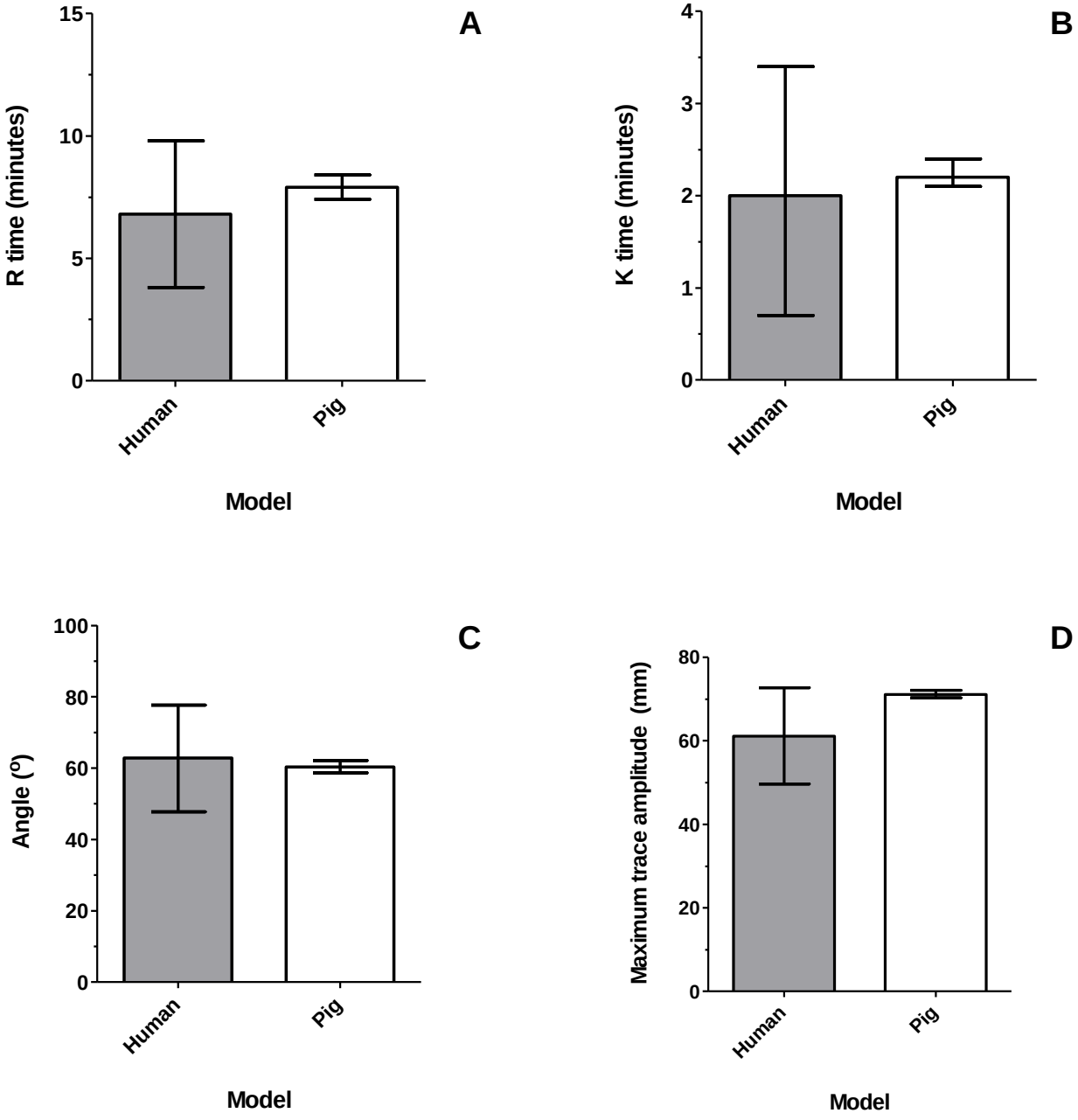

Figure 3.9: Reference range blood coagulation values (mean ± 95% confidence interval) from 118 healthy adult human volunteers[122], and corresponding pig values derived from this current study.

The parameters R time (A), K time (B), angle (C) and maximum amplitude (D) are in close agreement with the human reference range.

Stimulation of coagulatory pathways is the proposed mechanism of action for VG and FA [3,126]. Correspondingly, TEG identified that clotting kinetics were significantly enhanced in the presence of both products (Figure 3.5).

The effectiveness of these products as a function of dose was not investigated in this study: a set dose of 4.5 mg of test product was added to 1 ml of whole blood (4.5 mg ml^{-1}). *In vivo* studies of haemostatic products generally use much higher ratios of product to blood to more accurately model "in use" (emergency) conditions[7]. Therefore, this difference in dose may also account for some of the disparities observed in this *in vitro* study compared to *in vivo* investigations. However, the relatively low dose employed in this *in vitro* study was consistent with that from a previous study and provides a more challenging condition for the evaluation of haemostatic products and so would likely identify products of marginal efficacy. Further investigations of the effectiveness of products as a function of dose would assist both pre-clinical product development and evaluation of product efficacy "in-the-field".

Thrombelastography detected no significant effects of VX on coagulation parameters compared to untreated blood. This is in agreement with a previous study using the nerve agent soman, where no major effects of coagulation were noted[118]. There are no previous reports on the effects of JP8 on blood coagulation kinetics. In this study, treatment of blood with JP8 resulted in no measureable effect.

The lowest intra-venous dose for which a toxic response has been observed (TDLO) in humans is 1.5 µg kg^{-1} [28]. This equates to 0.1 mg for an average adult. The dose of VX applied to the blood in this study (~2 mg) is equivalent to ~20 x TDLO. This dose was intended to represent "worst-case scenario". At this relatively high dose, neither VX nor JP8 had a measureable effect on the clotting efficacy of the haemostatic products. The retention of haemostatic capability in the presence of such a high concentration of VX (or JP8) therefore justified further investigation of these products as haemostatic decontaminants. Even so, possible dose-response effects would be an important consideration for future investigations of the effects of contaminants on coagulation kinetics.In summary, the results of this *in vitro* study using TEG analysis of blood coagulation have demonstrated:

- The feasibility of acquiring serial blood samples from a relatively small number of animals for analysis of blood coagulation kinetics and has provided further evidence in support of validating this model.
- That thrombelastography (TEG) may be utilised for the relatively high throughput evaluation of haemostatic products which are not dependent on physical mechanisms of action such as tamponade effect or spontaneous blood vessel sealing.
- That four products (WS, PQR, FA and VG) have demonstrable haemostatic properties which are retained in the presence of potentially toxic contaminants such as VX and JP8.

Therefore, the haemostatic products were advanced for further assessment as topical skin decontaminants (Chapter 4) as part of the overall aims of identifying a haemostatic decontaminant for haemorrhaging wounds contaminated with potentially toxic chemicals.

This study has identified the need for further work in the following areas:

- Direct comparison of pig and human coagulation kinetics to further contribute to *in vitro* model validation.
- Development of a definitive reference range for pig blood coagulation kinetics.
- Effect of haemostatic product “dose” on coagulation performance.
- Dose-response effect of contaminants such as VX and JP8.

CHAPTER 4. *In vitro* percutaneous absorption assay to assess the effect of haemostat or decontaminant application on VX penetration in isolated porcine skin

Chapter 4. *In vitro* percutaneous absorption assay to assess the effect of haemostat or decontaminant application on VX penetration in isolated porcine skin

4.1 Introduction

The physicochemical characteristics of VX (namely lipophilicity and volatility) relative to other organophosphate chemical warfare agents (CWAs) means that the primary hazard from VX is dermal exposure to the liquid. Swift decontamination of exposed sites is a priority for first responders. In a penetrating injury or haemorrhage the integrity of the skin and the ability of the skin to function as a barrier to contaminants would be compromised. A haemostatic decontaminant must therefore be capable of reducing or preventing penetration of contaminants at the injury site.

The uppermost layer of the skin surface, the *stratum corneum*, is regarded as the primary barrier for dermal absorption[83,127]. *In vivo* models have been used previously to study absorption and toxicity of nerve agents, however differences in physiology and biochemistry between animal models and humans must be accounted for in interpretations. *In vitro* experiments allow preliminary investigations of decontamination properties of potential formulations. These may generally be higher throughput than *in vivo* studies and reduce the numbers of animals required.

This study used *in vitro* diffusion cells to assess penetration of VX across intact and damaged pig abdominal skin. Test decontaminants, including "commercial off-the-shelf" (COTS) haemostats, novel decontaminant liquids and currently deployed decontaminant

formulations, were assessed on their ability to reduce penetration of VX across damaged and undamaged pig skin *in vitro*.

4.2 Materials and Methods

The materials and methods are described in detail in Chapter 2 and are briefly outlined in Figure 4.1. The results presented are the averages of six replications of each condition.

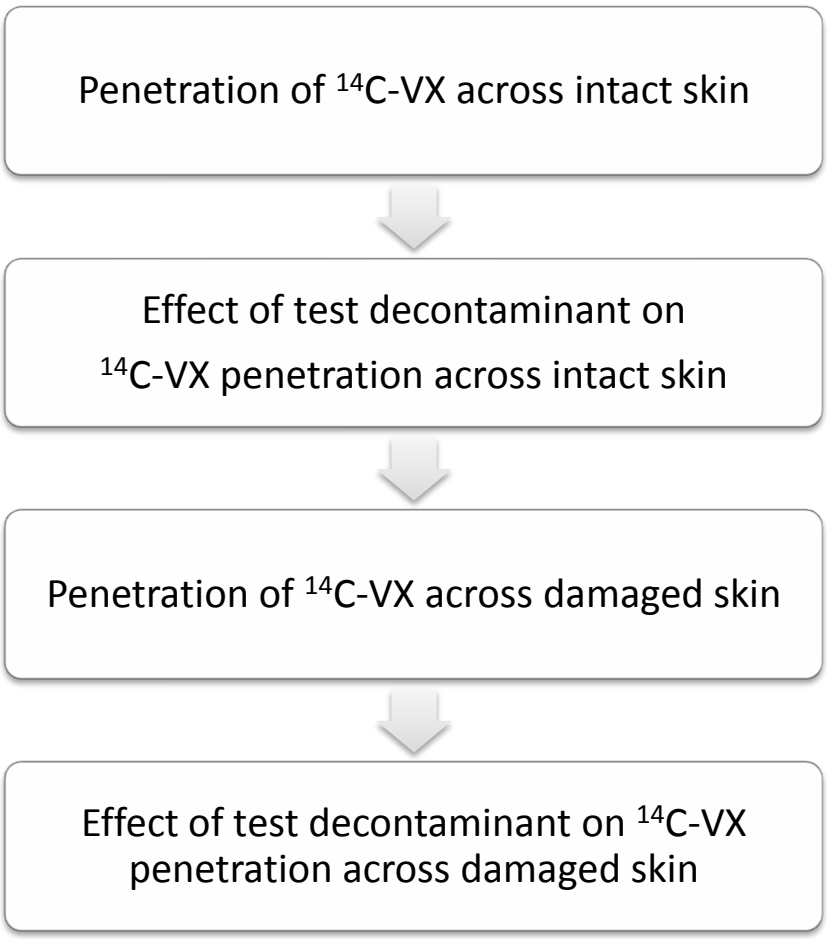

Figure 4.1: Workflow design for the *in vitro* analysis of the efficacy of haemostatic products (as test decontaminants) in reducing penetration of ^{14}C-VX across intact and damaged pig abdominal skin, using Franz-type diffusion cells.

4.3 Results

Pooled control data (undamaged skin; n=24) were normally distributed (Shapiro-Wilk normality test). Subsequent analyses were based on parametric tests.

4.3.1 Effect of application of QuikClot™, WoundStat™, Celox™, ProQR™ or Fuller's Earth on penetration of ^{14}C-VX across intact pig skin over 24 hours

1. Quantification of ^{14}C-VX in receptor fluid at 3 hourly intervals (µg cm^{-2})

Total ^{14}C-VX penetration at 24 hours (µg cm^{-2}) was significantly lower for diffusion cells treated with QuikClot™ (QC), WoundStat™ (WS), Celox™ (CX), ProQR™ (PQR) or Fuller's Earth (FE) compared to control cells ($p<0.0001$; Figure 4.2). The amount of ^{14}C which had penetrated into the receptor fluid (RF) of WS or FE-treated intact skin was significantly lower than that of controls from 3 hours onwards ($p<0.01$). Significantly lower amounts of ^{14}C-VX had penetrated across PQR-treated skin compared to that of controls from 6 hours onwards ($p<0.05$), and QC or CX-treated cells had significantly lower penetrated amounts of ^{14}C-VX than control cells from 9 hours onwards ($p<0.01$).

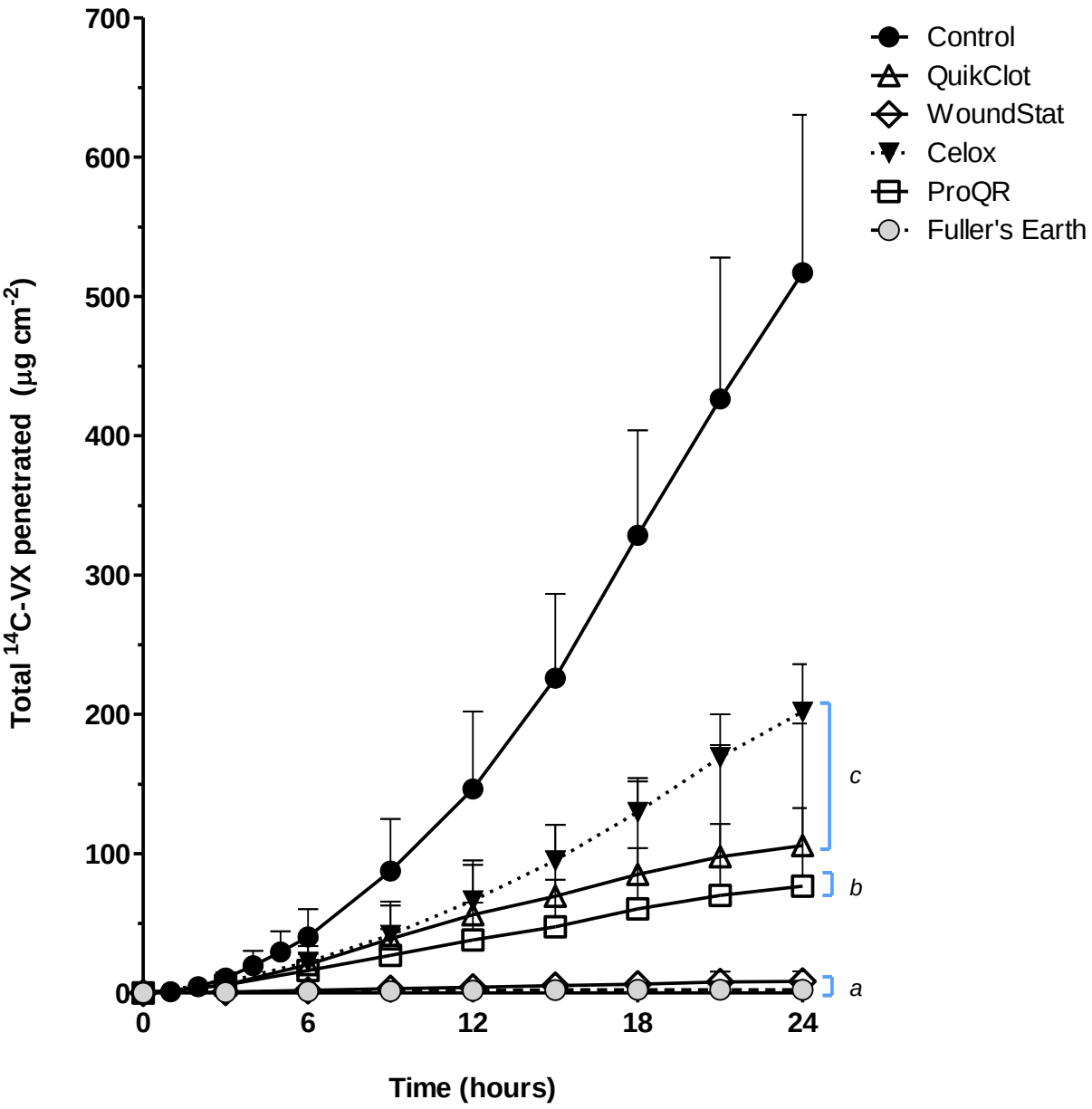

Figure 4.2: Penetration of ^{14}C-VX across intact pig skin over 24 hours in the first group, measured in the receptor fluid at 3 hour intervals and quantified as µg cm^{-2} (mean ± standard deviation; n=6).

Total ^{14}C-VX penetration at 24 hours (µg cm^{-2}) was significantly lower for diffusion cells treated with QC, WS, CX, PQR or FE compared to controls ($p<0.0001$). Bars indicate that amount of ^{14}C-VX penetrated was significantly different to control: (a) from 3 hours onwards for WS and FE, $p<0.01$; (b) from 6 hours onwards for PQR, $p<0.05$; (c) from 9 hours onwards for CX and QC, $p<0.01$).

2. Difference in quantification of ^{14}C-VX in receptor fluid at 3 hourly intervals (µg cm^{-2})

Fuller's Earth and WoundStat had significantly lower rates of penetration of ^{14}C-VX throughout the experiment compared to controls ($p<0.01$; Figure 4.3; Table 4.1).

The rate of penetration of ^{14}C-VX through QC-treated skin was significantly lower than controls between 3 and 6 hours exposure ($p<0.05$) and from 15 hours onwards ($p<0.01$). The rate of penetration of ^{14}C-VX through PQR-treated skin was also significantly lower than controls between 3 and 6 hours exposure ($p<0.01$); but then significantly lower than controls from 12 hours onwards ($p<0.01$). Celox-treated cells only had significantly lower penetration rates compared to controls between 3 and 6 hours of exposure ($p<0.05$).

In control cells, the highest rate of penetration of ^{14}C-VX was 34 ± 6.7 µg cm^{-2} hr^{-1} and was reached between 15 and 18 hours of exposure (Table 4.1).

Treatment	Time interval (hours post-exposure)							
	0-3	3-6	6-9	9-12	12-15	15-18	18-21	21-24
	Flux (μg cm^{-2} hr^{-1})							
Control	3.6 ± 2.1	10 ± 4.6	16 ± 6.0	20 ± 7.6	27 ± 7.1	34 ± 6.7	33 ± 11	30 ± 7.7
QuickClot	1.9 ± 1.1	4.9* ± 3.3	13 ± 8.9	19 ± 13	17 ± 13	15*** ± 13	14** ± 14	12*** ± 12
WoundStat	0.25** ± 0.12	0.37**** ± 0.70	1.1*** ± 1.3	1.4** ± 1.6	1.2**** ± 1.0	1.0**** ± 0.86	1.3**** ± 0.88	1.0**** ± 0.54
Celox	2.6 ± 0.99	4.8* ± 2.8	14 ± 7.1	22 ± 8.6	24 ± 3.8	29 ± 3.6	34 ± 2.8	36 ± 4.5
ProQR	1.9 ± 1.2	3.4** ± 2.8	9.0 ± 6.3	13 ± 8.9	10** ± 7.3	11**** ± 8.4	11*** ± 8.3	9.7**** ± 7.7
Fuller's Earth	0.19** ± 0.14	0.20**** ± 0.25	0.46*** ± 0.71	0.56** ± 0.84	0.29**** ± 0.24	0.30**** ± 0.24	0.21**** ± 0.10	0.12**** ± 0.14

Table 4.1: Changes in rate of penetration (μg cm^{-2} hr^{-1}) during 24 hours exposure to ^{14}C-VX and treatment with test decontaminants (mean ± standard deviation).

Asterisks indicate significant difference between treatment condition and controls (*p<0.05; **p<0.01; ***p<0.001; ****p<0.0001).

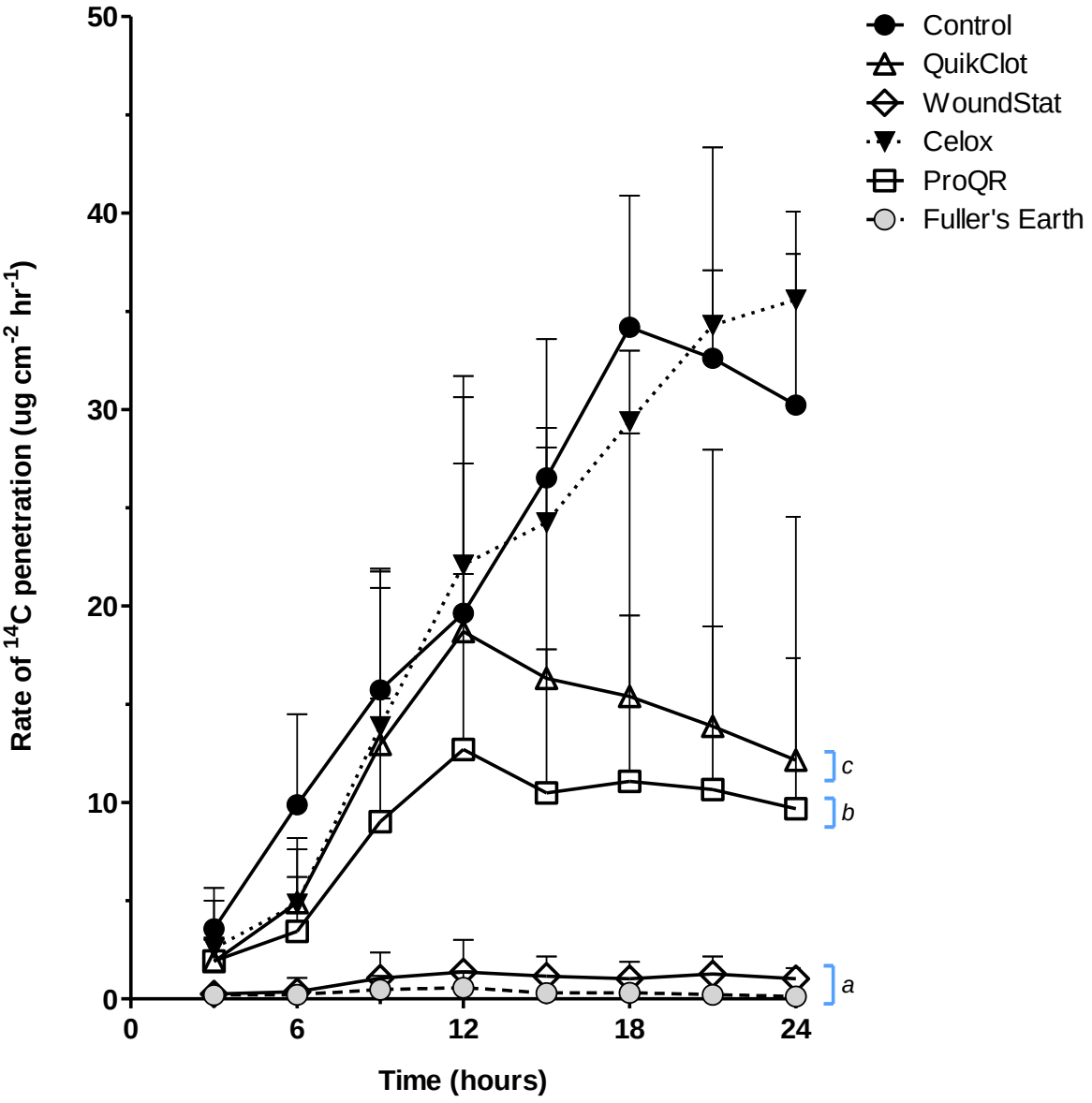

Figure 4.3: Rate of penetration of ^{14}C-VX across intact pig skin in the first group, according to the amounts of ^{14}C-VX quantified in the receptor fluid at three hour intervals (µg cm^{-2} hr^{-1}; mean ± standard deviation; n=6).

Bars indicate that rate of ^{14}C-VX penetration was significantly different to control: (a) throughout the experiment for WS and FE, $p<0.01$; (b) from 12 hours onwards for PQR, $p<0.01$; (c) from 15 hours onwards for QC, $p<0.01$).

3. Distribution of mass of ^{14}C-VX quantified as "penetrated", "remaining in skin" or "not penetrated" after 24 hours of exposure of intact porcine skin to ^{14}C-VX

The amount of ^{14}C-VX quantified in the penetrated fraction, skin fraction and not penetrated (collected decontaminant and swabs) fraction of all the treated cells was significantly different to that in control cells ($p<0.0001$), relative to the total mass recovered in the corresponding fraction of controls and relative to the dose applied (Figure 4.4, 4.5). The amount of ^{14}C-VX quantified in the penetrated fraction and skin fraction was significantly higher in the control condition compared to the treated conditions ($p<0.0001$); correspondingly the amount of ^{14}C-VX quantified in the not penetrated fraction was significantly lower in the control condition compared to the treated conditions ($p<.0001$).

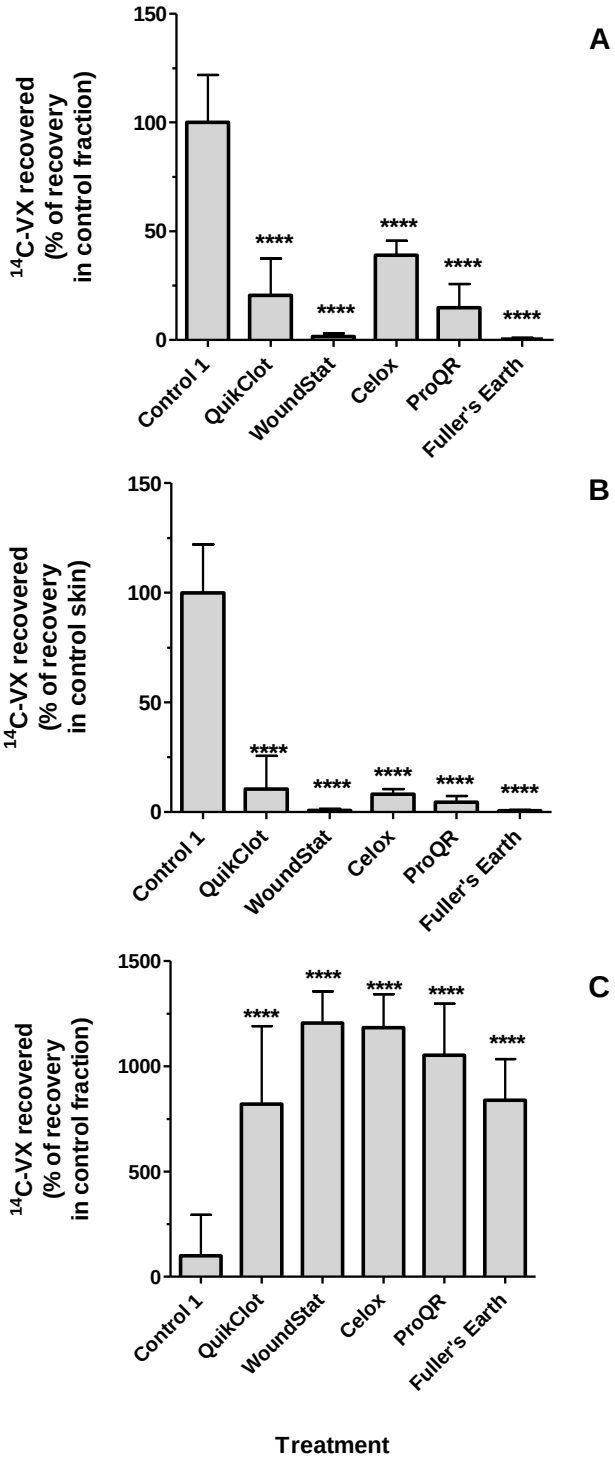

Figure 4.4: Recovery of ^{14}C-VX in the first group in (A) penetrated fraction; (B) skin; (C) not penetrated fraction.

Data are presented as mass (mean ± standard deviation; n=6) recovered relative to that in corresponding control fraction (%) following 24 hours exposure of intact skin to ^{14}C-VX and treatment with test decontaminants. Asterisks indicate significant differences (****$p<0.0001$) in recovery between control and treated cells.

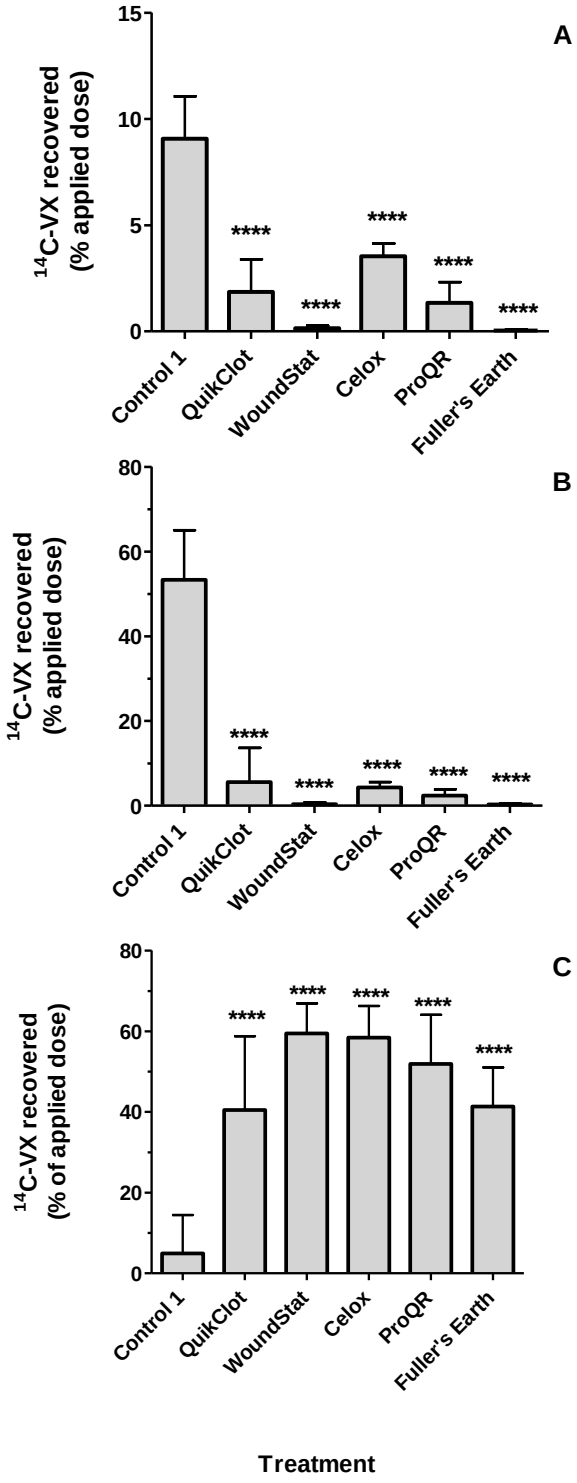

Figure 4.5: Recovery of ^{14}C-VX in the first group in (A) penetrated fraction; (B) skin; (C) not penetrated fraction.

Data are presented as mass (mean ± standard deviation; n=6) recovered relative to the dose of ^{14}C-VX applied (%) following 24 hours exposure of intact skin to ^{14}C-VX and treatment with test decontaminants. Asterisks indicate significant differences (****p<0.0001) in recovery between control and treated cells.

4.3.2 Effect of application of HemCon™, Reactive Skin Decontamination Lotion®, Vitagel™, FastAct™ or tetragylme-oxime-polyethyleneimine mixture on penetration of ^{14}C-VX across intact pig skin over 24 hours

1. Quantification of ^{14}C-VX in receptor fluid at 3 hourly intervals (μg cm^{-2})

Total ^{14}C-VX penetration at 24 hours (μg cm^{-2}) was significantly lower for diffusion cells treated with TOP ($p<0.001$) and significantly higher in RSDL-treated cells ($p<0.0001$) compared to control cells (Figure 4.6). Cells treated with RSDL had significantly larger amounts of ^{14}C-VX penetrated than controls from 9 hours onwards ($p<0.01$). Penetration of ^{14}C-VX in TOP-treated cells became significantly lower than controls after 12 hours exposure ($p<0.05$). The amount of ^{14}C-VX which had penetrated across VG or FA-treated skin was significantly higher than controls until 6 hours exposure ($p<0.001$).

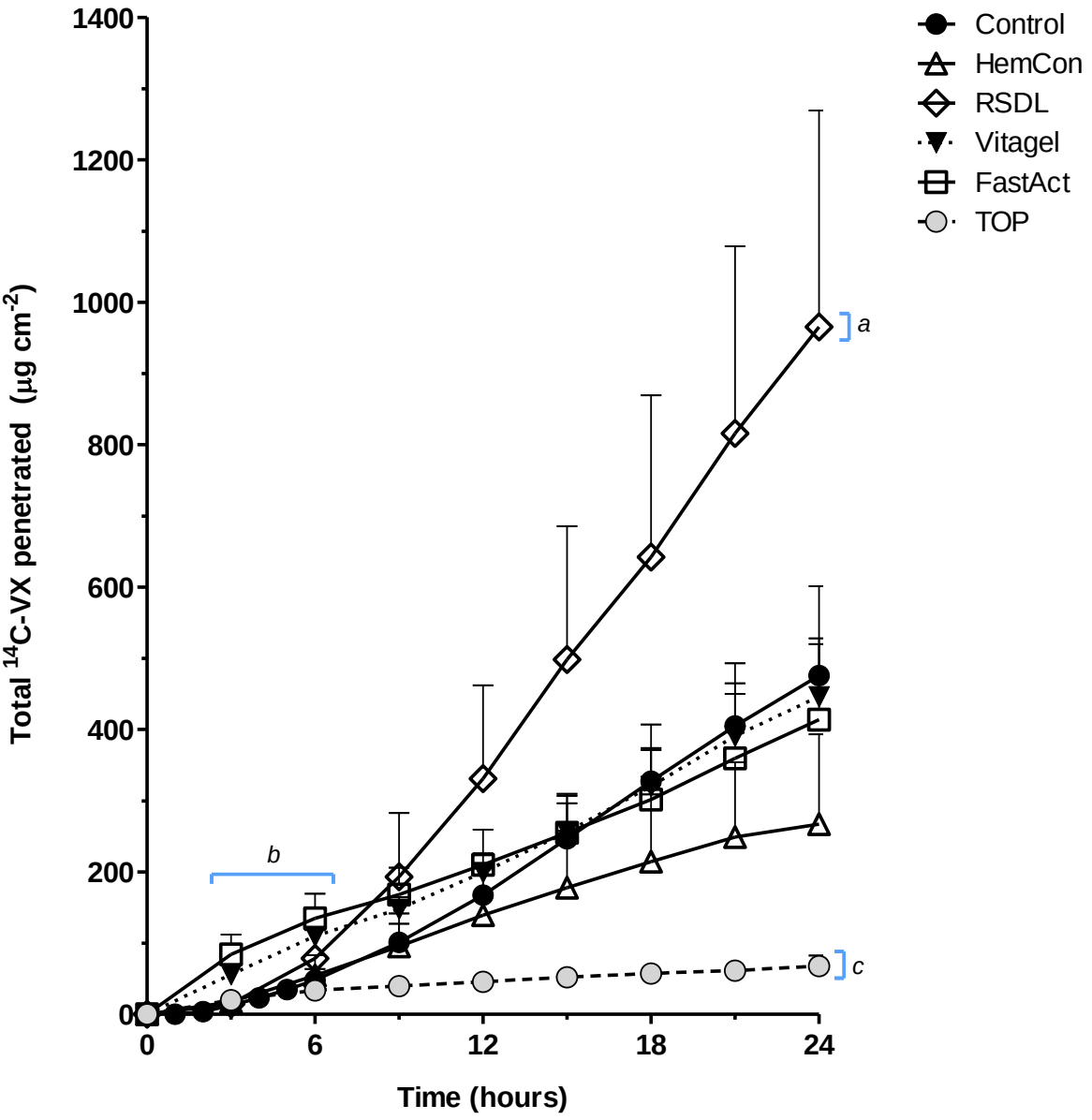

Figure 4.6: Penetration of 14C-VX across intact pig skin over 24 hours in the second group, measured in the receptor fluid at 3 hour intervals and quantified as µg cm-2 (mean ± standard deviation; n=6).

Bars indicate that amount of ^{14}C-VX penetrated was significantly different to control: (a) from 9 hours onwards for RSDL, $p<0.01$; (b) until 6 hours exposure for VG or FA, $p<0.0001$; (c) from 12 hours onwards for TOP, $p<0.05$).

2. Difference in quantification of ^{14}C-VX in receptor fluid at 3 hourly intervals (µg cm^{-2})

The rate of penetration of ^{14}C-VX across skin treated with TOP was significantly lower than that of control skin from the 6-9 hour period until 21 hours post-exposure ($p<0.01$; Figure 4.7). Cells treated with HemCon had significantly lower penetration rate than controls from the 15-18 hour period onwards ($p<0.05$). In contrast, the ^{14}C-VX penetration rate for RSDL-treatment was significantly higher than control cells from the 3-6 hour period onwards ($p<0.05$). The rate of ^{14}C-VX penetration across cells treated with VG or FA was initially significantly higher than controls ($p<0.0001$ in the 0-3 hour time period), but there were no further significant differences in penetration rate between these and control cells during the remainder of the exposure period.

In the control cells the maximum rate of penetration was 27 µg cm^{-2} hr^{-1} and was reached between 15 and 18 hours of exposure (Table 4.2).

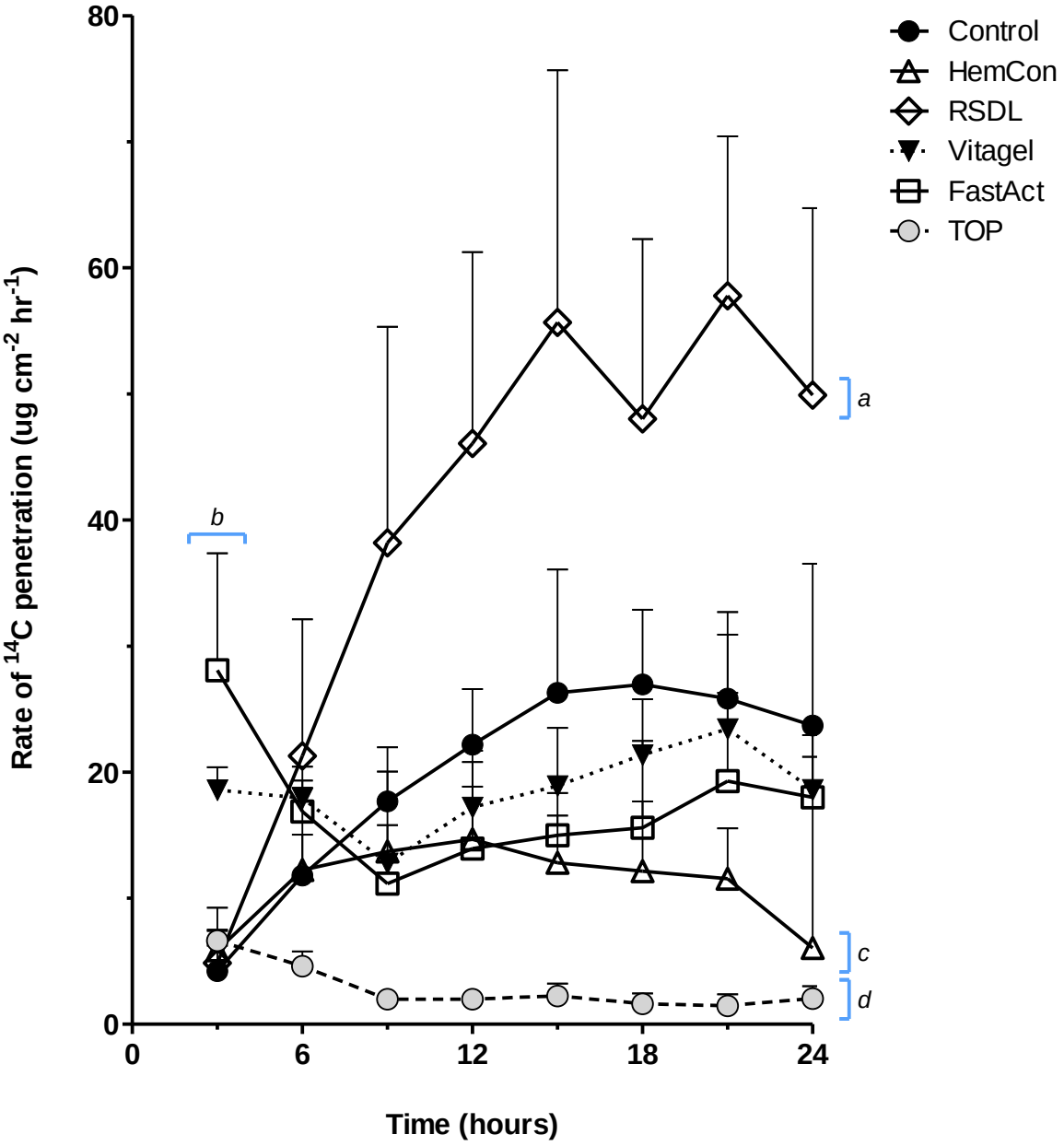

Figure 4.7: Rate of penetration of ^{14}C-VX across intact pig skin in the second group, according to the amounts of ^{14}C-VX quantified in the receptor fluid at three hour intervals (µg cm^{-2} hr^{-1}; mean ± standard deviation; n=6).

Bars indicate that rate of ^{14}C-VX penetration was significantly different to control: (a) from 3-6 hours onwards, $p<0.05$; (b) until 3 hours for VG or FA ($p<0.0001$); (c) from 15-18 hours onwards for HC, $p<0.05$; (d) from 6-9 hours onwards for TOP ($p<0.01$).

Treatment	Time interval (hours post-exposure)							
	0-3	3-6	6-9	9-12	12-15	15-18	18-21	21-24
	Flux (μg cm^{-2} hr^{-1})							
Control	4.2 ± 2.0	2.7 ± 0.75	18 ± 4.3	22 ± 4.4	26 ± 9.8	27 ± 5.9	26 ± 6.9	24 ± 13
HemCon	5.9 ± 3.4	2.8 ± 1.5	14 ± 6.3	14 ± 7.0	13 ± 5.5	12** ± 5.5	12* ± 4.0	6.1* ± 17
RSDL	4.9 ± 2.5	4.9* ± 2.5	38*** ± 17	46**** ± 15	56**** ± 20	48*** ± 14	58**** ± 13	50** ± 15
Vitagel	19**** ± 1.8	4.1 ± 0.6	13 ± 3.0	17 ± 3.6	19 ± 4.6	21 ± 4.4	23 ± 7.5	19 ± 2.6
FastAct	28**** ± 9.3	3.9 ± 0.6	11 ± 2.0	14 ± 4.9	15 ± 1.6	16 ± 6.9	19 ± 7.0	18 ± 5.8
TOP	6.6 ± 0.9	1.1 ± 0.3	2.0** ± 0.5	2.0*** ± 0.5	2.2*** ± 1.0	1.6**** ± 0.8	1.5**** ± 0.91	2.0** ± 1.0

Table 4.2: Changes in rate of penetration (μg cm^{-2} hr^{-1}) during 24 hours exposure to ^{14}C-VX and treatment with test decontaminants (mean ± standard deviation).

Asterisks indicate significant difference between treatment condition and controls (*p<0.05; **p<0.01; ***p<0.001; ****p<0.0001).

3. Distribution of mass of ^{14}C-VX quantified as "penetrated", "remaining in skin" or "not penetrated" after 24 hours of exposure of intact porcine skin to ^{14}C-VX

The amount of ^{14}C-VX quantified in the penetrated fraction of VG-treated cells was significantly lower than that in control cells, ($p<0.001$; Figure 4.8-4.9). The penetrated fraction of RSDL-treated cells contained significantly higher amounts of ^{14}C-VX than controls ($p<0.0001$; Figure 4.8-4.9).

The amount of ^{14}C-VX quantified in the skin ($p<0.01$) of all treated cells was significantly lower than that of controls (Figure 4.8-4.9).

In the not penetrated fraction, cells treated with RSDL or TOP had significantly higher amounts of ^{14}C-VX than controls (relative to that of the controls and relative to the dose applied: $p<0.05$; Figure 4.8-4.9).

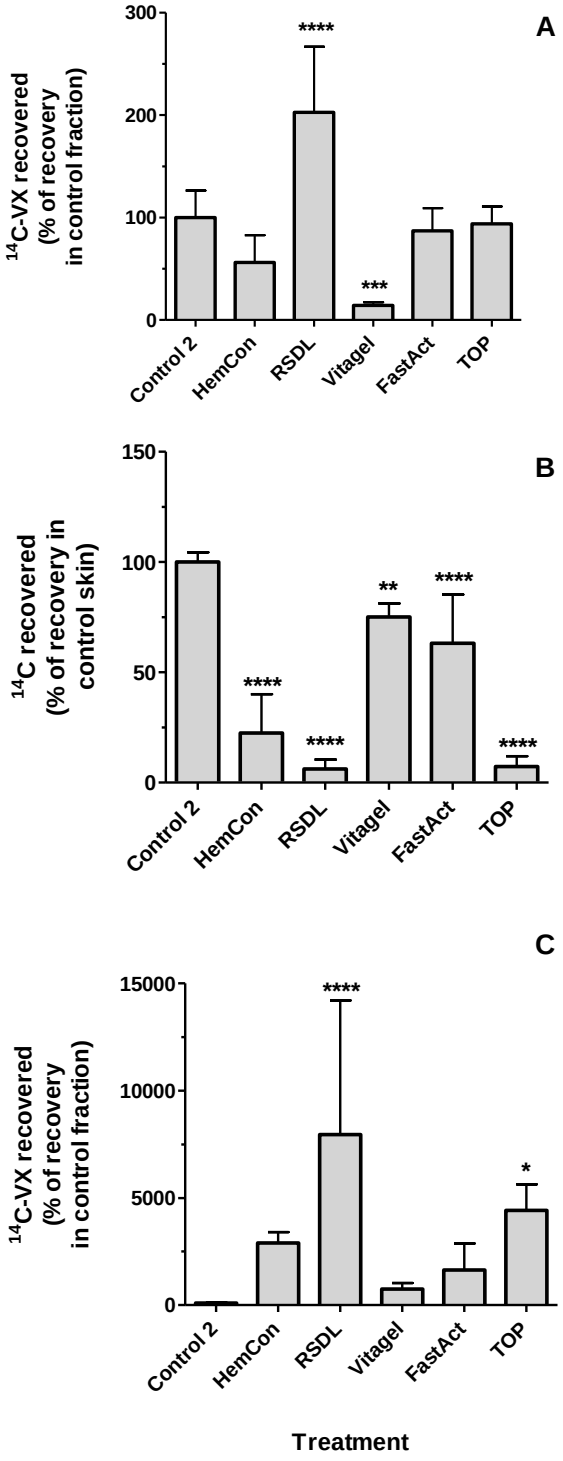

Figure 4.8: Recovery of ^{14}C-VX in the second group in (A) penetrated fraction; (B) skin; (C) not penetrated fraction.

Data are presented as mass (mean ± standard deviation; n=6) recovered relative to that in corresponding control fraction (%) following 24 hours exposure of intact skin to ^{14}C-VX and treatment with test decontaminants. Asterisks indicate significant differences in recovery between control and treated cells (*p<0.05; **p<0.01; ***p<0.001; ****p<0.0001).

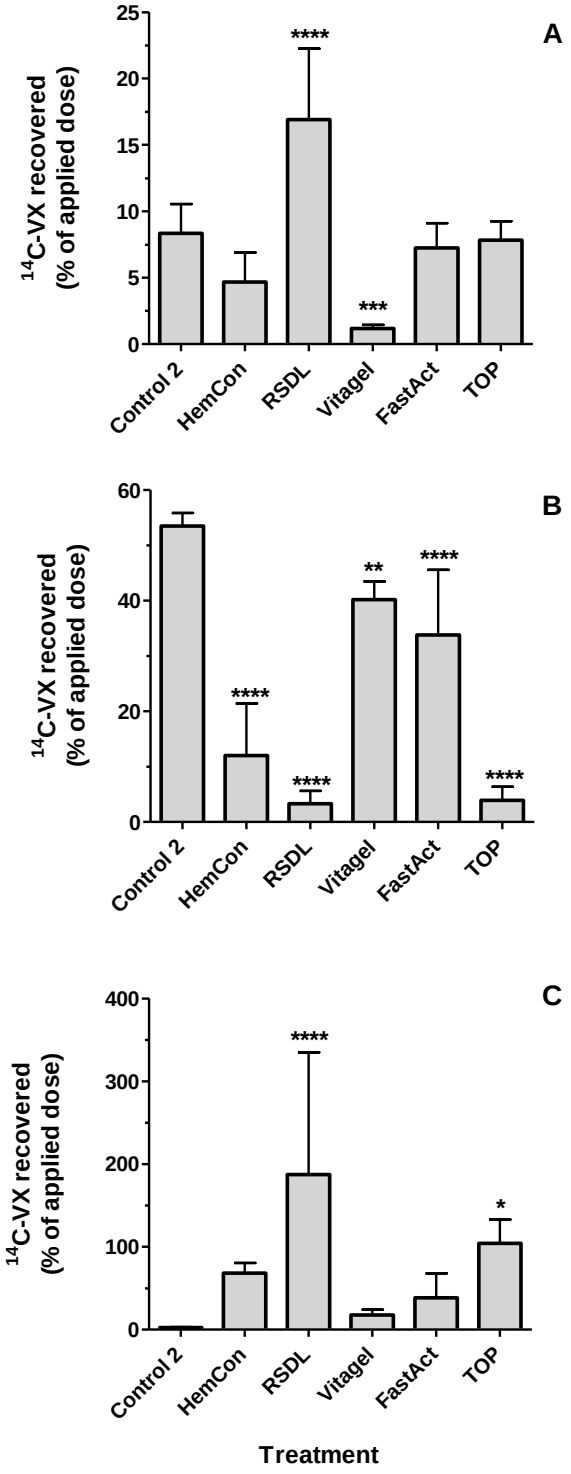

Figure 4.9: Recovery of ^{14}C-VX in the second group in (A) penetrated fraction; (B) skin; (C) not penetrated fraction.

Data are presented as mass (mean ± standard deviation; n=6) recovered relative to the dose of ^{14}C-VX applied (%) following 24 hours exposure of intact skin to ^{14}C-VX and treatment with test decontaminants. Asterisks indicate significant differences in recovery between control and treated cells (*p<0.05; **p<0.01; ***p<0.001; ****p<0.0001).

4.3.3 Effect of application of Vitagel™ + TOP, FastAct™ + TOP, M291 or occlusion on penetration of ^{14}C-VX across intact pig skin over 24 hours

1. Quantification of ^{14}C-VX in receptor fluid at 3 hourly intervals (µg cm^{-2})

The amount of ^{14}C-VX which had penetrated across cells treated with VG+TOP, FA+TOP or M291 was significantly lower than controls after 24 hours exposure ($p<0.0001$; Figure 4.10). The amount of ^{14}C-VX penetrating across M291-treated cells was significantly lower than control cells after 6 hours exposure ($p<0.0001$).

Initially, cells treated with VG+TOP or FA+TOP had significantly higher amounts of ^{14}C-VX penetrating than control cells until 6 hours post-exposure ($p<0.05$). From then on the penetration of ^{14}C-VX was lower than control cells: the difference between these treatments and control cells was significant after 9 hours for FA+TOP and 12 hours for VG+TOP.

Occlusion had no significant effect on the amount of ^{14}C-VX penetrating across intact skin during the experiment.

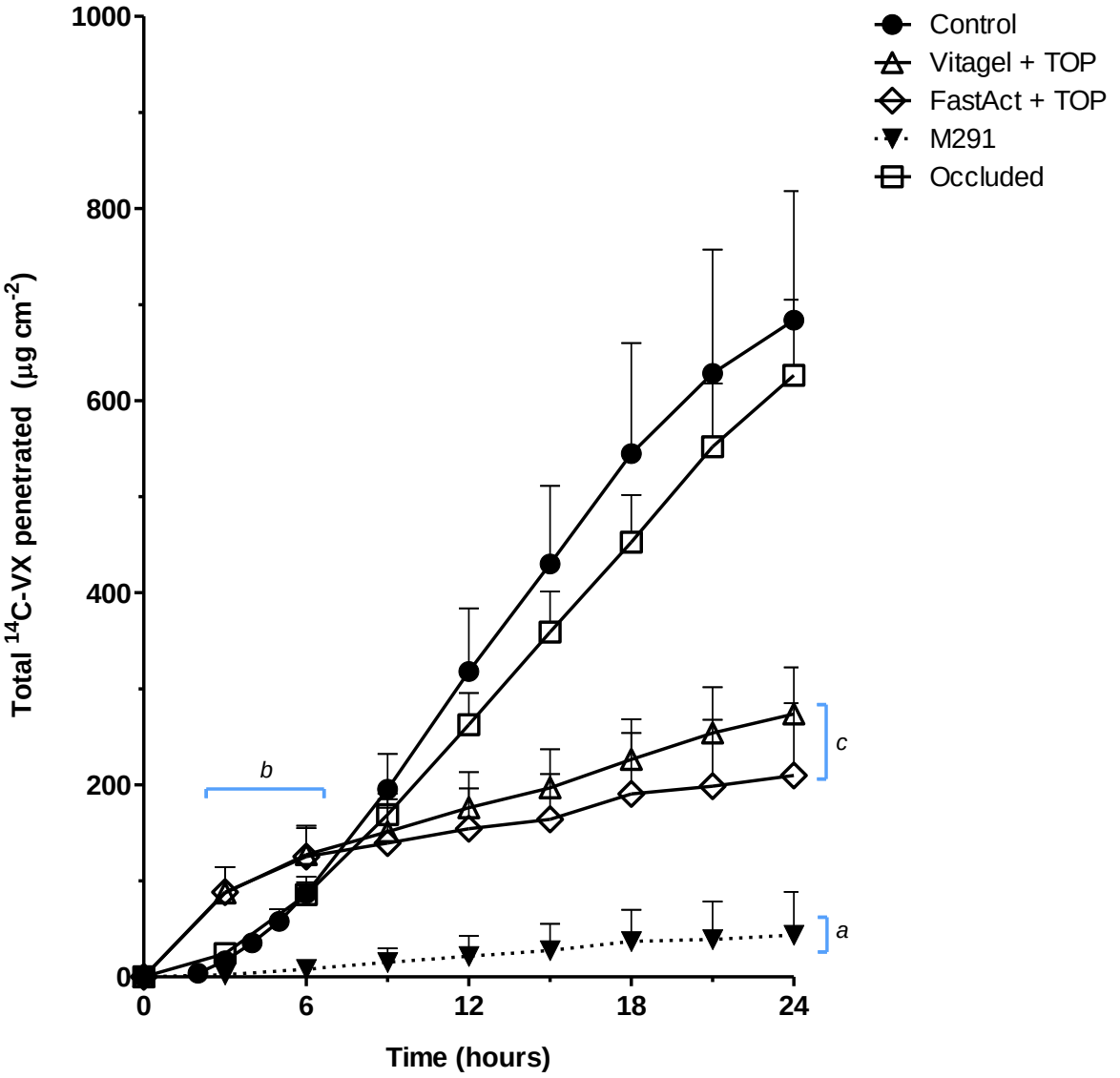

Figure 4.10: Penetration of ^{14}C-VX across intact pig skin over 24 hours in the first group, measured in the receptor fluid at 3 hour intervals and quantified as µg cm^{-2} (mean ± standard deviation; n=6).

Total ^{14}C-VX penetration at 24 hours (µg cm^{-2}) was significantly lower for diffusion cells treated with QC, WS, CX, PQR or FE compared to controls ($p<0.0001$). Bars indicate that amount of ^{14}C-VX penetrated was significantly different to control: (a) from 6 hours onwards for M291, $p<0.0001$; (b) until 6 hours for VG+TOP and FA+TOP, $p<0.05$; (c) from 12 hours onwards for VG+TOP and FA+TOP).

2. Difference in quantification of ^{14}C-VX in receptor fluid at 3 hourly intervals (µg cm^{-2})

The rate of penetration of ^{14}C-VX across skin treated with M291 was significantly lower than control cells from 3 hours onwards (Figure 4.11 and Table 4.3).

During the first 3 hours of exposure, the rate of penetration of ^{14}C-VX across skin treated with FA+TOP or VG+TOP was initially significantly higher than controls ($p<0.0001$); from then on the rate of penetration was significantly lower than controls ($p<0.001$).

In control cells the maximum penetration rate was 41µg cm^{-2} hr^{-1} and was reached between 9 and 12 hours exposure (Table 4.3).

The rate of penetration across occluded cells was only significantly lower than that of control cells between 6 and 12 hours exposure. In contrast, the rate of penetration across occluded cells was significantly higher than control cells between 21 and 24 hours exposure.

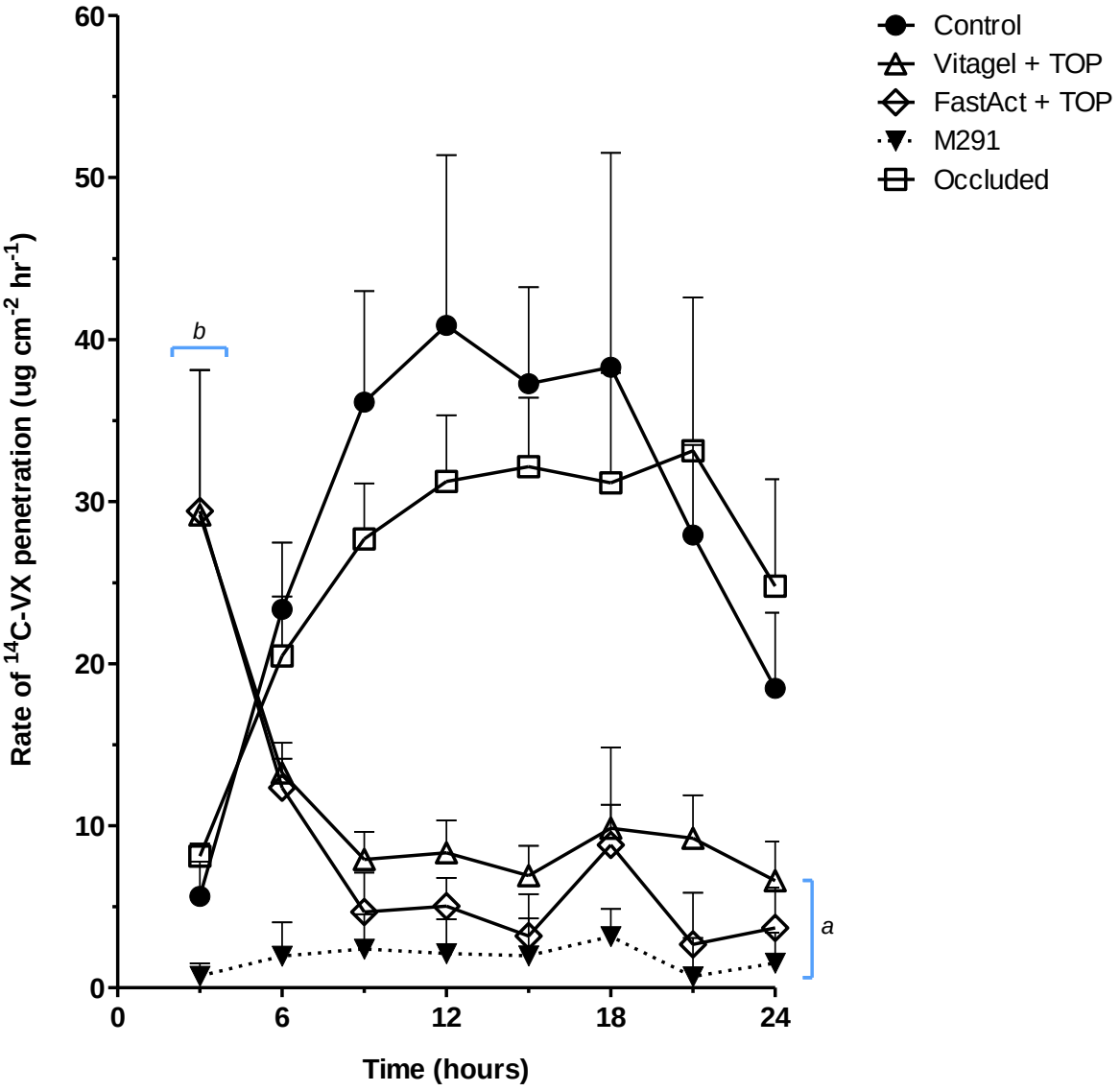

Figure 4.11: Rate of penetration of ^{14}C-VX across intact pig skin in the third group, according to the amounts of ^{14}C-VX quantified in the receptor fluid at three hour intervals (µg cm^{-2} hr^{-1}; mean ± standard deviation; n=6).

Bars indicate that rate of ^{14}C-VX penetration was significantly different to control: (a) from 3-6 hours onwards for M291, VG+TOP and FA+TOP, $p<0.05$; (b) until 3 hours for VG or FA ($p<0.0001$).

Treatment	Time interval (hours post-exposure)							
	0-3	3-6	6-9	9-12	12-15	15-18	18-21	21-24
	Flux (μg cm^{-2} hr^{-1})							
Control	5.6 ± 2.1	23 ± 4.1	36 ± 6.9	41 ± 11	37 ± 6.0	38 ± 13	28 ± 5.6	18 ± 4.7
Vitagel + TOP	29**** ± 8.9	13**** ± 1.9	7.9**** ± 1.7	8.3**** ± 2.0	6.9**** ± 1.9	9.8**** ± 1.4	9.2**** ± 2.7	6.6 *** ± 2.4
FastAct + TOP	29**** ± 8.7	12**** ± 1.8	4.7**** ± 2.4	5.0**** ± 1.8	3.2**** ± 2.6	8.8**** ± 6.0	2.7**** ± 3.2	3.7**** ± 2.5
M291	0.7 ± 0.8	2.0**** ± 2.1	2.4**** ± 2.2	2.1**** ± 2.1	2.0**** ± 2.3	3.2**** ± 1.7	0.7**** ± 2.4	1.5**** ± 1.9
Occluded	8.0 ± 0.8	20 ± 3.7	28** ± 3.4	31* ± 4.1	32 ± 4.3	31 ± 6.8	33 ± 9.5	25* ± 6.6

Table 4.3: Changes in rate of penetration (μg cm-2 hr-1) during 24 hours exposure to 14C-VX and treatment with test decontaminants (mean ± standard deviation).

Asterisks indicate significant difference between treatment condition and controls (*p<0.05; **p<0.01; ***p<0.001; ****p<0.0001).

3. Distribution of mass of ^{14}C-VX quantified as "penetrated", "remaining in skin" or "not penetrated" after 24 hours of exposure of intact porcine skin to ^{14}C-VX

The amount of ^{14}C-VX quantified in the penetrated fraction and skin of FA+TOP, VG+TOP or M291-treated cells was significantly lower than that in control cells, relative to that which was penetrated in the control condition and relative to the dose applied ($p<0.0001$; Figure 4.12-4.13). Correspondingly, significantly larger amounts of ^{14}C-VX were quantified in the "not penetrated" fraction of FA+TOP, VG+TOP or M291 treated cells compared to control cells, when expressed relative to that which was quantified in the control "not penetrated" fraction or relative to the applied dose of ^{14}C-VX ($p<0.0001$).

The collected decontaminant fraction of M291-treatment contained a significantly larger proportion of the applied dose than that of VG+TOP or FA+TOP-treatment ($p<0.001$).

There were no significant differences in amounts of ^{14}C-VX quantified in each fraction between occluded and control cells (figure 4.12-4.13).

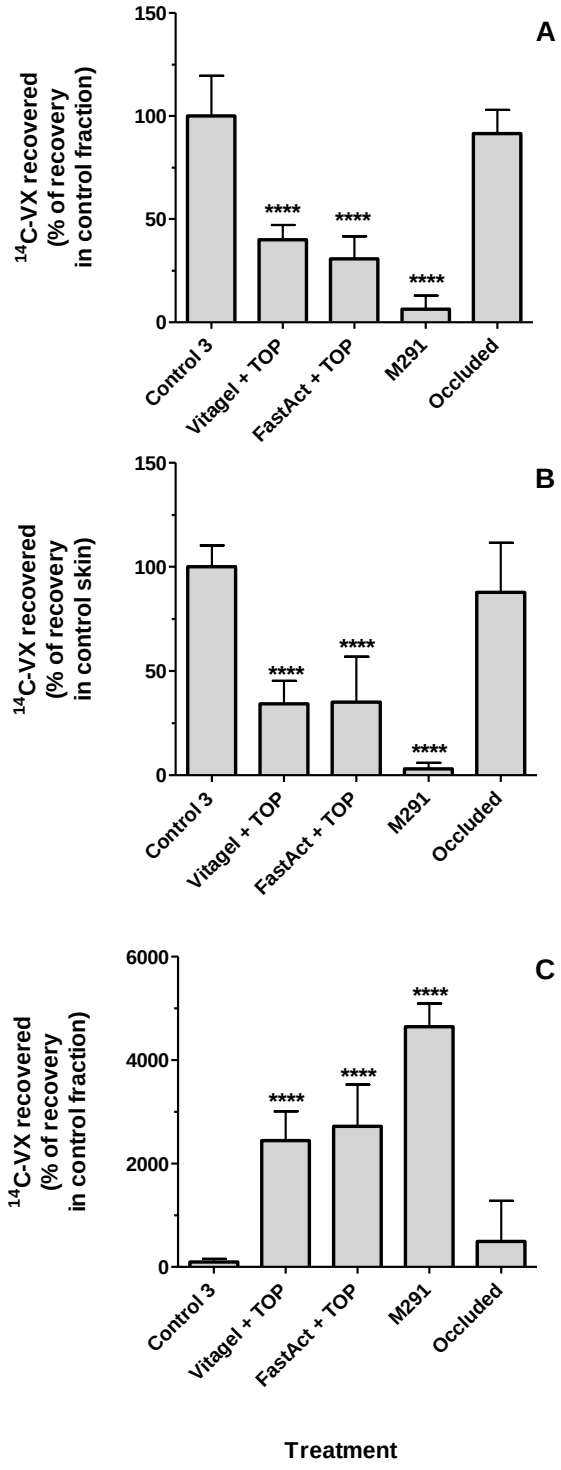

Figure 4.12: Recovery of ^{14}C-VX in the third group in (A) penetrated fraction; (B) skin; (C) not penetrated fraction.

Data are presented as mass (mean ± standard deviation; n=6) recovered relative to that in corresponding control fraction (%) following 24 hours exposure of intact skin to ^{14}C-VX and treatment with test decontaminants. Asterisks indicate significant differences in recovery between control and treated cells (****$p<0.0001$).

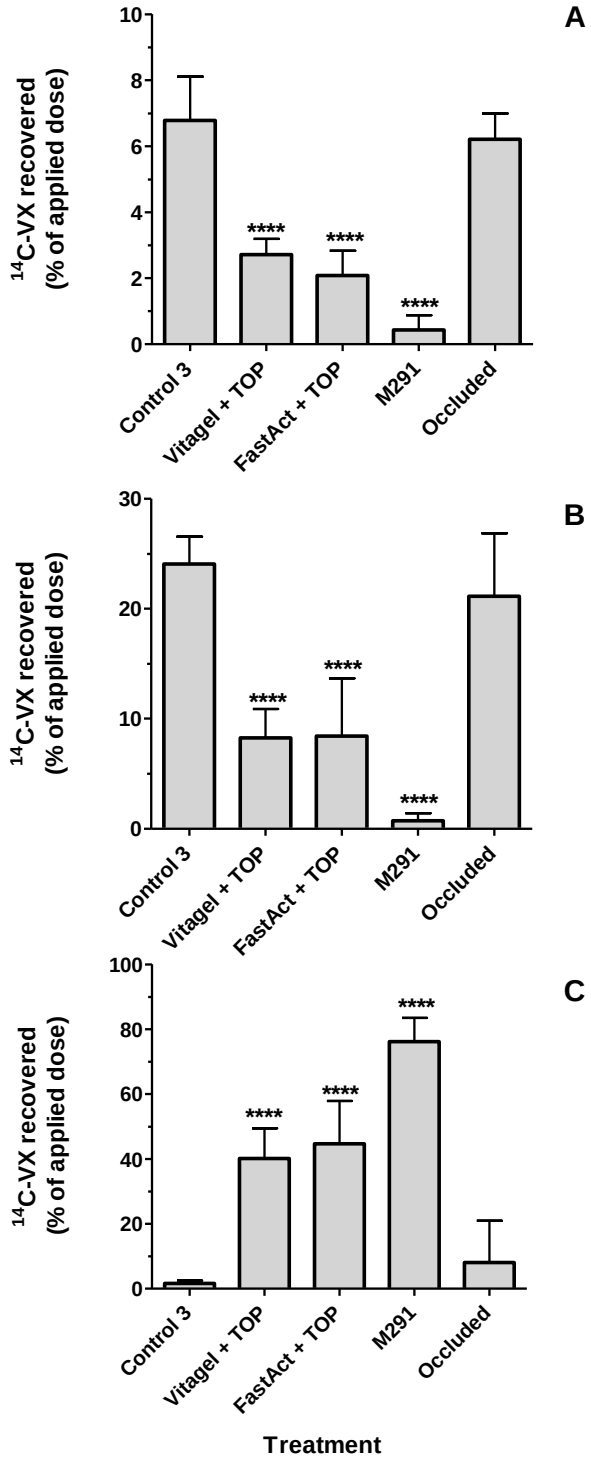

Figure 4.13:. Recovery of ^{14}C-VX in the third group in (A) penetrated fraction; (B) skin; (C) not penetrated fraction.

Data are presented as mass (mean ± standard deviation; n=6) recovered relative to the dose of ^{14}C-VX applied (%) following 24 hours exposure of intact skin to ^{14}C-VX and treatment with test decontaminants. Asterisks indicate significant differences in recovery between control and treated cells (****p<0.0001).

4.3.4 Decontaminant efficacy

There were significant differences in the mass of ^{14}C-VX recovered in the decontaminant fraction (relative to applied dose) between RSDL and VG or FA-treated cells ($p<0.01$; Figure 4.14). The mass of ^{14}C-VX recovered in collected M291 (relative to applied dose) was also significantly higher than in collected VG+TOP or FA+TOP ($p<0.001$; Figure 4.14).

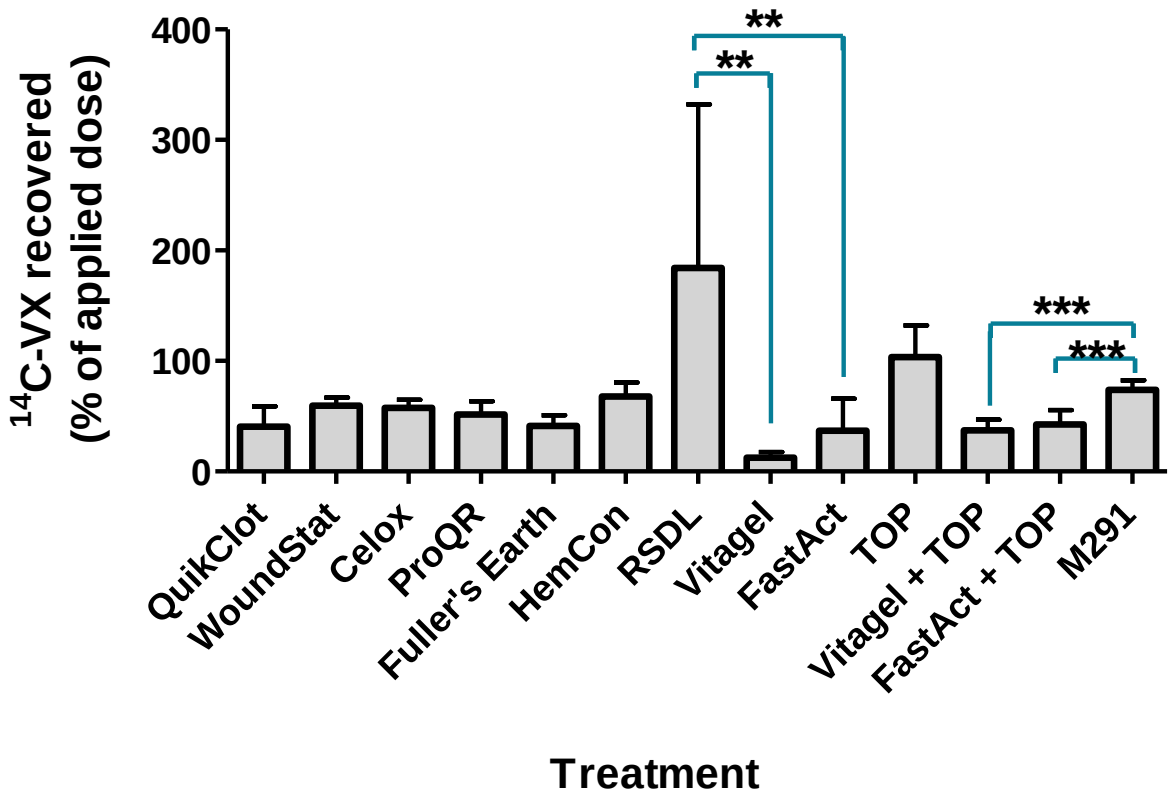

Figure 4.14: Amount of ^{14}C-VX quantified in the decontaminant fraction of diffusion cells treated with test and current decontaminants, relative to the applied dose (mean ± standard deviation; n=6).

Statistical analyses (1-way ANOVA with post-hoc Tukey's test) compared treatments within each individual study (to account for variation between control conditions). Bars indicate significant differences between treatments (within each study; **p<0.01; ***p<0.001).

4.3.5 Effect of application of QuikClot® ACS+, WoundStat™, ProQR™ or Fuller's Earth™ on penetration of ^{14}C-VX across damaged pig skin over 24 hours

1. Quantification of ^{14}C-VX in receptor fluid at 3 hourly intervals (µg cm^{-2})

Total ^{14}C-VX penetration (µg cm^{-2}) at 24 hours was significantly ($p<0.001$) higher in damaged skin (897 ± 176 µg cm^{-2}) compared to undamaged skin (563 ± 71 µg cm^{-2}; Figure 4.15). All the treatments (QC, WS, PQR, FE) significantly reduced the amount of ^{14}C-VX which had penetrated damaged skin at 24 hours ($p<0.0001$; Figure 4.15).

The amount of ^{14}C-VX penetrating across damaged skin was significantly higher than undamaged skin, and all the treated damaged-skin cells from 3 hours onwards ($p<0.001$; Figure 4.15).

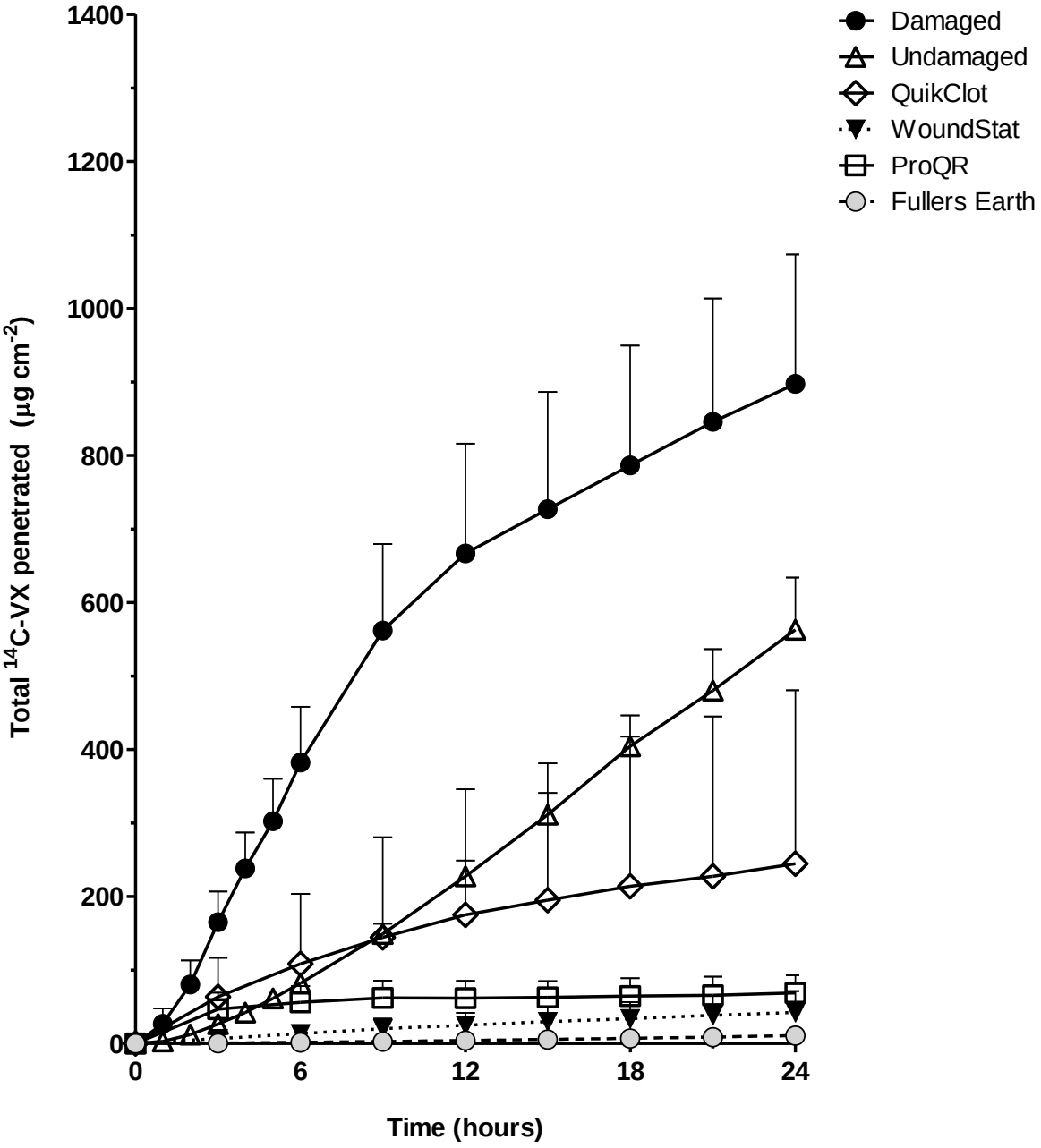

Figure 4.15: Penetration of ^{14}C-VX across damaged pig skin over 24 hours, measured in the receptor fluid at 3 hour intervals and quantified as µg cm^{-2} (mean ± standard deviation; n=6). Total ^{14}C-VX penetration at 24 hours (µg cm^{-2}) was significantly higher through damaged skin than untreated skin and damaged skin treated diffusion cells treated with QC, WS, PQR or FE throughout the exposure period.

2. Difference in quantification of ^{14}C-VX in receptor fluid at 3 hourly intervals (µg cm^{-2})

Initially, the rate of penetration across intact skin was significantly lower than damaged skin, until 9 hours of exposure ($p<0.0001$; Figure 4.16). After 12 hours of exposure, the rate of penetration across intact skin was significantly higher than that of damaged skin, until 18 hours post-exposure ($p<0.01$), and again between 21 and 24 hours exposure ($p<0.05$). The rate of penetration across treated damaged skin was significantly lower than that of untreated damaged skin for all treatments throughout the exposure period ($p<0.001$).

In damaged skin, the maximum penetration rate of ^{14}C-VX was 72 µg cm^{-2} hr^{-1} and was reached between 3 and 6 hours exposure. In contrast, the maximum ^{14}C-VX penetration rate was 31µg cm^{-2} hr^{-1} and was reached between 15 and 18 hours exposure (Table 4.4).

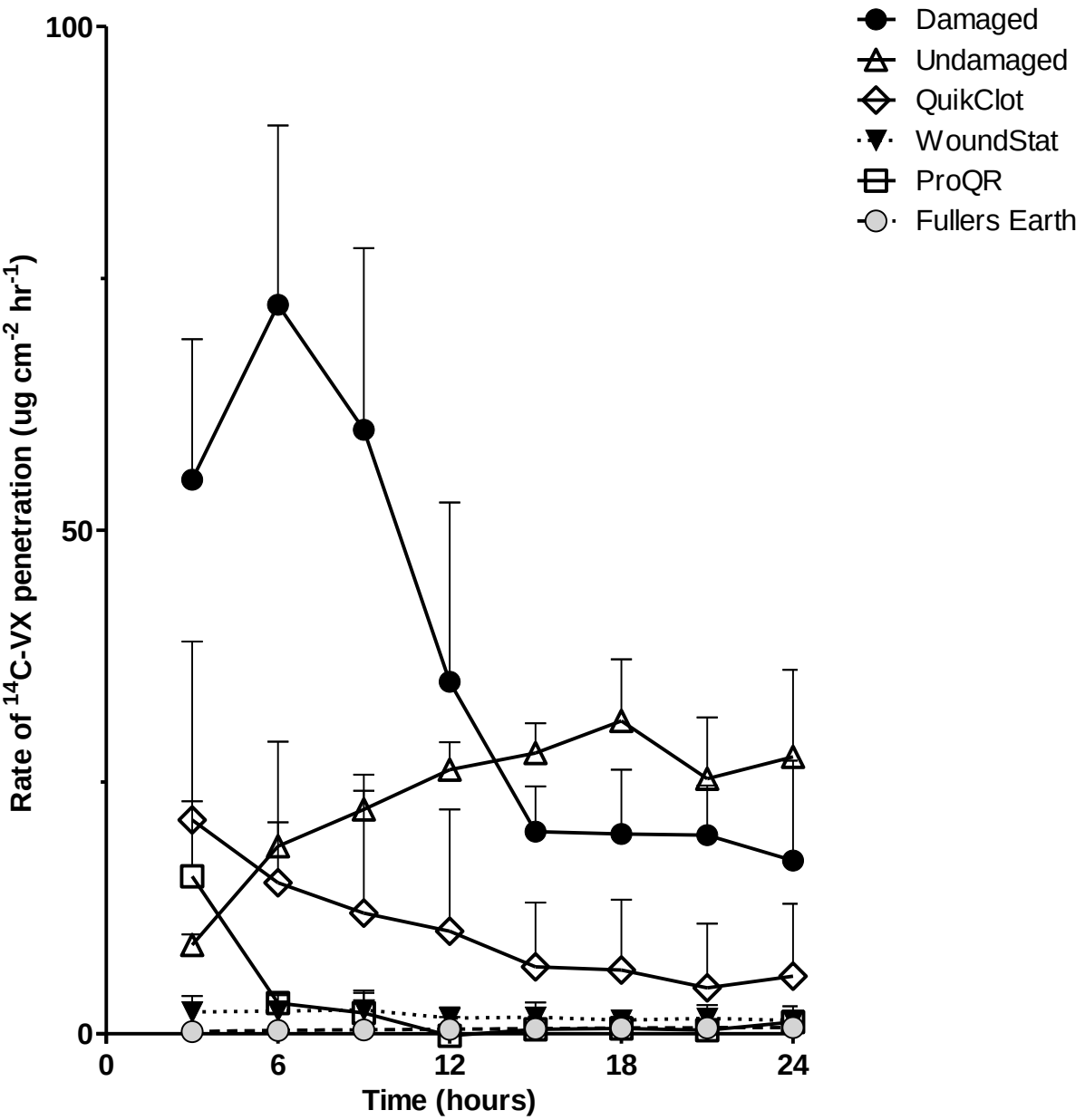

Figure 4.16: Rate of penetration of ^{14}C-VX across damaged pig skin in the second group, according to the amounts of ^{14}C-VX quantified in the receptor fluid at three hour intervals (μg cm^{-2} hr^{-1}; mean ± standard deviation; n=6).

Penetration rate of ^{14}C-VX across damaged skin was significantly different to that of undamaged skin at all time intervals except for 9-12 hours and 18-21 hours ($p<0.05$). The treated cells had significantly lower penetration rates than damaged skin throughout the study period ($p<0.001$).

Treatment	Time interval (hours post-exposure)							
	0-3	3-6	6-9	9-12	12-15	15-18	18-21	21-24
	Flux ($\mu g\ cm^{-2}\ hr^{-1}$)							
Damaged	55 ± 14	72 ± 18	60 ± 18	35 ± 18	20 ± 4.5	20 ± 6.4	20 ± 4.9	17 ± 9.9
Undamaged	8.8**** ± 1.0	19**** ± 2.4	22**** ± 1.8	26 ± 3.0	28** ± 3.0	31** ± 6.1	25 ± 6.1	27* ± 8.6
QuikClot	21**** ± 17	15**** ± 14	12**** ± 14	10**** ± 12	6.6**** ± 6.4	6.3*** ± 7.0	4.6**** ± 6.4	5.7* ± 7.2
WoundStat	2.2**** ± 1.6	2.2**** ± 1.6	2.4**** ± 1.9	1.5**** ± 1.1	1.6**** ± 1.5	1.3**** ± 0.8	1.5**** ± 1.3	1.3*** ± 1.4
ProQR	16**** ± 7.4	3.0**** ± 0.8	2.1**** ± 2.0	-0.2**** ± 1.8	0.5**** ± 0.93	0.5**** ± 1.1	0.3**** ± 0.6	1.2*** ± 0.6
Fuller's Earth	0.2**** ± 0.3	0.3**** ± 0.4	0.4**** ± 0.5	0.4**** ± 0.5	0.5**** ± 0.5	0.5**** ± 0.5	0.6**** ± 0.6	0.6*** ± 0.6

Table 4.4: Changes in rate of penetration Flux ($\mu g\ cm^{-2}\ hr^{-1}$) during 24 hours exposure to ^{14}C-VX and treatment with test decontaminants (mean ± standard deviation).

Asterisks indicate significant difference between treatment condition and controls (*p<0.05; **p<0.01; ***p<0.001; ****p<0.0001).

3. Distribution of mass of ^{14}C-VX quantified as "penetrated", "remaining in skin" or "not penetrated" after 24 hours of exposure of damaged porcine skin to ^{14}C-VX

The "penetrated" fraction from damaged skin was significantly larger than undamaged ($p<0.001$) and all treated cells (Figure 4.17- 4.18 (A); $p<0.0001$).

The amount of ^{14}C-VX quantified in undamaged skin was significantly larger than that quantified in damaged skin (Figure 4.17-4.18 (B); $p<0.0001$). In contrast, all the treatments significantly reduced the amount of ^{14}C-VX quantified in the damaged skin fraction, compared to the damaged skin controls ($p<0.0001$).

There was no difference in amount of ^{14}C-VX "not penetrated" between damaged and undamaged skin (Figure 4.17-4.18 (C)). The not penetrated fraction was significantly larger for all treatments compared to damaged skin ($p<0.0001$).

There were significant inter-treatment differences in the proportion of applied dose quantified in the decontaminant fractions. The QC and FE fractions contained significantly less ^{14}C-VX than WS or PQR fractions (Figure 4.19; $p<0.001$).

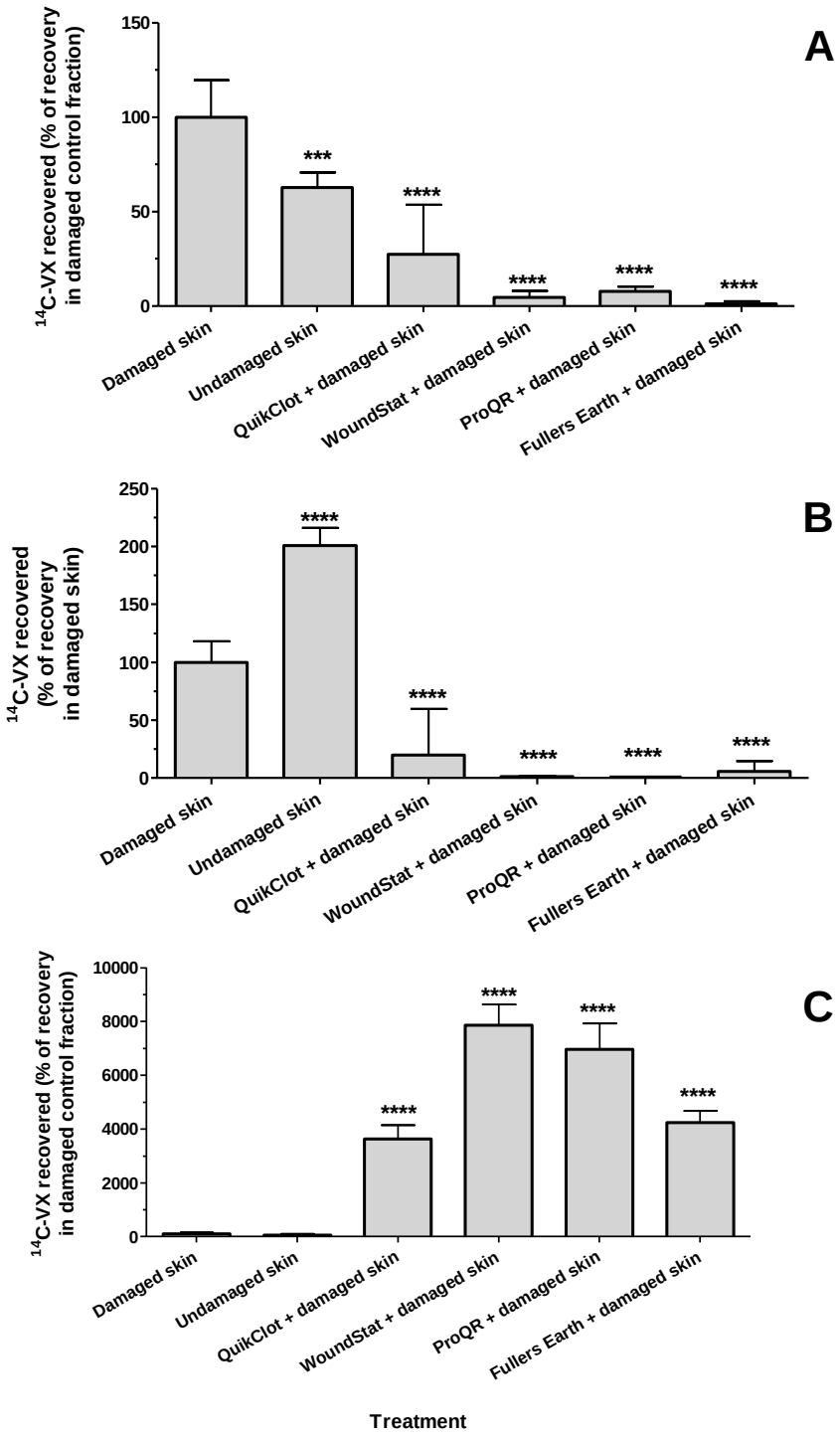

Figure 4.17: Recovery of ^{14}C-VX in the fourth group in (A) penetrated fraction; (B) skin; (C) not penetrated fraction.

Data are presented as mass (mean ± standard deviation; n=6) recovered relative to that in corresponding control fraction (%) following 24 hours exposure of intact skin to ^{14}C-VX and treatment with test decontaminants. Asterisks indicate significant differences in recovery between control and treated cells (****$p<0.0001$).

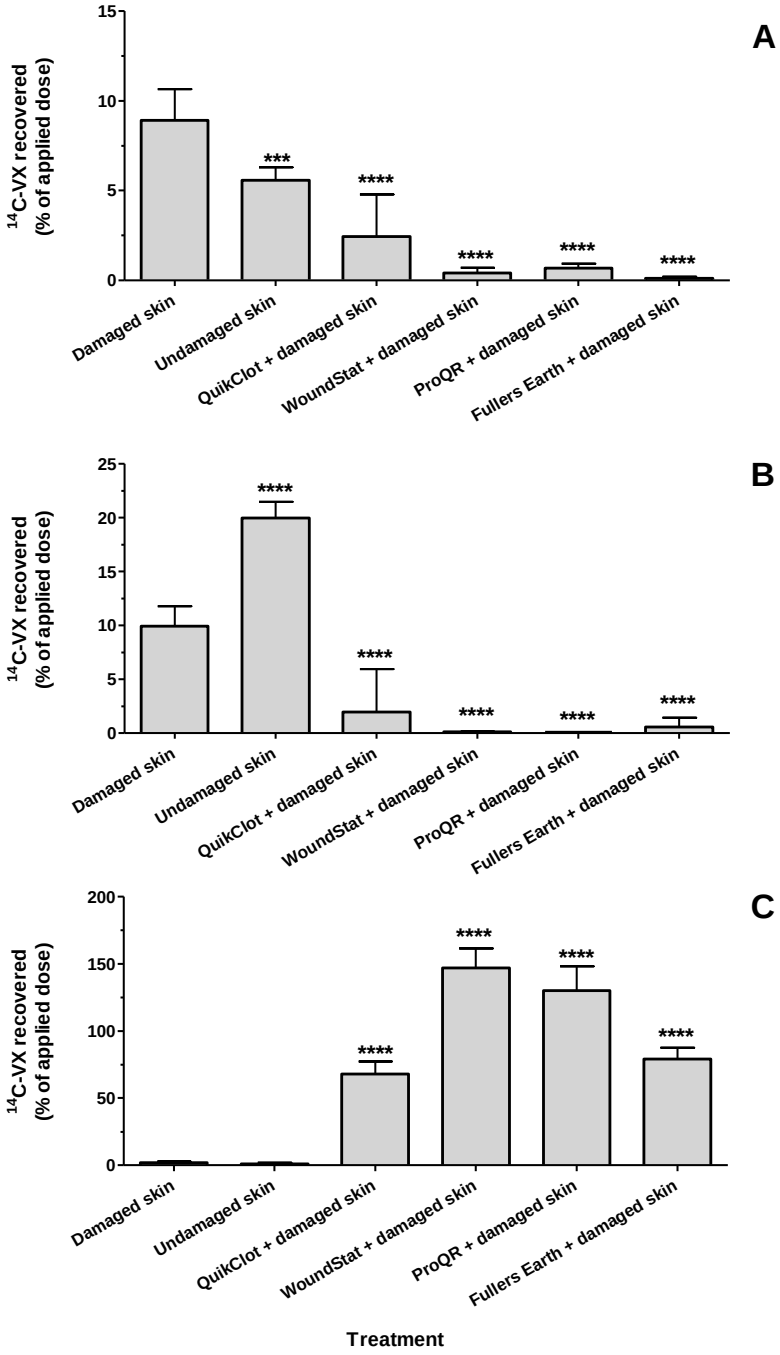

Figure 4.18: Recovery of ^{14}C-VX in the fourth group in (A) penetrated fraction; (B) skin; (C) not penetrated fraction.

Data are presented as mass (mean ± standard deviation; n=6) recovered relative to the dose of ^{14}C-VX applied (%) following 24 hours exposure of intact skin to ^{14}C-VX and treatment with test decontaminants. Asterisks indicate significant differences in recovery between control and treated cells (****$p<0.0001$).

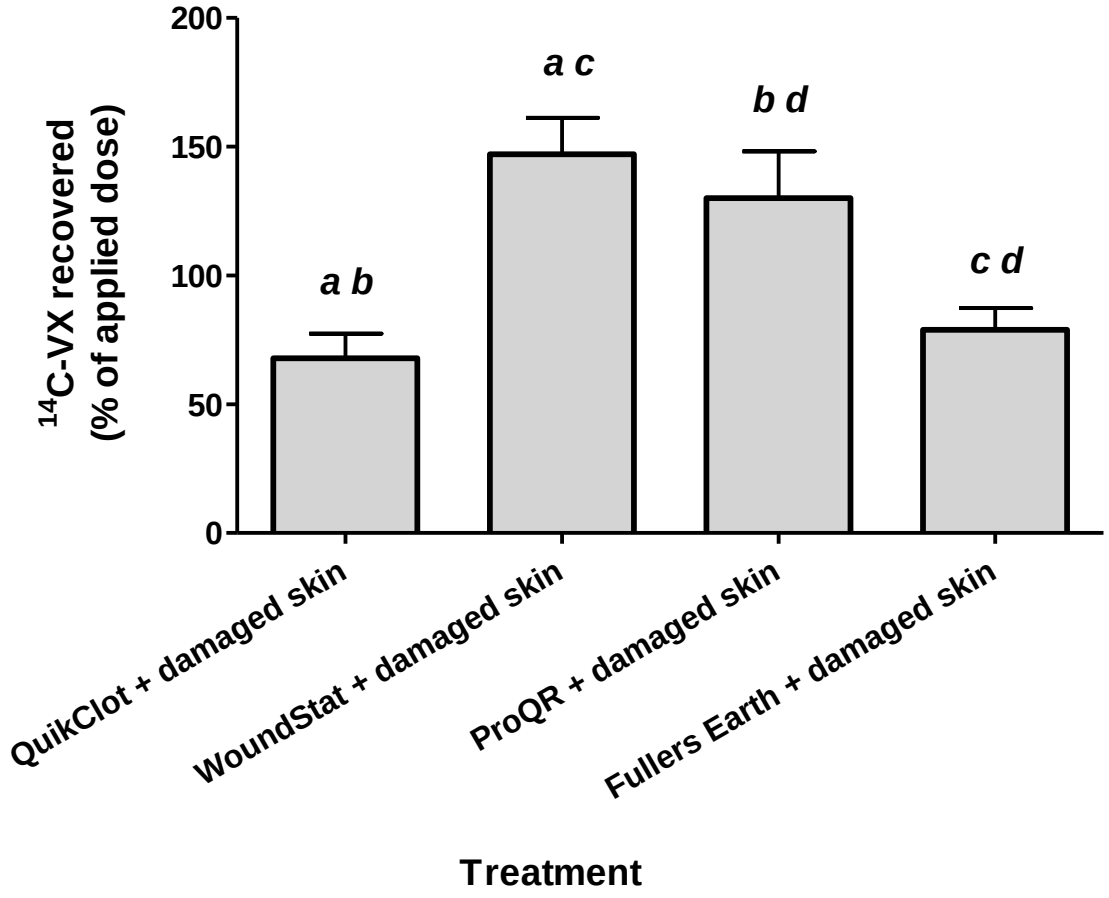

Figure 4.19: Recovery of ^{14}C-VX in the decontaminant fraction following 24 hours exposure on damaged skin.

Data are presented as the mass of ^{14}C-VX recovered relative to the applied dose (%; mean ± standard deviation; n=6). Annotations indicate significant differences between treatments which bear the same annotation ($p<0.001$).

4.4 Discussion

This experiment utilised *in vitro* diffusion cells to quantify penetration of ^{14}C-VX through intact, occluded and damaged pig abdominal skin over a 24 hour period. Penetration of ^{14}C-VX was significantly enhanced by removal of the top 100µm layer of skin prior to exposure. Along with the currently in-use military decontaminants FE and M291, five test products (QuikClot® ACS+™, WoundStat™, Celox™, ProQR™ and a novel decontaminant liquid (TOP)) were able to reduce ^{14}C-VX penetration across undamaged skin during the 24 hour exposure period QuikClot® ACS+™, WoundStat™, ProQR™ and Fuller's Earth also reduced ^{14}C-VX penetration across damaged skin. Occluding the skin did not significantly affect penetration of ^{14}C-VX across intact pig abdominal skin.

Treatment of undamaged skin with certain haemostats or decontaminants also resulted in significantly altered profiles of penetration rate across intact skin during the 24 hour exposure period compared to untreated control skin. For example, WS was the only haemostat which significantly reduced ^{14}C-VX penetration rate at all time-points throughout the 24 hour exposure period. Fuller's Earth was the only currently "in-use" decontaminant which shared this trait. In contrast, QC, WS, PQR (and FE) all significantly reduced the rate of ^{14}C-VX penetration across damaged skin at all time-points during the exposure period.

Human skin would be the "gold-standard" for the *in vitro* assessment of percutaneous penetration of VX. However, human skin was unavailable for this study. *In vitro* studies have provided some comparative data between pig and human abdominal skin for penetration of VX and nerve agent simulants [101,107,108,110]. The toxicokinetics of VX have also been described for the pig *in vivo*, following VX application to inner ear skin[58,100]. Therefore,

pig skin was chosen for this *in vitro* study. The use of pig abdominal skin allowed more products to be assessed simultaneously in skin from a common original source. Whilst quantitative data obtained here may not be directly predictive of penetration in humans as a result of species or anatomical differences, this study should permit an empirical assessment of the basic efficacy of the products. This also served to reduce the numbers of animals required to provide skin samples. The data obtained in this study compare favourably with a previous *in vitro* study of pig abdominal skin permeability to VX, taking into account (and assuming a linear relationship) between the variation in doses between studies[101].

Some of the measured parameters differed significantly between the third studies and the others. This may be due to differences in skin type between groups: this may have occurred because skin may have been sampled more distally or proximally to the abdomen midline between sources depending on damage.

There are no previous studies reporting differences in permeability of undamaged and damaged pig skin for VX specifically. However, varied efficacy of a selection of decontamination regimes in the context of VX-exposure in a full-thickness swine skin wound has been demonstrated *in vivo*[105]. Various other methods, such as tape stripping, abrasion or needle puncture have been employed to study effects of skin surface damage or compromised barrier function on penetration of compounds *in vitro*[128].

There are potential disadvantages of using *in vitro* assays of penetration to predict human absorption or toxicity *in vivo*. Isolating skin penetration experiments to an *in vitro* setting eliminates systemic circulation and distribution (and excretion), deposition in organs and metabolism. However, this enables the empirical assessment of skin absorption kinetics.

Flow-through diffusion cells can address the issue of removal of the penetrant from the exposure or absorption site, but this is not always a reliable estimation[129]. Owing to the toxicity of VX, the ability of the products to reduce, or indeed prevent, penetration of VX across the stratum corneum in the first instance was the main factor under investigation.

In addition, using radiolabelled VX allows penetration of the compound to be followed at each sampling time-point, as well as quantification of ^{14}C-VX in each fraction (skin, decontaminant, receptor fluid, swabs) at the conclusion of the experiment. However, this can only be interpreted as an estimation of the progress of penetration, as radioactivity is measured, not specifically VX. Due to the period of exposure, the relatively slow hydrolysis kinetics of VX (compared to other OP nerve agents) and the limited metabolic capacity of *ex vivo* skin, this quantified amount of ^{14}C is assumed to be the parent compound for the purposes of analysis[108,110,130]. However, the possibility that breakdown products may account for some of the quantified ^{14}C cannot be ignored.

Indeed, the increased penetration kinetics induced by RSDL here are in apparent contrast with the efficacy of RSDL already demonstrated *in vivo*[38,105]. This apparent inconsistency may be partly explained by penetration of, and thus quantification of, decontamination products, rather than ^{14}C-VX. Additionally, in contrast to previous studies, RSDL was not removed in this experiment.

The uncertainty of the exact molecules which are quantified in the mass balance should not affect the qualitative net interpretation of the results, *viz* toxicity *in vivo*, as some of the known metabolites and breakdown products of VX are also toxic. Gas chromatographic and mass spectrometric analysis of solvent extracts from the skin (or other exposed areas) would

address this uncertainty and enable speciation of penetrated substances. This would be particularly useful for products where the primary mechanism of action is to decontaminate exposed skin, rather than prevent or reduce penetration.

The total recovery of ^{14}C-VX from RSDL treated cells was above 100% of the applied mass: this is most notable in the recovery of ^{14}C-VX from the decontaminant fraction alone (Figure 4.14) and thus the significant difference in recovery from the decontaminant fraction between RSDL and VG or FA is not surprising. The standard deviation for the ^{14}C-VX quantification for the RSDL treatment condition is large and reflects large variations in the quantification of ^{14}C-VX in the different fractions between the individual replicates. Reasons for this variation could include a chemiluminescence effect of RSDL influencing scintillation counts (which could be determined with further investigation); dosing errors resulting in variations in the amount of ^{14}C-VX applied to the individual skin sections or decontaminant standard reference samples for this condition; or sampling errors. Consequently the ^{14}C-VX quantification data for the RSDL condition are unreliable. In the damaged skin model, the ^{14}C-VX extracted from WS and PQR conditions (the "not penetrated" fraction, and in particular the decontaminant fraction) were also calculated to be above 100% of the applied mass, so the significant difference between those treatments and QC and FE are also unsurprising (Figure 4.19). Similarly, sampling or dosing errors (either of the reference decontaminant standards or the skin sections) may have contributed to this error. A further possibility is that if these particular decontaminants had a quenching effect on scintillation, any variations in mass of the decontaminant between the reference standards and experimental samples may have resulted in samples being quenched to different extents. Insufficient mixing of the decontaminant during extraction may also have contributed to this

observation. The ^{14}C-VX quantification data for the WS and PQR decontaminant fraction (in the damaged skin model) are unreliable, although further experiments would be useful to investigate these observations further.

The effectiveness of products as a function of dose was not investigated in this study. A set dose of 200mg was added to 10µl of contaminant. As described earlier (chapter 1 & 3), *in vivo* studies of haemostats generally use much higher ratios of product to blood in order to more accurately model "in use" (emergency) conditions[7]. Analysis of the effects of product dose on decontamination ability may be useful for product development. However, inability of a product to prevent or reduce VX penetration (at a given dose of product) whilst other products are effective at the same dose, should preclude its inclusion in further studies.

In this *in vitro* experiment of percutaneous penetration, the mechanism by which these haemostatic products are presumed to reduce penetration of VX is by adsorption of the contaminant onto or into the product matrix. Previously, the possibility that discrepancies in product efficacy between *in vitro* and *in vivo* models was due to dose-response effects or mechanism of action was put forward. For example, it was suggested that QC may not act (primarily) via passive absorption to promote blood coagulation (Chapter 3). The apparent contradiction of this suggestion by the results of the diffusion cell study may partly be explained by the higher ratio of product mass to contaminant mass (1µl VX: 9mg product for TEG; 1µl VX : 20mg product for diffusion cells). Reactions with VX on the surface of the decontaminants may also be involved.

The dose of VX applied (5.7mg cm^{-2}; 10µl volume) in this study was intended to be representative of a "worst-case" scenario: indeed, this models a finite dose *in vivo*[101] and

represents a multiple LD_{50} for both humans and pigs[58]. An apparent inability to reduce or prevent absorption of this dose would preclude inclusion of a product in further studies of decontamination of a multiple LD_{50} *in vivo*.

Furthermore, the test decontaminants remained in contact with the skin for the duration of the experiment. This contrast to standard "in-use" procedure enabled identification of products which were immediately ineffective, or products in which efficacy may be inversely proportional to length of exposure (Figure 4.20). Indeed, the mass of unabsorbed contaminant may arguably be considered as "mass available to penetrate with prolonged exposure". Desorption kinetics for test decontaminants is also an important point for product development with regards to secondary exposure due to "off-gassing". Therefore, desorption kinetics along with gas chromatographic and speciation analysis studies would be important to assess "in-use" efficacy of test decontaminants.

In comparison with other chemical warfare agents (such as sulphur mustard), enhanced penetration caused by occlusion of exposed skin is perhaps less likely for VX due to its relative lower volatility[105,131–133]. For volatile compounds, certain vehicles may act occlusively by preventing evaporation[132]. In this experiment, occlusion did not significantly enhance the penetration of ^{14}C-VX across intact pig abdominal skin. The novel liquid decontaminant mixture, TOP, significantly reduced penetration of ^{14}C-VX. In that case, the enhanced penetration kinetics observed following treatment with the other liquid products, VG and FA (and RSDL as described previously) may partly be explained by (a) reactions between VX and the vehicle, or; (b) reactions between the vehicle and the skin resulting in increased permeability.

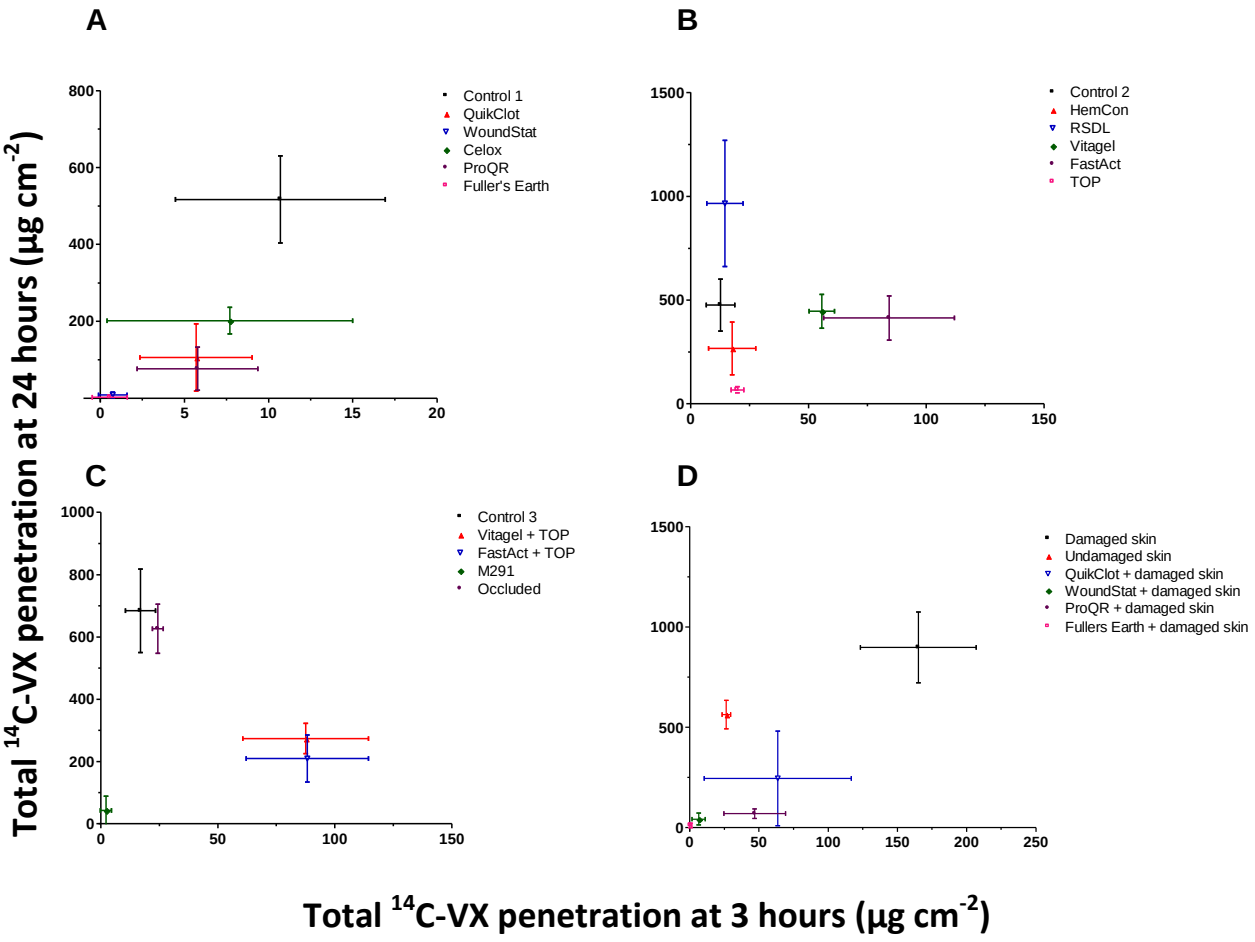

Figure 4.20: Short-term and long-term efficacy of test decontaminants on penetration of ^{14}C-VX across intact skin (n=6): (A) Study 1; (B) Study 2; (C) Study 3; and damaged skin: (D) Study 4.

In summary, the results of this *in vitro* diffusion cell study of ^{14}C-VX penetration across pig abdominal skin demonstrated:

- Enhanced permeability of pig skin following removal of the uppermost ~100µm layer.
- That four haemostatic products (WS, QC, PQR, CX) and a novel liquid decontaminant mixture (TOP) have demonstrable efficacy in reducing penetration of VX across undamaged skin.
- That three haemostatic products (WS, QC, PQR) have demonstrable efficacy in reducing penetration of VX across damaged skin, to a similar level as the currently "in-use" military decontaminant, Fuller's Earth.

Taken together with the favourable pro-coagulative characteristics measured by TEG (Chapter 3), WoundStat was advanced for further assessment in an *in vivo* model of percutaneous VX exposure in swine.

This study has identified the need for further work in the following areas:

- Dose-response effects of contaminant penetration at finite doses.
- Dose-response effects of test decontaminants on penetration of contaminants.
- More detailed characterisation of anatomical differences in penetration between species.
- Reactions between contaminants and decontaminant vehicles.
- Speciation analysis of resultant mixtures following decontamination.

Desorption ("off-gassing") kinetics (and speciation analysis) for test decontaminants.

CHAPTER 5. Decontamination of ^{14}C-VX applied to damaged skin *in vivo*

CHAPTER 5. DECONTAMINATION OF ^{14}C-VX APPLIED TO DAMAGED SKIN *IN VIVO*

5.1 Introduction

The skin is a potential route of entry for toxic organophosphate nerve agents such as VX. The toxicity of these compounds clearly prohibits investigations in humans. Much of the data relating to toxicity, and indeed, decontamination, of nerve agents is obtained from *in vivo* models. Swine models are frequently chosen as a closely representative model for extrapolation or prediction of effects in humans, following skin exposure to VX. The efficacy of decontamination products or regimes, in response to VX exposure, has been demonstrated in swine models[105,134].

An increased hazard was demonstrated by the enhanced penetration kinetics of ^{14}C-VX across damaged pig skin measured *in vitro* (Chapter 4), along with the efficacy of WoundStat™, a haemostatic product, to counter this effect. WoundStat™ was also one of a small number of haemostatic products which retained demonstrable pro-coagulative characteristics in the presence of VX, *in vitro*. The aim of a haemostatic decontaminant would be to facilitate haemostasis in the presence of contaminants and prevent fatal toxicity. An *in vivo* feasibility study of swine exposure to VX via superficially damaged skin, and subsequent treatment with a test decontaminant, should provide useful, empirical toxicokinetic data, which may be used as evidence to either support or reject further investigation of this product as a potential haemostatic decontaminant. Hence, the purpose

of this study was to assess the efficacy of the haemostat WoundStat as a decontaminant on a VX-exposed, non-haemorrhaging, superficial wound *in vivo*.

5.2 Materials and Methods

The materials and methods are described in detail in Chapter 2 and are briefly outlined in Figure 5.1.

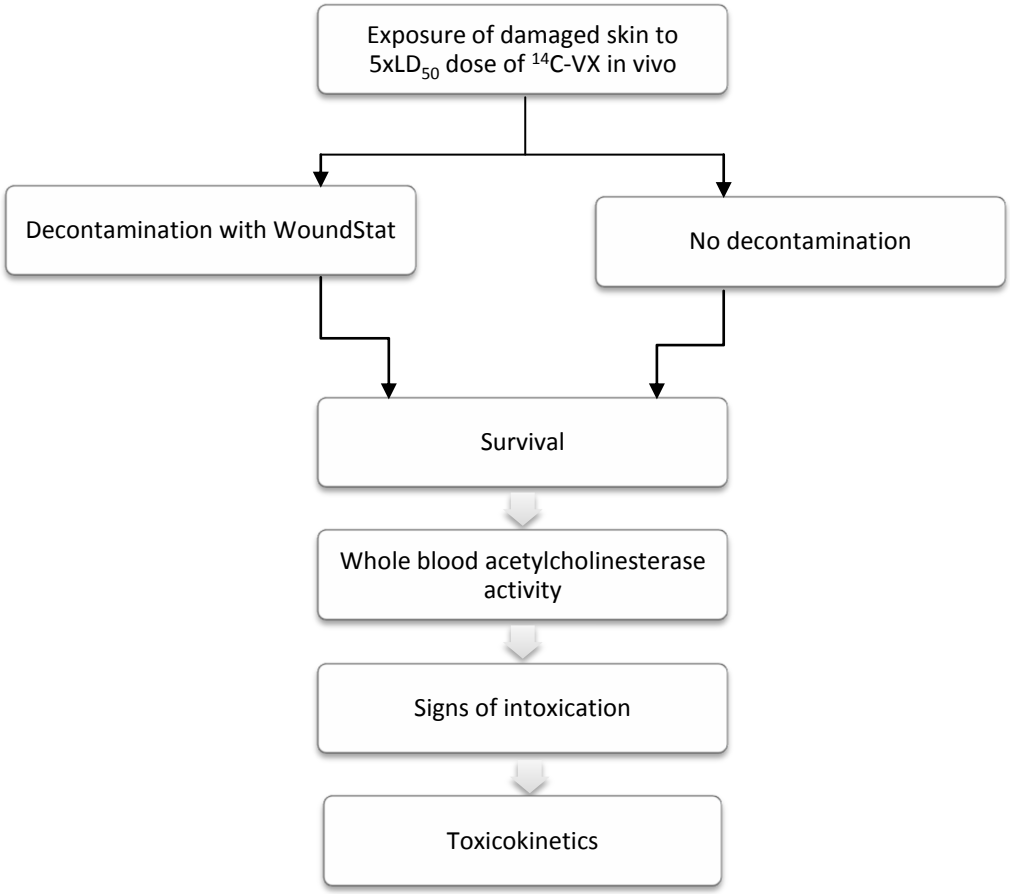

Figure 5.1: Workflow design for the *in vivo* analysis of the efficacy of the haemostatic product WoundStat as a decontaminant.

5.3 Results

5.3.1 Animal weight and dosage

The weights of all 31 animals included in the study were normally distributed (Shapiro-Wilk test). The mean body weight was 20.6 ± 1.6kg (mean ± standard deviation; range 16.6-23.1kg) and there was no significant difference in mean body weight between groups (Figure 5.2). The mean mass of ^{14}C-VX applied to the skin was 6.3 ± 0.4mg (range 5.4–7.0mg).

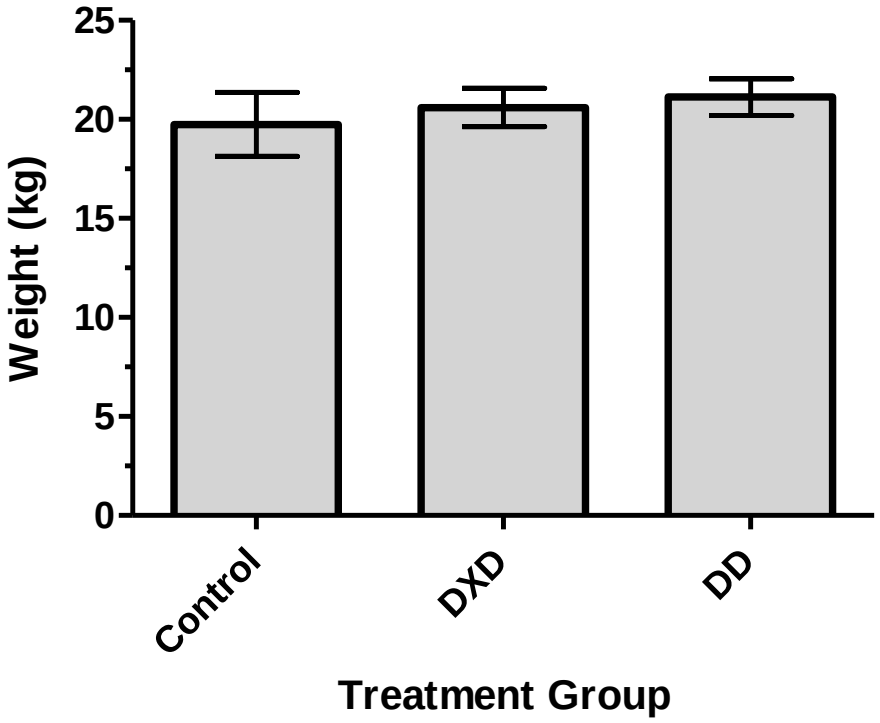

Figure 5.2: Body weight (mean ± standard deviation) of swine included in the ^{14}C-VX exposure and decontamination study, measured prior to commencement of the experiment. Animals were fasted overnight before the experiment and allowed access to water *ad libitum*. Body weight did not significantly differ between the control (n=7), not-decontaminated (DXD, n=12) and decontaminated (DD, n=12) groups ($p>0.05$).

5.3.2 Survival

1. Survival fractions and curve analysis

After 360 minutes the survival fractions were 100% (6/6) in the control group; 92% (11/12) for the decontaminated group; and 25% (3/12) for the not-decontaminated group. Gehan-Brislow-Wilcoxon analysis showed that the survival curve for the not-decontaminated (DXD) group differed significantly from that of control group ($p<0.01$), and the decontaminated (DD) group (Figure 5.3).

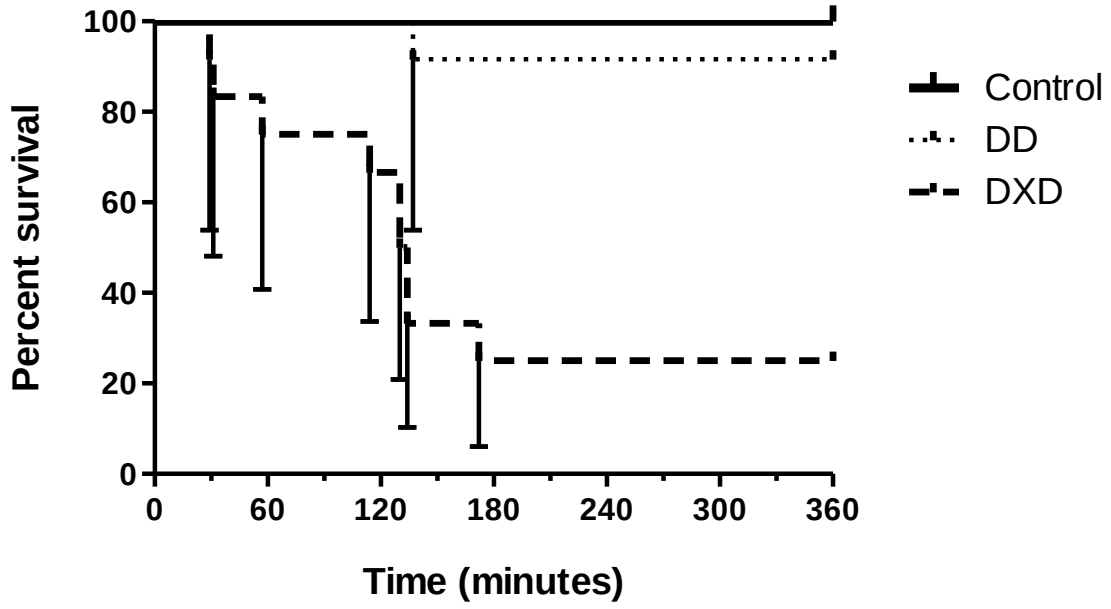

Figure 5.3: Survival curve for anaesthetised swine exposed to a 5xLD_{50} (300µg kg^{-1}) dose of neat ^{14}C-VX via damaged ear skin (DXD; n=12); similarly exposed swine treated with a test decontaminant (DD; n=12); and anaesthetised control (un-exposed) animals (mean percentage of group survival ± 95% confidence interval).

The survival curve for the DXD group differed significantly from the control group and the DD group (Gehan-Brislow-analysis; $p<0.01$).

2. Survival time

The mean survival times for the non-decontaminated group and decontaminated group were 168 ± 79 and 341 ± 41 minutes respectively (mean ± 95% CI; Figure 5.4). The survival time for the not-decontaminated group was significantly lower than the control ($p<0.01$) and decontaminated ($p<0.01$) groups.

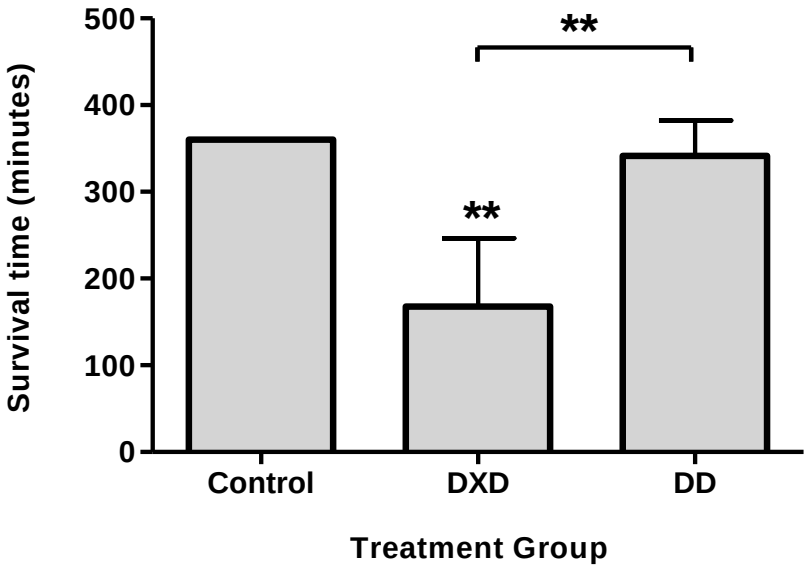

Figure 5.4: Mean survival times for anaesthetised swine exposed to a 5xLD_{50} (300µg kg^{-1}) dose of neat ^{14}C-VX via damaged ear skin (DXD; n=12); similarly exposed swine treated with a test decontaminant (DD; n=12); and anaesthetised control (un-exposed) animals (mean percentage of group survival ± 95% confidence interval).

Asterisks indicate groups with mean survival times which are significantly different to that of the control group (**p<0.01). The bar indicates a significant difference in survival time between treatment groups (**p<0.01).

5.3.3 Acetylcholinesterase activity

1. Effect of ^{14}C-VX exposure on whole blood acetylcholinesterase activity

There were no significant differences in whole blood acetylcholinesterase (AChE) activity in the control group at 15, 60, or 360 minutes (during the 6 hour observation period[1].

Exposure to ^{14}C-VX resulted in a rapid, significant decrease in whole blood AChE activity, to below 30% of mean pre-dose activity within 15 minutes for both exposed groups ($p<0.05$; Figure 5.5). At 15, 60 and 360 minutes post-exposure, mean whole blood AChE activity of the exposed animals was significantly lower than non-exposed controls[2]. Whole blood AChE activity was not significantly different between the exposed groups at 15, 60 or 360 minutes post-exposure).

[1] *Data for the intervening timepoints for the control group are unavailable.*
[2] *NB: only 3 animals in the DXD groups survived to 360 minutes which may reduce the power of these interpretations.*

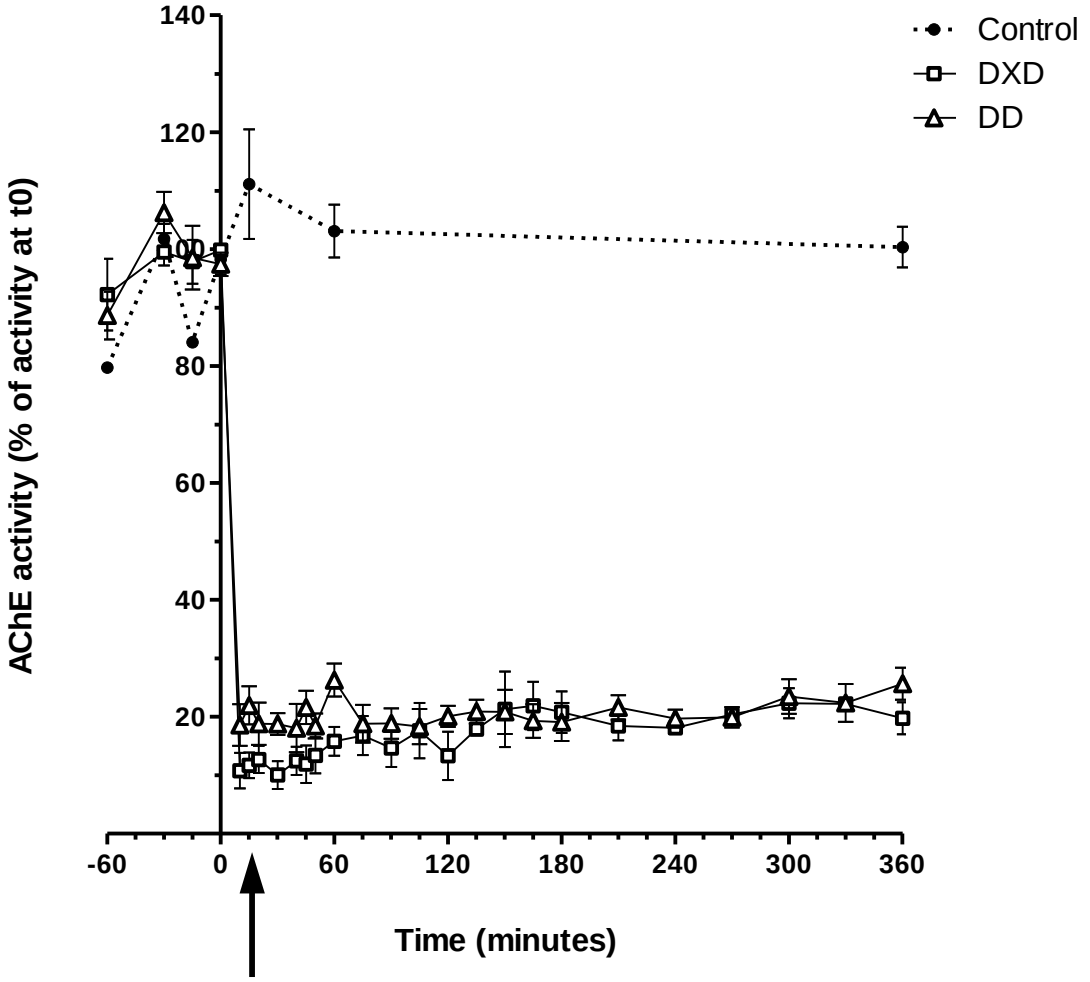

Figure 5.5: Whole blood acetylcholinesterase (AChE) activity of anaesthetised swine exposed to a 5xLD_{50} (300µg kg^{-1}) dose of neat ^{14}C-VX via damaged ear skin (DXD; n=12); similarly exposed swine treated with a test decontaminant (DD; n=12); and anaesthetised control (un-exposed) animals (mean ± SEM).

Data presented are relative to the mean activity at time of dose, or 0 minutes for controls. Within 15 minutes post-exposure, AChE activity decreased to below 30% of mean pre-dose levels (indicated by arrow; $p<0.05$) and remained significantly lower than that of control animals for the remainder of the exposure period.

2. Whole blood acetylcholinesterase activity at time of death.

For animals exposed to ^{14}C-VX, whole blood AChE activity of the final blood sample (i.e. at the time of death or 360 minutes post-exposure) was significantly lower than that of control animals (after 360 minutes anaesthesia). Whole blood AChE activity of the final blood sample was not significantly different between the decontaminated and not-decontaminated groups (Figure 5.6).

Furthermore, in animals which did not survive the 6 hour exposure period, the AChE activity at time of death did not correlate with survival time (Spearman's rank-order correlation coefficient analysis; Figure 5.7).

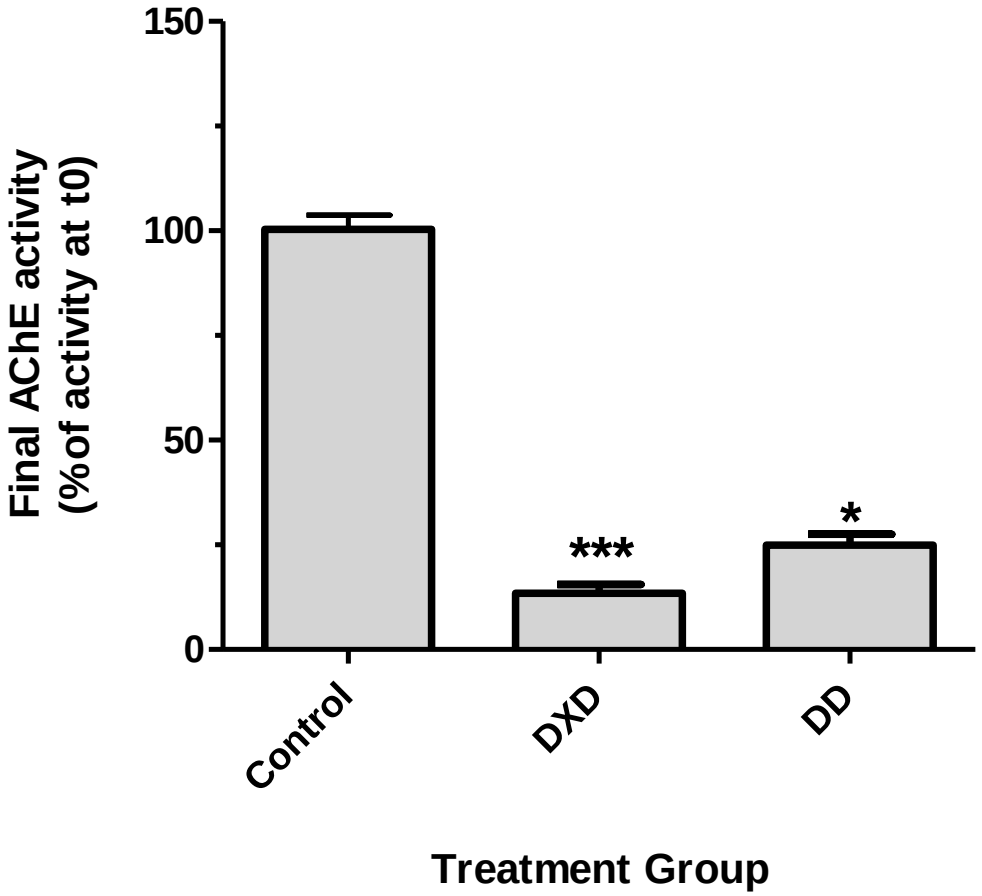

Figure 5.6: Whole blood acetylcholinesterase activity (relative to that of time zero) of the final blood sample obtained from anaesthetised swine exposed to a $5xLD_{50}$ (300µg kg^{-1}) dose of neat ^{14}C-VX via damaged ear skin (DXD; n=12); similarly exposed swine treated with a test decontaminant (DD; n=12); and control (un-exposed) animals (mean ± SEM).

The final blood sample was taken either at the time of death or 360 minutes post-exposure in surviving animals. Asterisks indicate a significant difference between ^{14}C-VX-exposed groups (DXD and DD) and control group (*$p<0.05$; ***$p<0.001$). There was no significant difference between the DXD and DD groups.

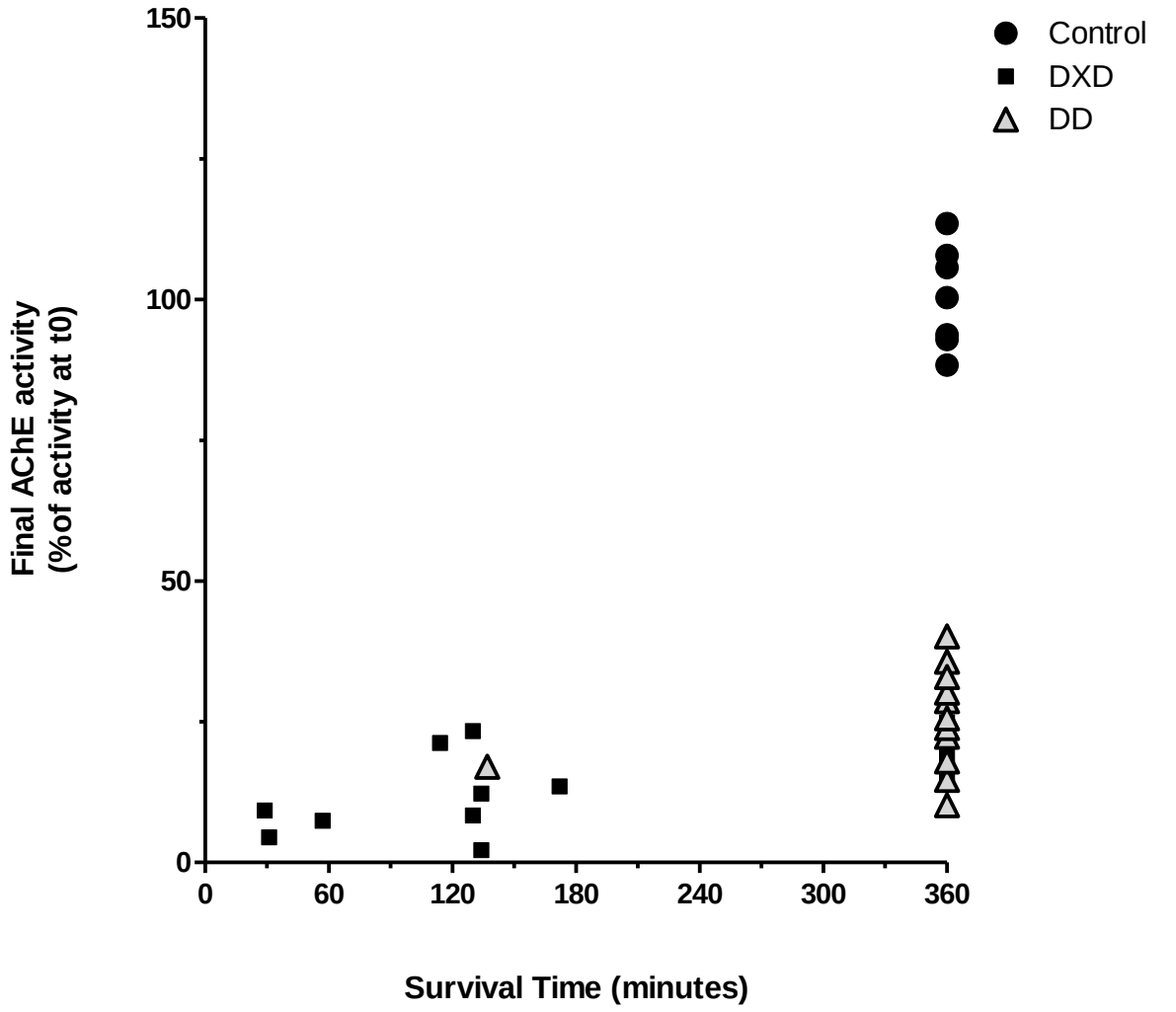

Figure 5.7: Individual scatter plot relating AChE activity of the final blood sample (relative to pre-dose activity) to survival time (up to 6 hours) of anaesthetised swine exposed to a 5xLD_{50} (300µg kg^{-1}) dose of neat ^{14}C-VX via damaged ear skin (DXD; n=12); similarly exposed swine treated with a test decontaminant (DD; n=12); and control (un-exposed) animals (mean ± SEM).

When surviving animals were excluded, Spearman's rank-order correlation coefficient analysis showed no significant correlation between AChE activity at time of death and survival time.

5.3.4 Toxicokinetics

Analysis of ^{14}C-VX recovery and distribution was conducted in cohort 2 only. Toxicokinetic data are presented as the percentage of applied mass which was recovered from each compartment (mean ± standard deviation), rather than the total mass, to account for the variation in mass of ^{14}C-VX applied according to differences in animal weight. Data were analysed by Mann-Whitney tests.

1. Total recovery

Total ^{14}C-VX recovery in the decontaminated group (55 ± 11% of the applied mass) was significantly higher than that of the non-decontaminated group (20 ± 4.1% of applied mass; $p<0.01$; Figure 5.8).

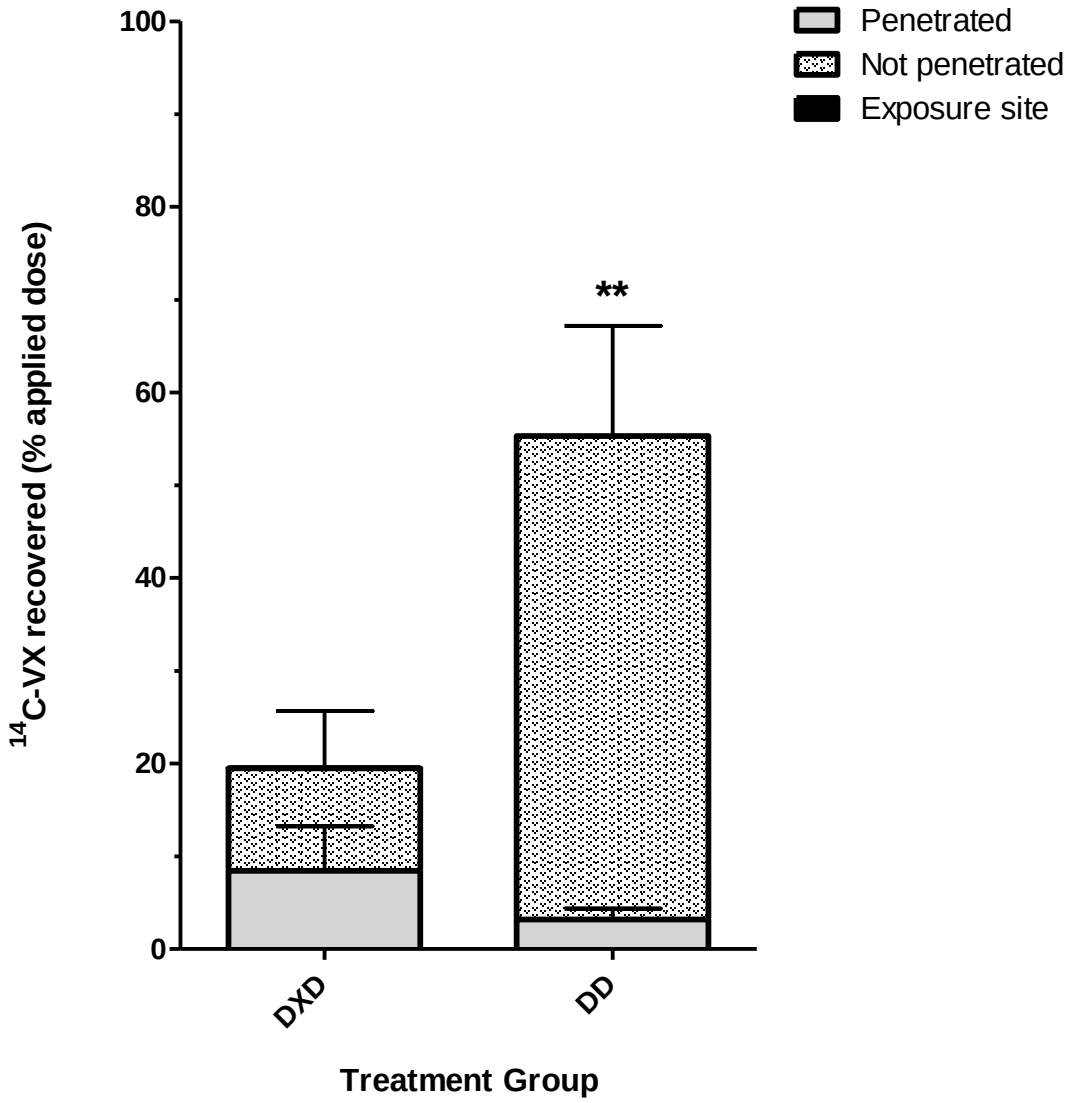

Figure 5.8: Total post-mortem recovery (and distribution) of ^{14}C-VX from anaesthetised swine exposed to a 5xLD_{50} (300µg kg^{-1}) dose of neat ^{14}C-VX via damaged ear skin (DXD; n=6); and similarly exposed swine (DD; n=6) treated with a test decontaminant (percentage of mass applied; mean ± standard deviation).

Total recovery of ^{14}C-VX was significantly lower in the DXD group compared to the DD group (**$p<0.01$). Total recovery of ^{14}C-VX from the exposure site was not above 0.05% in either treatment group.

2. Not penetrated

Recovery of ^{14}C-VX from the not penetrated fraction (decontaminant, dose chamber and swabs) was significantly higher in the decontaminated group (52 ± 12% of the applied mass) than in the non-decontaminated group (11 ± 6.2%; $p<0.01$; Figure 5.9).

Decontaminant

For the decontaminated group, the ^{14}C-VX extracted from the collected WoundStat accounted for 47 ± 12% of the applied mass (range 34 – 66%; Figure 5.10). Indeed, this also accounted for the bulk of the total ^{14}C-VX recovery (as shown in Figure 5.8).

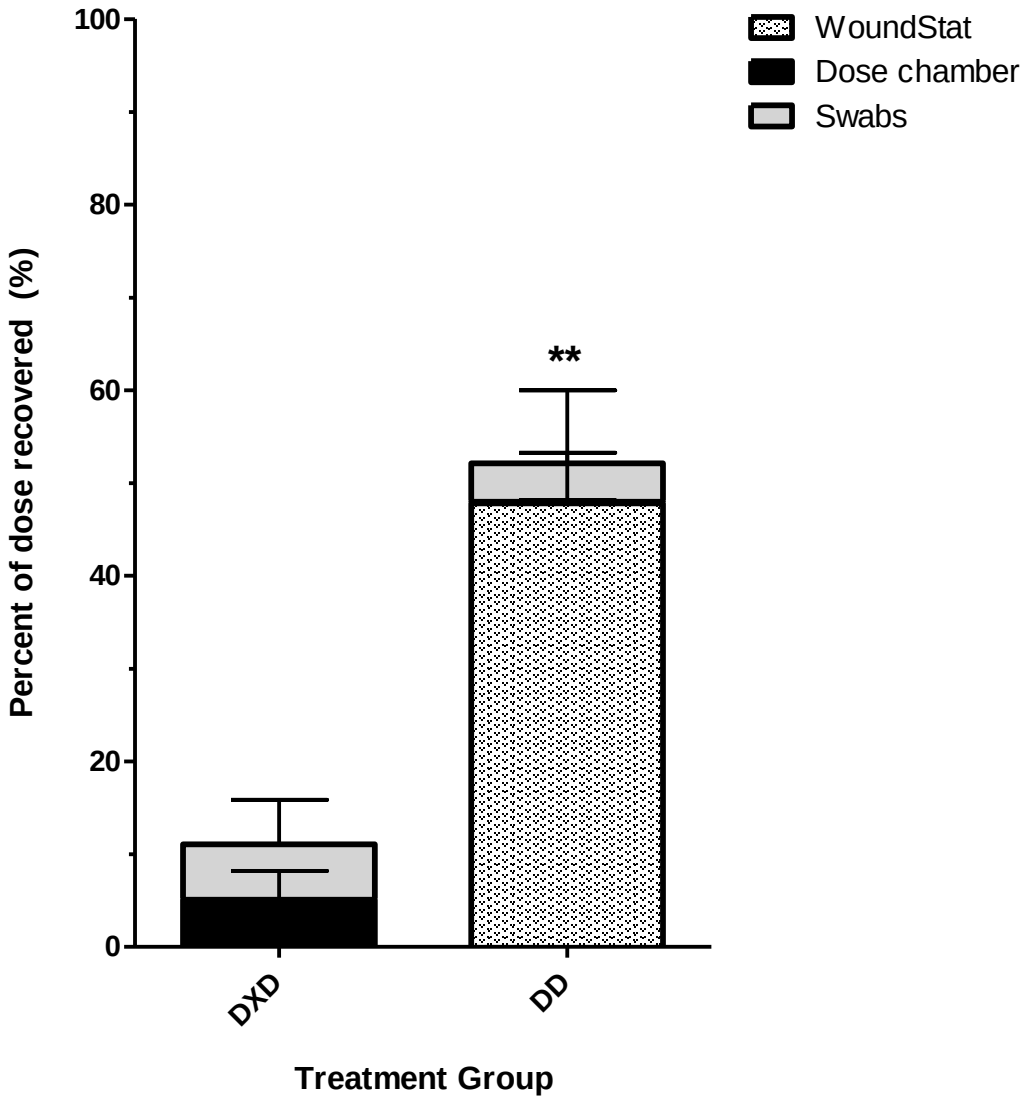

Figure 5.9: Total post-mortem recovery of ^{14}C-VX in the "not penetrated" fraction from anaesthetised swine exposed to a 5xLD_{50} (300µg kg^{-1}) dose of neat ^{14}C-VX via damaged ear skin (DXD; n=6); and from similarly exposed swine treated with a test decontaminant (WoundStat; DD; n=6).

The total recovery is presented relative to the applied mass (%; mean ± standard deviation). The amount of ^{14}C-VX which was not penetrated was significantly higher in the decontaminated group (**$p<0.01$): the bulk of this was extracted from the decontaminant itself.

Dosing chamber and swabs

Recovery of ^{14}C-VX from the dosing chambers was significantly higher for the DXD group (5.1 ± 3.1% of the applied dose) compared to the DD group (0.18 ± 0.17%; $p<0.01$; Figure 5.11A). Recovery from swabs of the exposure site was 6.0 ± 4.8% in the DXD group and 4.1 ± 1.1% for the DD group (figure 5.10B). The bulk of this was removed in the first swab compared to subsequent swabs (up to 3 per animal) and there was no significant difference in recovery of ^{14}C-VX from swabs between treatment groups.

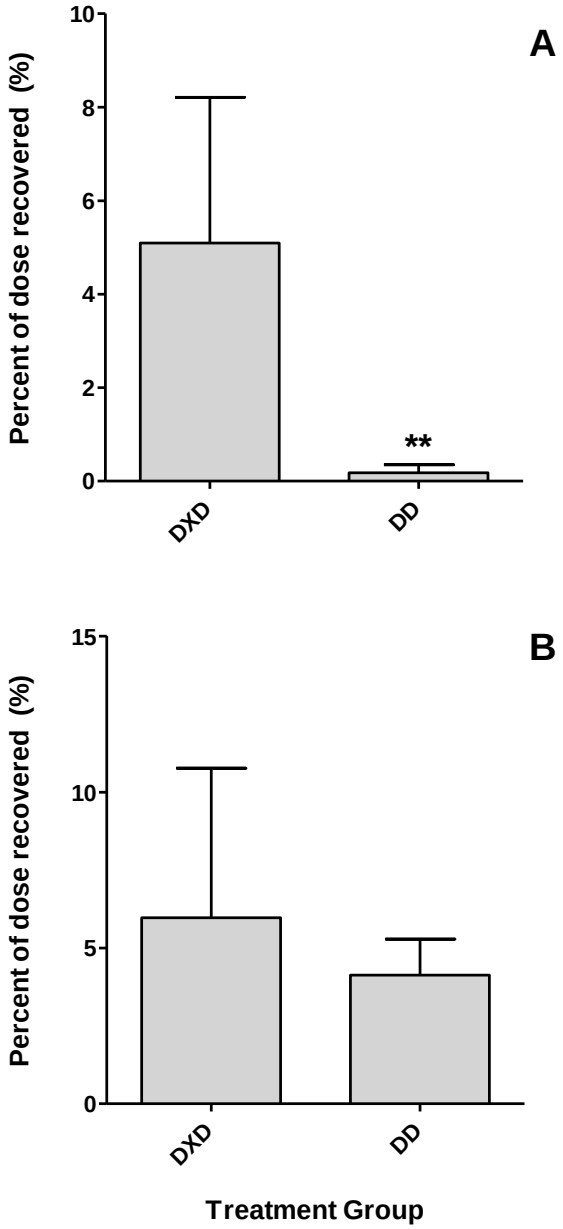

Figure 5.10: Total post-mortem recovery of ^{14}C-VX from the dosing chamber (A) and swabs of the exposure site (B), taken from anaesthetised swine exposed to a 5xLD_{50} (300µg kg^{-1}) dose of neat ^{14}C-VX via damaged ear skin (DXD; n=6); and from similarly exposed swine treated with a test decontaminant (DD; n=6).

The total recovery is presented relative to the applied mass (%; mean ± standard deviation). A significantly larger amount of ^{14}C-VX was extracted from the dose chambers in the not decontaminated group compared to the decontaminated group (**$p<0.01$). Swabs of the exposed skin recovered similar amounts of ^{14}C-VX in both groups.

3. Exposure site

The mean recovery of ^{14}C-VX from the exposed skin sections, excised from non-decontaminated animals (0.018 ± 0.0074% of the applied mass), was significantly higher than that from decontaminated animals (0.0011 ± 0.081 %; $p<0.01$; Figure 5.11).

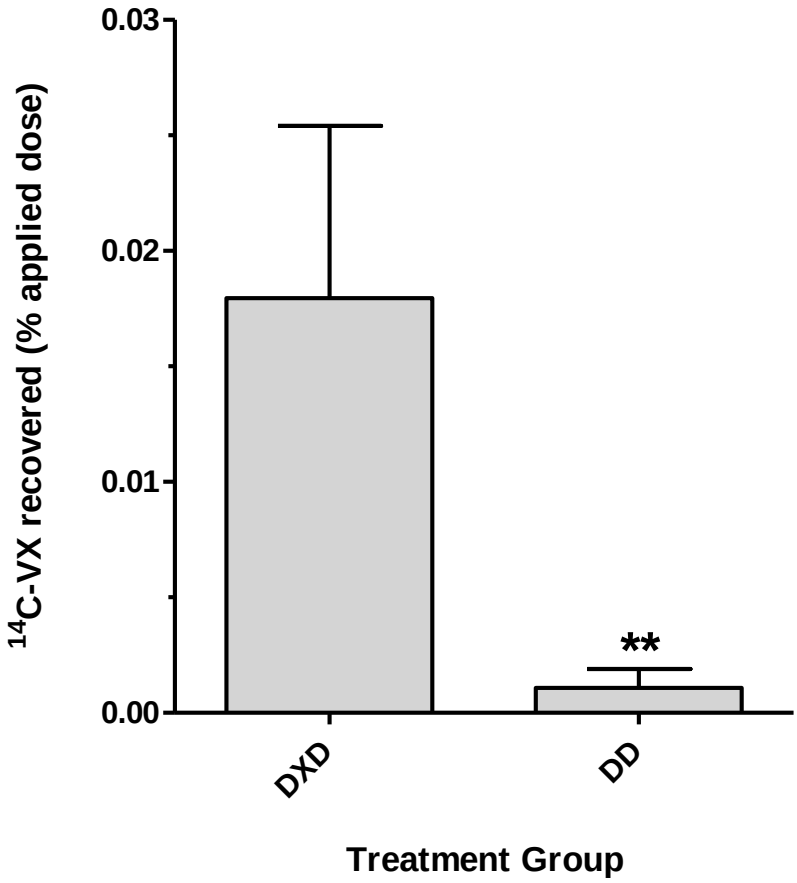

Figure 5.11: Total post-mortem recovery of ^{14}C-VX from solubilised, exposed skin sections, excised from anaesthetised swine exposed to a 5xLD_{50} (300µg kg^{-1}) dose of neat ^{14}C-VX via damaged ear skin (DXD; n=6); and from similarly exposed swine treated with a test decontaminant (DD; n=6).

The total recovery is presented relative to the applied mass (%; mean ± standard deviation). Significantly less ^{14}C-VX was recovered from the decontaminated exposure sites compared to the not-decontaminated sites (**$p<0.01$).

4. Absorbed

The total ^{14}C-VX recovered from the sampled organs was not significantly different between groups (Figure 5.12). Recovery from the liver accounted for the bulk of the absorbed fraction in both groups' liver (5.1 ± 3.2% and 1.9 ± 0.64% in the DXD and DD groups respectively); followed by the blood (1.9 ± 1.3% and 0.79 ± 0.45% in the DXD and DD groups respectively).

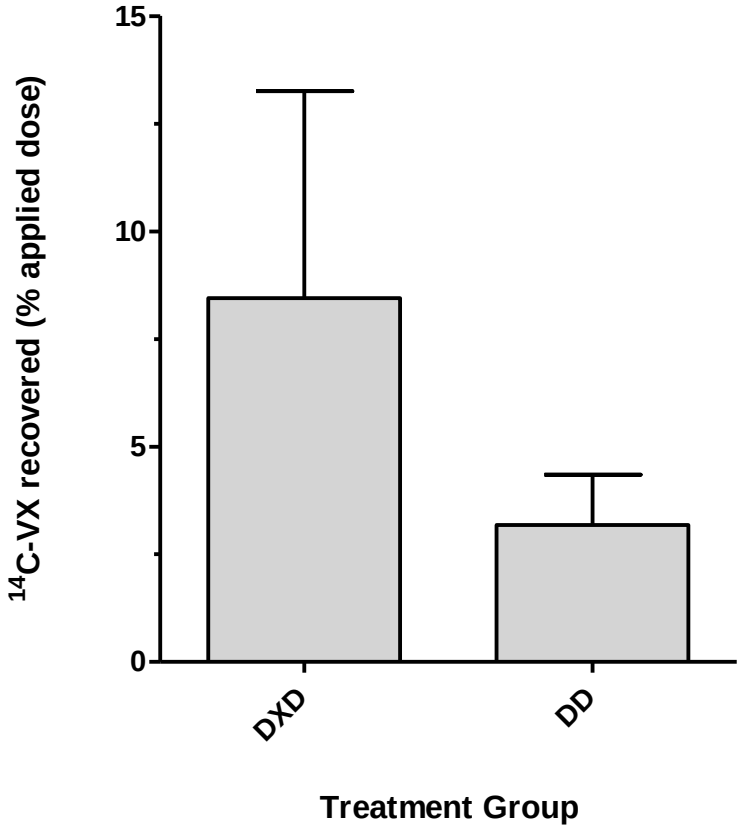

Figure 5.12: Total ^{14}C-VX recovered from the sampled organs, post-mortem, from anaesthetised swine exposed to a 5xLD_{50} (300µg kg^{-1}) dose of neat ^{14}C-VX via damaged ear skin (DXD; n=6); and from similarly exposed swine treated with a test decontaminant (DD; n=6).

The total recovery is presented relative to the applied mass (%; mean ± standard deviation) and there was no significant difference in total internal recovery between groups.

Internal organs

The mean mass (g) of the heart and liver of decontaminated animals was significantly lower than that of the not-decontaminated animals (Figure 5.13; $p<0.05$).

For both treatment groups, the largest amount of ^{14}C-VX recovered internally was located in the liver, followed by the blood, then kidney, (Figure 5.14). The brains, hearts, lungs and spleens of the non-decontaminated group contained significantly higher amounts of ^{14}C-VX compared to those of decontaminated animals (Figure 5.14). Recoveries of ^{14}C-VX from brain, heart, lung and spleen were significantly higher in the non-decontaminated group compared to the decontaminated group ($p<0.05$; Figure 5.14). The concentration of radiolabel in the diaphragm was also significantly higher in not-decontaminated animals than decontaminated animals ($p<0.05$), whilst ^{14}C-VX in the pancreas did not differ significantly between groups (Figure 5.15)[1].

[1] *As the total organ weights for pancreas and diaphragm could not be measured assuredly, the concentration of radiolabel (µg ^{14}C-VX g tissue^{-1}) in these organs was measured.*

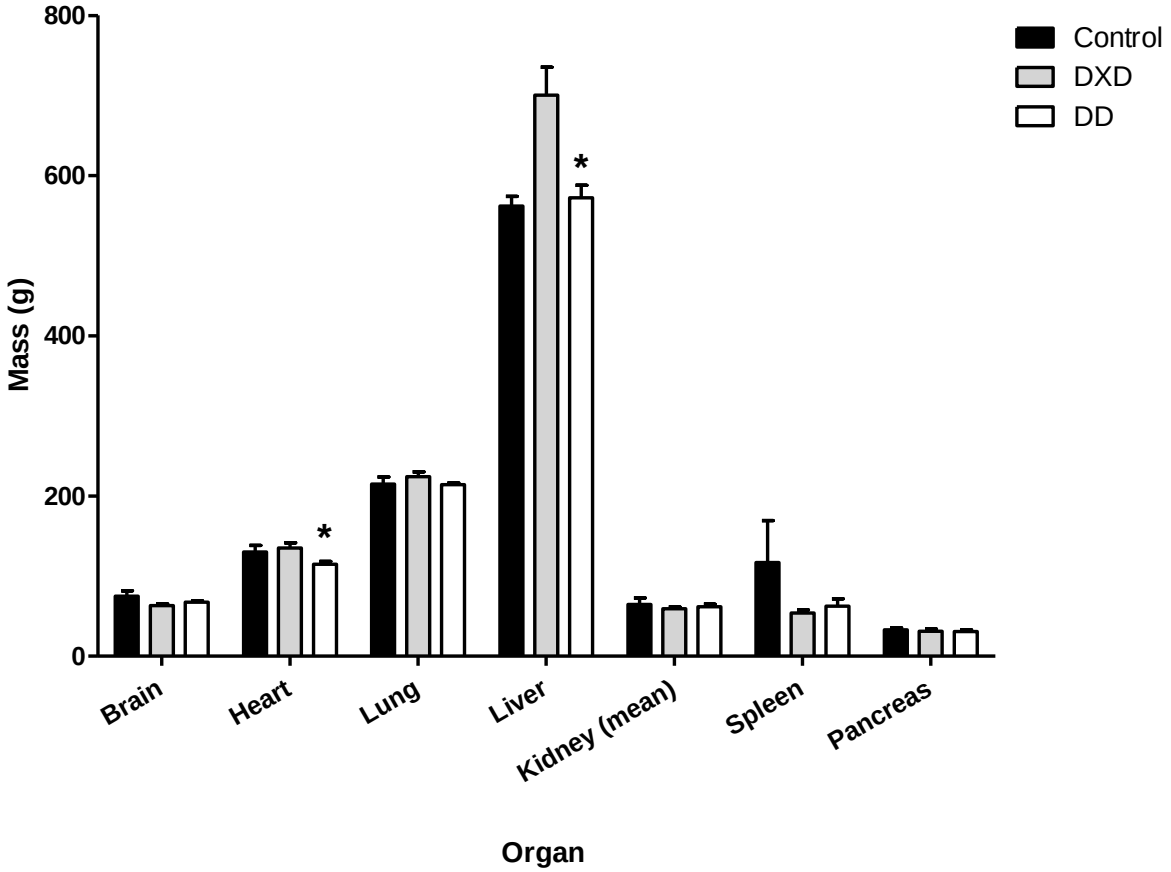

Figure 5.13: Mean (± standard error) mass of organs measured post-mortem, following 6 hours anaesthesia (control); exposure to 5xLD_{50} neat ^{14}C-VX via damaged ear skin untreated (DXD; survival time ranged from 29-360 minutes); and decontaminated (DD; survival time ranged from 137 to 360 minutes).

Asterisks indicate a significant ($p<0.05$) difference in heart and liver mass between DD and DXD groups. The data for the kidney is the mean mass of right and left kidneys per individual.

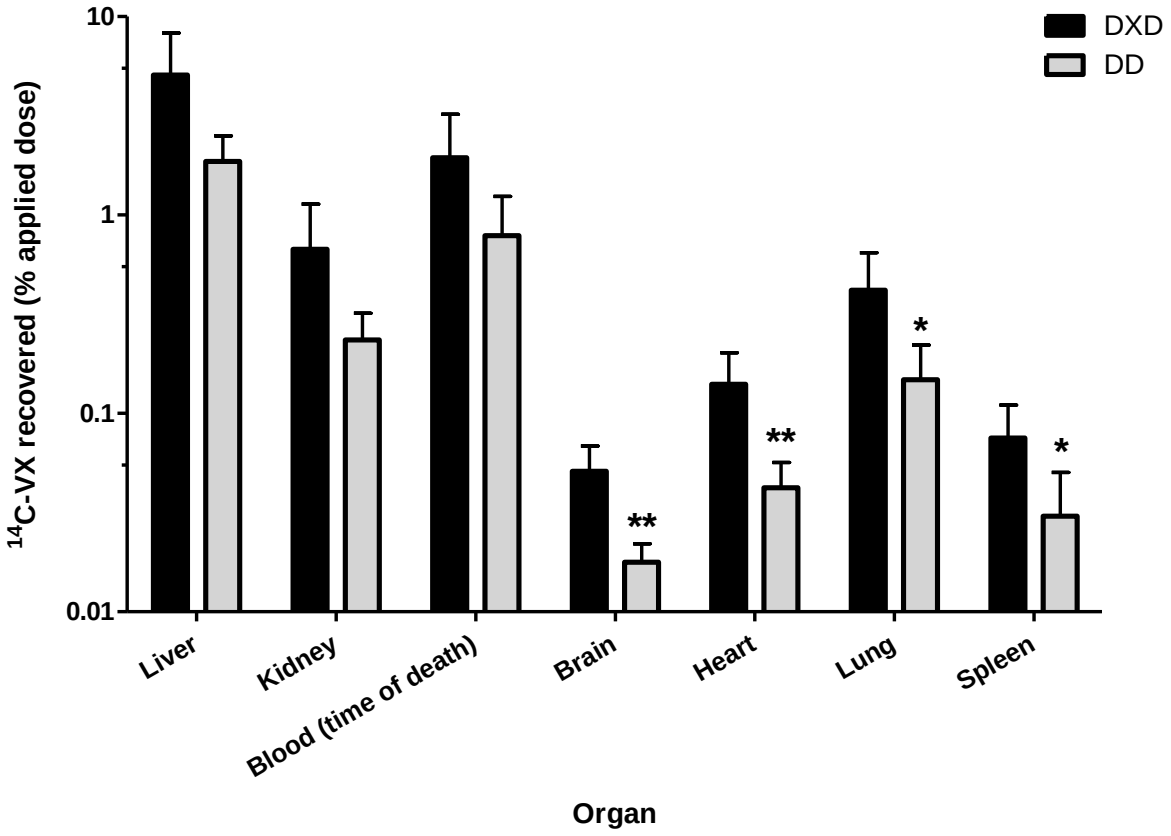

Figure 5.14: Distribution of ^{14}C-VX in specified organs, recovered (post-mortem) from anaesthetised swine exposed to a 5xLD_{50} (300µg kg^{-1}) dose of neat ^{14}C-VX via damaged ear skin (DXD; n=6); and from similarly exposed swine treated with a test decontaminant (DD; n=6).

The total recovery is presented relative to the applied mass (%; mean ± standard deviation). Asterisks indicate significant differences between treatment groups (*p<0.05; **p<0.01).

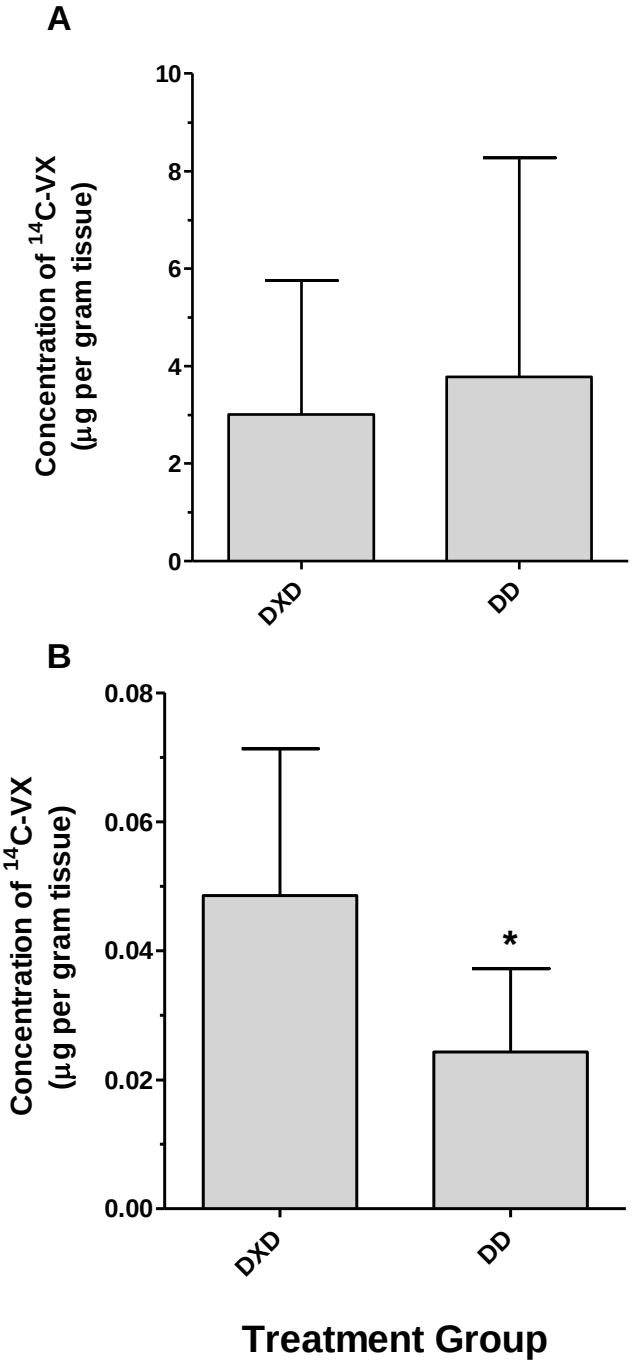

Figure 5.15: Concentration of ^{14}C-VX (µg g tissue^{-1}) in pancreas (A) and diaphragm (B), recovered (post-mortem) from anaesthetised swine exposed to a 5xLD_{50} (300µg kg^{-1}) dose of neat ^{14}C-VX via damaged ear skin (DXD; n=6); and from similarly exposed swine treated with a test decontaminant (DD; n=6).

The total recovery is presented relative to the applied mass (%; mean ± standard deviation). Asterisks indicate significant differences between treatment groups (*p<0.05).

Blood

The concentration of ^{14}C-VX in blood became significantly different between the DXD and DD groups at 120 minutes post-exposure ($p<0.05$; Figure 5.17)[1]. There was no significant difference between groups in concentration of ^{14}C-VX in blood at the time of death (described previously, Figure 5.14). However, the animals that died at 20, 105 (DXD) and 135 minutes (DD) after exposure had quantitatively lower ^{14}C-VX concentration in their final blood sample compared to the mean concentrations at other timepoints in their respective groups (Figure 5.16).

In animals which survived to 6 hours (in either group), radiolabel concentration generally (but not exclusively) decreased as time progressed (Figure 5.17). In contrast, the highest concentrations of radiolabel in the non-decontaminated animals which did not survive to 6 hours were detected in the final blood samples (time of death).

[1] *However only 2 animals in the DXD group, cohort 2, survived past 120 minutes which may reduce power of statistical comparisons beyond this point.*

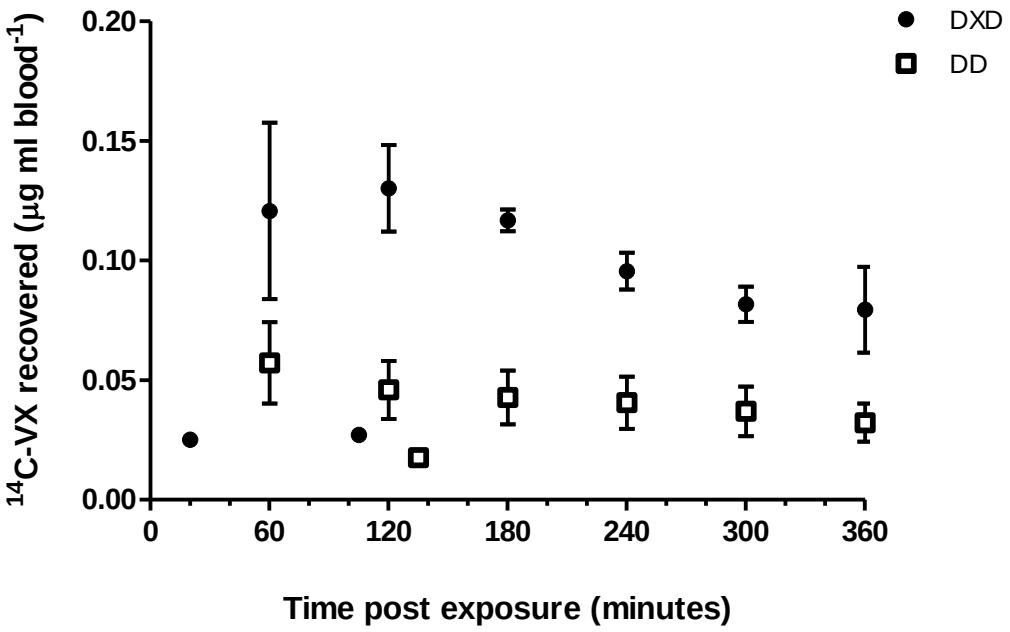

Figure 5.16: Concentration (mean ± SEM) of ^{14}C-VX in consecutive blood samples of anaesthetised swine exposed to a 5xLD_{50} (300µg kg^{-1}) dose of neat ^{14}C-VX via damaged ear skin (DXD; n=6); and from similarly exposed swine treated with a test decontaminant (DD; n=6).

Concentration became significantly different between the decontaminated (DD) and not-decontaminated groups (DXD) at 120 minutes[1]. The individual plots of concentration for animals which died at 20, 105 and 135 minutes are also presented: these were quantitatively lower than the mean concentrations of their respective groups at other time-points.

[1] *Only 2 animals in the DXD group survived longer than 120 minutes so statistical comparisons between exposed groups are not powerful beyond this time-point.*

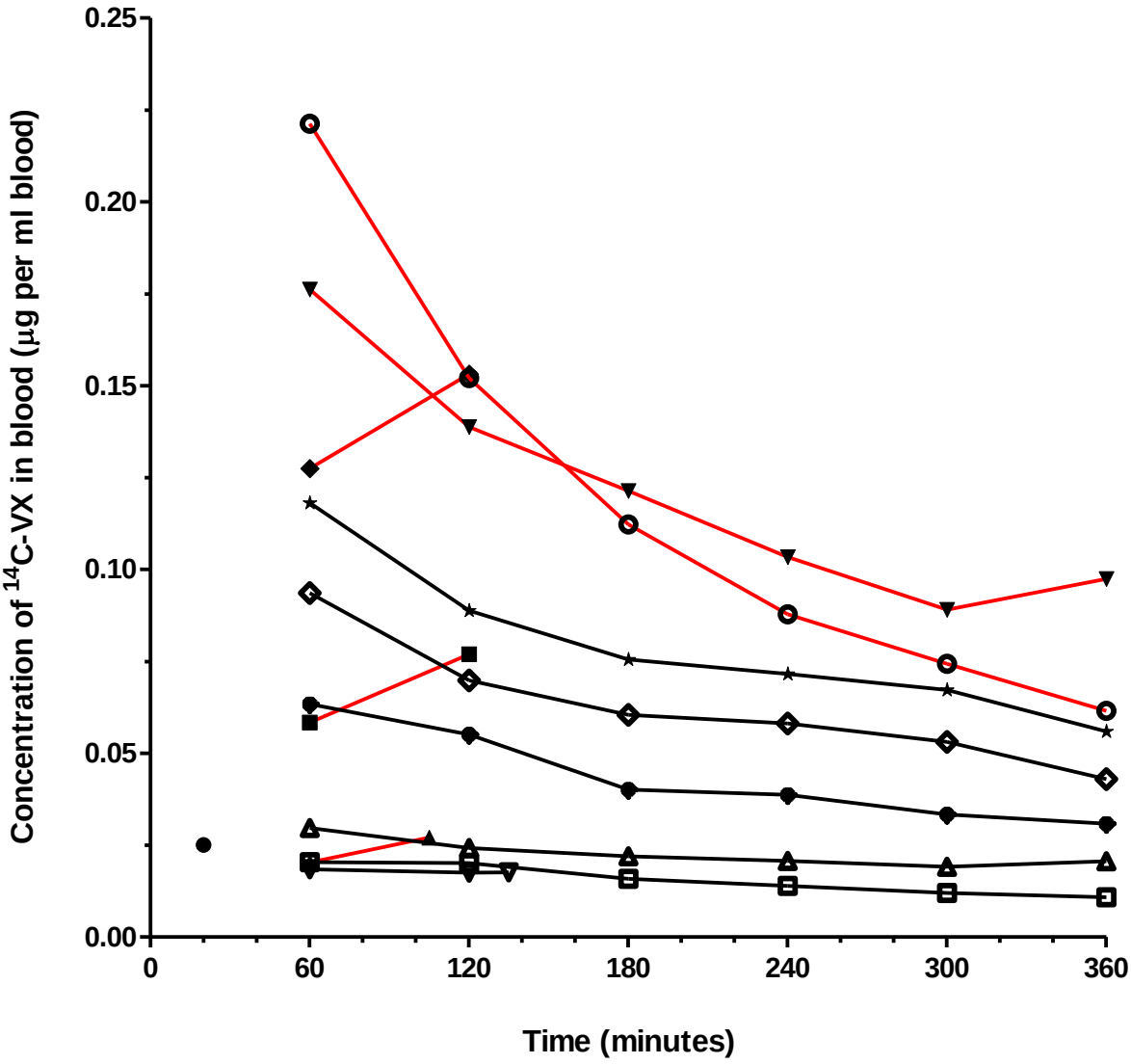

Figure 5.17: Concentration (mean ± SEM) of ^{14}C-VX in consecutive blood samples of individual, anaesthetised swine exposed to a 5xLD_{50} (300µg kg^{-1}) dose of neat ^{14}C-VX via damaged ear skin (red connecting lines and individual plot at x=20; n=6); and from similarly exposed swine treated with a test decontaminant (black connecting lines; n=6).

Generally, concentration decreased during the exposure period, particularly for animals which survived until 360 minutes. In contrast, the concentration of ^{14}C-VX blood was highest at the time of death in animals which did not survive the exposure period.

5.3.5 Physiological recordings

1. Pulse rate and mean arterial pressure

Exposure to ^{14}C-VX without decontamination resulted in a rapid decrease in pulse rate (PR) and mean arterial pressure (MAP; Figure 5.18): within 15 minutes, PR and MAP of not-decontaminated animals was significantly lower than control animals ($p<0.05$), and remained so until 120 minutes post-exposure[1].

There was also a significant, transient reduction in the pulse rate of decontaminated animals, compared to pre-exposure pulse rate, between 60 and 120 minutes post-exposure. A prolonged, late onset period of significantly decreased MAP (compared to pre-exposure MAP) was observed between 2 and 4 hours exposure in the decontaminated group.

[1] *Only three animals in the DXD group survived beyond 180 minutes exposure, which may reduce the power of statistical comparisons beyond this time.*

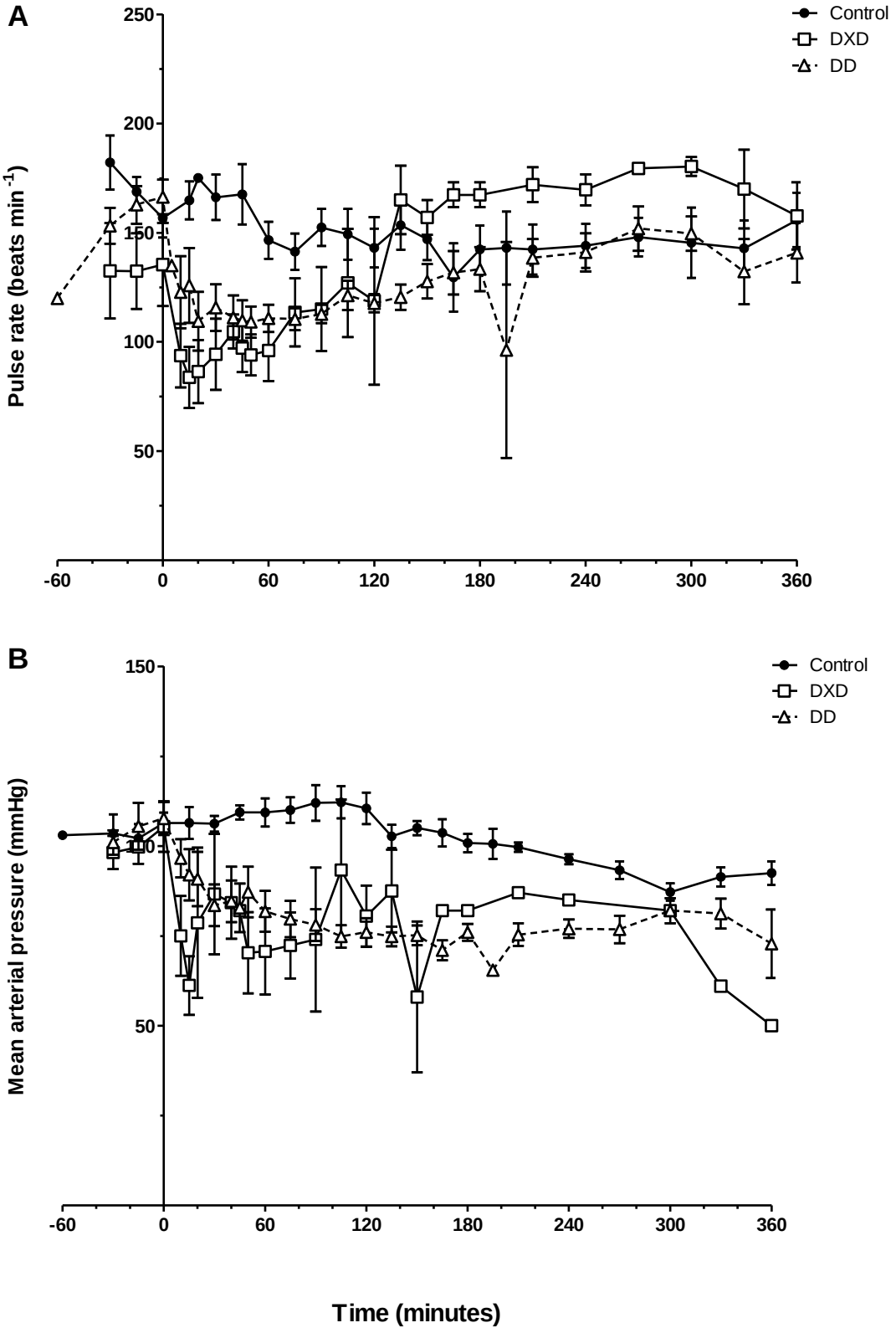

Figure 5.18: Pulse rate (A) and mean arterial pressure (B) for anaesthetised (control), ^{14}C-VX exposed (DXD) and ^{14}C-VX-exposed and decontaminated (DD) swine.

Data are mean ± SEM for *up to* 12 animals per group, recorded over 6 hours from exposure at 0 minutes.

2. Breathing rate, expired CO_2 and saturated O_2

Exposure to ^{14}C-VX without decontamination resulted in a rapid reduction of breathing rate: within 15 minutes post-exposure, breathing rate in not-decontaminated animals had significantly slowed compared to the pre-dose rate (Figure 5.19A; $p<0.05$) and remained so until 2 hours post-exposure. The mean breathing rate of both groups was significantly slower than the pre-dose rate at 6 hours post-exposure.

In contrast, the expired CO_2 levels in exposed and non-decontaminated animals were only significantly higher than the pre-dose level at 60 minutes post-dose (Figure 5.19B). For the three surviving animals in the DXD group, expired CO_2 was significantly higher than control animals from 180 minutes post-exposure.

In practice, decreasing saturated oxygen level was usually a good indicator of deterioration of condition; however there were no significant differences in SpO_2 levels between groups during the 6 hours (Figure 5.20C).

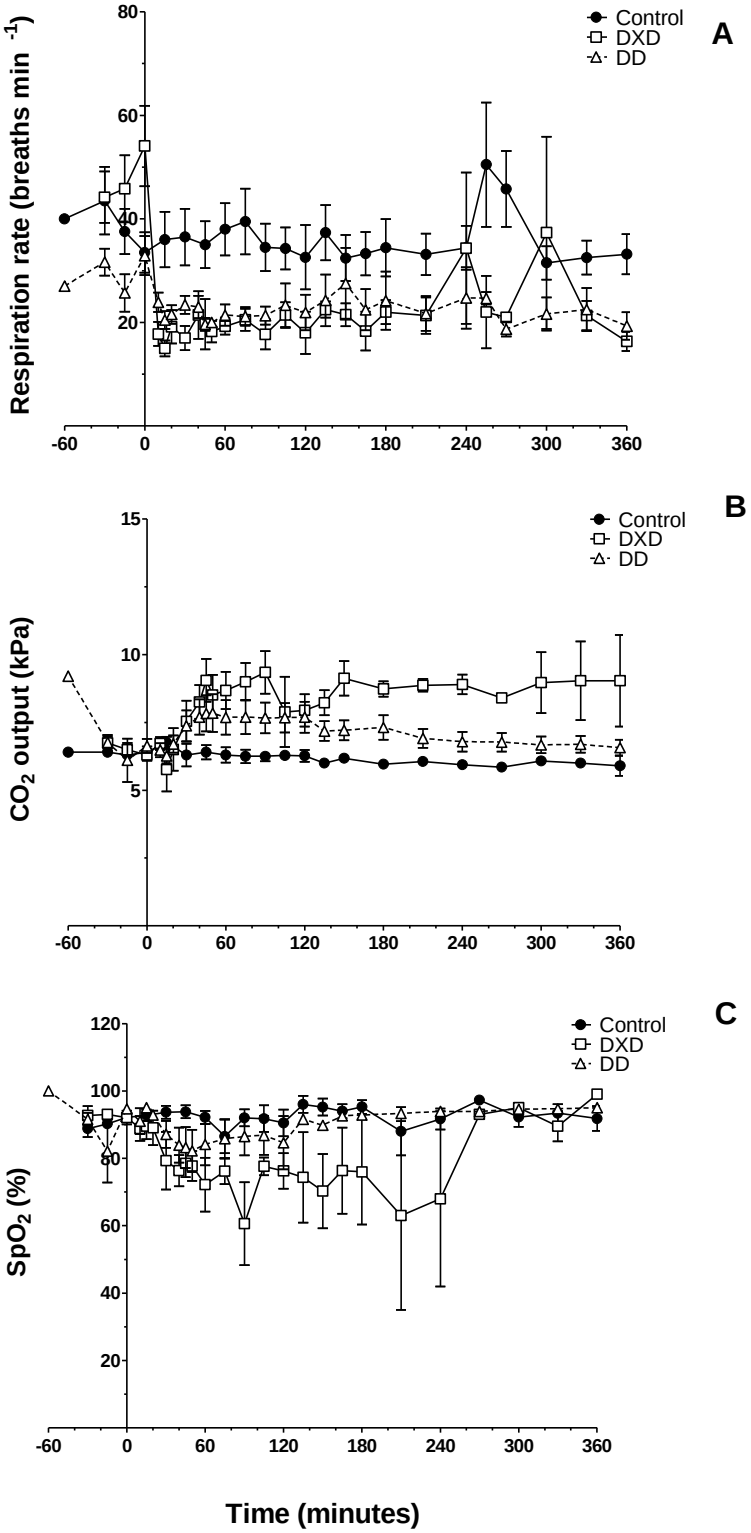

Figure 5.19: Respiration rate (A), expired CO_2 level (B) and saturated oxygen level (SpO_2; C) for anaesthetised (control), ^{14}C-VX exposed (DXD) and ^{14}C-VX-exposed and decontaminated (DD) swine.

Data are mean ± SEM for *up to* 12 animals per group, recorded over 6 hours from exposure at 0 minutes.

3. Haematocrit

Exposure to ^{14}C-VX caused without decontamination resulted in an increase in haematocrit, which was significantly higher than pre-exposure level at 60 and 120 minute post-exposure (Figure 5.20). The haematocrit-time curves were almost parallel for the decontaminated and not-decontaminated group.

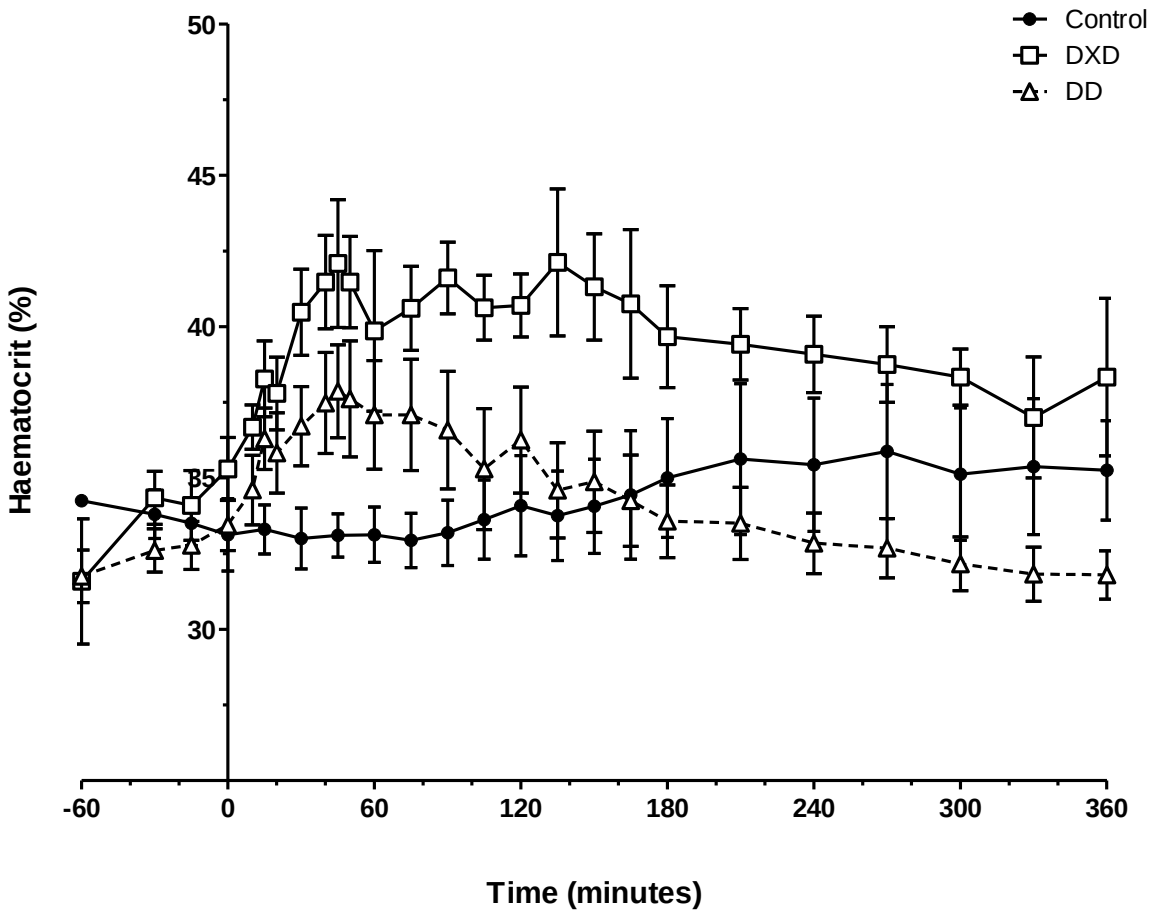

Figure 5.20: Haematocrit values for anaesthetised (control), ^{14}C-VX exposed (DXD) and ^{14}C-VX exposed and decontaminated (DD) swine.

Data are mean ± SEM for *up to* 12 animals per group, recorded over 6 hours from exposure at 0 minutes.

4. Variations

Clear (inter-)individual variations were observed between animals within groups, which may complicate overall interpretations based on treatment (decontamination or no decontamination). For example, in decontaminated animals, PR and MAP generally recovered during the remainder of the exposure period (Figure 5.18); however, in one decontaminated animal, a decrease in PR (from ~140 to <40bpm between 300 and 330 minutes) and MAP (from 80 to <40mmHg after 330 minutes) was observed. A similar profile was observed for one of the surviving animals from the not decontaminated group (Figure 5.21). These animals were both classified as displaying moderate signs of intoxication. Similarly, the deterioration of the condition of the decontaminated animal which did not survive the exposure period, more closely paralleled that of the not-decontaminated group (as a whole) than the decontaminated group.

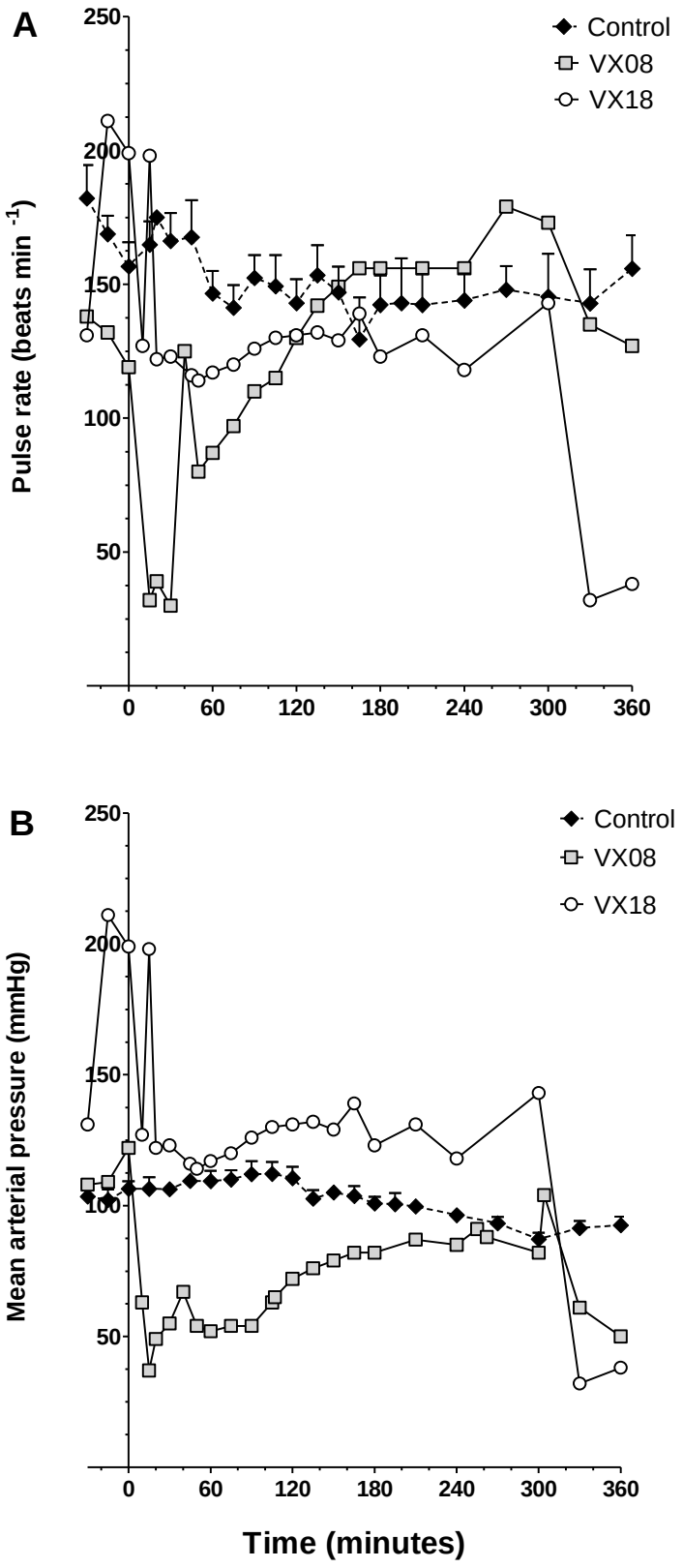

Figure 5.21: Pulse rate (A) and MAP (B) for two, anaesthetised ^{14}C-VX exposed swine. One animal was decontaminated (VX18); the other was not (VX08). The mean ± SEM for *up to* 7 anaesthetised (control) animals, observed over 6 hours, are also presented.

5.3.6 Signs of intoxication

During the exposure period the signs of intoxication observed could be distinguished using thirty-two separate descriptions, taking into account both the type and location of the sign (described in Table 5.1). To enable further analysis, a selection of the more commonly observed signs were organised into the following groups:

i. Any motor effect (including fasciculations, tremors, spasms etc.);

ii. Any secretory effect (including salivation, rhinorrhea, lacrimation; bronchorrhea);

iii. Any regular /continuing / not sporadic abnormality observed on the ECG trace;

iv. Mastication;

v. Any pupil effect (miosis or mydriasis).

These 5 groups were used to describe the severity of signs of intoxication in animals as follows:

- Fatal: animals died within 360 minutes.
- Severe: rapid onset (<30 minutes) of at least two of the groups (i-v) of signs of intoxication described above.
- Moderate: onset of only 1 of the above groups (i-v) within 30 minutes OR onset of any of the above groups (i-v) after 30 minutes.
- Mild: late onset (>60 minutes) of any of the groups (i-v) described above.

The proportion of animals which were classified as moderately or fatally intoxicated was significantly different between the treatment groups (Table 5.2).

Location	Description
Face, head and neck	fasciculations, tremors (including shaking or shivering-like movements, not twitches), side-to-side movements of the head, twitches or jerks, skin colour changes.
Body and back	fasciculations, tremors (including shaking or shivering-like movements, not twitches), twitches or jerks (including convulsions), skin colour changes.
Limbs, shoulders and feet	fasciculations, tremors, including shaking or shivering-like movements (not twitches), twitches or jerks, including convulsions, skin colour changes, blood pooling in the limbs or feet.
Other signs	
Mastication, salivation, lacrimation, nasal secretions, bronchorrhea (interpreted by noisy or gurgling breaths when secretions themselves weren't visible), defecation or urination, beading on the snout, *cutis anserina* and piloerection, gasping or gulping breaths, agonal breathing, cyanosis on the face, arrhythmia or any other unusual ECG traces, swollen snout, bloodshot eyes, bulging or sinking of the eyes in the sockets, movement of the eyes within the sockets (including rolling forward or backward, up and down, vibrating), pupil constriction or dilation.	

Table 5.1: Descriptions of the signs of intoxication, and their localisation, observed in animals exposed to a $5xLD_{50}$ (300µg kg^{-1}) dose of neat ^{14}C-VX via damaged ear skin (DXD; n=12); and in similarly exposed swine treated with a test decontaminant (DD; n=12).

Group	Fatal**	Severe	Moderate*	Mild
DXD	9/12	2/12	1/12	0/12
DD	1/12	2/12	7/12	2/12

Table 5.2: Severity of signs of intoxication in anaesthetised animals exposed to a $5xLD_{50}$ (300µg kg^{-1}) dose of neat ^{14}C-VX via damaged ear skin (DXD) and a test decontaminant (DD). Asterisks indicate a significant difference between groups in the proportion of animals within the category (Fisher's two-tailed exact test: *$p<0.05$; **$p<0.01$).

Onset of particular signs of intoxication

The proportion of each treatment group which displayed any of the groups of signs previously described (i-v) were analysed using Fisher's two-tailed exact test (Table 5.3). The time of onset of these signs was also included in this analysis.

There was no significant difference in occurrence or onset time of any motor or secretory effects or mastication between groups. There was not a significant difference in occurrence of pupil effects between the groups. However, within the animals which did display pupil effects, the onset of these within 30 minutes occurred in a significantly larger proportion of the not-decontaminated group than the decontaminated group. Also, the onset of pupil effects after 30 minutes occurred in a significantly lower proportion of the not-decontaminated group than the decontaminated group.

Electrocardiograph irregularities were observed in a significantly larger proportion of the not-decontaminated group compared to the decontaminated group.

Sign of intoxication	Treatment group	Not observed	Observed		
			Total	<30 minutes	30+
Alive at timepoint	DXD		12	12	11
	DD		12	12	12
Any motor effect	DXD	0/12	12/12	11/12	1/11
	DD	0/12	12/12	6/12	6/12
Any secretory effect	DXD	2/12	10/12	7/10	3/10
	DD	1/12	11/12	3/11	8/11
Mastication	DXD	1/12	11/12	9/11	2/10
	DD	6/12	6/12	3/6	3/6
Any pupil effect (constriction or dilation)	DXD	2/12	10/12	9/10 [a]	1/9 [b]
	DD	6/12	6/12	1/6 [a]	5/6 [b]
Any ECG effect or arrhythmia	DXD	4/12	8/12 [c]	4/8	4/7
	DD	11/12	1/12 [c]	1/12	0/1

Table 5. 3: Observations of onset of signs of intoxication in anaesthetised animals exposed to a 5xLD_{50} (300µg kg^{-1}) dose of neat ^{14}C-VX via damaged ear skin (DXD) and a test decontaminant (DD).

For the onset period, the denominator takes into account both the number of animals in each group which displayed the given sign in the first instance *and* the number of animals which were alive in the given timeframe. Superscript letters indicate a significant difference in proportions between groups bearing the same annotation: [a]$p<0.01$; [b]$p<0.05$; [c]$p<0.01$.

5.4 Discussion

This study demonstrated the efficacy of swift application of a haemostatic product, WoundStat™, to prevent death and reduce the severity of intoxication in swine exposed to a supra-lethal ($5xLD_{50}$) dose of ^{14}C-VX via damaged ear skin. This efficacy was evident despite a rapid, significant decrease in acetylcholinesterase (AChE) activity. Application of WoundStat™ within 30 seconds of exposure resulted in retention of almost 50% of the applied dose within the decontaminant matrix, and effectively reduced deposition of ^{14}C-VX in the brain, heart, lung, spleen, diaphragm and blood.

The toxicity of VX clearly prohibits investigations in humans. However, *in vitro* and *in vivo* studies have provided some comparative toxicokinetic data for VX between pig and human models[44,58,101,105,108]. The pig ear in particular has been reported to be an appropriate model for human abdominal penetration of VX[101]. Furthermore, swine models are also used for studies of haemostat treatment of severely haemorrhaging wounds[5,7]. However, data obtained from animal models should always be interpreted within the limitations of the model, *viz* its relevance to effects in humans.

This model was designed to be representative of a "worst-case" scenario, in all but haemorrhaging conditions. Whilst dose-response effects of VX were not investigated in this study, the dose applied was a supra-lethal toxic challenge. Application of neat, undiluted contaminant (>98% pure), rather than a less toxic simulant, allowed the clinical effects and outcome of exposure via damaged skin to be observed. The pig ear has also been demonstrated to be more permeable to VX than pig abdomen[102]. Dose-response effects of

the decontaminant were not investigated in the present study. Furthermore, the decontaminant was left in place for the duration of the experiment, which is representative of "in use" procedure for an advanced haemostat, but not for a decontaminant. Application of ^{14}C-VX to damaged skin *in vitro* resulted in significantly enhanced penetration kinetics (Chapter 4). The skin damage induced, whilst not a complex, haemorrhaging wound, may have created an environment favouring VX-penetration. These elements of the study design provide a thorough "worst-case" scenario to assess efficacy of the test decontaminant.

In this study the dorsal aspect of the ear (pinna) was exposed to VX. Creating a uniform area of damage (that was also distal to pre-experimental superficial damage that can often be present on co-housed pigs) was deemed to be less complicated on the dorsal aspect of the pinna than the ventral aspect. The interval between exposure and decontamination (30 seconds) was selected to be reflective of a response time beyond which an arterial haemorrhaging wound may become unsalvageable.

Interestingly, the mean survival time for animals exposed to 5xLD_{50} ^{14}C-VX via damaged skin (without decontamination) in this study was not dissimilar to that of a previous study of an equivalent dose to intact ear skin in swine[105]. However, three of the animals also survived the 5xLD_{50} dose of ^{14}C-VX in the present study, compared to none in Bjarnason *et al*'s study. The reported percutaneous LD_{50} for swine (specifically, ear) has differed between 50 - 80 µg kg^{-1}) between previous studies of *in vivo* VX exposure[58,102,105]. Variations in protocol, anaesthesia, dosing regimen or simply individual subjects may partly explain the range of LD_{50} values, and in turn may partly account for the discrepancy in survival between studies

using “equivalent” multiple LD_{50}s. Arguably, the lethality of the dose used in this study is supported by the death of one decontaminated animal.

The test decontaminant was evaluated in a superficial skin wound, rather than a complex haemorrhaging injury. Application of Fuller’s Earth pre-contaminated with an 80 μg kg^{-1} dose of VX to a full-thickness skin wound resulted in zero fatalities within 6 hours exposure[105]. In contrast, one animal in the decontaminated group in the present study died 137 minutes post-exposure. The present model is more representative of an exposure-decontamination event; rather than a secondary exposure event due to cross-contamination. Furthermore, it has previously been suggested that contact with the skin is the limiting factor for VX-spreading[100]; thus spread of the agent (and, hence, the total size of the exposed area) may be affected to different extents between the two models.

Autoradiography of the ear was not used to measure radiolabel spread in the present experiment, although a Geiger-Muller probe was used to direct excision of all contaminated regions in the vicinity of the exposure site for radiometric analysis. Previously, agent spread over pig ear skin (measured *in vivo*) was shown to be approximately 5-fold lower than human forearm skin (measured in volunteers)[44,58]. Characterisation of agent spread in different models would be useful for future decontamination studies, particularly to demonstrate whether products with different mechanisms of decontaminant action (e.g. absorptive material rather than barrier) have differing effects on agent spread. The discrepancies between this experiment and previous swine studies (using similar or

equivalent doses) may partly be attributable to spread of the contaminant beyond the damaged skin area.

The use of a radiolabelled contaminant does not provide a complete profile of VX-absorption and distribution, as radiometric analysis does not distinguish between ^{14}C-VX and breakdown products or metabolites. Furthermore, radiolabel excretion was not measured in this study, and it is probable that some of the un-recovered dose is contained within un-sampled tissue. Speciation analysis, for example GC-MS, would be essential to attempt to predict the hazard posed by absorbed material.

This approach, however, does permit some interpretations of basic toxicokinetics. The amount of radiolabel recovered in the skin sections in this study was noticeably lower than that of previous *in vivo* investigations of exposures to pig ear, despite a larger dose of VX being applied in the present study[58,100]. Previous studies of VX exposure in humans and swine have been suggestive of the presence of a dermal reservoir of VX within the skin[44,100]. It is possible that the skin damage induced in the present model may have prevented the formation of a reservoir. The longer exposure period used in the present study (6 hours rather than 3 hours) may also have prolonged the opportunity for excretion or deposition in unsampled tissues. Indeed, blood concentration decreased with time in the surviving animals, which may represent mobilisation of radiolabel from the blood. Furthermore, of the tissues that were sampled, the largest amount of ^{14}C-VX was recovered from the liver. However, without a detailed speciation analysis, there is also no certainty about the

presence of structures other than ^{14}C-VX (i.e. potential breakdown products), or their relative abundance and distribution, within the sampled tissues.

The radiometric approach can also demonstrate basic decontamination efficacy. Approximately 47% of the applied dose was extracted from collected WoundStat alone. Despite this, the total ^{14}C-VX recovery from internal organs and blood was not significantly different between groups; whilst recovery from brain, heart, lung, spleen and diaphragm (inferred by concentration) was significantly reduced by decontamination. A possible explanation could be that the decontaminant may reduce the rate of penetration of ^{14}C-VX, rather than preventing penetration altogether. However, if swift decontamination reduces the rate of penetration to a clinically relevant extent, or prevents build-up of a reservoir, then this should improve prognosis. Analyses of desorption kinetics for VX from decontaminant matrices, or of dose-response effects of decontaminant may provide some data to support or oppose this possibility. Comparative spectrometric analysis (for example of extracted samples from blood or urine) would be useful to determine differences in the metabolic profiles (i.e. the presence or absence of structures other than ^{14}C-VX and relative abundance) between decontaminated and not-decontaminated groups.

In the present study, approximately 10% of the applied dose was recovered unabsorbed, extracted from the exposure chamber and swabs of the exposure site. This is approximately 10x higher than the unabsorbed fraction recovered following exposure to a lower dose ($2xLD_{50}$) to intact skin[58]. The proportion of the applied dose which was absorbed in the present study was lower (approximately one fifth) of that which was absorbed in the

previous study. The differences in total recovery between these studies may be attributed to variations in the doses applied or distribution of radiolabel in unsampled tissues.

In contrast to previous *in vivo* studies, anaesthesia was maintained by intravenous alphaxalone, rather than inhaled isoflurane or halothane. Isoflurane anaesthesia has been previously shown to produce up to a 15-20% reduction in acetyl cholinesterase activity[74].

A detailed analysis of prolonged alphaxalone exposure on acetylcholinesterase activity in swine has not been conducted. However, althesin, a discontinued anaesthetic mixture containing alphaxalone, was reported to have negligible effect on cholinesterase activity[135]. A clear difference was evident between the control and VX-exposed animals; and there were negligible changes in acetylcholinesterase activity in control animals throughout the study period. Therefore, it can be reasonably assumed that any effects on cholinesterase function induced by the anaesthetic regime would have had a negligible contribution to the overall outcome of the experiment. Nevertheless, characterisation of anaesthetic suitability for *in vivo* nerve agent experiments is worthy of further investigation.

It is also important to note that mild fasciculations or shivers were observed in some animals prior to VX-exposure, which has been reported previously following anaesthesia induction in swine[105]. Signs of intoxication in each animal were recorded relative to any initial observations made prior to exposure: i.e. fasciculations and tremors etc. were recorded when the status of the animal worsened from that of the pre-dose period.

There was no detectable correlation between final acetylcholinesterase activity and survival time in non-surviving animals in this study. There were also no general significant differences in acetylcholinesterase activity between decontaminated and not-decontaminated animals during the exposure period (except for at the time of death). These results compare favourably with previous reports that cholinesterase activity is a robust indicator of exposure, but not prognosis[70,74]. This is particularly important following a recent demonstration of plasma cholinesterase rebound following VX-exposures in swine[136]. This also suggests the requirement for further investigations and characterisations of the cholinesterase response in pig and human blood fractions; and the investigation of other possible mechanisms of VX (and indeed, organophosphate nerve agents in general) toxicity[70–72]. Contributively or protective effects resulting from VX interaction with other esterases were not explored in this study. A detailed investigation of activity of other esterases, including tissues other than blood, may provide useful supporting information relating to VX-toxicokinetics.

In contrast to previous reports, a clear order of occurrence of signs of intoxication was not observed; although significant differences were identified in severity of intoxication between treatment groups [37,74]. This may partly be attributable to the different doses applied between studies. There were, however, apparent differences in physiological parameter recordings between animals which died or survived, regardless of treatment group. For example, the pulse rate and mean arterial pressure of two surviving individuals, one from each treatment group, closely paralleled each-other. Similarly, the physiological recordings of the decontaminated animal which did not survive, more closely paralleled that of the not-

decontaminated group. This may be interpreted as further evidence that physiological parameters alongside signs of intoxication may be more useful as prognostic indicators.

The predominance of different effects of VX exposure and their relative contribution to overall outcome (i.e. death or survival) was not clear. Death was confirmed following a 15 minute period of uninterrupted apnoea; but whether apnoea had resulted from central depression of respiratory regulation or paralysis of respiratory muscles was not clear. The changes in pulse rate or blood pressure and their contribution to outcome may have causal, effector, synergistic or contradictory interactions. For example, a change in pulse rate may be an effect of exposure, but could also be reasonably expected to affect distribution of VX.

Core temperature was monitored but not included as an experimental endpoint. Temperature was artificially maintained where necessary, for monitoring of stable anaesthesia; furthermore, use of a rectal probe meant that a reduction in temperature often indicated defecation. However, a more detailed analysis of temperature at exposure sites (and other anatomical locations) could provide useful information regarding temperature effects on penetration rates and resultant toxicity[44,137].

The present evidence cannot be used to determine whether variations in types of signs of intoxication observed (inter-treatment), or changes in physiological parameters observed during the 6 hour period (inter-individual), are due to the relative predominance of muscarinic or nicotinic effects of cholinesterase inhibition; non cholinesterase effects; or subsequent recovery following an initial period of intoxication.

To summarise, the results of this *in vivo* decontamination study demonstrated:

- The efficacy of swift application of a haemostatic product, WoundStat™, to reduce fatality and reduce the severity of signs of intoxication following exposure of swine to a 5xLD_{50} dose of ^{14}C-VX via damaged ear skin.
- That WoundStat™, applied 30 seconds after exposure of the damaged skin, was effective in retaining almost 50% of the applied dose.
- That swift decontamination of the exposed area altered distribution of ^{14}C-VX, specifically in the brain, heart, lung, spleen, diaphragm, and blood, although the mechanisms involved are not clear.
- That acetylcholinesterase activity, following exposure to a supra-lethal dose of ^{14}C-VX, was not as useful for assessing prognosis as physiological monitoring.

This study has identified the requirement for further work in the following areas:

- *In vitro* comparisons of VX penetration kinetics in similarly damaged human and pig skin;
- Dose-response investigations for VX application to intact and damaged pig skin, particularly for toxicokinetic analysis and characterisation of clinical signs of intoxication;
- Effects of the dose-decontamination interval and decontaminant dose on product efficacy;
- Speciation analysis of blood and tissues following *in vivo* experiments of VX exposure;
- Analysis of desorption of compounds from test decontaminants;
- Characterisation of anaesthetic suitability for *in vivo* nerve agent experiments.

CHAPTER 6. Analysis of gene expression following exposure to ^{14}C-VX: effects of decontamination and outcome

CHAPTER 6. ANALYSIS OF GENE EXPRESSION FOLLOWING EXPOSURE TO ^{14}C-VX: EFFECTS OF DECONTAMINATION AND OUTCOME

6.1 Introduction

The primary mechanism of toxic action of organophosphate nerve agents is inhibition of acetylcholinesterase. Previous *in vivo* investigations have demonstrated the efficacy of various decontaminants to prevent death following nerve agent exposure (Chapter 5) [105,106,134]. However, previous reports have investigated the suggestion that VX toxicity may not be completely explained by acetylcholinesterase inhibition[71,72]. Indeed, in the preceding experiment, 14 animals survived 6 hours exposure to a supra-lethal (5xLD_{50}) dose of ^{14}C-VX, with marked levels of acetylcholinesterase inhibition which were not significantly dissimilar to subjects which did not survive. A microarray experiment was conducted to investigate changes in gene expression in whole blood samples obtained from the preceding *in vivo* decontamination study, in order to investigate processes which may have been involved in responses to VX-exposure.

6.2 Materials and Methods

The experimental groups, acquisition of blood samples, extraction of RNA and microarray hybridisation (preparation and post-hybridisation) are detailed in Chapter 2 and an experimental overview is summarised in Figure 6.1.

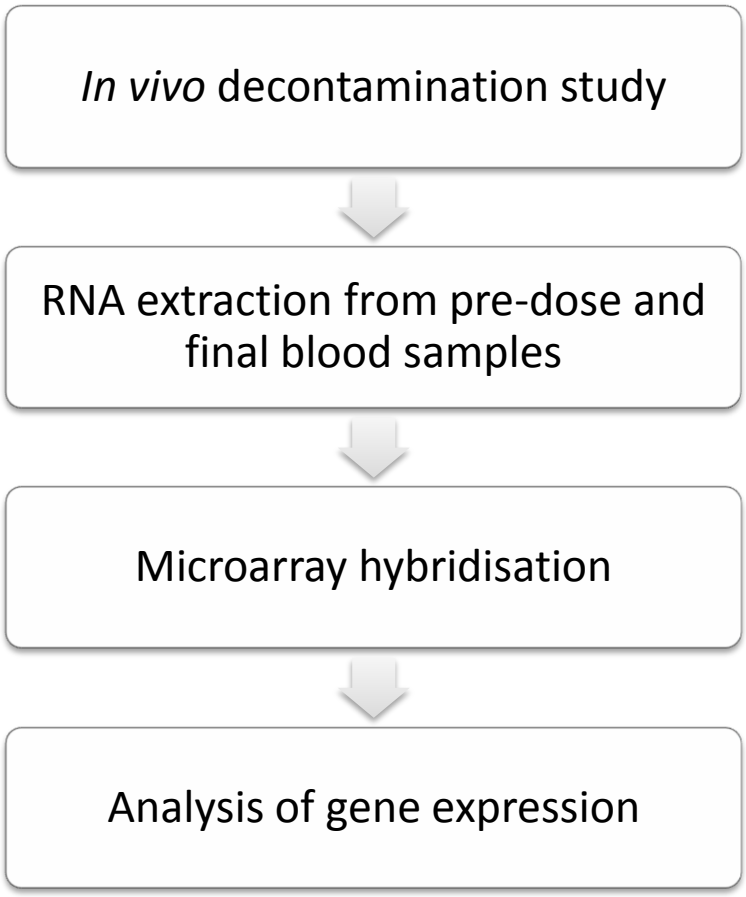

Figure 6.1: Workflow design for analysis of gene expression in blood samples of swine exposed to a 5xLD_{50} dose of ^{14}C-VX via damaged ear skin.

6.3 Results

Normalisation and filtering on flags (detected in all conditions) resulted in 10,110 probes for inclusion in subsequent data analysis. The highest number of significant changes in gene expression were identified when comparing the pre-dose and final blood samples of the decontaminated (22% of the analysed genes) or survivor (37%) groups (Table 6.1). In comparison, 3% and 7% of the analysed genes were significantly changed in whole blood samples from non-surviving or non-decontaminated animals respectively. Gene ontology analyses did not identify a shortlist of significant functional groups for any of the comparisons made. Many of the features were shared between groups. A visual representation of the overlap of significantly changed genes between groups is shown in Figure 6.2.

Comparison	Down	No change	Up	Total change
No decontamination: **Pre-dose *vs* final**	591	9455	64	655
Decontamination: **Pre-dose *vs* final**	1246	7920	944	2190
Survivor: **Pre-dose vs final**	2324	6417	1369	3693
Non-survivor: **Pre-dose vs final**	197	9853	60	257

Table 6.1: Statistical summary for number of probes showing differential expression (FC>1.0; p<0.05) in each comparison, between the pre-dosage and final blood sample, following exposure of swine to a 5x LD_{50} dose of ^{14}C-VX via damaged ear skin.
Data were analysed by paired T-test with Welch's correction and no false discovery rate limit.

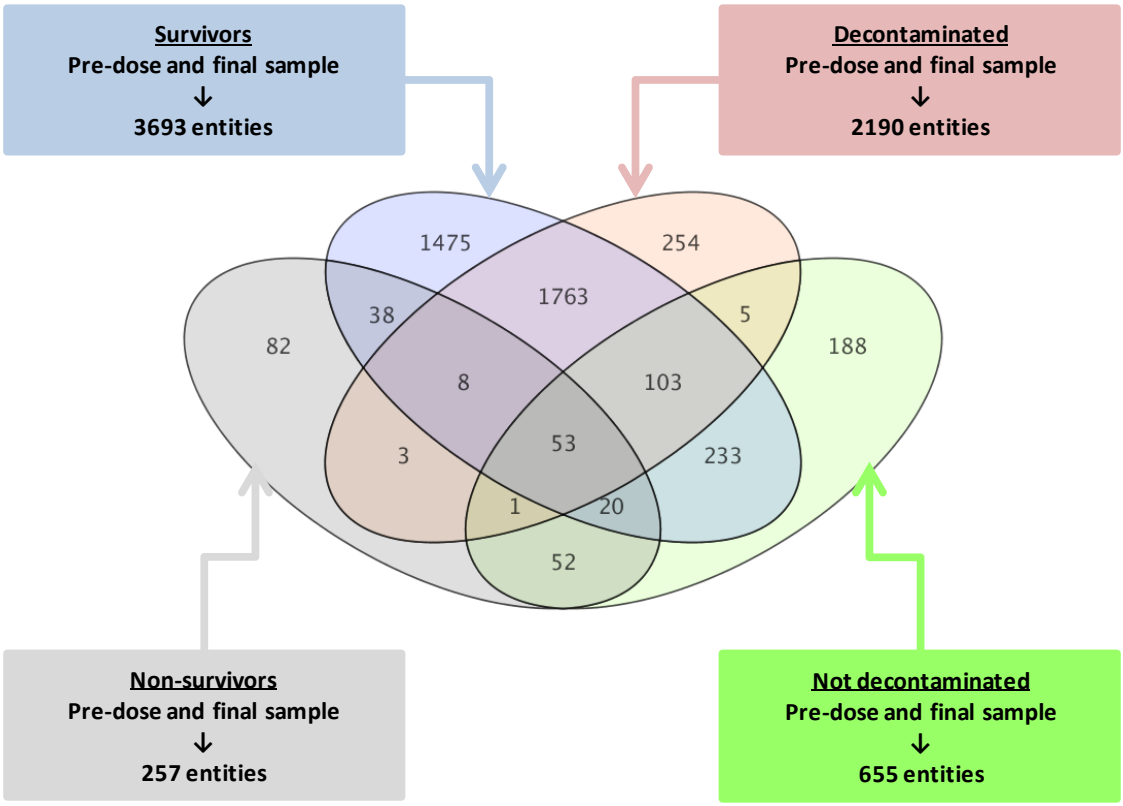

Figure 6.2: Venn diagram (not proportional) showing the frequency of the genes which were identified to be significantly ($p<0.05$) differently regulated (fold change >1.0) during exposure to ^{14}C-VX in different conditions.

The diagram shows the entities which are shared between groups, and entities which are isolated to particular groups: Survivors, Non-survivors, Decontaminated and Not decontaminated.

6.3.1 Changes in gene expression following fatal or non-fatal exposure to ^{14}C-VX.

Comparing expression in the final blood sample to pre-dose blood samples in the surviving animals identified 3693 entities (37% of those analysed) with a significant fold change ($p<0.05$; $FC>1.0$) following exposure to ^{14}C-VX. Comparing expression in the final blood sample to pre-dose blood samples in the animals which did not survive identified 257 entities (3% of those analysed) with a significant fold change ($p<0.05$; $FC>1.0$) following exposure to ^{14}C-VX (Figure 6.3).

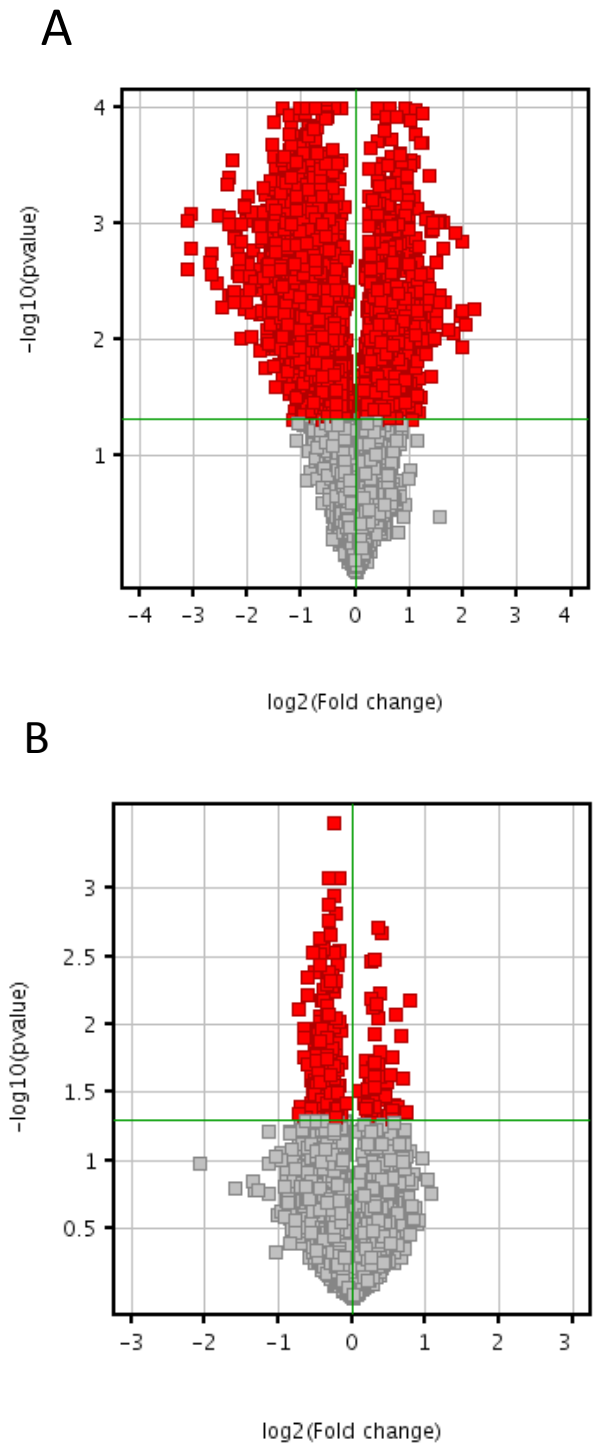

Figure 6.3: Volcano plot showing entities with a significant fold change ($p<0.05$; $FC>1.0$) in whole blood of swine which survived (A; n=7; 3693 entities) or did not survive (B; n=5; 257 entities) exposure to a $5xLD_{50}$ dose of ^{14}C-VX via damaged ear skin.

Data were analysed by paired T-tests with no false discovery rate limit.

Opposite regulation of genes in samples from survivors and non-survivors

Expression of 119 genes were significantly changed during exposure in both the survivor and non-survivor groups. Of these, 38 were oppositely regulated between the groups (i.e. 19 were down-regulated in the survivor group and up-regulated in the death group; 19 were up-regulated in the death group and down-regulated in the survival group; Table S6.1). None of these significantly linked to gene ontology terms. Three entities had significant fold changes above 1.5 in both survival or death groups; one with opposing regulation between groups (Table 6.2). Some of the entities identified were not annotated with any Gene Ontology terms, whereas others were linked to up to 80 Gene Ontology terms. Gene ontology analyses did not identify a shortlist of significant functional groups for any of the comparisons made.

Probe Name	FC Survival	Regulation	FC Death	Regulation	Gene Symbol	Description	GenBank Accession	Gene Name
A_72_P107181	1.74	down	1.51	down	TTI1	Uncharacterized protein [Source:UniProtKB/TrEMBL;Acc:F1SEK2] [ENSSSCT00000008032]	AK346364	Tel2 interacting protein 1 homolog (S. pombe)
A_72_P330288	2.69	down	1.54	down		Rep: Chromosome undetermined SCAF3439, whole genome shotgun sequence - Tetraodon nigroviridis (Green puffer), partial (6%) [TC538063]		
A_72_P204972	1.98	down	1.60	up				

Table 6.2: Three genes had significantly changed expression in surviving (n=7) and non-surviving (n=5) swine following exposure to a 5xLD_{50} dose of ^{14}C-VX via damaged ear skin, with fold-change greater than 1.5.

6.3.2 Changes in gene expression in decontaminated or non decontaminated animals following exposure to ^{14}C-VX.

Comparing expression in the final blood sample to pre-dose blood samples in the decontaminated animals identified 2190 entities (22% of those analysed) with a significant fold change ($p<0.05$; $FC>1.0$) following exposure to ^{14}C-VX. Comparing expression in the final blood sample to pre-dose blood samples in the animals which were not decontaminated identified 655 entities (7% of those analysed) with a significant fold change ($p<0.05$; $FC>1.0$) following exposure to ^{14}C-VX (Figure 6.4).

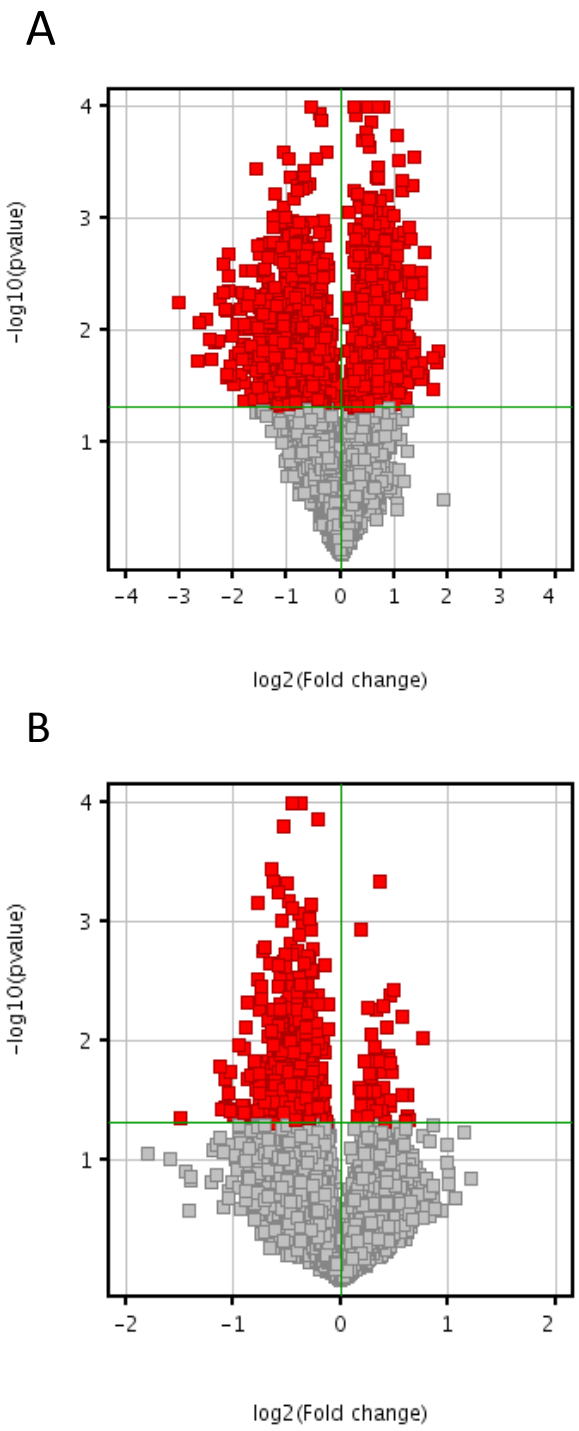

Figure 6.4: Volcano plot showing entities with a significant fold change ($p<0.05$; $FC>1.0$) in whole blood of swine which were decontaminated (A; n=6; 2190 entities) or not decontaminated (B; n=6; 655 entities) following (*up to* 6 hours) exposure to a $5xLD_{50}$ dose of ^{14}C-VX via damaged ear skin.

Data were analysed by paired T-tests with no false discovery rate limit.

Differences in gene expression between decontaminated or non decontaminated animals

Expression of 162 genes were significantly changed during exposure in both the decontaminated and not-decontaminated groups.

In order to further focus the results on the most marked changes, the fold change limit was raised to 2.0, which identified 396 significantly differentially expressed entities (Figure 6.5). Of these, 3 were represented in both treatment groups (Table 6.3), and 5 were isolated to the “not decontaminated” group (Figure 6.5; Table 6.4). In the “not decontaminated” group, no entities were identified to have a significant fold-change above 3.0 between the pre-dose and final blood sample.

The most marked changes (i.e. highest fold change) were evident in the “decontaminated” group. In this group, 65 entities were identified with a significant fold change between 3.0 and 9.0 (Table S6.2). One entity had a significant fold change above 7.0 in this group.

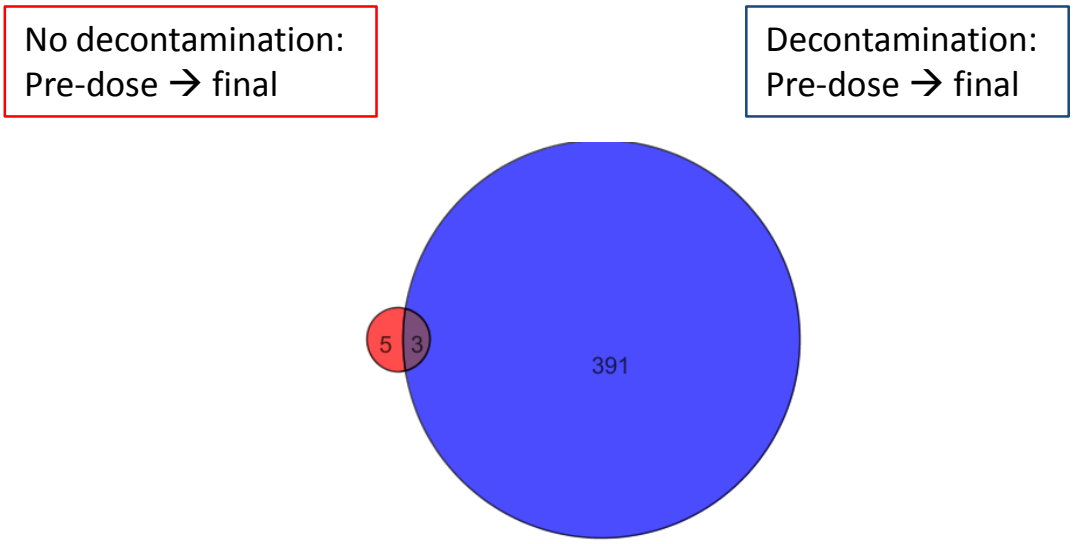

Figure 6.5: Proportional Venn diagram showing frequency of significantly differentially expressed entities (FC>2.0; p<0.05) in pre-dose and "final" blood samples obtained from swine exposed to a 5xLD_{50} dose of ^{14}C-VX via damaged ear skin treated with a test decontaminant (Decontamination) or not (No decontamination).

The entities were obtained by Volcano plot and unpaired T-test with Welch's correction and no false discovery rate limit; no probes passed the Benjamini & Hochberg FDR limit). In total, 396 entities were identified with significant differential expression between the pre-dose and "final" blood samples. Of these, 3 were identified in both treatment groups and 5 were only identified in the not decontaminated group.

Probe Name	P Value	Fold change	Gene Symbol	Description
A_72_P153566	0.044	2.82		Sus scrofa mRNA, clone:THY010092F01, expressed in thymus. [AK239319]
A_72_P330288	0.037	2.15		Rep: Chromosome undetermined SCAF3439, whole genome shotgun sequence - Tetraodon nigroviridis (Green puffer), partial (6%) [TC538063]
A_72_P000091	0.039	2.04	LOC100512978	Uncharacterized protein [Source:UniProtKB/TrEMBL;Acc:F1SAL1] [ENSSSCT00000016455]

Table 6.3: Three genes were identified which were significantly down-regulated by a fold-change greater than 2.0, during (*up to*) 6 hours exposure of anaesthetised swine to a $5xLD_{50}$ dose of ^{14}C-VX via damaged ear skin, in blood samples of both decontaminated (n=6) and not-decontaminated (n=6) animals (FC>2; $p<0.05$).
Data were analysed by paired T-test with Welch's correction and no false discovery rate limit.

Probe Name	P Value	Fold change	Gene Symbol	Description
A_72_P217812	0.037	2.12	ZCCHC6	Uncharacterized protein [Source:UniProtKB/TrEMBL;Acc:F1S4J1] [ENSSSCT00000011987]
A_72_P165046	0.021	2.10	CD55	Sus scrofa CD55 molecule, decay accelerating factor for complement (Cromer blood group) (CD55), mRNA [NM_213815]
A_72_P413368	0.038	2.15		Sus scrofa mRNA, clone:ITT010040H02, expressed in intestine. [AK231345]
A_72_P374023	0.039	2.04		Sus scrofa mRNA, clone:AMP010092E08, expressed in alveolar macrophage. [AK231094]
A_72_P149411	0.017	2.18	ADAM8	Uncharacterized protein [Source:UniProtKB/TrEMBL;Acc:F1SCV2] [ENSSSCT00000011786]

Table 6.4: Five genes were identified which were significantly down-regulated by a fold-change greater than 2.0, during (*up to*) 6 hours exposure of anaesthetised swine to a 5xLD_{50} dose of ^{14}C-VX via damaged ear skin (n=6).

Four animals did not survive the 6 hour observation period: the mean survival time for these four animals was 103 ± 50 minutes (mean ± standard deviation; range 29 to 172 minutes). The remaining two animals were euthanized at 6 hours post-exposure. Data were analysed by paired T-test with Welch's correction and no false discovery rate limit. No entities in the not-decontaminated group were significantly differentially expressed by a fold-change greater than 3.0.

6.3.3 Changes in gene expression with successful decontamination (survival) following exposure to ^{14}C-VX

Of the significantly differently expressed entities ($p<0.05$; $FC>1.0$), 1763 were specific to samples from decontaminated animals which survived (Figure 6.2). Six of these entities were significantly regulated with a fold change between 5.0 and 9.0 (Table 6.5).

Probe Name	FC Survival	FC Decontaminated	Regulation	Gene Symbol	Description	GenBank Accession	Gene Name
A_72_P160596	6.46	5.05	down	CD163	Sus scrofa CD163 mRNA, complete cds. [DQ067278]	DQ067278	CD163 molecule
A_72_P004066	8.64	6.38	down		Sus scrofa mRNA, clone:THY010119H01, expressed in thymus. [AK351987]	AK351987	
A_72_P178006	6.57	6.22	down	HP	Sus scrofa haptoglobin (HP), mRNA [NM_214000]	NM_214000	haptoglobin
A_72_P131846	8.35	5.44	down	RETN	Sus scrofa resistin (RETN), mRNA [NM_213783]	NM_213783	resistin
A_72_P177496	8.67	5.37	down	RETN	Sus scrofa resistin (RETN), mRNA [NM_213783]	NM_213783	resistin
A_72_P088736	8.32	8.10	down	LTF	Sus scrofa lactotransferrin (LTF), mRNA [NM_214362]	NM_214362	Lactotransferrin

Table 6.5: Of 1763 significantly differently expressed entities which were isolated to decontaminated survivor samples (n=7), six had fold changes between 5.0 and 9.0 in both interpretations.

6.3.4 Changes in gene expression with un-successful decontamination (death) following exposure to ^{14}C-VX

Of the significantly differently expressed entities ($p<0.05$; FC>1.0), 3 were specific to the samples from the decontaminated animal which died (Table 6.6)[1].

[1] *NB: Only one decontaminated animal did not survive.*

Probe Name	FC Death	Regulation	FC DD	Regulation	Gene Symbol	Description	GenBank Accession	Gene Name
A_72_P088121	1.72	up	1.47	up	CCL25	Sus scrofa chemokine (C-C motif) ligand 25 (CCL25), mRNA [NM_001025214]	NM_001025214	chemokine (C-C motif) ligand 25
A_72_P058551	1.21	up	1.39	up				
A_72_P178516	1.23	down	1.16	down	PITPNC1	Sus scrofa phosphatidylinositol transfer protein, cytoplasmic 1 (PITPNC1), mRNA [NM_001143722]	NM_001143722	Phosphatidyl-inositol transfer protein, cytoplasmic 1

Table 6.6: One decontaminated (DD) animal did not survive despite decontamination. Three entities were only significantly differently expressed in non-surviving decontaminated samples. The fold change of these entities was between 1.0 and 2.0.

6.3.5 Changes in gene expression with non-fatal (survival) exposure to ^{14}C-VX without decontamination

Two animals survived the exposure of damaged ear skin to 5xLD_{50} ^{14}C-VX, without any decontamination treatment. Of the significantly differently expressed entities ($p<0.05$; FC>1.0), 233 were specific to samples from these survivors of the not-decontaminated group (Figure 6.2). Thirty six of these were differently regulated with a fold-change greater than 1.5 (Table S6.3). Three entities were differently regulated with a fold change greater than 2.0 in both groups; whereas one had a fold change greater than 3.0 within the survivor group only (but less than 2.0 in the not-decontaminated group): this was un-annotated and did not map to a Gene Ontology term (Table 6.7).

Probe Name	FC Survival	FC DXD	Regulation	Gene Symbol	Description	GenBank Accession	Gene Name
A_72_P165046	2.18	2.10	down	CD55	Sus scrofa CD55 molecule, decay accelerating factor for complement (Cromer blood group) (CD55), mRNA [NM_213815]	NM_213815	CD55 molecule, decay accelerating factor for complement (Cromer blood group)
A_72_P217812	2.27	2.12	down	ZCCHC6	Uncharacterized protein [Source:UniProtKB/TrEMBL; Acc:F1S4J1] [ENSSSCT00000011987]	XM_003130637	zinc finger, CCHC domain containing 6
A_72_P413368	2.99	2.15	down		Sus scrofa mRNA, clone:ITT010040H02, expressed in intestine. [AK231345]	AK231345	
A_72_P229897	3.35	1.89	down				

Table 6.7: Of 233 significantly differently expressed entities which were isolated to not-decontaminated survivor samples (n=2), three had fold changes greater than 2.0 in both interpretations. One was significantly down-regulated with a fold-change greater than 3.0 in the survivor group.

6.3.6 Changes in gene expression with fatal exposure to ^{14}C-VX and no decontamination

Four animals which received no decontamination did not survive exposure to a 5xLD_{50} dose of ^{14}C-VX via damaged ear skin. Of the significantly differently expressed entities ($p<0.05$; FC>1.0), 52 were specific to samples from these non-survivors of the not-decontaminated group (n=4; Table S6.4). Two entities were differently regulated with a fold-change greater than 1.5 (Table 6.8).

Probe Name	FC Death	FC DXD	Regulation	Gene Symbol	Description	GenBank Accession	Gene Name
A_72_P124386	1.54	1.55	down		Sus scrofa mRNA, clone:LVR010018C03, expressed in liver. [AK232317]	AK232317	AK350727
A_72_P150236	1.65	1.55	down		Uncharacterized protein [Source:UniProtKB/TrEMBL;Acc: F1SCM0] [ENSSSCT00000002493]		

Table 6.8: Of 52 significantly differently expressed entities which were isolated to not-decontaminated non-surviving samples (n=4), two had fold changes greater than 1.5 in both interpretations.

6.3.7 Changes in gene expression in swine blood, common to "survivor", "non-survivor", "decontaminated" and "non-decontaminated" groups following exposure to 5xLD_{50} ^{14}C-VX via damaged ear skin

Of the significantly differently expressed entities ($p<0.05$; FC>1.0), 53 were identified across all groups (i.e. the "survivor" group, the "death" group, the "decontaminated" group and the "not-decontaminated" group; Figure 6.2 and Table S6.5). Fold change was between 1.0 and 3.0 and only one entity had fold change greater than 1.5 in all interpretations (Table 6.9).

Probe Name	FC Survival	FC Death	FC DXD	FC DD	Regulation	Gene Symbol	Description	GenBank Accession	Gene Name
A_72_P330288	2.69	1.54	2.04	2.23	down		Rep: Chromosome undetermined SCAF3439, whole genome shotgun sequence - Tetraodon nigroviridis (Green puffer), partial (6%) [TC538063]		

Table 6.9: Of 53 entities which were significantly differently expressed in all 4 groups, one had fold changes greater than 1.5 in all 4 interpretations

6.4 Discussion

This extension of an *in vivo* study of decontamination efficacy in response to a supra-lethal ^{14}C-VX exposure (5xLD_{50}) via damaged ear skin of anaesthetised swine, allowed identification of 4278 entities (42% of the probes included in the analysis) which were significantly differently expressed in the blood cells during the exposure period. However, interpretation of these results *viz* prediction of responses in humans must be made within the limits of the experimental design.

The toxicity of VX clearly precludes its use in human volunteer studies. Toxicological data must, therefore, be obtained from relevant *in vitro* or *in vivo* animal models. Swine models have been used previously for numerous investigations of VX-toxicity, decontamination and medical countermeasures. The preceding *in vivo* study, in which swine were exposed to a supra-lethal dose of ^{14}C-VX (Chapter 5), provided blood samples in which gene expression could be assessed.

Obtaining samples from an *in vivo* investigation enabled analysis of gene expression in the blood of animals experiencing clinical signs of toxicity: thus, the results should be representative of the whole organism response (as represented via the blood). The results may provide useful information for development of medical countermeasures for severe VX intoxication, particularly in terms of survival and long-term prognosis following exposure to a usually, and indeed, likely (i.e. without medical intervention or decontamination) fatal exposure to VX.

Gene expression analysis does not automatically infer functional protein expression. Furthermore quantitative confirmations of gene transcription were not validated by quantitative-PCR analysis. Validation of gene expression data and proteomic analyses would provide a more complete reference for relationships between gene expression and protein expression following exposure to VX.

In terms of quantification following the initial *in vivo* experiment, the mass of ^{14}C-VX extracted from the blood (1.9 ± 1.3% and 0.79 ± 0.45% in the not decontaminated and decontaminated groups respectively; mean ± standard deviation) was second only to the liver. The pre-dose blood sample for each subject could also be used as an intrinsic control. Analysis was performed on RNA extracted from whole blood samples. This also brought the array analysis into line with the assay of AChE inhibition. The brain, diaphragm, lungs, heart and liver would be of particular interest for future studies of organophosphate-induced changes in gene expression, as VX toxicity is frequently reported to be manifest in these organs.

The observed differences in gene expression between groups cannot be exclusively attributed to VX–exposure and/or decontamination. The *in vivo* model also included anaesthetic administration, and application of a >98% pure radio-labelled contaminant (i.e. <2% unspecified impurities). Without a comprehensive speciation analysis of the exogenous compounds present in the blood, i.e. a profile of the relative concentrations of ^{14}C-VX, impurities, metabolites or breakdown products, the relative influence of VX and/or other compounds on gene expression of the blood cannot be confirmed. Nevertheless, by

comparing decontaminated to non-decontaminated groups, the effects of the exposures was investigated.

Genes involved in inflammatory and immune system responses were identified to be significantly differently regulated in all of the groups. This may be attributed to a response to the skin injury which all animals had received. However, recent microarray analyses of gene expression in brain tissue following soman exposure in rodents has also identified the involvement of inflammatory pathways[138,139]. These observations could be particularly pertinent for studies of haemostatic decontaminant performance in a contaminated haemorrhaging wound.

Information pertaining to effects of alphaxalone effects on gene expression is limited, so the influence of alphaxalone administration on these results cannot be confirmed. Alphaxalone has been shown to have transcriptional activity at the chicken progesterone receptor and in cultured human neuroblastoma (SK-N-MC cells) but not at the human progesterone receptor[140]. However, all animals were anaesthetised so any gene expression changes caused by the anaesthetic will be common to all groups. The final blood sample was obtained prior to administration of pentobarbital, so the method of euthanasia has not contributed to the results presented.

Nineteen common genes were oppositely regulated between samples from survivors (down-regulated) and non-survivors (up-regulated). The majority of these were un-annotated, but the list did include genes involved in cell signalling processes and genes specifically expressed in hematopoietic cells (PTPRC). A separate common set of nineteen genes were also oppositely regulated between samples from survivors (up-regulated) and samples from

non-survivors (down-regulated). A number of these were un-annotated, but the list did include genes which are involved in acute liver failure (HMGB1)[141], inflammatory responses and wound healing (AIMP)[142,143], responses to oxidative stress (SOD1), endoplasmic reticulum structural formation (ATL3)[144], distal myopathy (including muscle weakness; MATR3)[145], nucleic acid binding, ribosome structure and endonuclease activity (CNBP, RPL6, RPL7, RSP3)[146]. The TTI1 gene was down-regulated in both survivor and death groups with one of the highest fold-changes: this gene is involved in the DNA Damage Response (DDR) which is initiated following DNA damage[147]. Whilst liver function or damage was not directly under investigation, the identification of changes in HMGB1 expression in the blood cells could be reflective of detrimental processes taking place in the liver.

The comparisons of genes expressed in the blood samples of survivors and non-survivors indicate the differential induction or suppression of responses to oxidative stress, DNA damage, disruption of DNA replication, stimulation of inflammatory responses or liver toxicity. In addition to DNA damage, oxidative stress (OS) can also have a detrimental effect on cell membrane integrity via lipid peroxidation and disturbance of Ca^{2+} homeostasis. Oxidative stress has been demonstrated following organophosphate exposure[93,94]. Indeed, mild hyperkalaemia and hyperphosphataemia has been measured in blood of swine exposed to a $2xLD_{50}$ dose of VX[74], which could possibly be a result of OS-induced reduced membrane integrity.

A gene involved in immunoregulatory functions and the haemostasis pathway, particularly cell surface interactions at the vascular wall (Entrez Gene ID 100512978 sequence derived

from AMICA1), was one of the highest down-regulated genes in samples from both decontaminated and non-decontaminated groups exposed to VX[148].

Three genes which were isolated to the not-decontaminated survivor group (with the highest magnitude fold-change) encoded genes involved in complement cascade regulation (CD55)[149], and zinc finger formation (ZCCHC6). One of the genes of interest in not-decontaminated samples (regardless of outcome) is involved in cellular interactions and adhesion processes, perhaps with particular relationships to immunological and inflammatory responses (ADAM8)[150].

The genes identified with the largest fold-change in the decontaminated samples were down-regulated (fold-change >6.0). Many of these were also identified in the survivor interpretation. Thus, these genes were identified in samples of surviving decontaminated animals. These genes included *S. scrofa* lactotransferrin, *S. scrofa* haptoglobin, *S. scrofa* CD163 and resistin. Resistin (RETN) is expressed in porcine leukocytes and secreted by adipocytes[151,152]. Lactotransferrin (LF), which is an iron-binding protein expressed in neutrophils, has been detected in secretions including mucosal secretions, tears and saliva, as well as human, cattle and swine milk[153–155]. Antimicrobial, antioxidant, iron absorption regulation and transcription activation roles for LF have also been demonstrated[153–155]. Haptoglobin (HP) is also a haem-binding protein, with suggested involvement in oxidative stress and responses to infection[156,157]. Elevated levels of HP have been detected in sera of pigs in the early stages of porcine reproductive and respiratory syndrome (PRSS) infection[157]. CD163 has a role in binding specific glycoproteins of the PRRS virus (PRSSv)[158–161]. An investigation of LF and HP, and iron and haem protein levels in blood may be an useful point

of investigation, as changes in permeability of blood cells have been demonstrated following organophosphate exposure *in vitro*[162].

In the samples taken from decontaminated animal which did not survive, genes of interest included a chemokine (CCL25) usually expressed in the porcine small intestine, which was up-regulated[163,164]; and *S. scrofa* phosphatidylinositol transfer protein, cytoplasmic 1 (PITPNC1), which was down-regulated. Similar proteins are involved in phospholipid trafficking. However, in non-surviving animals, many of the changes seen are likely to be secondary to the detrimental effects on cell biochemistry and physiology caused by intoxication, rather than being a direct mechanistic effect of VX.

The majority of the significant differential expressions identified were down-regulated. This could be suggestive of an overall inhibitory effect on gene expression or transcription, but not entirely as only approximately 42% of the analysed genes on the array were affected in any way. Additional mechanisms which may manifest as changes in gene expression may also be induced by processes contributing to mortality which are secondary to (i.e. resulting from) primary VX toxicity. The predominant cause of death was not determined in this study, but death was confirmed following 15 minutes of apnoea, which may be caused by respiratory paralysis, either centrally or peripherally. Gene expression changes and changes in transcriptional regulation have been reported due to hypoxia or asphyxia[148,165–167].

In summary, gene expression analysis identified a number of genes which were significantly differentially expressed in whole blood samples obtained from decontaminated or not-decontaminated survivors or non-survivors of a supra-lethal ^{14}C-VX exposure via damaged ear skin of swine. In particular, genes of interest were identified with involvement in

oxidative stress, inflammatory and immunoregulatory responses, liver failure, and iron binding. These processes may be important to consider in future studies of VX intoxication, mechanisms of action, protective measures and medical treatments.

This experiment identified the need for further investigations of:

- gene expression in other tissues following VX exposure.
- characterisation of the effects of anaesthetics on gene expression.
- inclusion of speciation analysis in *in vivo* exposure models to relate gene expression results to specific substances.
- inclusion of specific haematology measurements in *in vivo* exposure models.
- relative contributions of radiolabel and impurities to gene expression results.
- sub-lethal VX exposures to investigate gene expression with equivalent exposure times.
- microarray data, by validation of results using qPCR.

CHAPTER 7. General Discussion and Summary

CHAPTER 7. GENERAL DISCUSSION AND SUMMARY

The aim of the work presented was to identify a product with haemostatic capability, which was able to prevent death following exposure of a wound contaminated with an otherwise lethal dose of VX (Figure 7.1). In chapter 3, the feasibility of using thrombelastography to investigate inherent pro-coagulative activity of a number of commercially available haemostatic products was successfully demonstrated. This was a relatively novel approach to investigating haemostat efficacy. Using this *in vitro* technique, it was shown that a relatively high dose of VX had no effect on coagulation kinetics of swine blood *in vitro*. Furthermore, it was shown that VX contamination did not adversely affect the efficacy of the haemostats which were tested. However, for some of the products tested, no advantage in coagulation kinetics was observed, despite documented *in vivo* evidence in the literature. The benefit of *in vitro* tests for product efficacy cannot be under-estimated, however, clearly physical mechanisms of action other than inherent pro-coagulation are involved for some of these products, which were not exploited or clearly demonstrated by the thrombelastographic method. This provides supporting evidence that whilst an *in vitro* coagulation assay may be utilised for demonstrations of haemostatic efficacy, and even "screening" of advantageous products, efforts must be made in study designs to ensure that physical mechanisms of action such as compression or tamponade can be represented *in vitro*.

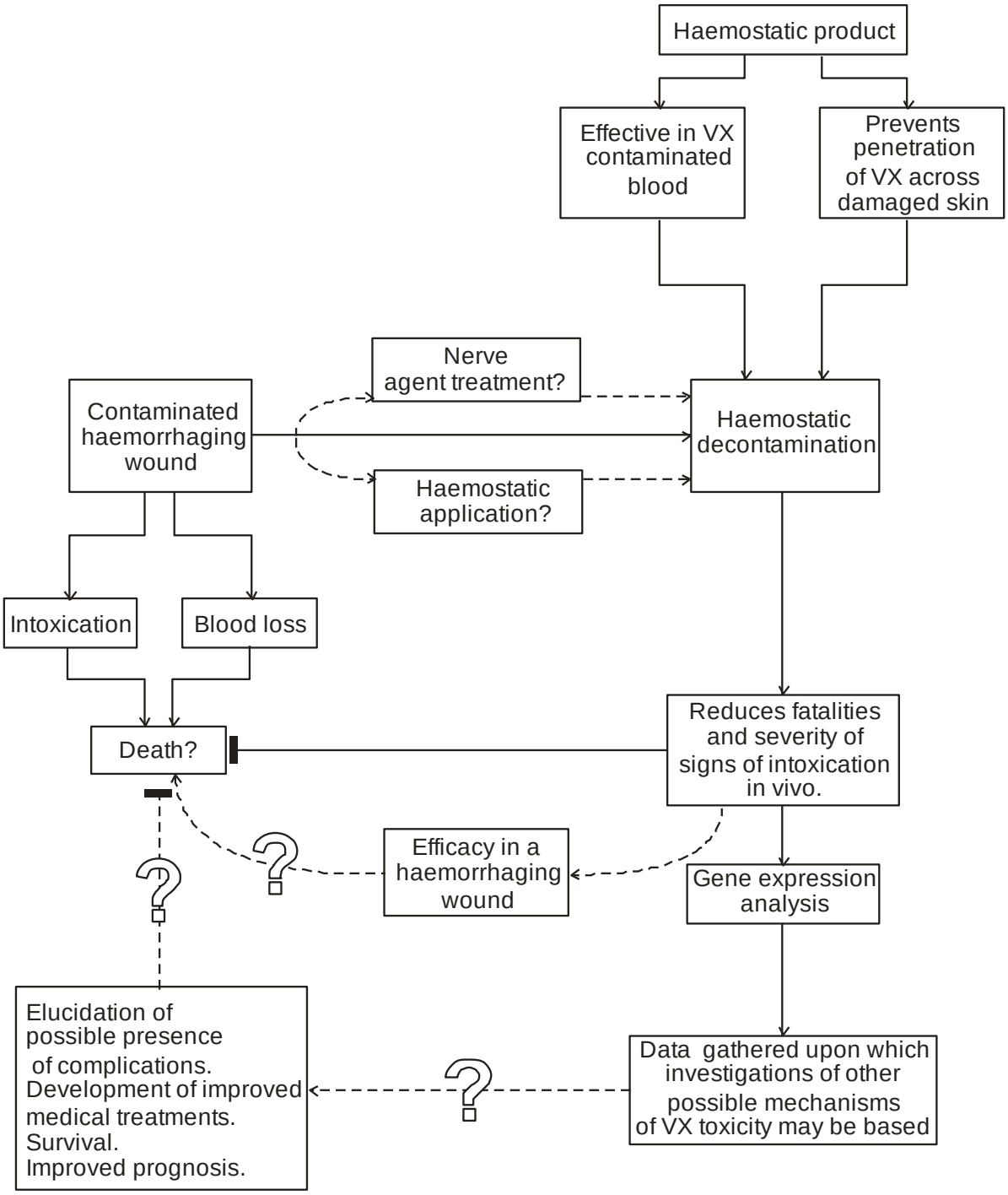

Figure 7.1: Schematic summary of the results presented and inferences drawn from the studies evaluating the feasibility of applying a haemostat to a wound contaminated with VX in order to prevent death from blood loss or intoxication.

Points that require further investigation are indicated by the dotted lines.

Further supporting evidence for the feasibility of using a haemostat as a decontaminant was provided by the ability of a selection of haemostats to effectively prevent, or at the very least reduce, penetration of VX across intact and damaged pig skin (Chapter 4). A number of products compared favourably to currently "in use" decontaminants. Including damaged skin in the experiments was particularly useful to assess simple mechanistic characteristics of these products in conditions relevant to the ultimate intended setting: a contaminated haemorrhaging wound. However, the merits of products with chemical-decontamination mechanisms of action, rather than prevention of penetration, were perhaps not fully represented by this approach. Interestingly, one novel liquid decontamination product was able to effectively reduce penetration. This was particularly encouraging and merits further investigation of chemical-decontamination mechanisms, including speciation analysis of breakdown products, and the consideration of combination therapies.

Following successful demonstrations of pro-coagulative and decontamination efficacy, one product, from a starting list of 7 candidates, was selected for evaluation in a superficial skin wound *in vivo* (Chapter 5). Application of WoundStat^{TM} was successful in reducing the number of fatalities, prolonging survival time and reducing the severity of signs of intoxication, without any additional medical treatment (other than anaesthesia). However, signs of intoxication were not eliminated, and the total (estimated) internal absorption and extent of acetylcholinesterase inhibition were not dissimilar between decontaminated and non-decontaminated animals. Acetylcholinesterase inhibition did not correlate with survival time and similarities were observed in physiological parameters and signs of intoxication between animals which did or did not survive between the treatment groups. This evidence further supported the clinical need for rapid medical treatment along with effective

decontamination, and that acetylcholinesterase activity was not a robust indicator of prognosis. The results provided further evidence for the existence of mechanisms involved in VX toxicity, other than acetylcholinesterase inhibition, in agreement with previous experimental reports in the literature. The long-term effects and prognosis of the demonstrated efficacy of decontamination were not investigated. With continuing improvements in decontamination methods, products and medical interventions, future investigations should include analysis of long term prognosis and sequelae following survival of severe nerve agent intoxication. Desorption kinetics also remain to be investigated, as although WoundStat™ was able to retain almost 50% of the mass of ^{14}C-VX which was applied, the desorption (or "off-gassing") of VX from the decontaminant matrix could become a secondary hazard. This is particularly pertinent for situations such as a battlefield or a mass casualty incident where evacuation to a medical centre, or receipt of treatment, may be delayed[168,169].

With these points in mind, changes in gene expression in the exposed animals was analysed (Chapter 6). Currently, this is the only microarray investigation of gene expression changes in the blood of animals exposed to a supra-lethal dose of VX. The changes in expression of genes involved in inflammatory responses could be attributed to the induced skin damage, but has also been reported following exposure of rodents to sarin or VX (without skin damage)[138,139,170]. Genes involved in responses to oxidative stress and DNA damage were also identified, in accordance with reports of genotoxicity effects of organophosphate pesticides, along with genes involved in iron binding and liver failure. In the context of a contaminated haemorrhaging wound, these findings, in particular the involvement of

inflammatory responses, can be a further complication to consider for successful medical treatment, and as a target for development of effective medical countermeasures.

During the *in vivo* experimentation stage, reports of clinical safety concerns ultimately led to the withdrawal of WoundStat™ from use[171]. Nevertheless, this work clearly demonstrated the proof-of-principle of a possible haemostatic decontaminant, and the resultant benefits of development and evaluation of standard haemostatic decontaminants cannot be under-emphasised.

Further work

The results presented support the principle and feasibility of successful application of a haemostatic decontaminant, based on an adsorptive mechanism of action, to prevent death from intoxication following contamination of a superficial skin wound. The efficacy of WoundStat™ (or a similar product) to prevent death from intoxication and blood loss in a severely haemorrhaging contaminated wound *in vivo* has yet to be established. Validation and detailed investigation of the gene analysis results is also necessary. The inclusion of biochemical analyses of blood during exposure to VX (*in vivo*) would also be useful to further investigate extra mechanisms of VX intoxication. The hypothetical benefit of developing products with combinations of adsorptive and decontaminating mechanisms of action is also clearly supported. Future investigations based on the work presented, should ultimately lead to enhanced decontamination products, improved medical treatments and ultimately life-saving results.

CHAPTER 8. References

CHAPTER 8. REFERENCES

1. Bellamy RF. The causes of death in conventional land warfare: implications for combat casualty care research. Military Medicine 1984;149:55–62.

2. Sauaia A, Moore FA, Moore EE, Moser KS, Brennan R, Read RA, Pons PT. Epidemiology of trauma deaths: a reassessment. The Journal of Trauma - Injury, Infection & Critical Care 1995;38:185–93.

3. Alam HB, Chen Z, Jaskille A, Ireneo R, Querol LC, Koustova E, Inocencio R, Conran R, Seufert A, Ariaban N, Toruno K, Rhee P. Application of a Zeolite Hemostatic Agent Achieves 100 % Survival in a Lethal Model of Complex Groin Injury in Swine. The Journal of Trauma - Injury, Infection & Critical Care 2004;56(May):974–83.

4. Alam HB, Uy GB, Miller D, Koustova E, Hancock T, Inocencio R, Anderson D, Llorente O, Rhee P. Comparative Analysis of Hemostatic Agents in a Swine Model of Lethal Groin Injury. The Journal of Trauma - Injury, Infection & Critical Care 2003;54(6):1077–1082.

5. Pusateri AE, Holcomb JB, Kheirabadi BS, Alam HB, Wade CE, Ryan KL. Making Sense of the Preclinical Literature on Advanced Hemostatic Products. The Journal of Trauma - Injury, Infection & Critical Care 2006;60(3):674–682.

6. Wedmore I, Mcmanus JG, Pusateri AE, Holcomb JB. A Special Report on the Chitosan-based Hemostatic Dressing: Experience in Current Combat Operations. The Journal of Trauma - Injury, Infection & Critical Care 2006;60(3):655–658.

7. Pusateri AE, Modrow HE, Harris RA, Holcomb JB, Hess JR, Mosebar RH, Reid TJ, Nelson JH, Goodwin CW, Fitzpatrick GM, Mcmanus AT, Zolock DT, Sondeen JL, Cornum RL, Martinez RS. Advanced Hemostatic Dressing Development Program: Animal Model Selection Criteria and Results of a Study of Nine Hemostatic Dressings in a Model of Severe Large Venous Hemorrhage and Hepatic Injury in Swine. The Journal of Trauma - Injury, Infection & Critical Care 2003;(September):518–526.

8. Pusateri AE, Delgado AV, Dick EJ, Martinez RS, Holcomb JB, Ryan KL. Application of a Granular Mineral-Based Hemostatic Agent (QuikClot) to Reduce Blood Loss After Grade V Liver Injury in Swine. The Journal of Trauma - Injury, Infection & Critical Care 2004;57(3):555–562.

9. Pusateri AE, Mccarthy SJ, Gregory KW, Harris RA, Cardenas L, Mcmanus AT, Goodwin CW. Effect of a Chitosan-Based Hemostatic Dressing on Blood Loss and Survival in a Model of Severe Venous Hemorrhage and Hepatic Injury in Swine. The Journal of Trauma - Injury, Infection & Critical Care 2003;54(1):177–182.

10. Holcomb JB, Pusateri AE, Harris RA, Charles NC, Gomez RR, Cole JP, Beall LD, Bayer V, MacPhee MJ, Hess JR. Effect of Dry Fibrin Sealant Dressings versus Gauze Packing on Blood Loss in Grade V Liver Injuries in Resuscitated Swine. The Journal of Trauma - Injury, Infection & Critical Care 1999;46(1):49–57.

11. Holcomb JB, Pusateri AE, Harris RA, Reid TJ, Beall LD, Hess JR, MacPhee MJ. Dry Fibrin Sealant Dressings Reduce Blood Loss, Resuscitation Volume, and Improve Survival in Hypothermic Coagulopathic Swine with Grade V Liver Injuries. The Journal of Trauma - Injury, Infection & Critical Care 1999;47(2):233–242.

12. Pusateri AE, Kheirabadi BS, Delgado AV, Doyle JW, Kanellos J, Uscilowicz JM, Martinez RS, Holcomb JB, Modrow HE. Structural Design of the Dry Fibrin Sealant Dressing and Its Impact on the Hemostatic Efficacy of the Product. Journal of Biomedical Materials Research Part B: Applied Biomaterials 2004;70(1):114–121.

13. Arnaud F, Tomori T, Saito R, Mckeague A, Prusaczyk WK, Mccarron RM. Comparative Efficacy of Granular and Bagged Formulations of the Hemostatic Agent QuikClot. The Journal of Trauma - Injury, Infection & Critical Care 2007;63(4):775–782.

14. Kozen BG, Kircher SJ, Henao J, Godinez FS, Johnson AS. An Alternative Hemostatic Dressing: Comparison of CELOX, HemCon, and QuikClot. Journal of Academic Emergency Medicine 2008;15(1):74–81.

15. Acheson EM, Kheirabadi BS, Deguzman R, Dick EJ, Holcomb JB. Comparison of Hemorrhage Control Agents Applied to Lethal Extremity Arterial Hemorrhages in Swine. The Journal of Trauma - Injury, Infection & Critical Care 2005;59(4):865–875.

16. Ward KR, Tiba MH, H HW, Blocher CR, Draucker GT, Proffitt EK, Bowlin GL, Ivatury RR, Diegelmann RF. Comparison of a New Hemostatic Agent to Current Combat Hemostatic Agents in a Swine Model of Lethal Extremity Arterial Hemorrhage. The Journal of Trauma - Injury, Infection & Critical Care 2007;63(August):276–284.

17. Kheirabadi BS, Acheson EM, Deguzman R, Sondeen JL, Ryan KL, Delgado A, Dick Jr EJ, Holcomb JB. Hemostatic Efficacy of Two Advanced Dressings in an Aortic Hemorrhage Model in Swine. The Journal of Trauma - Injury, Infection & Critical Care 2005;59(1):25–35.

18. Sondeen JL, Pusateri AE, Coppes VG, Gaddy CPTCE, Holcomb JB. Comparison of 10 Different Hemostatic Dressings in an Aortic Injury. The Journal of Trauma - Injury, Infection & Critical Care 2003;54(2):280–285.

19. Jewelewicz DD, Cohn SM, Crookes BA, Proctor KG. Modified Rapid Deployment Hemostat Bandage Reduces Blood Loss and Mortality in Coagulopathic Pigs with Severe Liver Injury. The Journal of Trauma - Injury, Infection & Critical Care 2003;55(2):275–281.

20. Mathias M, Liesner R. Understanding haemostasis. Paediatrics and Child Health 2007;17(8):317–321.

21. Coakley M, Reddy K, Mackie I, Mallett S. Transfusion Triggers in Orthotopic Liver Transplantation: A Comparison of the Thromboelastometry Analyzer , the Thromboelastogram, and Conventional Coagulation Tests. Journal of Cardiothoracic and Vascular Anesthesia 2006;20(4):548–553.

22. Valeri CR, Srey R, Tilahun D, Ragno G. In Vitro Effects of Poly-N-Acetyl Glucosamine on the Activation of Platelets in Platelet-Rich Plasma with and without Red Blood Cells. The Journal of Trauma - Injury, Infection & Critical Care 2004;57:S22–25.

23. Fischer TH, Connolly R, Thatte HS, Schwaitzberg SS. Comparison of Structural and Hemostatic Properties of the Poly-N-Acetyl Glucosamine Syvek Patch With Products Containing Chitosan. Microscopy Research and Technique 2004;63:168 –174.

24. Kheirabadi BS, Scherer MR, Estep JS, Dubick M a, Holcomb JB. Determination of efficacy of new hemostatic dressings in a model of extremity arterial hemorrhage in swine. The Journal of Trauma - Injury, Infection & Critical Care 2009 Sep;67(3):450–9; discussion 459–60.

25. Ahuja N, Ostomel TA, Rhee P, Stucky GD, Conran R, Chen Z, Al-Mubarack G, Velmahos G, DeMoya M. Testing of Modified Zeolite Hemostatic Dressings in a Large Model of Lethal Grion Injury. The Journal of Trauma - Injury, Infection & Critical Care 2006;61(6):1312–1320.

26. Okumura T, Takasu N, Ishimatsu S, Miyanoki S, Mitsuhashi A, Kumada K, Tanaka K, Hinohara S. Report on 640 Victims of the Tokyo Subway Sarin Attack. Annals of Emergency Medicine 1996;28(2):129–134.

27. Nozaki H, Aikawa N, Fujishima S, Suzuki M, Shinozawa Y, Hori S, Nogawa S. A case of VX poisoning and the difference from sarin. Lancet 1995;346(8976):698–699.

28. Marrs TC. Toxicology of Organophosphate Nerve Agents. In: Marrs TC, Maynard RL, Sidell F, editors. Chemical Warfare Agents: Toxicology and Treatment. Wiley-Blackwell; 2007 p. 191–222.

29. Okumura T, Nomura T, Suzuki T, Sugita M, Takeuchi Y, Naito T, Okumura S, Maekawa H, Ishimatsu S, Takasu N, Miura K, Suzuki K. The Dark Morning: The Experiences and Lessons Learned from the Tokyo Subway Sarin Attack. In: Marrs TC, Maynard RL, Sidell F, editors. Chemical Warfare Agents: Toxicology and Treatment. Wiley-Blackwell; 2007 p. 277–286.

30. Timbrell J. Biochemical mechanisms of toxicity: specific examples. In: Principles of Biochemical Toxicology. Taylor & Francis; 2000 p. 297–303.

31. Vale A, Marrs TC, Rice P. Chemical terrorism and nerve agents. Medicine 2007 Oct;35(10):573–575.

32. Echobichon DJ. Toxic Effects of Pesticides. In: Klaassen CD, editor. Casarett & Doull's Toxicology: The Basic Science of Poisons. McGraw Hill; 2001 p. 779–784.

33. Worek F, Thiermann H, Szinicz L, Eyer P. Kinetic analysis of interactions between human acetylcholinesterase, structurally different organophosphorus compounds and oximes. Biochemical Pharmacology 2004 Dec;68(11):2237–48.

34. Aurbek N, Thiermann H, Szinicz L, Eyer P, Worek F. Analysis of inhibition, reactivation and aging kinetics of highly toxic organophosphorus compounds with human and pig acetylcholinesterase. Toxicology 2006;224:91–99.

35. Worek F, Reiter G, Eyer P, Szinicz L. Reactivation kinetics of acetylcholinesterase from different species inhibited by highly toxic organophosphates. Archives of Toxicology 2002;76(9):523–529.

36. Maxwell DM, Koplovitz I, Worek F, Sweeney RE. A structure-activity analysis of the variation in oxime efficacy against nerve agents. Toxicology and Applied Pharmacology 2008;231:157–164.

37. Mumford H, Price ME, Wetherell JR. A novel approach to assessing percutaneous VX poisoning in the conscious guinea-pig. Journal of Applied Toxicology 2008;28(5):694–702.

38. Bide RW, Schofield L, Risk DJ. Immediate post-dosing paralysis following severe Soman and VX toxicosis in guinea pigs. Journal of Applied Toxicology 2005 Sep;25(5):410–417.

39. McGuire JM, Taylor JT, Byers CE, Jakubowski EM, Thomson SA. Determination of VX-G analogue in red blood cells via gas chromatography-tandem mass spectrometry following an accidental exposure to VX. Journal of Analytical Toxicology 2008 Jan;32(1):73–77.

40. Solano MI, Thomas JD, Taylor JT, McGuire JM, Jakubowski EM, Thomson SA, Maggio VL, Holland KE, Smith JR, Capacio B, Woolfitt AR, Ashley DL, Barr JR. Quantification of nerve agent VX-butyrylcholinesterase adduct biomarker from an accidental exposure. Journal of Analytical Toxicology 2008 Jan;32(1):68–72.

41. Morita H, Yanagisawa N, Nakajima T, Shimizu M, Hirabayashi H, Okudera H, Nohara M, Midorikawa Y, Mimura S. Sarin poisoning in Matsumoto, Japan. Lancet 1995 Jul;346(8970):290–3.

42. Macilwain C. Study proves Iraq used nerve gas. Nature 1993;363:3.

43. Black RM, Clarke RJ, Read RW, Reid MT. Application of gas chromatography-mass spectrometry and gas chromatography-tandem mass spectrometry to the analysis of chemical warfare samples, found to contain residues of the nerve agent sarin, sulphur mustard and their degradation products. Journal of Chromatography A 1994 Feb;662(2):301–21.

44. Craig FN, Cummings EG, Sim VM. Environmental temperature and the percutaneous absorption of a cholinesterase inhibitor, VX. The Journal of Investigative Dermatology 1977 Jun;68(6):357–361.

45. Okudera H, Morita H, Iwashita T, Shibata T, Otagiri T, Kobayashi S, Yanagisawa N. Unexpected Nerve Gas Exposure in the City of Matsumoto: Report of Rescue Activity in the First Sarin Gas Terrorism. The American Journal of Emergency Medicine 1997 Sep;15(5):527–8.

46. Hilmas CJ, Poole MJ, Finneran K, Clark MG, Williams PT. Galantamine is a novel post-exposure therapeutic against lethal VX challenge. Toxicology and Applied Pharmacology 2009;240(2):166–173.

47. Wetherell J, Price M, Mumford H. A novel approach for medical countermeasures to nerve agent poisoning in the guinea-pig. NeuroToxicology 2006;27(4):485–491.

48. Shih T-M, Skovira JW, McDonough JH. Effects of 4-pyridine aldoxime on nerve agent-inhibited acetylcholinesterase activity in guinea pigs. Archives of Toxicology 2009 Dec;83(12):1083–9.

49. Shih T-M, Skovira JW, O'Donnell JC, McDonough JH. In vivo reactivation by oximes of inhibited blood, brain and peripheral tissue cholinesterase activity following exposure to nerve agents in guinea pigs. Chemico-Biological Interactions 2010 Sep;187:207–14.

50. Skovira JW, O'Donnell JC, Koplovitz I, Kan RK, McDonough JH, Shih T-M. Reactivation of brain acetylcholinesterase by monoisonitrosoacetone increases the therapeutic efficacy against nerve agents in guinea pigs. Chemico-Biological Interactions 2010 Sep;187:318–24.

51. Lenz DE, Maxwell DM, Koplovitz I, Clark CR, Capacio BR, Cerasoli DM, Federko JM, Luo C, Saxena A, Doctor BP, Olson C. Protection against soman or VX poisoning by human butyrylcholinesterase in guinea pigs and cynomolgus monkeys. Chemico-Biological Interactions 2005;157-158(0009-2797):205–210.

52. Valiyaveettil M, Alamneh Y, Rezk P, Perkins MW, Sciuto AM, Doctor BP, Nambiar MP. Recombinant paraoxonase 1 protects against sarin and soman toxicity following microinstillation inhalation exposure in guinea pigs. Toxicology Letters 2011 May;202(3):203–8.

53. Mumford H, Price ME, Cerasoli DM, Teschner W, Ehrlich H, Peter H, Lenz DE. Efficacy and physiological effects of human butyrylcholinesterase as a post-exposure therapy against percutaneous poisoning by VX in the guinea-pig. Chemico-Biological Interactions 2010;187:304–308.

54. Worek F, Aurbek N, Wetherell J, Pearce P, Mann T, Thiermann H. Inhibition, reactivation and aging kinetics of highly toxic organophosphorus compounds: Pig versus minipig acetylcholinesterase. Toxicology 2008;244(1):35–41.

55. Balboa A, Buchanan JH, Buettner LC, Sewell T, Tevault DE. Vapor Pressure of GD. Edgewood Chemical Biological Center ECBC-TR-575 2007;(October):1–18.

56. Buchanan JH, Buettner LC, Butrow AB, Tevault DE. Vapor Pressure of VX. Edgewood Chemical Biological Center ECBC-TR-068 1999;(November)

57. Van Der Schans MJ, Lander BJ, Van Der Wiel H, Langenberg JP, Benschop HP. Toxicokinetics of the nerve agent (+/-)-VX in anesthetized and atropinized hairless guinea pigs and marmosets after intravenous and percutaneous administration. Toxicology and Applied Pharmacology 2003;191(1):48–62.

58. Chilcott RP, Dalton CH, Hill I, Davison CM, Blohm KL, Clarkson ED, Hamilton MG. In vivo skin absorption and distribution of the nerve agent VX (O-ethyl-S-[2(diisopropylamino)ethyl] methylphosphonothioate) in the domestic white pig. Human & Experimental Toxicology 2005 Jul;24(7):347–352.

59. van der Schans MJ, Lander BJ, Moes GWH, Wiel HJVD, Langenberg JP, Benschop HP. Toxicokinetics of (±)-VX and results of an exploratory study on the in vitro metabolism of (+/-)-VX. 2000;1–11. Paper presented at the meeting of NATO TG 004 Task Group on Prophylaxis and Therapy of Chemical Agents, 2000. ftp://ftp.rta.nato.int/Pubfulltext/RTO/TR/RTO-TR-HFM-041/TR-HFM-041-2000-Files/Papers/Marcelvxtoxicokinetiek.pdf

60. Hoskin FCG, Walker JE. Malathion as a Model for the Enzymatic Hydrolysis of the Neurotoxic Agent, VX. Bulletin of Environmental Contamination and Toxicology 1997 Jul;59(1):9–13.

61. Hoskin FCG, Walker JE, Dettbarn W-D, Wild JR. Hydrolysis of tetriso by an enzyme derived from Pseudomonas diminuta as a model for the detoxication of O-ethyl S-(2-diisopropylaminoethyl) methylphosphonothiolate (VX). Biochemical Pharmacology 1995;49(5):711–715.

62. Jokanović M. Current understanding of the mechanisms involved in metabolic detoxification of warfare nerve agents. Toxicology Letters 2009 Jul;188(1):1–10.

63. Peterson MW, Fairchild SZ, Otto TC, Mohtashemi M, Cerasoli DM, Chang WE. VX Hydrolysis by Human Serum Paraoxonase 1: A Comparison of Experimental and Computational Results. PLoS One 2011 Jan;6(5):e20335, 1–7.

64. Black RM. History and perspectives of bioanalytical methods for chemical warfare agent detection. Journal of Chromatography B 2010 May;878(17-18):1207–1215.

65. Munro NB, Talmage SS, Griffin GD, Waters LC, Watson AP, King JF, Hauschild V. The sources, fate, and toxicity of chemical warfare agent degradation products. Environmental Health Perspectives 1999;107(12):933–974.

66. Bonierbale E, Debordes L, Coppet L. Application of capillary gas chromatography to the study of hydrolysis of the nerve agent VX in rat plasma. Journal of Chromatography B: Biomedical Sciences and Applications 1997;688(2):255–264.

67. Miki A, Katagi M, Tsuchihashi H, Yamashita M. Determination of alkylmethylphosphonic acids, the main metabolites of organophosphorus nerve agents, in biofluids by gas chromatography-mass spectrometry and liquid-liquid-solid-phase-transfer-catalyzed pentafluorobenzylation. Journal of Analytical Toxicology 1999;23(2):86–93.

68. Tsuchihashi H, Katagi M, Nishikawa M, Tatsuno M. Identification of metabolites of nerve agent VX in serum collected from a victim. Journal of Analytical Toxicology 1998 Sep;22(5):383–388.

69. Reiter G, Mikler J, Hill I, Weatherby K, Thiermann H, Worek F. Simultaneous quantification of VX and its toxic metabolite in blood and plasma samples and its application for in vivo and in vitro toxicological studies. Journal of Chromatography B 2011 Sep;879(26):2704–13.

70. Fawcett WP, Aracava Y, Adler M, Pereira EFR, Albuquerque EX. Acute Toxicity of Organophosphorus Compounds in Guinea Pigs is Sex- and Age-Dependent and Cannot be Solely Accounted for by Acetylcholinesterase Inhibition. The Journal of Pharmacology and Experimental Therapeutics 2009;328(2):516–524.

71. Lockridge O, Duysen EG, Voelker T, Thompson CM, Schopfer LM. Life without acetylcholinesterase: the implications of cholinesterase inhibitor toxicity in AChE-knockout mice. Environmental Toxicology and Pharmacology 2005 May;19:463–469.

72. Duysen EG, Li B, Xie W, Schopfer LM, Anderson RS, Broomfield CA, Lockridge O. Evidence for Nonacetylcholinesterase Targets of Organophosphorus Nerve Agent: Supersensitivity of Acetylcholinesterase Knockout Mouse to VX Lethality. The Journal of Pharmacology and Experimental Therapeutics 2001;299(2):528–535.

73. Rocksen D, Elfsmark D, Heldestad V, Wallgren K, Cassel G, Goransson Nyberg A. An animal model to study health effects during continuous low-dose exposure to the nerve agent VX. Toxicology 2008 Aug;250(1):32–8.

74. Chilcott R, Dalton C, Hill I, Davidson C, Blohm K, Hamilton M. Clinical manifestations of VX poisoning following percutaneous exposure in the domestic white pig. Human & Experimental Toxicology 2003 May;22(5):255–261.

75. Wilkinson SC, Maas WJM, Nielsen JB, Greaves LC, van de Sandt JJM, Williams FM. Interactions of skin thickness and physicochemical properties of test compounds in percutaneous penetration studies. International Archives of Occupational and Environmental Health 2006 May;79(5):405–13.

76. Sun T-T, Green H. Keratin Filaments of Cultured Human Epidermal Cells. The Journal of Biological Chemistry 1978;253(6):2053–2060.

77. Sun T-T, Green H. Differentiation of the epidermal keratinocyte in cell culture: formation of the cornified envelope. Cell 1976 Dec;9(4, Part 1):511–21.

78. Sun T-T, Green H. Cultured epithemial cells of cornea, conjunctiva and skin: absence of marked intrinsic divergence of their differentiated states. Nature 1977;269:489–493.

79. Doran TI, Vidrich A, Sun T-T. Intrinsic and Extrinsic Regulation of the Differentiation of Skin, Corneal and Esophageal Epithelial Cells. Cell 1980 Nov;22(1, Part 1):17–25.

80. Ovaere P, Lippens S, Vandenabeele P, Declercq W. The emerging roles of serine protease cascades in the epidermis. Trends in Biomedical Sciences 2009 Sep;34(9):453–63.

81. Lechler T, Fuchs E. Asymmetric cell divisions promote stratification and differentiation of mammalian skin. Nature 2005 Sep;437(7056):275–80.

82. Plewig G, Marples RR. Regional differences of cell sizes in the human stratum corneum. Part 1. The Journal of Investigative Dermatology 1970;54(1):13–18.

83. Scheuplein RJ. Permeability of the skin: a review of major concepts and some new developments. The Journal of Investigative Dermatology 1976;67(5, part 2 of 2):672–676.

84. Rougier A, Dupuis D, Lotte C, Roguet R. The Measurement of the Stratum Corneum Reservoir. A Predictive Method for In Vivo Percutaneous Absorption Studies: Influence of Application Time. The Journal of Investigative Dermatology 1985;84(1):66 – 68.

85. Dupuis D, Rougier A, Roguet R, Lotte C, Kalopissis G. In Vivo Relationship Between Horny Layer Reservoir Effect and Percutaneous Absorption in Human and Rat. The Journal of Investigative Dermatology 1984;82(4):353–356.

86. Rougier A, Dupuis D, Lotte C, Roguet R, Schaefer H. In Vivo Correlation Between Stratum Corneum Reservoir Function and Percutaneous Absorption. The Journal of Investigative Dermatology 1983;81(3):275–278.

87. Scott RC, Ramsey JD. Comparison of the In Vivo and In Vitro Percutaneous Absorption of a Lipophilic Molecule (Cypermethrin, a Pyrethroid Insecticide). The Journal of Investigative Dermatology 1987;89(2):142–146.

88. Grasso P, Lansdown ABG. Methods of measuring , and factors affecting, percutaneous absorption. Journal Of The Society Of Cosmetic Chemists 1972;521:481–521.

89. Haftek M, Teillon M-H, Schmitt D. Stratum Corneum, Corneodesmosomes and Ex Vivo Percutaneous Penetration. Microscopy Research and Technique 1998 Nov;43(3):242–9.

90. Scott RC, Corrigan MA, Smith F, Mason H. The Influence of Skin Structure on Permeability: An Intersite and Interspecies Comparison with Hydrophilic Penetrants. The Journal of Investigative Dermatology 1991;96(6):921–925.

91. Nakajima T, Ohta S, Fukushima Y, Yanagisawa N. Sequelae of Sarin Toxicity at One and Three Years After Exposure in Matsumoto, Japan. Journal of Epidemiology 1999;9(5):337–343.

92. Thiermann H, Szinicz L, Eyer P, Felgenhauer N, Zilker T, Worek F. Lessons to be learnt from organophosphorus pesticide poisoning for the treatment of nerve agent poisoning. Toxicology 2007;233(1-3 SPEC. ISS):145–154.

93. Hernández AF, López O, Rodrigo L, Gil F, Pena G, Serrano JL, Parrón T, Alvarez JC, Lorente JA, Pla A. Changes in erythrocyte enzymes in humans long-term exposed to pesticides: Influence of several markers of individual susceptibility. Toxicology Letters 2005 Oct;159(1):13–21.

94. López O, Hernández AF, Rodrigo L, Gil F, Pena G, Serrano JL, Parrón T, Villanueva E, Pla A. Changes in antioxidant enzymes in humans with long-term exposure to pesticides. Toxicology Letters 2007 Jul;171(3):146–53.

95. Wilkinson SC, Williams FM. Effects of experimental conditions on absorption of glycol ethers through human skin in vitro. International Archives of Occupational and Environmental Health 2002 Oct;75(8):519–27.

96. Monteiro-Riviere NA, Bristol DG, Manning TO, Rogers RA, Riviere JE. Interspecies and Interregional Analysis of the Comparative Histological Thickness and Laser Doppler Blood Flow Measurements at Five Cutaneous Sites in Nine Species. The Journal of Investigative Dermatology 1990;95(5):582–586.

97. Bartek MJ, LaBudde JA, Maibach HI. Skin Permeability In Vivo: Comparison in Rat, Rabbit, Pig and Man. The Journal of Investigative Dermatology 1972;58(3):114–123.

98. Ferry LL, Argentieri G, Lochner DH. The comparative histology of porcine and guinea pig skin with respect to iontophoretic drug delivery. Pharmaceutica Acta Helvetiae 1995 Apr;70:43–56.

99. Graham JS, Chilcott RP, Rice P, Milner SM, Hurst CG, Maliner BI. Wound Healing of Cutaneous Sulfur Mustard Injuries: Strategies for the Development of Improved Therapies. Journal of Burns and Wounds 1996;4:1–45.

100. Chilcott RP, Dalton CH, Hill I, Davison CM, Blohm KL, Clarkson ED, Hamilton MG. Evaluation of a Barrier Cream against the Chemical Warfare Agent VX using the Domestic White Pig. Basic & Clinical Pharmacology & Toxicology 2005 Jul;97(1):35–38.

101. Dalton CH, Hattersley IJ, Rutter SJ, Chilcott RP. Absorption of the nerve agent VX (O-ethyl-S- [2(di-isopropylamino)ethyl] methyl phosphonothioate) through pig, human and guinea pig skin in vitro. Toxicology in Vitro 2006 Dec;20(8):1532–1536.

102. Duncan EJS, Brown A, Lundy P, Sawyer TW, Hamilton M, Hill I, Conley JD. Site-specific percutaneous absorption of methyl salicylate and VX in domestic swine. Journal of Applied Toxicology 2002;22(3):141–148.

103. Read RW, Riches JR, Stevens J a, Stubbs SJ, Black RM. Biomarkers of organophosphorus nerve agent exposure: comparison of phosphylated butyrylcholinesterase and phosphylated albumin after oxime therapy. Archives of Toxicology 2010 Jan;84(1):25–36.

104. Dorandeu F, Mikler JR, Thiermann H, Tenn C, Davidson C, Sawyer TW, Lallement G, Worek F. Swine models in the design of more effective medical countermeasures against organophosphorus poisoning. Toxicology 2007 Apr;233(1-3):128–44.

105. Bjarnason S, Mikler J, Hill I, Tenn C, Garrett M, Caddy N, Sawyer TW. Comparison of selected skin decontaminant products and regimens against VX in domestic swine. Human & Experimental Toxicology 2008 Mar;27(3):253–261.

106. Taysse L, Daulon S, Delamanche S, Bellier B, Breton P. Skin decontamination of mustards and organophosphates: comparative efficiency of RSDL and Fuller's earth in domestic swine. Human & Experimental Toxicology 2007 Feb;26(2):135–141.

107. Vallet V, Cruz C, Josse D, Bazire A, Lallement G, Boudry I. In vitro percutaneous penetration of organophosphorus compounds using full-thickness and split-thickness pig and human skin. Toxicology in Vitro 2007 Sep;21(6):1182–1190.

108. Vallet V, Cruz C, Licausi J, Bazire A, Lallement G, Boudry I. Percutaneous penetration and distribution of VX using in vitro pig or human excised skin. Validation of demeton-

S-methyl as adequate simulant for VX skin permeation investigations. Toxicology 2008;246(1):73–82.

109. Josse D, Barrier G, Cruz C, Ferrante M, Berthelot N. Delayed decontamination effectiveness following skin exposure to the chemical warfare agent VX. Toxicology Letters 2011 Aug;205(2011):S163.

110. Millerioux J, Cruz C, Bazire A, Lallement G, Lefeuvre L, Josse D. In vitro selection and efficacy of topical skin protectants against the nerve agent VX. Toxicology in Vitro 2009;23(3):539–545.

111. Davies DJ, Ward RJ, Heylings JR. Multi-species assessment of electrical resistance as a skin integrity marker for in vitro percutaneous absorption studies. Toxicology in Vitro 2004 Jun;18(3):351–8.

112. Eyer P, Worek F, Kiderlen D, Sinko G, Stuglin A, Simeon-Rudolf V, Reiner E. Molar absorption coefficients for the reduced Ellman reagent: reassessment. Analytical Biochemistry 2003;312:224–227.

113. Worek F, Mast U, Kiderlen D, Diepold C, Eyer P. Improved determination of acetylcholinesterase activity in human whole blood. Clinical Chimica Acta 1999 Oct;288(1-2):73–90.

114. Agilent Technologies. One Color Microarray-Based Gene Expression Analysis Low Input Quick Amp Labeling Protocol. 2010;(May)

115. Petroianu G, Toomes M, Maleck W, Bergler W, Rufer R. Intravenous paraoxon (POX) exposure: coagulation studies in mini pigs. Chemico-Biological Interactions 1999;119-120:489 – 495.

116. Quistad GB, Casida JE. Sensitivity of Blood-Clotting Factors and Digestive Enzymes to Inhibition by Organophosphorus Pesticides. Journal of Biochemical and Molecular Toxicology 2000;14(1):1–6.

117. Murray JC, Stein F, McGlothlin JC, McClain KL. Prolongation of the prothrombin time after organophosphate poisoning. Pediatric Emergency Care 1994;10:289–93.

118. Lee MJ, Clement JG. Effects of soman poisoning on hematology and coagulation parameters and serum biochemistry in rabbits. Military Medicine 1990;155:244–9.

119. Russell WMS, Burch RL. The Principles of Humane Experimental Technique. In: The Principles of Humane Experimental Technique. Methuen; 1959

120. Russell WMS. The Increase of Humanity in Experimentation: Replacement, Reduction and Refinement. Paper read at UFAW Symposium on Humane Technique in the

Laboratory, May, 1957, London. Collected Papers of the Laboratory Animals Bureau 1957;6:23–5.

121. Kheirabadi BS, Edens JW, Terrazas IB, Estep JS, Klemcke HG, Dubick MA, Holcomb JB. Comparison of New Hemostatic Granules/Powders With Currently Deployed Hemostatic Products in a Lethal Model of Extremity Arterial Hemorrhage in Swine. The Journal of Trauma - Injury, Infection & Critical Care 2009 Feb;66(2):316–26; discussion 327–8.

122. Scarpelini S, Rhind SG, Nascimento B, Tien H, Shek PN, Peng HT, Huang H, Pinto R, Speers V, Reis M, Rizoli SB. Normal range values for thromboelastography in healthy adult volunteers. Brazilian Journal of Medical and Biological Research 2009;42(12):1210–1217.

123. Schreiber MA, Tieu B. Hemostasis in Operation Iraqi Freedom III. Surgery 2007;142:S61–S66.

124. Wright JK, Kalns J, Wolf EA, Traweek F, Schwarz S, Loeffler CK, Snyder W, Yantis LD, Eggers J. Thermal Injury Resulting from Application of a Granular Mineral Hemostatic Agent. The Journal of Trauma - Injury, Infection & Critical Care 2004;57(2):224–230.

125. Wright FL, Hong TH, Thoman D, Demitriades D, Rhee PM. Intracorporeal Use of the Hemostatic Agent QuickClot in a Coagulopathic Patient with Combined Thoracoabdominal Penetrating Trauma. The Journal of Trauma - Injury, Infection & Critical Care 2004;56(1):205–208.

126. Turner AS, Parker D, Egbert B, Maroney M, Armstrong R, Powers N. Evaluation of a Novel Hemostatic Device in an Ovine Parenchymal Organ Bleeding Model of Normal and Impaired Hemostasis. Journal of Biomedical Materials Research Part A 2001;63:37–47.

127. Zhai H, Maibach HI. Occlusion vs. skin barrier function. Skin Research and Technology 2002 Feb;8(1):1–6.

128. Wu X-M, Todo H, Sugibayashi K. Effects of pretreatment of needle puncture and sandpaper abrasion on the in vitro skin permeation of fluorescein isothiocyanate (FITC)-dextran. International Journal of Pharmacetics 2006 Jun;316(1-2):102–8.

129. Marzulli FN, Callaghan JF, Brown DWC. Chemical Structure and Skin Penetrating Capacity of a Short Series of Organic Phosphates and Phosphoric Acid. The Journal of Investigative Dermatology 1965;44(5):339–344.

130. Morris AP, Brain KR, Heard CM. Skin permeation and ex vivo skin metabolism of O-acyl haloperidol ester prodrugs. International Journal of Pharmaceutics 2009 Feb;367(1-2):44–50.

131. Chilcott RP, Jenner J, Carrick W, Hotchkiss SAM, Rice P. Human Skin Absorption of Bis-2- (chloroethyl) sulphide (Sulphur Mustard) In Vitro. Journal of Applied Toxicology 2000;20(August 1999):349–355.

132. Chilcott RP. Toxicity of sulphur mustard. Toxicology and Applied Pharmacology 2005;204:99–100.

133. Chilcott RP, Jenner J, Hotchkiss SAM, Rice P. In Vitro Skin Absorption and Decontamination of Sulphur Mustard: Comparison of Human and Pig-ear Skin. Journal of Applied Toxicology 2001;21:279–283.

134. Taysse L, Dorandeu F, Daulon S, Foquin A, Perrier N, Lallement G, Breton P. Cutaneous challenge with chemical warfare agents in the SKH-1 hairless mouse (II): effects of some currently used skin decontaminants (RSDL and Fuller's earth) against liquid sulphur mustard and VX exposure. Human and Experimental Toxicology 2011 Jun;30(6):491–8.

135. Clarke RS, Dundee JW, Doggart JR, Lavery T. The Effects of Single and Intermittent Administrations of Althesin and Other Intravenous Anesthetic Agents on Liver Function. Anesthesia and Analgesia 1974;53(3):461–8.

136. Dorandeu F, Foquin A, Briot R, Delacour C, Denis J, Alonso A, Froment MT, Renault F, Lallement G, Masson P. An unexpected plasma cholinesterase activity rebound after challenge with a high dose of the nerve agent VX. Toxicology 2008 Jun;248(2-3):151–157.

137. Mikler J, Tenn C, Worek F, Reiter G, Thiermann H, Garrett M, Bohnert S, Sawyer TW. Immobilization of Russian VX skin depots by localized cooling: Implications for decontamination and medical countermeasures. Toxicology Letters 2011 Sep;206(1):47–53.

138. Spradling KD, Lumley LA, Robison CL, Meyerhoff JL, Dillman JF 3rd. Transcriptional analysis of rat piriform cortex following exposure to the organophosphonate anticholinesterase sarin and induction of seizures. Journal of Neuroinflammation 2011 Jan;8(1):83.

139. Spradling KD, Lumley L a, Robison CL, Meyerhoff JL, Dillman JF 3rd. Transcriptional responses of the nerve agent-sensitive brain regions amygdala, hippocampus, piriform cortex, septum, and thalamus following exposure to the organophosphonate anticholinesterase sarin. Journal of Neuroinflammation 2011 Jan;8(1):84.

140. Rupprecht R, Berning B, Hauser C, Holsboer F, Reul JM. Steroid receptor-mediated effects of neuroactive steroids: characterization of structure-activity relationship. European Journal of Pharmacology 1996 May;303(3):227–34.

141. Jaeschke H, Hasegawa T. Role of neutrophils in acute inflammatory liver injury. Liver International 2006 Oct;26(8):912–9.

142. Kim E, Hong H-J, Cho D, Han JM, Kim S, Kim TS. Enhancement of toll-like receptor 2-mediated immune responses by AIMP1, a novel cytokine, in mouse dendritic cells. Immunology 2011 Sep;134(1):73–81.

143. Park SG, Schimmel P, Kim S. Aminoacyl tRNA synthetases and their connections to disease. Proceedings of the National Academy of Sciences of the United States of America 2008;105(32):11043–11049.

144. Hu J, Shibata Y, Zhu P-P, Voss C, Rismanchi N, Prinz WA, Rapoport TA, Blackstone C. A Class of Dynamin-like GTPases Involved in the Generation of the Tubular ER Network. Cell 2009;138(3):549–561.

145. Senderek J, Garvey SM, Krieger M, Guergueltcheva V, Urtizberea A, Roos A, Elbracht M, Stendel C, Tournev I, Mihailova V, Feit H, Tramonte J, Hedera P, Crooks K, Bergmann C, Rudnik-Schöneborn S, Zerres K, Lochmüller H, Seboun E, Weis J, Beckmann JS, Hauser MA, Jackson CE. Autosomal-Dominant Distal Myopathy Associated with a Recurrent Missense Mutation in the Gene Encoding the Nuclear Matrix Protein, Matrin 3. The American Journal of Human Genetics 2009 Apr;84(4):511–8.

146. Taylor DJ, Devkota B, Huang AD, Topf M, Narayanan E, Sali A, Harvey SC, Frank J. Comprehensive molecular structure of the eukaryotic ribosome. Structure 2009 Dec;17(12):1591–604.

147. Hurov KE, Cotta-Ramusino C, Elledge SJ. A genetic screen identifies the Triple T complex required for DNA damage signaling and ATM and ATR stability. Genes & Development 2010;24:1939–1950.

148. Weber C, Fraemohs L, Dejana E. The role of junctional adhesion molecules in vascular inflammation. Nature Reviews. Immunology 2007 Jun;7(6):467–77.

149. Pérez de la Lastra JM, Harris CL, Hinchliffe SJ, Holt DS, Rushmere NK, Morgan BP. Pigs Express Multiple Forms of Decay-Accelerating Factor (CD55), All of Which Contain Only Three Short Consensus Repeats. The Journal of Immunology 2000 Sep;165(5):2563–73.

150. Yamamoto S, Higuchi Y, Yoshiyama K, Shimizu E, Kataoka M, Hijiya N, Matsuura K. ADAM family proteins in the immune system. Immunology Today 1999;5699(6):278–284.

151. Dai MH, Xia T, Chen XD, Gan L, Feng SQ, Qiu H, Peng Y, Yang ZQ. Cloning and characterization of porcine resistin gene. Domestic Animal Endocrinology 2006 Feb;30(2):88–97.

152. Cepica S, Rohrer G, Masopust M, Kubickova S, Musilova P, Rubes J. Partial cloning, cytogenetic and linkage mapping of the porcine resistance (RSTN) gene. Animal Genetics 2002;33(5):381.

153. Wu S-C, Chen H-L, Yen C-C, Kuo M-F, Yang T-S, Wang S-R, Weng C-N, Chen C-M, Cheng WTK. Recombinant Porcine Lactoferrin Expressed in the Milk of Transgenic Mice Enhances Offspring Growth Performance. Journal of Agricultural and Food Chemistry 2007 Jun;55(12):4670–7.

154. Lydon JP, O'Malley BR, Saucedo O, Lee T, Headon DR, Conneely OM. Nucleotide and primary amino acid sequence of porcine lactoferrin. Biochimica et Biophysica Acta 1992 Aug;1132(1):97–9.

155. Steffl M, Telgen L, Schweiger M, Amselgruber WM. Estrous cycle-dependent activity of neutrophils in the porcine endometrium: Possible involvement of heat shock protein 27 and lactoferrin. Animal Reproduction Science 2010 Aug;121(1-2):159–66.

156. Clapperton M, Bishop SC, Piñeiro M, Campbell FM, Glass EJ. The association between plasma levels of acute phase proteins, haptoglobin, alpha-1 acid glycoprotein (AGP), Pig-MAP, transthyretin and serum amyloid A (SAA) in Large White and Meishan pigs. Veterinary Immunology and Immunopathology 2007 Oct;119:303–9.

157. Gnanandarajah JS, Dvorak CMT, Johnson CR, Murtaugh MP. Presence of free haptoglobin alpha 1S-subunit in acute porcine reproductive and respiratory syndrome virus infection. Journal of General Virology 2008 Nov;89:2746–53.

158. Lee YJ, Park C-K, Nam E, Kim S-H, Lee O-S, Lee DS, Lee C. Generation of a porcine alveolar macrophage cell line for the growth of porcine reproductive and respiratory syndrome virus. Journal of Virological Methods 2010 Feb;163(2):410–5.

159. Du Y, Pattnaik AK, Song C, Yoo D, Li G. Glycosyl-phosphatidylinositol (GPI)-anchored membrane association of the porcine reproductive and respiratory syndrome virus GP4 glycoprotein and its co-localization with CD163 in lipid rafts. Virology 2012 Mar;424(1):18–32.

160. Das PB, Dinh PX, Ansari IH, de Lima M, Osorio FA, Pattnaik AK. The minor envelope glycoproteins GP2a and GP4 of porcine reproductive and respiratory syndrome virus interact with the receptor CD163. Journal of Virology 2010 Feb;84(4):1731–40.

161. Calvert JG, Slade DE, Shields SL, Jolie R, Mannan RM, Ankenbauer RG, Welch S-KW. CD163 Expression Confers Susceptibility to Porcine Reproductive and Respiratory Syndrome Viruses. Journal of Virology 2007 Jul;81(14):7371–9.

162. Greig ME. The effect of physostigmine and acetyl choline on the permeability of erythrocytes. (Papers presented at the meeting of the Society of General Physiologists, June 21-23, 1950). Energy 1950;311–312.

163. Ledger TN, Pinton P, Bourges D, Roumi P, Salmon H, Oswald IP. Development of a Macroarray To Specifically Analyze Immunological Gene Expression in Swine. Clinical and Diagnostic Laboratory Immunology 2004;11(4):691–698.

164. Meurens F, Berri M, Whale J, Dybvig T, Strom S, Thompson D, Brownlie R, Townsend HGG, Salmon H, Gerdts V. Expression of TECK/CCL25 and MEC/CCL28 chemokines and their respective receptors CCR9 and CCR10 in porcine mucosal tissues. Veterinary Immunology and Immunopathology 2006 Oct;113(3-4):313–27.

165. Brogi E, Wu T, Namiki A, Isner JM. Indirect Angiogenic Cytokines Upregulate VEGF and bFGF Gene Expression in Vascular Smooth Muscle Cells, Whereas Hypoxia Upregulates VEGF Expression Only. Circulation 1994;90:649–652.

166. Wenger RH. Cellular adaptation to hypoxia: O2-sensing protein hydroxylases, hypoxia-inducible transcription factors, and O2-regulated gene expression. The Journal of the Federation of American Societies for Experimental Biology 2002 Aug;16(10):1151–62.

167. Liu Y, Cox SR, Morita T, Kourembanas S. Hypoxia Regulates Vascular Endothelial Growth Factor Gene Expression in Endothelial Cells: Identification of a 5' Enhancer. Circulation Research 1995 Sep;77(3):638–643.

168. Gerhardt RT, De Lorenzo RA, Oliver J, Holcomb JB, Pfaff JA. Out-of-Hospital Combat Casualty Care in the Current War in Iraq. Annals of Emergency Medicine 2009;53(2):169–174.

169. Okumura T, Suzuki K, Fukuda A, Kohama A, Takasu N, Ishimatsu S, Hinohara S. The Tokyo Subway Sarin Attack: Disaster Management, Part 2: Hospital Response. Academic Emergency Medicine 1998 Jun;5(6):618–24.

170. Blanton JL, D'Ambrozio JA, Sistrunk JE, Midboe EG. Global Changes in the Expression Patterns of RNA Isolated from the Hippocampus and Cortex of VX Exposed Mice. Journal of Biochemical and Molecular Toxicology 2004;18(3):115–123.

171. Kheirabadi BS, Mace JE, Terrazas IB, Fedyk CG, Estep JS, Dubick MA, Blackbourne LH. Safety Evaluation of New Hemostatic Agents, Smectite Granules, and Kaolin-Coated Gauze in a Vascular Injury Wound Model in Swine. The Journal of Trauma - Injury, Infection & Critical Care 2010 Feb;68(2):269–278.

APPENDIX: Tables Supplementary to Chapter 6

Probe Name	"Survivor" FC (up-regulated)	"Death" FC (down-regulated)	Gene Symbol	Description	GenBank Accession	Gene Name
A_72_P417944	1.29	1.49	HMGB1	Sus scrofa high mobility group box 1 (HMGB1), mRNA [NM_001004034]	NM_001004034	high mobility group box 1
A_72_P123316	1.17	1.36	AIMP1	Sus scrofa aminoacyl tRNA synthetase complex-interacting multifunctional protein 1 (AIMP1), mRNA [NM_001114283]	NM_001114283	aminoacyl tRNA synthetase complex-interacting multifunctional protein 1
A_72_P166216	1.53	1.32		Sus scrofa mRNA, clone:AMP010005H07, expressed in alveolar macrophage. [AK230520]	AK230520	
A_72_P051516	1.14	1.29	LOC100512835	Uncharacterized protein [Source:UniProtKB/TrEMBL;Acc:F1SKJ5] [ENSSSCT00000000147]	AK234726	eukaryotic translation initiation factor 3 subunit D-like
A_72_P043501	1.36	1.36		Rep: CG10107 - Drosophila miranda (Fruit fly), partial (6%) [TC545141]		

Table S6.1a: Thirty-eight genes were oppositely regulated between the "survivor" and "death" groups. Nineteen of these were up-regulated in the "survivor" group and down-regulated in the "death" group.

Probe Name	"Survivor" FC (up-regulated)	"Death" FC (down-regulated)	Gene Symbol	Description	GenBank Accession	Gene Name
A_72_P293799	1.24	1.17	LOC100520446	PREDICTED: Sus scrofa phosphatidylinositol-5-phosphate 4-kinase type-2 alpha-like (LOC100520446), mRNA [XM_003130778]	XM_003130778	phosphatidylinositol-5-phosphate 4-kinase type-2 alpha-like
A_72_P124171	1.21	1.25	RPL6	Sus scrofa ribosomal protein L6 (RPL6), mRNA [NM_001044542]	NM_001044542	ribosomal protein L6
A_72_P237542	1.31	1.27	ATL3	PREDICTED: Sus scrofa atlastin GTPase 3 (ATL3), mRNA [XM_003122603]	XM_003122603	atlastin GTPase 3
A_72_P043131	1.43	1.24	MATR3	Uncharacterized protein [Source:UniProtKB/TrEMBL;Acc:F1RGI7] [ENSSSCT00000015671]	AK230971	matrin 3
A_72_P351373	1.15	1.23		Sus scrofa mRNA, clone:LVRM10164B01, expressed in liver. [AK233516]	AK233516	

Table S6.1a (continued): Thirty-eight genes were oppositely regulated between the "survivor" and "death" groups. Nineteen of these were up-regulated in the "survivor" group and down-regulated in the "death" group.

Probe Name	"Survivor" FC (up-regulated)	"Death" FC (down-regulated)	Gene Symbol	Description	GenBank Accession	Gene Name
A_72_P315983	1.11	1.20		Sus scrofa mRNA, clone:OVRM10011C12, expressed in ovary. [AK234726]	AK234726	
A_72_P301774	1.28	1.27	RPL7	Sus scrofa ribosomal protein L7 (RPL7), mRNA [NM_001113217]	NM_001113217	ribosomal protein L7
A_72_P407373	1.17	1.13		Sus scrofa mRNA, clone:OVRM10053F02, expressed in ovary. [AK235147]	AK235147	
A_72_P296699	1.26	1.29		Uncharacterized protein [Source:UniProtKB/TrEMBL;Acc:F1SJA1] [ENSSSCT00000005809]	AK237752	
A_72_P181041	1.51	1.16	SOD1	Sus scrofa mRNA, clone:TES010065D08, expressed in testis. [AK351289]	AK351289	superoxide dismutase 1, soluble
A_72_P041136	1.28	1.28	RPS3	Sus scrofa ribosomal protein S3 (RPS3), mRNA [NM_001044601]	NM_001044601	ribosomal protein S3

Table S6.1a (continued): Thirty-eight genes were oppositely regulated between the "survivor" and "death" groups. Nineteen of these were up-regulated in the "survivor" group and down-regulated in the "death" group.

Probe Name	"Survivor" FC (up-regulated)	"Death" FC (down-regulated)	Gene Symbol	Description	GenBank Accession	Gene Name
A_72_P381933	1.18	1.26		Sus scrofa mRNA, clone:THY010111H04, expressed in thymus. [AK239542]	AK239542	
A_72_P035951	1.19	1.15	SUCLG1	Sus scrofa succinate-CoA ligase, alpha subunit (SUCLG1), nuclear gene encoding mitochondrial protein, mRNA [NM_214409]	NM_214409	succinate-CoA ligase, alpha subunit
A_72_P127776	1.33	1.40	CNBP	Sus scrofa clone Clu_4372.scr.msk.p1.Contig4, mRNA sequence. [AY609917]	AY609917	CCHC-type zinc finger, nucleic acid binding protein

Table S6.1a (continued): Thirty-eight genes were oppositely regulated between the "survivor" and "death" groups. Nineteen of these were up-regulated in the "survivor" group and down-regulated in the "death" group.

Probe Name	"Survivor" FC (down-regulated)	"Death" FC (up-regulated)	Gene Symbol	Description	GenBank Accession	Gene Name
A_72_P319703	1.43	1.17		BP463284 full-length enriched swine cDNA library, adult uterus Sus scrofa cDNA clone UTR010061C02 5', mRNA sequence [BP463284]	BP463284	
A_72_P315823	1.51	1.21		Rep: VACUOLAR ATP SYNTHASE SUBUNIT C - Encephalitozoon cuniculi, partial (5%) [TC609086]		
A_72_P436894	1.18	1.16				
A_72_P041341	1.69	1.32		Rep: Dihydroorotate dehydrogenase 1 - Mariprofundus ferrooxydans PV-1, partial (5%) [TC581282]		
A_72_P122626	1.39	1.19		Rep: Ubiquitin-conjugating enzyme E2 Z - Rattus norvegicus (Rat), partial (5%) [TC574178]		

Table S6.1b: Thirty-eight genes were oppositely regulated between the "survivor" and "death" groups. Nineteen of these were down-regulated in the "survivor" group and up-regulated in the "death" group.

Probe Name	"Survivor" FC (down-regulated)	"Death" FC (up-regulated)	Gene Symbol	Description	GenBank Accession	Gene Name
A_72_P267002	1.70	1.13	C2CD2L	Uncharacterized protein [Source:UniProtKB/TrEMBL;Acc:F1SAH4] [ENSSSCT00000016477]	XM_003129928	C2CD2-like
A_72_P287269	2.01	1.19		Uncharacterized protein [Source:UniProtKB/TrEMBL;Acc:F1S705] [ENSSSCT00000016896]	XM_003130329	
A_72_P170936	1.42	1.29		Rep: Uncharacterized tatC-like protein ymf16 - Marchantia polymorpha (Liverwort), partial (5%) [TC598884]		
A_72_P330563	1.56	1.30				
A_72_P186806	1.75	1.07	PTPRC	Uncharacterized protein [Source:UniProtKB/TrEMBL;Acc:F1S5D7] [ENSSSCT00000011937]	AK236971	protein tyrosine phosphatase, receptor type, C
A_72_P072301	1.76	1.27				

Table S6.1b (continued): Thirty-eight genes were oppositely regulated between the "survivor" and "death" groups. Nineteen of these were down-regulated in the "survivor" group and up-regulated in the "death" group.

Probe Name	"Survivor" FC (down-regulated)	"Death" FC (up-regulated)	Gene Symbol	Description	GenBank Accession	GeneName
A_72_P205202	1.33	1.47		Sus scrofa mRNA, clone:THY010066B02, expressed in thymus. [AK351708]	AK351708	
A_72_P050411	2.38	1.21		Sus scrofa mRNA, clone:SPL010073E05, expressed in spleen. [AK237647]	AK237647	
A_72_P225502	1.35	1.45		937553 MARC 4PIG Sus scrofa cDNA 3', mRNA sequence [CK466354]	CK466354	
A_72_P400518	1.34	1.24				
A_72_P346773	1.35	1.11				
A_72_P030816	1.31	1.42				
A_72_P419449	2.03	1.15		Rep: VirB2 - Agrobacterium tumefaciens, partial (8%) [TC570679]		
A_72_P204972	1.98	1.60				

Table S6.1b (continued): Thirty-eight genes were oppositely regulated between the "survivor" and "death" groups. Nineteen of these were down-regulated in the "survivor" group and up-regulated in the "death" group.

Probe Name	p	FC	Regulation	Gene Symbol	Description	Genbank Accession	Gene Name
A_72_P219772	0.005	3.02	down	LOC100513077	PREDICTED: Sus scrofa max dimerization protein 1-like (LOC100513077), mRNA [XM_003125065]	XM_003125065	max dimerization protein 1-like
A_72_P050971	0.024	3.02	down	CD14	Sus scrofa CD14 molecule (CD14), mRNA [NM_001097445]	NM_001097445	CD14 molecule
A_72_P226012	0.000	3.03	down	LIMK2	PREDICTED: Sus scrofa LIM domain kinase 2, transcript variant 1 (LIMK2), mRNA [XM_001926065]	XM_001926065	LIM domain kinase 2
A_72_P188166	0.014	3.04	down		AJ950630 KN404_1 Sus scrofa cDNA clone C0007735b23 5', mRNA sequence [AJ950630]	AJ950630	
A_72_P141156	0.022	3.04	down		Sus scrofa mRNA, clone:LVRM10008D06, expressed in liver. [AK346027]	AK346027	
A_72_P048361	0.018	3.05	down		Sus scrofa mRNA, clone:OVRM10193D12, expressed in ovary. [AK236447]	AK236447	
A_72_P320963	0.042	3.06	down		Rep: contactin 1 - Mus musculus, partial (20%) [TC556852]		
A_72_P288384	0.022	3.09	down		Sus scrofa mRNA, clone:OVRM10148D01, expressed in ovary. [AK236053]	AK236053	
A_72_P356133	0.009	3.12	down				
A_72_P055401	0.003	3.17	down	LOC100523979	Uncharacterized protein [Source:UniProtKB/TrEMBL;Acc:F1RYS3] [ENSSSCT00000009845]	AK344675	cyclin-G2-like
A_72_P155761	0.014	3.18	down		Rep: predicted gene, ENSMUSG00000074232 - Mus musculus, partial (12%) [TC625156]		

Table S6.2: In the decontaminated group, 65 entities were identified with a significant fold change between 3.0 and 9.0.

Probe Name	p	FC	Regulation	Gene Symbol	Description	Genbank Accession	Gene Name
A_72_P136946	0.033	3.19	down		rspc003_l7.y1 spc Sus scrofa cDNA 5', mRNA sequence [EW572445]	EW572445	
A_72_P031421	0.009	3.21	down				
A_72_P088666	0.022	3.26	down	CD14	Sus scrofa CD14 molecule (CD14), mRNA [NM_001097445]	NM_001097445	CD14 molecule
A_72_P080016	0.018	3.27	up		Rep: NADH-ubiquinone oxidoreductase chain 2 - Lichmera indistincta, partial (5%) [TC530628]		
A_72_P207457	0.014	3.27	down	ALOX5AP	Sus scrofa arachidonate 5-lipoxygenase-activating protein (ALOX5AP), mRNA [NM_001164001]	NM_001164001	arachidonate 5-lipoxygenase-activating protein
A_72_P165431	0.009	3.27	down	TLR4	Sus scrofa toll-like receptor 4 (TLR4), mRNA [NM_001113039]	NM_001113039	toll-like receptor 4
A_72_P303724	0.009	3.28	down	TLR4	Sus scrofa toll-like receptor 4 (TLR4), mRNA [NM_001113039]	NM_001113039	toll-like receptor 4
A_72_P381428	0.021	3.28	down				
A_72_P008841	0.034	3.30	up		Sus scrofa mRNA, clone:AMP010017G07, expressed in alveolar macrophage. [AK230622]	AK230622	
A_72_P385368	0.005	3.31	down				
A_72_P330938	0.006	3.32	down		Sus scrofa mRNA, clone:AMP010002E09, expressed in alveolar macrophage. [AK230491]	AK230491	
A_72_P297879	0.018	3.33	down	SGMS1	Sus scrofa sphingomyelin synthase 1 (SGMS1), mRNA [NM_001097438]	NM_001097438	sphingomyelin synthase 1

Table S6.2 (continued): In the decontaminated group, 65 entities were identified with a significant fold change between 3.0 and 9.0.

Probe Name	p	FC	Regulation	Gene Symbol	Description	Genbank Accession	Gene Name
A_72_P369763	0.020	3.41	up		Sus scrofa mRNA, clone:ADR010084E08, expressed in adrenal gland. [AK343528]	AK343528	
A_72_P320648	0.010	3.44	down		Sus scrofa mRNA, clone:LVR010029A05, expressed in liver. [AK232355]	AK232355	
A_72_P146566	0.003	3.44	down	LOC396867	Sus scrofa stefin A8 (LOC396867), mRNA [NM_213860]	NM_213860	stefin A8
A_72_P085766	0.015	3.47	up	LOC100521616	Sus scrofa mRNA, clone:PBL010087G05, expressed in periphral blood mononuclear cell. [AK237064]	AK237064	interleukin-9 receptor-like
A_72_P076666	0.030	3.48	down				
A_72_P079266	0.013	3.51	down	LOC100519123	Uncharacterized protein [Source:UniProtKB/TrEMBL;Acc:F1SP55] [ENSSSCT00000005966]	XM_003122054	ATP-binding cassette sub-family A member 1-like
A_72_P075026	0.009	3.51	down	CHIT1	Uncharacterized protein [Source:UniProtKB/TrEMBL;Acc:F1S7U2] [ENSSSCT00000016860]	EF090909	chitinase 1 (chitotriosidase)
A_72_P352528	0.006	3.52	down				
A_72_P237572	0.043	3.53	down	LOC100520761	PREDICTED: Sus scrofa c4b-binding protein alpha chain-like (LOC100520761), mRNA [XM_003130456]	XM_003130456	c4b-binding protein alpha chain-like
A_72_P164781	0.005	3.54	down	C5AR1	Sus scrofa mRNA, clone:DCI010005C10, expressed in dendritic cells (immature). [AK344310]	AK344310	complement component 5a receptor 1

Table S6.2 (continued): In the decontaminated group, 65 entities were identified with a significant fold change between 3.0 and 9.0.

Probe Name	p	FC	Regulation	Gene Symbol	Description	Genbank Accession	Gene Name
A_72_P178346	0.018	3.56	down				
A_72_P289749	0.015	3.62	down				
A_72_P345443	0.006	3.63	down				
A_72_P037841	0.016	3.63	down		Rep: Latency-associated nuclear antigen - Macaca nemestrina rhadinovirus 2, partial (5%) [TC544206]		
A_72_P266432	0.025	3.65	down		Sus scrofa mRNA, clone:AMP010057A04, expressed in alveolar macrophages. [AK343821]	AK343821	
A_72_P213242	0.017	3.75	down		Sus scrofa mRNA, clone:ITT010062E10, expressed in small intestine. [AK345112]	AK345112	
A_72_P033811	0.016	3.76	down		Sus scrofa mRNA, clone:ITT010100C12, expressed in small intestine. [AK345293]	AK345293	
A_72_P299774	0.009	3.80	down		Rep: Decay-accelerating factor CD55 - Sus scrofa (Pig), partial (9%) [TC563365]		
A_72_P025326	0.017	3.90	down				
A_72_P032716	0.031	4.00	down	EMR1	Sus scrofa mRNA, clone:AMP010018D08, expressed in alveolar macrophage. [AK230628]	AK230628	egf-like module containing, mucin-like, hormone receptor-like 1
A_72_P035486	0.011	4.13	down	SGMS1	Sus scrofa sphingomyelin synthase 1 (SGMS1), mRNA [NM_001097438]	NM_001097438	sphingomyelin synthase 1

Table S6.2 (continued): In the decontaminated group, 65 entities were identified with a significant fold change between 3.0 and 9.0.

Probe Name	p	FC	Regulation	Gene Symbol	Description	Genbank Accession	Gene Name
A_72_P368263	0.025	4.15	down	LOC100156489	Uncharacterized protein [Source:UniProtKB/TrEMBL;Acc:F1SGP9] [ENSSSCT00000002231]	XM_001927895	protein-glutamine gamma-glutamyltransferase K-like
A_72_P340983	0.021	4.17	down	FN1	Uncharacterized protein [Source:UniProtKB/TrEMBL;Acc:F1SS23] [ENSSSCT00000017611]	AK236279	fibronectin 1
A_72_P189121	0.021	4.20	down				
A_72_P262237	0.002	4.25	down		Sus scrofa mRNA, clone:UTR010017A02, expressed in uterus. [AK239973]	AK239973	
A_72_P188846	0.003	4.30	down		Sus scrofa mRNA, clone:TES010027B04, expressed in testis. [AK351197]	AK351197	
A_72_P293619	0.004	4.31	down		Sus scrofa mRNA, clone:UTR010017A02, expressed in uterus. [AK239973]	AK239973	
A_72_P055186	0.026	4.33	down	CD163	Sus scrofa mRNA, clone:SPL010088G03, expressed in spleen. [AK237746]	AK237746	CD163 molecule
A_72_P412988	0.025	4.37	down				
A_72_P306144	0.007	4.41	down	TGFA	Sus scrofa mRNA, clone:OVRM10010E08, expressed in ovary. [AK347880]	AK347880	transforming growth factor, alpha
A_72_P130606	0.007	4.50	down		Rep: Glycogenin - Bos taurus (Bovine), partial (16%) [TC543772]	XM_003358602	

Table S6.2 (continued): In the decontaminated group, 65 entities were identified with a significant fold change between 3.0 and 9.0.

Probe Name	p	FC	Regulation	Gene Symbol	Description	Genbank Accession	Gene Name
A_72_P097366	0.005	4.54	down	LOC100520641	Uncharacterized protein [Source:UniProtKB/TrEMBL;Acc:F1SKC4] [ENSSSCT00000012806]	AK236587	glycogenin-1-like
A_72_P268229	0.003	4.55	down		Rep: Phospholipase D/Transphosphatidylase precursor - Polaromonas sp. (strain JS666 / ATCC BAA-500), partial (11%) [TC621826]		
A_72_P001376	0.005	4.74	down	LOC100512873	Sus scrofa mRNA, clone:AMP010041A03, expressed in alveolar macrophage. [AK230779]	AK230779	antileukoproteinase-like
A_72_P177981	0.012	4.91	down	CD163	Sus scrofa CD163 molecule (CD163), mRNA [NM_213976]	NM_213976	CD163 molecule
A_72_P160596	0.013	5.05	down	CD163	Sus scrofa CD163 mRNA, complete cds. [DQ067278]	DQ067278	CD163 molecule
A_72_P177496	0.018	5.37	down	RETN	Sus scrofa resistin (RETN), mRNA [NM_213783]	NM_213783	resistin
A_72_P131846	0.012	5.44	down	RETN	Sus scrofa resistin (RETN), mRNA [NM_213783]	NM_213783	resistin
A_72_P121576	0.008	5.70	down				
A_72_P178006	0.008	6.22	down	HP	Sus scrofa haptoglobin (HP), mRNA [NM_214000]	NM_214000	haptoglobin
A_72_P004066	0.019	6.38	down		Sus scrofa mRNA, clone:THY010119H01, expressed in thymus. [AK351987]	AK351987	
A_72_P088736	0.006	8.10	down	LTF	Sus scrofa lactotransferrin (LTF), mRNA [NM_214362]	NM_214362	lactotransferrin

Table S6.2 (continued): In the decontaminated group, 65 entities were identified with a significant fold change between 3.0 and 9.0.

Probe Name	"Survivor" FC	"DXD" FC	Gene Symbol	Description	Genbank Accession	Gene Name
A_72_P074056	1.52	1.67		BW979405 full-length enriched swine cDNA library, adult intestine Sus scrofa cDNA clone ITT010038B10 5', mRNA sequence [BW979405]	BW979405	
A_72_P364398	1.54	1.61	LOC100511072	Uncharacterized protein [Source:UniProtKB/TrEMBL;Acc:F1RMT5] [ENSSSCT00000015724]	XM_003123999	protein diaphanous homolog 1-like
A_72_P408748	1.59	1.53				
A_72_P254562	1.64	1.71	LOC100153550	Uncharacterized protein [Source:UniProtKB/TrEMBL;Acc:F1S8Y4] [ENSSSCT00000011508]	AY609998	exosomal core protein CSL4
A_72_P258182	1.68	1.86		susfleck_PG_18_F11 SUSFLECK Pituitary Gland Sus scrofa cDNA clone 18_F11, mRNA sequence [FD592765]	FD592765	
A_72_P072416	1.68	1.54		Uncharacterized protein [Source:UniProtKB/TrEMBL;Acc:F1SD10] [ENSSSCT00000011405]	AK343385	
A_72_P223132	1.69	1.61		Sus scrofa mRNA, clone:THY010094A09, expressed in thymus. [AK239334]	AK239334	

Table S6.3: Thirty-six genes were significantly ($p<0.05$) differently regulated with a fold change (FC) above 1.5 in samples from non-decontaminated (DXD) survivors. These were all down-regulated.

Probe Name	"Survivor" FC	"DXD" FC	Gene Symbol	Description	Genbank Accession	Gene Name
A_72_P163356	1.69	1.54	LOC100511865	Uncharacterized protein [Source:UniProtKB/TrEMBL;Acc:F1S3C2] [ENSSSCT00000015340]	AY609632	ras-related protein Rab-24-like
A_72_P098516	1.74	1.56	LOC100515356	Uncharacterized protein [Source:UniProtKB/TrEMBL;Acc:F1ST88] [ENSSSCT00000005878]	AK352242	golgi-associated plant pathogenesis-related protein 1-like
A_72_P363878	1.74	1.53				
A_72_P213067	1.80	1.52	BRWD3	PREDICTED: Sus scrofa bromodomain and WD repeat-containing protein 3-like (LOC100520060), mRNA [XM_003135212]	XM_003135212	bromodomain and WD repeat domain containing 3
A_72_P216567	1.82	1.60	DOK1	Sus scrofa docking protein 1, 62kDa (downstream of tyrosine kinase 1) (DOK1), mRNA [NM_001143705]	NM_001143705	docking protein 1, 62kDa (downstream of tyrosine kinase 1)
A_72_P402708	1.84	1.72	LOC100519082	Uncharacterized protein [Source:UniProtKB/TrEMBL;Acc:F1RGC4] [ENSSSCT00000015915]	AK237820	interferon-induced transmembrane protein 1-like

Table S6.3 (continued): Thirty-six genes were significantly ($p<0.05$) differently regulated with a fold change (FC) above 1.5 in samples from non-decontaminated survivors. These were all down-regulated.

Probe Name	"Survivor" FC	"DXD" FC	Gene Symbol	Description	Genbank Accession	Gene Name
A_72_P085651	1.86	1.67		Sus scrofa mRNA, clone:AMP010048B11, expressed in alveolar macrophage. [AK230816]	AK230816	
A_72_P164771	1.86	1.55		Rep: MGC151858 protein - Bos taurus (Bovine), partial (65%) [TC550554]	XM_003129158	
A_72_P317048	1.91	1.61		930738 MARC 4PIG Sus scrofa cDNA 5', mRNA sequence [CK460460]	CK460460	
A_72_P189756	1.92	1.61		BX920065 Sus Scrofa library (scan) Sus scrofa cDNA clone scan0010.l.14 5prim, mRNA sequence [BX920065]	BX920065	
A_72_P180891	1.92	1.55	FGL2	Sus scrofa fibrinogen-like 2 (FGL2), mRNA [NM_001005152]	NM_001005152	fibrinogen-like 2
A_72_P000771	1.93	1.64	BACH1	Uncharacterized protein [Source:UniProtKB/TrEMBL;Acc:F1SHM8] [ENSSSCT00000013161]	XM_003132749	BTB and CNC homology 1, basic leucine zipper transcription factor 1

Table S6.3 (continued): Thirty-six genes were significantly ($p<0.05$) differently regulated with a fold change (FC) above 1.5 in samples from non-decontaminated survivors. These were all down-regulated.

Probe Name	"Survivor" FC	"DXD" FC	Gene Symbol	Description	Genbank Accession	Gene Name
A_72_P197885	1.95	1.54	DEDD	PREDICTED: Sus scrofa death effector domain-containing protein-like, transcript variant 2 (LOC100156474), mRNA [XM_003125653]	XM_003125653	death effector domain containing
A_72_P030191	1.97	1.54		Rep: Olfactomedin-like protein 3 precursor - Homo sapiens (Human), complete [TC539943]		
A_72_P377998	1.97	1.57		Sus scrofa mRNA, clone:DCI010109D09, expressed in dendritic cells (immature). [AK344690]	AK344690	
A_72_P345513	1.98	1.57		Rep: Brain protein I3 - Bos taurus (Bovine), complete [TC534832]	XM_003354451	
A_72_P326028	2.10	1.74	LOC100516039	Uncharacterized protein [Source:UniProtKB/TrEMBL;Acc:F1S1A0] [ENSSSCT00000019268]	AK230835	c-C motif chemokine 23-like
A_72_P002361	2.10	1.63		Sus scrofa mRNA, clone:SPL010015B04, expressed in spleen. [AK237234]	AK237234	

Table S6.3 (continued): Thirty-six genes were significantly ($p<0.05$) differently regulated with a fold change (FC) above 1.5 in samples from non-decontaminated survivors. These were all down-regulated.

Probe Name	"Survivor" FC	"DXD" FC	Gene Symbol	Description	Genbank Accession	Gene Name
A_72_P290549	2.11	1.60	TNFAIP8L2	Sus scrofa tumor necrosis factor, alpha-induced protein 8-like 2 (TNFAIP8L2), mRNA [NM_001204370]	NM_001204370	tumor necrosis factor, alpha-induced protein 8-like 2
A_72_P055151	2.11	1.65		Rep: Dof15 - Glycine max (Soybean), partial (7%) [TC632217]		
A_72_P002561	2.14	1.59		Rep: Cellulose synthase - Synechococcus sp. (strain CC9605), partial (3%) [TC530941]	XM_003354775	
A_72_P165046	2.18	2.10	CD55	Sus scrofa CD55 molecule, decay accelerating factor for complement (Cromer blood group) (CD55), mRNA [NM_213815]	NM_213815	CD55 molecule, decay accelerating factor for complement (Cromer blood group)
A_72_P094941	2.25	1.83				
A_72_P217812	2.27	2.12	ZCCHC6	Uncharacterized protein [Source:UniProtKB/TrEMBL;Acc:F1S4J1] [ENSSSCT00000011987]	XM_003130637	zinc finger, CCHC domain containing 6
A_72_P258487	2.35	1.69	ZNF467	Sus scrofa mRNA, clone:OVR010064E12, expressed in ovary. [AK347604]	AK347604	zinc finger protein 467

Table S6.3 (continued): Thirty-six genes were significantly ($p<0.05$) differently regulated with a fold change (FC) above 1.5 in samples from non-decontaminated survivors. These were all down-regulated.

Probe Name	"Survivor" FC	"DXD" FC	Gene Symbol	Description	Genbank Accession	Gene Name
A_72_P088056	2.65	1.78	LY96	Sus scrofa lymphocyte antigen 96 (LY96), mRNA [NM_001104956]	NM_001104956	lymphocyte antigen 96
A_72_P136176	2.73	1.84				
A_72_P413368	2.99	2.15		Sus scrofa mRNA, clone:ITT010040H02, expressed in intestine. [AK231345]	AK231345	
A_72_P229897	3.35	1.89				

Table S6.3 (continued): Thirty-six genes were significantly ($p<0.05$) differently regulated with a fold change (FC) above 1.5 in samples from non-decontaminated survivors. These were all down-regulated.

Probe Name	"Death" FC	"DXD" FC	Regulation	Gene Symbol	Description	Genbank Accession	Gene Name
A_72_P115951	1.32	1.37	down		Rep: Transmembrane and coiled-coil domain-containing protein C6orf129 - Homo sapiens (Human), complete [TC558016]		
A_72_P274654	1.20	1.22	up		Rep: Chromosome 11 SCAF14979, whole genome shotgun sequence - Tetraodon nigroviridis (Green puffer), partial (3%) [TC552531]		
A_72_P359418	1.31	1.24	down	WDHD1	Uncharacterized protein [Source:UniProtKB/TrEMBL;Acc:F1SSP1] [ENSSSCT00000005569]	XM_001924194	WD repeat and HMG-box DNA binding protein 1
A_72_P153536	1.39	1.45	down		BX666888 Sus Scrofa library (scac) Sus scrofa cDNA clone scac0025.o.23 3prim, mRNA sequence [BX666888]	BX666888	
A_72_P229677	1.26	1.35	up		Rep: Isoform 3 of Q924C1 - Mus musculus (Mouse), partial (12%) [TC549174]		

Table S6.4: Fifty-two genes were identified with a significant ($p<0.05$) differently regulated with a fold change (FC) above 1.0 in samples from non-decontaminated (DXD) animals which did not survive.

Probe Name	"Death" FC	"DXD" FC	Regulation	Gene Symbol	Description	Genbank Accession	Gene Name
A_72_P268254	1.25	1.22	down		Sus scrofa mRNA, clone:AMP010021H04, expressed in alveolar macrophage. [AK230658]	AK230658	
A_72_P108426	1.35	1.34	down	LOC100523873	Sus scrofa mRNA, clone:LVRM10157D07, expressed in liver. [AK233485]	AK233485	modulator of retrovirus infection homolog
A_72_P237527	1.25	1.28	down	LOC100511525	Uncharacterized protein [Source:UniProtKB/TrEMBL;Acc:F1S775] [ENSSSCT00000016580]	AK230495	dolichyl-diphosphooligosaccharide--protein glycosyltransferase subunit STT3A-like
A_72_P281339	1.32	1.29	down				
A_72_P182836	1.26	1.25	up				
A_72_P344858	1.58	1.49	up		CJ013650 full-length enriched swine cDNA library, adult mesenteric lymph node Sus scrofa cDNA clone MLN01B060076 5', mRNA sequence [CJ013650]	CJ013650	

Table S6.4 (continued): Fifty-two genes were identified with a significant ($p<0.05$) differently regulated with a fold change (FC) above 1.0 in samples from non-decontaminated (DXD) animals which did not survive.

Probe Name	"Death" FC	"DXD" FC	Regulation	Gene Symbol	Description	Genbank Accession	Gene Name
A_72_P104776	1.32	1.29	down	LOC100153480	Sus scrofa mRNA, clone:OVRT10035E05, expressed in ovary. [AK348676]	AK348676	small nuclear ribonucleoprotein Sm D3-like
A_72_P124386	1.54	1.55	down		Sus scrofa mRNA, clone:LVR010018C03, expressed in liver. [AK232317]	AK232317	
A_72_P337618	1.18	1.30	down		Uncharacterized protein [Source:UniProtKB/TrEMBL;Acc:F1SFU9] [ENSSSCT00000007202]	EU814888	
A_72_P296819	1.39	1.21	down		PREDICTED: Sus scrofa CD93 molecule (CD93), mRNA [XM_001927042]	XM_001927042	
A_72_P080576	1.52	1.46	down	LOC100154056	PREDICTED: Sus scrofa calmodulin (LOC100154056), mRNA [XM_001928187]	XM_001928187	calmodulin
A_72_P221872	1.25	1.25	up				
A_72_P063496	1.34	1.38	down		Uncharacterized protein [Source:UniProtKB/TrEMBL;Acc:F1SV46] [ENSSSCT00000004033]	AK232614	

Table S6.4 (continued): Fifty-two genes were identified with a significant ($p<0.05$) differently regulated with a fold change (FC) above 1.0 in samples from non-decontaminated (DXD) animals which did not survive.

Probe Name	"Death" FC	"DXD" FC	Regulation	Gene Symbol	Description	Genbank Accession	Gene Name
A_72_P120391	1.30	1.29	down	LOC100521387	Uncharacterized protein [Source:UniProtKB/TrEMBL;Acc:F1STS6] [ENSSSCT00000016272]	AK235125	uncharacterized protein C11orf73 homolog
A_72_P145521	1.27	1.25	down		1533070 MARC 3PIG Sus scrofa cDNA 5', mRNA sequence [DY417983]	DY417983	
A_72_P379698	1.27	1.24	down	LOC100524500	Non-histone chromosomal protein HMG-17 [Source:UniProtKB/Swiss-Prot;Acc:P80272] [ENSSSCT00000003949]	AK236192	non-histone chromosomal protein HMG-17-like
A_72_P206962	1.32	1.29	down	ATAD2	Uncharacterized protein [Source:UniProtKB/TrEMBL;Acc:F1RR16] [ENSSSCT00000006566]	AK235138	ATPase family, AAA domain containing 2
A_72_P349623	1.15	1.26	down	LOC733637	Sus scrofa myosin regulatory light chain 2 protein (LOC733637), mRNA [NM_001044572]	NM_001044572	myosin regulatory light chain 2 protein
A_72_P223752	1.16	1.33	down	LOC733646	Sus scrofa lysosomal 9kDa H+ transporting ATPase V0 subunit e (LOC733646), mRNA [NM_001044579]	NM_001044579	lysosomal 9kDa H+ transporting ATPase V0 subunit e

Table S6.4 (continued): Fifty-two genes were identified with a significant ($p<0.05$) differently regulated with a fold change (FC) above 1.0 in samples from non-decontaminated (DXD) animals which did not survive.

Probe Name	"Death" FC	"DXD" FC	Regulation	Gene Symbol	Description	Genbank Accession	Gene Name
A_72_P410588	1.21	1.35	up		Uncharacterized protein [Source:UniProtKB/TrEMBL;Acc:F1SE96] [ENSSSCT00000009656]	BP438150	
A_72_P185306	1.48	1.42	down	RPL35	Sus scrofa ribosomal protein L35 (RPL35), mRNA [NM_214326]	NM_214326	ribosomal protein L35
A_72_P302514	1.22	1.25	down	LOC100524500	Non-histone chromosomal protein HMG-17 [Source:UniProtKB/Swiss-Prot;Acc:P80272] [ENSSSCT00000003949]	AK349259	non-histone chromosomal protein HMG-17-like
A_72_P049556	1.19	1.21	up		Rep: Uncharacterized protein FAM91A1 - Homo sapiens (Human), partial (14%) [TC550796]		
A_72_P407543	1.22	1.33	down		Sus scrofa mRNA, clone:THY010110B03, expressed in thymus. [AK239520]	AK239520	
A_72_P202462	1.24	1.17	down		Rep: tRNA pseudouridine synthase 3 (EC 5.4.99.-) (tRNA-uridine isomerase 3) (tRNA pseudouridylate synthase 3). - Bos Taurus, partial (50%) [TC584687]		

Table S6.4 (continued): Fifty-two genes were identified with a significant ($p<0.05$) differently regulated with a fold change (FC) above 1.0 in samples from non-decontaminated (DXD) animals which did not survive.

Probe Name	"Death" FC	"DXD" FC	Regulation	Gene Symbol	Description	Genbank Accession	Gene Name
A_72_P369808	1.22	1.17	up		Sus scrofa mRNA, clone:TCH010079F10, expressed in trachea. [AK238305]	AK238305	
A_72_P147081	1.35	1.26	down		Uncharacterized protein [Source:UniProtKB/TrEMBL;Acc:F1RPK5] [ENSSSCT00000007401]	AK233940	
A_72_P107981	1.27	1.25	down	LOC100520359	Uncharacterized protein [Source:UniProtKB/TrEMBL;Acc:F1SJY0] [ENSSSCT00000014397]	XM_003122715	mediator of RNA polymerase II transcription subunit 19-like
A_72_P040436	1.24	1.18	down		Sus scrofa mRNA, clone:PBL010012G03, expressed in periphral blood mononuclear cell. [AK236819]	AK236819	
A_72_P113886	1.18	1.16	down		Sus scrofa mRNA, clone:AMP010018H04, expressed in alveolar macrophages. [AK343693]	AK343693	
A_72_P227762	1.16	1.11	down	UBC	Pig poly-ubiquitin mRNA, 3' end. [M18159]	M18159	ubiquitin C

Table S6.4 (continued): Fifty-two genes were identified with a significant ($p<0.05$) differently regulated with a fold change (FC) above 1.0 in samples from non-decontaminated (DXD) animals which did not survive.

Probe Name	"Death" FC	"DXD" FC	Regulation	Gene Symbol	Description	Genbank Accession	Gene Name
A_72_P122296	1.41	1.39	down				
A_72_P397313	1.14	1.12	up		Rep: MGC137767 protein - Bos taurus (Bovine), partial (93%) [TC541708]		
A_72_P304269	1.23	1.19	up	THOP1	Sus scrofa thimet oligopeptidase 1 (THOP1), mRNA [NM_214223]	NM_214223	thimet oligopeptidase 1
A_72_P333508	1.35	1.37	down				
A_72_P127706	1.18	1.14	down		Sus scrofa mRNA, clone:SPL010027C01, expressed in spleen. [AK237351]	AK237351	
A_72_P309698	1.21	1.24	down		AJ952826 KN404_1 Sus scrofa cDNA clone C0007738k19 3', mRNA sequence [AJ952826]	AJ952826	
A_72_P286104	1.22	1.13	down	LOC100152655	PREDICTED: Sus scrofa lysM and putative peptidoglycan-binding domain-containing protein 4-like (LOC100152655), mRNA [XM_001928238]	XM_001928238	lysM and putative peptidoglycan-binding domain-containing protein 4-like

Table S6.4 (continued): Fifty-two genes were identified with a significant ($p<0.05$) differently regulated with a fold change (FC) above 1.0 in samples from non-decontaminated (DXD) animals which did not survive.

Probe Name	"Death" FC	"DXD" FC	Regulation	Gene Symbol	Description	Genbank Accession	Gene Name
A_72_P437959	1.44	1.41	down		Rep: UPF0215 protein APE_0476.1 - Aeropyrum pernix, partial (8%) [TC616255]		
A_72_P097596	1.18	1.17	down		Sus scrofa mRNA, clone:ITT010044D03, expressed in small intestine. [AK345045]	AK345045	
A_72_P051741	1.11	1.08	down		Uncharacterized protein [Source:UniProtKB/TrEMBL;Acc:F1SNN9] [ENSSSCT00000017690]	AK239087	
A_72_P282504	1.16	1.27	down		Rep: Alpha/beta hydrolase fold - Saccharopolyspora erythraea (strain NRRL 23338), partial (9%) [TC552936]		
A_72_P257442	1.57	1.30	down		Sus scrofa mRNA, clone:LVRM10063C11, expressed in liver. [AK232987]	AK232987	
A_72_P150236	1.65	1.55	down		Uncharacterized protein [Source:UniProtKB/TrEMBL;Acc:F1SCM0] [ENSSSCT00000002493]	AK350727	
A_72_P174356	1.16	1.17	down	TBP10	26S protease regulatory subunit 8 [Source:UniProtKB/Swiss-Prot;Acc:P62197] [ENSSSCT00000018819]	AK234194	Tat-binding protein 10

Table S6.4 (continued): Fifty-two genes were identified with a significant ($p<0.05$) differently regulated with a fold change (FC) above 1.0 in samples from non-decontaminated (DXD) animals which did not survive.

Probe Name	"Death" FC	"DXD" FC	Regulation	Gene Symbol	Description	Genbank Accession	Gene Name
A_72_P420559	1.13	1.18	up	LOC100517385	PREDICTED: Sus scrofa hypothetical protein LOC100517385 (LOC100517385), mRNA [XM_003121502]	XM_003121502	hypothetical protein LOC100517385
A_72_P233767	1.28	1.24	down		Uncharacterized protein [Source:UniProtKB/TrEMBL;Acc:F1SJP7] [ENSSSCT00000000048]	XM_003125991	

Table S6.4 (continued): Fifty-two genes were identified with a significant ($p<0.05$) differently regulated with a fold change (FC) above 1.0 in samples from non-decontaminated (DXD) animals which did not survive.

Probe Name	"Survivor" FC	"Death" FC	"DXD" FC	"DD" FC	Gene Symbol	Description	Genbank Accession	Gene Name
A_72_P281644	1.35	1.46	1.44	1.35		Glutaredoxin-1 [Source:UniProtKB/Swiss-Prot;Acc:P12309] [ENSSSCT00000015476]	AY550049	
A_72_P350248	1.40	1.14	1.21	1.36		Rep: RNA-binding tegument protein - Cercopithecine herpesvirus 16, partial (15%) [TC526559]		
A_72_P201747	1.19	1.38	1.45	1.10		Rep: COX6B - Sus scrofa (Pig), partial (20%) [TC541904]		
A_72_P193407	1.35	1.48	1.42	1.38	LOC100520751	Uncharacterized protein [Source:UniProtKB/TrEMBL;Acc:F1SDZ8] [ENSSSCT00000002683]	XM_003128681	protein sel-1 homolog 1-like
A_72_P303239	2.14	1.36	1.56	2.02	VNN1	Sus scrofa vanin 1 (VNN1), mRNA [NM_214133]	NM_214133	vanin 1
A_72_P376378	1.26	1.41	1.33	1.31	ERP44	Sus scrofa endoplasmic reticulum protein 44 (ERP44), mRNA [NM_001137629]	NM_001137629	endoplasmic reticulum protein 44

Table S6.5a: Of 53 genes which were identified to be significantly ($p<0.05$) differently regulated with a fold change (FC) above 1.0 (and up to 3.0) during the exposure period in all interpretations (survivors, non-survivors (death), decontaminated (DD) and not-decontaminated (DXD)), 47 were down-regulated. Only 1 entity had FC>1.5 in all interpretations.

Probe Name	"Survivor" FC	"Death" FC	"DXD" FC	"DD" FC	Gene Symbol	Description	Genbank Accession	Gene Name
A_72_P121841	1.31	1.13	1.20	1.26		Rep: Plasmid replication protein - Clostridium perfringens, partial (5%) [TC560818]		
A_72_P092691	1.25	1.17	1.24	1.20		Uncharacterized protein [Source:UniProtKB/TrEMBL;Acc:F1SSD2] [ENSSSCT00000005929]	AK235387	
A_72_P034906	1.25	1.20	1.24	1.21	LOC100518251	Uncharacterized protein [Source:UniProtKB/TrEMBL;Acc:F1SFJ6] [ENSSSCT00000000604]	XM_003126427	GTPase KRas-like
A_72_P119756	1.23	1.19	1.21	1.22	NPTN	PREDICTED: Sus scrofa neuroplastin (NPTN), mRNA [XM_001928665]	XM_001928665	neuroplastin
A_72_P262732	1.24	1.21	1.22	1.23	SLA-1	Sus scrofa MHC class I antigen 1 (SLA-1), mRNA [NM_001097431]	NM_001097431	MHC class I antigen 1
A_72_P209872	1.33	1.18	1.32	1.21	LOC100515483	Uncharacterized protein [Source:UniProtKB/TrEMBL;Acc:F1RKI9] [ENSSSCT00000003279]	AK239689	26S proteasome non-ATPase regulatory subunit 8-like
A_72_P257732	1.56	1.19	1.31	1.48				

Table S6.5a (continued): Of 53 genes which were identified to be significantly ($p<0.05$) differently regulated with a fold change (FC) above 1.0 (and up to 3.0) during the exposure period in all interpretations (survivors, non-survivors (death), decontaminated (DD) and not-decontaminated (DXD)), 47 were down-regulated. Only 1 entity had FC>1.5 in all interpretations.

Probe Name	"Survivor" FC	"Death" FC	"DXD" FC	"DD" FC	Gene Symbol	Description	Genbank Accession	Gene Name
A_72_P340103	2.18	1.47	1.82	1.88	LOC100525312	Uncharacterized protein [Source:UniProtKB/TrEMBL;Acc:F1SKV5] [ENSSSCT00000018446]	AK234414	importin-11-like
A_72_P079156	1.43	1.37	1.40	1.41	LOC100525087	Sus scrofa mRNA, clone:LVRM10066C06, expressed in liver. [AK233003]	AK233003	CCR4-NOT transcription complex subunit 8-like
A_72_P107181	1.74	1.51	1.46	1.84	TTI1	Uncharacterized protein [Source:UniProtKB/TrEMBL;Acc:F1SEK2] [ENSSSCT00000008032]	AK346364	Tel2 interacting protein 1 homolog (S. pombe)
A_72_P092501	1.87	1.33	1.48	1.78	MBP	Sus scrofa myelin basic protein (MBP), mRNA [NM_001001546]	NM_001001546	myelin basic protein
A_72_P016631	1.81	1.26	1.42	1.71	LOC100518503	Uncharacterized protein [Source:UniProtKB/TrEMBL;Acc:F1SMC9] [ENSSSCT00000016388]	AK231752	UPF0686 protein C11orf1 homolog
A_72_P205857	1.16	1.42	1.38	1.15	NANS	Sus scrofa N-acetylneuraminic acid synthase (NANS), mRNA [NM_001185139]	NM_001185139	N-acetylneuraminic acid synthase

Table S6.5a (continued): Of 53 genes which were identified to be significantly ($p<0.05$) differently regulated with a fold change (FC) above 1.0 (and up to 3.0) during the exposure period in all interpretations (survivors, non-survivors (death), decontaminated (DD) and not-decontaminated (DXD)), 47 were down-regulated. Only 1 entity had FC>1.5 in all interpretations.

Probe Name	"Survivor" FC	"Death" FC	"DXD" FC	"DD" FC	Gene Symbol	Description	Genbank Accession	Gene Name
A_72_P168881	1.87	1.29	1.60	1.61		Rep: AP-4 complex subunit beta-1 (Adapter-related protein complex 4 beta 1 subunit) (Beta subunit of AP-4) (AP-4 adapter complex beta subunit). - Canis familiaris, partial (52%) [TC523497]		
A_72_P202087	1.79	1.31	1.48	1.66				
A_72_P378588	1.42	1.43	1.34	1.51	LOC100 511905	Uncharacterized protein [Source:UniProtKB/TrEMBL;Acc:F1SE16] [ENSSSCT00000007705]	AY609592	arylamine N-acetyltransferase 1-like
A_72_P335098	1.79	1.19	1.41	1.62	LOC100 526122	Sus scrofa mRNA, clone:AMP010084E02, expressed in alveolar macrophage. [AK231033]	AK231033	ragulator complex protein LAMTOR3-like
A_72_P304394	1.28	1.22	1.32	1.19		Rep: Chromosome undetermined SCAF11230, whole genome shotgun sequence - Tetraodon nigroviridis (Green puffer), partial (9%) [TC525365]		
A_72_P241922	1.81	1.23	1.42	1.67		Rep: Transforming acidic coiled-coil-containing protein 3 (ERIC-1). - Bos Taurus, partial (34%) [TC535168]		

Table S6.5a (continued): Of 53 genes which were identified to be significantly ($p<0.05$) differently regulated with a fold change (FC) above 1.0 (and up to 3.0) during the exposure period in all interpretations (survivors, non-survivors (death), decontaminated (DD) and not-decontaminated (DXD)), 47 were down-regulated. Only 1 entity had FC>1.5 in all interpretations.

Probe Name	"Survivor" FC	"Death" FC	"DXD" FC	"DD" FC	Gene Symbol	Description	Genbank Accession	Gene Name
A_72_P161631	1.39	1.14	1.25	1.30		Uncharacterized protein [Source:UniProtKB/TrEMBL;Acc:F1SU59] [ENSSSCT00000011272]	AK236443	
A_72_P223957	1.81	1.24	1.48	1.61	SULT1A1	Sus scrofa sulfotransferase family, cytosolic, 1A, phenol-preferring, member 1 (SULT1A1), mRNA [NM_213765]	NM_213765	sulfotransferase family, cytosolic, 1A, phenol-preferring, member 1
A_72_P105491	1.31	1.52	1.46	1.33	UBCH5B	Sus scrofa mRNA, clone:SPL010093C06, expressed in spleen. [AK350560]	AK350560	E2 ubiquitin-conjugating enzyme UbcH5B
A_72_P296599	1.43	1.27	1.40	1.32	RCL1	Uncharacterized protein [Source:UniProtKB/TrEMBL;Acc:F1SK46] [ENSSSCT00000005750]	AK346045	RNA terminal phosphate cyclase-like 1
A_72_P415038	1.23	1.18	1.12	1.30	MORF4L1	Uncharacterized protein [Source:UniProtKB/TrEMBL;Acc:F1RKS0] [ENSSSCT00000001981]	AK343838	mortality factor 4 like 1
A_72_P127676	1.61	1.18	1.33	1.51		Sus scrofa mRNA, clone:LNG010095F07, expressed in lung. [AK232172]	AK232172	

Table S6.5a (continued): Of 53 genes which were identified to be significantly ($p<0.05$) differently regulated with a fold change (FC) above 1.0 (and up to 3.0) during the exposure period in all interpretations (survivors, non-survivors (death), decontaminated (DD) and not-decontaminated (DXD)), 47 were down-regulated. Only 1 entity had FC>1.5 in all interpretations.

Probe Name	"Survivor" FC	"Death" FC	"DXD" FC	"DD" FC	Gene Symbol	Description	Genbank Accession	Gene Name
A_72_P052726	2.16	1.34	1.57	2.00		Uncharacterized protein [Source:UniProtKB/TrEMBL;Acc:F1RZE9] [ENSSSCT00000005091]	AK230536	
A_72_P077771	2.39	1.47	1.87	2.04	HMGB2	Sus scrofa high mobility group box 2 (HMGB2), mRNA [NM_214063]	NM_214063	high mobility group box 2
A_72_P076931	1.23	1.19	1.21	1.21	TPM3	Sus scrofa tropomyosin 3 (TPM3), mRNA [NM_001001632]	NM_001001632	tropomyosin 3
A_72_P116461	1.75	1.24	1.43	1.62	GGNBP2	Uncharacterized protein [Source:UniProtKB/TrEMBL;Acc:F1S1C1] [ENSSSCT00000019252]	AK348998	gametogenetin binding protein 2
A_72_P431299	1.61	1.16	1.32	1.50	LOC100520095	Sus scrofa mRNA, clone:THY010049D07, expressed in thymus. [AK351624]	AK351624	sorting nexin-11-like
A_72_P322008	1.26	1.25	1.25	1.26		Uncharacterized protein [Source:UniProtKB/TrEMBL;Acc:F1RUD0] [ENSSSCT00000001457]	AK233371	

Table S6.5a (continued): Of 53 genes which were identified to be significantly ($p<0.05$) differently regulated with a fold change (FC) above 1.0 (and up to 3.0) during the exposure period in all interpretations (survivors, non-survivors (death), decontaminated (DD) and not-decontaminated (DXD)), 47 were down-regulated. Only 1 entity had FC>1.5 in all interpretations.

Probe Name	"Survivor" FC	"Death" FC	"DXD" FC	"DD" FC	Gene Symbol	Description	Genbank Accession	Gene Name
A_72_P330288	2.69	1.54	2.04	2.23		Rep: Chromosome undetermined SCAF3439, whole genome shotgun sequence - Tetraodon nigroviridis (Green puffer), partial (6%) [TC538063]		
A_72_P097686	2.37	1.26	1.54	2.15	VNN2	Uncharacterized protein [Source:UniProtKB/TrEMBL;Acc:F1S3Q9] [ENSSSCT00000004618]	AK230630	vanin 2
A_72_P051611	1.45	1.23	1.23	1.49	PRPF38 B	PREDICTED: Sus scrofa pre-mRNA-splicing factor 38B-like (LOC100154667), mRNA [XM_001927806]	XM_001927806	PRP38 pre-mRNA processing factor 38 (yeast) domain containing B
A_72_P362328	1.42	1.32	1.38	1.37		Uncharacterized protein [Source:UniProtKB/TrEMBL;Acc:F1SU59] [ENSSSCT00000011272]	XM_003133077	
A_72_P293229	1.33	1.25	1.41	1.19	RAB11A	Sus scrofa clone Clu_4682.scr.msk.p1.Contig1, mRNA sequence. [AY609947]	AY609947	RAB11A, member RAS oncogene family
A_72_P331833	1.82	1.36	1.51	1.72	ARHGAP25	Sus scrofa mRNA, clone:UTR010010D09, expressed in uterus. [AK239912]	AK239912	Rho GTPase activating protein 25

Table S6.5a (continued): Of 53 genes which were identified to be significantly ($p<0.05$) differently regulated with a fold change (FC) above 1.0 (and up to 3.0) during the exposure period in all interpretations (survivors, non-survivors (death), decontaminated (DD) and not-decontaminated (DXD)), 47 were down-regulated. Only 1 entity had FC>1.5 in all interpretations.

Probe Name	"Survivor" FC	"Death" FC	"DXD" FC	"DD" FC	Gene Symbol	Description	Genbank Accession	Gene Name
A_72_P179366	1.44	1.23	1.27	1.44		Rep: Pherophorin-C4 protein precursor - Chlamydomonas reinhardtii, partial (5%) [TC571577]		
A_72_P431724	2.12	1.20	1.34	2.09		DB803791 full-length enriched swine cDNA library, adult skin Sus scrofa cDNA clone SKNB10062H08 5', mRNA sequence [DB803791]	DB803791	
A_72_P310598	1.23	1.23	1.25	1.22		Uncharacterized protein [Source:UniProtKB/TrEMBL;Acc:F1RPM5] [ENSSSCT00000005002]	XR_130280	
A_72_P003456	1.31	1.27	1.26	1.33	LOC100 524500	Non-histone chromosomal protein HMG-17 [Source:UniProtKB/Swiss-Prot;Acc:P80272] [ENSSSCT00000003949]	AK349259	non-histone chromosomal protein HMG-17-like

Table S6.5a (continued): Of 53 genes which were identified to be significantly ($p<0.05$) differently regulated with a fold change (FC) above 1.0 (and up to 3.0) during the exposure period in all interpretations (survivors, non-survivors (death), decontaminated (DD) and not-decontaminated (DXD)), 47 were down-regulated. Only 1 entity had FC>1.5 in all interpretations.

Probe Name	"Survivor" FC	"Death" FC	"DXD" FC	"DD" FC	Gene Symbol	Description	Genbank Accession	Gene Name
A_72_P430259	1.35	1.31	1.36	1.31	GGNBP2	Uncharacterized protein [Source:UniProtKB/TrEMBL;Acc:F1S1C1] [ENSSSCT00000019252]	AK348998	gametogenet in binding protein 2
A_72_P063621	1.43	1.27	1.29	1.44	LOC1005 20095	Sus scrofa mRNA, clone:THY010049D07, expressed in thymus. [AK351624]	AK351624	sorting nexin-11-like
A_72_P258962	1.21	1.32	1.20	1.31		Uncharacterized protein [Source:UniProtKB/TrEMBL;Acc:F1RUD0] [ENSSSCT00000001457]	AK233371	
A_72_P034856	1.73	1.42	1.38	1.84		Rep: Pherophorin-C4 protein precursor - Chlamydomonas reinhardtii, partial (5%) [TC571577]		
A_72_P221242	1.54	1.37	1.40	1.54		Rep: Chromosome undetermined SCAF3439, whole genome shotgun sequence - Tetraodon nigroviridis (Green puffer), partial (6%) [TC538063]		
A_72_P128671	1.60	1.23	1.29	1.59	VNN2	Uncharacterized protein [Source:UniProtKB/TrEMBL;Acc:F1S3Q9] [ENSSSCT00000004618]	AK230630	vanin 2

Table S6.5b: Of fifty-three genes which were identified to be significantly ($p<0.05$) differently regulated with a fold change (FC) above 1.0 (and up to 3.0) during the exposure period in all interpretations (survivors, non-survivors (death), decontaminated (DD) and not-decontaminated (DXD)), six were up-regulated.